

JENNI TIENAHO

Utilizing Nordic Forest Plant and Fungi Extracts

Bioactivity assessment with bacterial
whole-cell biosensors

JENNI TIENAHO

Utilizing Nordic Forest Plant and Fungi Extracts
Bioactivity assessment with bacterial whole-cell biosensors

ACADEMIC DISSERTATION

To be presented, with the permission of
the Faculty of Engineering and Natural Sciences
of Tampere University,
for public discussion in the auditorium Pieni sali 1
of the Festia building, Korkeakoulunkatu 8, Tampere,
on 29 April 2020, at 12 o'clock.

ACADEMIC DISSERTATION

Tampere University, Faculty of Engineering and Natural Sciences, Finland

Natural Resources Institute Finland (Luke)

*Responsible
supervisor
and Custos*

Assistant Professor
Ville Santala
Tampere University
Finland

Supervisors

Docent
Tytti Sarjala
Natural Resources Institute
Finland (Luke)
Finland

Professor
Matti Karp
Tampere University
Finland

Pre-examiners

Professor
Elisa Michelini
University of Bologna
Italy

Professor
Heikki Vuorela
University of Helsinki
Finland

Opponent

Docent
Anna Maria Pirttilä
University of Oulu
Finland

The originality of this thesis has been checked using the Turnitin OriginalityCheck service.

Copyright ©2020 author

Cover design: Roihu Inc.

ISBN 978-952-03-1534-4 (print)

ISBN 978-952-03-1535-1 (pdf)

ISSN 2489-9860 (print)

ISSN 2490-0028 (pdf)

<http://urn.fi/URN:ISBN:978-952-03-1535-1>

PunaMusta Oy – Yliopistopaino

Tampere 2020

PREFACE

This study was carried out in cooperation between the Bio and Circular Economy Research group of Tampere University (former Tampere University of Technology) and Natural Resources Institute Finland. Both organizations are thanked for providing the resources and valuable support required for the completion of this thesis. The European Regional Development Fund (project code A71142), Kone Foundation and Suoviljelysyhdistys ry are warmly acknowledged for the funding of this work. COST Action FA1103: Endophytes in Biotechnology and Agriculture is also thanked for the short-term scientific mission fund.

This thesis would have never reached its goals without my excellent supervisors: assistant professor Ville Santala and docent Tytti Sarjala. I also wish to thank Matti Karp and Robert Franzén for the initial supervision of this thesis. Thank you all for your support and patience as well as resources and overall help throughout the work. Especial thanks for Tytti for her eternal optimism, encouragement and friendship during the years. Grateful appreciation also to University lecturer Maarit Karonen for valuable discussions and encouragement as well as to other coauthors for their effort and aid during the writing process. Additionally, I am grateful to people from the Synbio for welcoming me warmly into their group. Thank you also Tarja Ylijoki-Kaiste and Tea Tanhuanpää for all the assistance and friendly discussions.

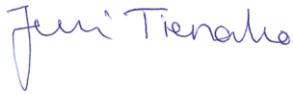
All my collaborators and friends at Natural Resources Institute Finland, I am eternally grateful. Especially Anneli Käenmäki, Eeva Pihlajaviita and Hanna Leppälampi are acknowledged for their professional help in the laboratory. I also wish to thank Riina Muilu-Mäkelä for the valuable discussions during the drives to Parkano. Appreciation also to Olli “local-IT-support” Seppälä for assistance and friendship. In addition, Leila Korpela and Niko Silvan have shared important knowledge about peatland environments. Additionally, Biomass Characterization and Properties Group of Luke and Tuula Jyske are acknowledged for support and encouragement during this work.

I wish to thank all my friends and especially Hanna Manninen, Jenna Mannoja, Emmi Poikulainen and Liisa Naskali for valuable discussions, never-ending encouragement and peer support without which I could not have made it this far.

You and your families have also been of great assistance and support during personal life obstacles. I wish to be able to return even a small bit of the loyalty and friendship that I have encountered during the years.

Lopuksi haluan kiittää perhettäni. Ilman teitä en olisi tässä. Äiti, isä, Olli ja Aira, te olette uskoneet minuun silloinkin, kun se on ollut itselleni vaikeaa ja olen saanut loputtomasti apua ja tukea. Siskoni Noora, sinulle on aina voinut soittaa ja olet tarjonnut tukea niin työhön ja tutkimukseen liittyvissä asioissa kuin kaikessa muussakin. Kiitos tuhannesti myös oikolukuavusta vuosien varrella, olet paras! Kiitos myös tyttäreni Emma; olet elämäni arvokkain asia ja suurin ilon lähde. Todistuksena siitä, että pystyt mihin vaan – kuuhun, tähtiin ja takaisin.

Tampere, March 2020



Jenni Tienaho

ABSTRACT

Efficient methods are needed in the search for novel biologically active components from natural sources. Bacterial whole-cell biosensors offer a less-examined alternative with high sensitivity. In this thesis, forest-derived extracts were screened for their bioactivity with bacterial whole-cell biosensors and complementary measures, such as antioxidant microplate tests. The main metabolites were also identified from endophytic fungi extracts using liquid chromatography-mass spectrometry (LC-MS).

Two novel applications of biosensors are described for *Escherichia coli* whole-cell biosensors. The first application provides an improved antioxidant method via increased high-throughput screening potential and the other describes a method for measuring the UV protection capacity for both the biological and absorbance-based shield. There is also an opportunity to obtain simultaneous information of the genotoxicity of the sample. The methodologies were validated using reference compounds and were found to be usable in the field of forest-derived extracts with certain limitations. The bacterial biosensors were used in an activity/inactivity type of screening. By using small concentrations of forest-derived extracts or fractionated samples, the limitations, such as possible sample matrix masking effect and induction delay phenomenon, can be reduced.

Endophytic fungi live asymptotically inside a plant host and are often beneficial for the host plant growth and stress resistance. They comprise a large untapped source of potential bioactive compounds to be utilized for different purposes. Many metabolites (318) were discovered using an LC-MS methodology from *Acephala applanata*, *Phialocephala fortinii* and *Humicolopsis cephalosporioides/Coniochaeta mutabilis* isolated from the roots of Scots pine seedlings. Out of the metabolites, 220 were identified with varying degree of certainty. The antioxidant and antimicrobial potential of the extracts and fractions were screened with the biosensors and complementary methods and various bioactivities were discovered.

In conclusion, endophytic fungi are a rich source of potential functional metabolites and whole-cell biosensor methodologies are usable for nature-based samples and provide valuable insights into both the bioactivity and bioavailability of the material, if their limitations are also considered.

TIIVISTELMÄ

Luonnonmateriaalien sisältämien biologisesti aktiivisten komponenttien seulontaan tarvitaan uusia tehokkaita menetelmiä. Tässä tutkimuksessa metsästä saatavien uutteen bioaktiivisuuden määrittämiseen käytettiin kokosolubiosensoreita. Tätä vaihtoehtoista seulontamenetelmää on tutkittu tarkoituksessa vain vähän, mutta herkkyytensä vuoksi se on varteenotettava. Tutkimuksessa aktiivisuushavainnot täydentämään käytettiin myös perinteisempiä menetelmiä kuten antioksidanttikuoppalevytestejä. Lisäksi aineenvaihduntatuotteet määritettiin bioaktiivisiksi havaituista endofyyttisieniuutteista nestekromatografia-massaspektrometriaa (LC-MS) käyttäen.

Tutkimuksen osana kehitettiin kaksi biosensorimenetelmää *Escherichia coli* -kokosolubiosensoreille. Ensimmäinen sovellus parantaa aiemmin kuvattua antioksidanttisuuden mittaamisen menetelmää sen seulonnan tehopotentialia lisäämällä. Toinen esittelee menetelmän UV-säteilysuojan mittaamiseksi määrittäen sekä biologista että absorbanssipohjaista suojauskykyä. Menetelmällä voidaan saada samalla tietoa myös näytteen genotoksisuudesta. Kehitettyjen menetelmien toimivuus vahvistettiin malliyhdisteitä käyttäen, ja ne todettiin toimiviksi myös luonnonaineuutteilla joillakin rajoituksilla. Bakteeribiosensoreita voidaan käyttää etenkin konsentraatioiltaan pienien näytteiden ja fraktioiden aktiivisuus- tai inaktiivisuusseulonnoissa, jolloin minimoidaan rajoitukset, kuten näytematriisin signaalin peittovaikutus ja induktioviive.

Endofyyttisienet elävät kasvien sisällä aiheuttamatta oireilua isäntäkasvissa, ja ne voivat lisätä esimerkiksi isäntien kasvua ja stressinsietokykyä. Endofyyttisienet sisältävät suuren määrän toistaiseksi hyödyntämättömiä bioaktiivisia yhdisteitä, joita voidaan käyttää erilaisiin tarkoituksiin. Tutkimuksessa männyn taimien juurista eristettiin *Acephala applanata*, *Philocephala fortinii* ja *Humicolopsis cephalosporioides/Coniochaeta mutabilis* -endofyyttisienilajit, ja niistä löydettiin suuri määrä yhdisteitä LC-MS:llä (yht. 318 kpl). Yhdisteistä tunnistettiin eri varmuusasteilla 220 kpl. Sienilajien uutteen ja fraktioiden antioksidantti- ja antibakteerisuuspotentiaali seulottiin käyttäen *E. coli* -biosensorimenetelmiä sekä täydentäviä menetelmiä ja havaittiin useita aktiivisuuksia.

Johtopäätöksenä endofyyttisienet sisältävät valtavan määrän mahdollisesti toiminnallisia aineenvaihduntatuotteita, ja kokosolubiosensorimenetelmät soveltuvat

erilaisten luontopohjaisten näytteiden tutkimiseen antaen samanaikaisesti tietoa sekä näytteen bioaktiivisuudesta että biosaatavuudesta, mikäli myös niiden heikkoudet huomioidaan mittausasettelussa.

CONTENTS

1	Introduction	1
2	Background	3
2.1	Endophytes	3
2.2	Bioluminescent bacterial biosensors	6
2.3	Antioxidants against oxidative stress	8
2.4	Biological UV protection	10
2.5	Antibacterial agents and antibiotics	12
3	Research objectives	14
4	Materials and methods	15
4.1	Sample pre-handling	17
4.2	Extraction	17
4.3	Fractionation of the fungal extracts	19
4.4	LC-MS and identification	19
4.5	Bacterial strains and cultivation	19
4.6	Biosensor measurements	21
4.6.1	Antioxidant screening using <i>E. coli</i> DPD2511	21
4.6.2	UV protection screening using <i>E. coli</i> DPD2794	21
4.6.2.1	Absorbance measurements	22
4.6.3	Antibacterial screening with biosensors	23
4.7	Other bioactivity measurements	23
4.7.1	Hydrogen peroxide scavenging, SCAV	23
4.7.2	Oxygen radical absorbance capacity, ORAC	23
4.7.3	Oxidative stress related diseases	24
4.8	Statistical methods	25
5	Results and discussion	26
5.1	Bacterial biosensor results	26
5.1.1	Antioxidant and antibacterial activity, <i>E. coli</i> DPD2511	26
5.1.2	UV protective and antibacterial activity, <i>E. coli</i> DPD2794	27
5.1.3	Color effect of berry extracts	28
5.1.4	Bacterial biosensor discussion	30
5.2	Bioactive metabolites of endophytic fungi	35

5.2.1	Bioactivities of endophytic fungi extracts and fractions.....	35
5.2.2	Bioactive metabolites from endophytic fungi.....	37
5.2.2.1	Amino acids and peptides	41
5.2.2.2	Osmolytes and siderophores.....	45
5.2.2.3	Amadori compounds, amino acid quinones and opine amino acids	46
5.2.2.4	Common metabolites.....	48
5.2.2.5	Specialized metabolites	52
5.2.3	Bioactive metabolites of endophytic fungi discussion	53
6	Conclusions	57
	References	60

ABBREVIATIONS

A fungi	Cultivation code of <i>Acephala applanata</i>
act	Active in a bioactivity test
ADP	Adenosine diphosphate
AMD	Age-related macular degeneration
AMP	Adenosine monophosphate
antiox ^{act/inact}	Active or inactive in the biosensor test for antioxidant activity
cADPR	Cyclic adenosine diphosphate ribose
cGMP	Cyclic guanosine monophosphate
CPS	Counts per second
cUMP	Cyclic uridine monophosphate
CV%	Coefficient of variation (%)
dAMP	Deoxyadenosine monophosphate
dGMP	Deoxyguanosine monophosphate
DNA ^{act/inact}	Active or inactive in the biosensor test for genotoxicity
DPPH	2,2-Diphenyl-1-picrylhydrazyl antioxidant assay
DSE	Dark septate endophytic fungi
FI	Fold induction compared with water blank (see IF)
FOX	Ferrous oxidation–xylenol orange assay (see SCAV)
HAT	Hydrogen atom transfer antioxidant mechanism
HTS	High-throughput screening
IF	Impact factor compared with water blank (see FI)
ITS	Internal transcribed spacer
LA	Lysogeny agar growth medium
LB	Lysogeny broth growth medium
LC-MS	Liquid chromatography–mass spectrometry
MSI	Metabolomics standards initiative
NAD	Nicotinamide adenine dinucleotide
NR	Nicotinamide riboside
ORAC	Oxygen radical absorbance capacity antioxidant test
OX ^{act/inact}	Active or inactive in the biosensor test for oxidative stress

PAC	<i>Philocephala fortinii</i> s.l. – <i>Acephala applanata</i> species complex
PC	Principal component
PCA	Principal component analysis
PD ^{act/inact}	Active or inactive in Parkinson’s disease cell model test
Pi _{Ne}	Pine needle methanol extract
R fungi	Cultivation code of <i>Pialocephala fortinii</i>
ROS	Reactive oxygen species
S16 fungi	Cultivation code of <i>Humicolopsis cephalosporioides/Coniochaeta mutabilis</i>
SCAV	Hydrogen peroxide scavenging (see FOX)
SET	Single electron transfer antioxidant mechanism
TE	Trolox equivalent
UDP	Uridine diphosphate
UV-R	Ultraviolet radiation

ORIGINAL PUBLICATIONS

- Publication I Jenni Tienaho, Tytti Sarjala, Robert Franzén, and Matti Karp. Method with High-Throughput Screening Potential for Antioxidative Substances Using *Escherichia coli* Biosensor *katG::lux*, *Journal of Microbiological Methods*, vol. 118, pp. 78–80, Aug. 2015.
- Publication II Jenni Tienaho, Emmi Poikulainen, Tytti Sarjala, Riina Muilu-Mäkelä, Ville Santala, and Matti Karp. A Bioscreening Technique for Ultraviolet Irradiation Protective Natural Substances, *Photochemistry and Photobiology*, vol. 94, pp. 1273–1280, May 2018.
- Publication III Jenni Tienaho, Maarit Karonen, Riina Muilu-Mäkelä, Kristiina Wähälä, Eduardo Leon Denegri, Robert Franzén, Matti Karp, Ville Santala, and Tytti Sarjala. Metabolic Profiling of Water-Soluble Compounds from the Extracts of Dark Septate Endophytic Fungi (DSE) Isolated from Scots Pine (*Pinus sylvestris* L.) Seedlings Using UPLC-Orbitrap-MS, *Molecules*, vol. 24, 2330, June 2019.
- Publication IV Jenni Tienaho, Maarit Karonen, Riina Muilu-Mäkelä, Janne Kaseva, Nuria de Pedro, Francisca Vicente, Olga Genilloud, Ulla Aapola, Hannu Uusitalo, Robert Franzén, Kristiina Wähälä, Matti Karp, Ville Santala, and Tytti Sarjala. Metabolites of the Endophytic Fungi of Scots Pine (*Pinus sylvestris*) Roots: An Abundant Source of Bioactive Compounds for Potential Utilization, *Planta Medica*, Submitted for publication.

AUTHOR CONTRIBUTIONS

- Publication I J. Tienaho planned and carried out the experiments, drafted the manuscript and is the corresponding author. T. Sarjala, R. Franzén, and M. Karp contributed in designing of the experiments and writing of the manuscript.
- Publication II J. Tienaho drafted the manuscript, is the corresponding author and planned the experiments as well as interpreted the results. E. Poikulainen carried out the UV measurements with biosensors and contributed in interpreting these results. T. Sarjala and R. Muilu-Mäkelä contributed in planning the absorbance measurements and T. Sarjala noticed a need for this screening methodology. V. Santala and M. Karp contributed in planning and developing the UV measurements with biosensors. All authors participated in writing of the manuscript.
- Publication III J. Tienaho drafted the manuscript and is the corresponding author. She planned the experiments and interpreted results together with M. Karonen, who also carried out LC-MS measurements. R. Muilu-Mäkelä identified the fungal strains. K. Wähälä and E. Leon Denegri contributed in synthesizing reference compounds. T. Sarjala, M. Karp, V. Santala and R. Franzén contributed in designing the experiments and supervision. All authors participated in writing the manuscript.
- Publication IV J. Tienaho drafted the manuscript and is the corresponding author. She also planned and carried out biosensor experiments and interpreted the results. M. Karonen carried out the LC-MS measurements and R. Muilu-Mäkelä identified the fungal strains. J. Kaseva conducted the statistical analysis. N. de Pedro, F. Vicente, O. Genilloud, U. Aapola and H. Uusitalo carried out and designed cell model testing. R. Franzén, K. Wähälä, M. Karp, V. Santala, and T. Sarjala contributed in designing the experiments and supervision. All authors participated in writing the manuscript.

1 INTRODUCTION

Finnish nature provides vast potential to provide beneficial natural products. The boreal region poses numerous challenges to the organisms to survive in the growing conditions and consequently these organisms have developed a wide range of strategies for survival including various beneficial metabolites with bioactive features. Biological activity or bioactivity is determined as a dose-dependent beneficial (for example antioxidant activity) or detrimental (for example antimicrobial activity) effect of a substance on living tissues, cells or organisms (Jackson *et al.*, 2007). On the other hand, bioavailability describes the extent and ability of a substance to cross the cellular membrane of an organism and, thus, enter their target in the cells (Chow, 2014). Both factors are fundamentally necessary for medicinal products and are desired for certain products in dermatology, cosmetics and fortified or functional foods. Additionally, such products could be used for applications such as antimicrobial packaging materials for the replacement of plastic products.

In fact, nature has already provided different bioactive substances for the use in fields such as pharmaceuticals, cosmetics and nutraceuticals for thousands of years. While estimates vary, it is safe to say that from 25 to 50% of prescription drugs are natural substance derivatives, semi-synthetic natural products or directly of natural origin (Kingston, 2011). Out of 1562 approved drugs during years 1981–2014, 23% are biological macromolecules, unaltered natural products, botanical drugs or natural product derivatives (Newman & Cragg, 2016). If synthetic products mimicking natural products are also considered, the share increases to 44% (Newman & Cragg, 2016). Nature is still the single most important source for finding new mechanisms of action for use of medicine. In addition, the dermatology and functional foods industries rely on beneficial substances that can enter tissues and cells. As an example, different parts of plants and plant extracts have been used as cosmeceuticals in skincare and hair care products, antioxidants and fragrances for decades (Yahya *et al.*, 2018). Furthermore, functional or fortified foods or herbal medicines draw benefit from phytochemicals and bioactive animal products such as phenolic and polyphenolic compounds and omega-3 fatty acids from marine oils.

Microorganisms, such as fungi and bacteria, are a diverse source of bioactive metabolites and have yielded some of the most important products of the pharmaceutical industry, such as penicillin and tetracycline (Cragg & Newman, 2013). It has been estimated that out of up to 1.5 to 5.1 million fungal species living on earth no more than 5% have been studied for their health promoting or bioactive properties (Hawksworth, 2001; O'Brien *et al.*, 2005). In a recently published study, it was found that with regard of the contained functional groups, plant products were least diverse when compared to molecules obtained from bacteria, animals and fungi (Ertl & Schuhmann, 2019). This is interesting because it is by far the most thoroughly investigated and largest group. However, the plants produce most complex scaffolds out of the investigated organisms (Ertl & Schuhmann, 2020). Less examined fungal species could, thus, offer an enormous bioactive and medicinal product potential. In fact, six of the 20 most commonly prescribed commercial drugs are of fungal origin (Schulz *et al.*, 2002). Metabolites produced by fungi have also been found to contain a large range of biological activities for example in the antimicrobial, antiviral, insecticidal, antioxidant and anticancer fields (Strobel *et al.*, 2004; Zhao *et al.*, 2010).

In this thesis bacterial whole-cell biosensors are used in the screening of bioactivity of forest-derived plant and fungi extracts. With these bacterial biosensors, in order to show bioactivity, the sample needs to also be able to enter the bacterial cell and therefore pose bioavailability as well. Two novel applications of biosensor methodologies are described in Papers **I** and **II**. Paper **I** introduces a microplate technique of an antioxidant screening method with improved high throughput screening potential whereas Paper **II** shows a new method of screening the ultraviolet (UV) radiation protection capacity of samples. In Paper **IV**, the search for antioxidant and antibacterial properties from endophytic fungi is described using whole-cell bacterial biosensors. This information is combined with the metabolite identification obtained in Paper **III**. To my knowledge, this is the first time that the water-extractable metabolites of Scots pine roots associated endophytes are described and combined with bioactivity information.

2 BACKGROUND

This chapter introduces endophytic fungi, which are used as forest-derived sample material. Bioluminescent bacterial biosensors are also introduced as well as the functional properties sought for: antioxidant activity, UV radiation protection and antibacterial activity.

2.1 Endophytes

Endophyte, from Greek ‘endon’, meaning within, and ‘phyton’, meaning a plant, is a term literally referring to an organism living inside a plant host (**Figure 1**). The most common endophytes are fungi or bacteria and the term usually refers to these microbial species (Wilson, 1995). Endophytic infections are inconspicuous, and an endophyte must live asymptotically inside the plant host for at least some part of its lifecycle (Stone *et al.*, 2000). The host plant benefits from the infection through enhanced growth, nutrient intake and various stress tolerance improvements, whereas the endophyte can access the nutrients from the plant apoplastic space and benefits from being able to spread asexually via vertical transmission through the seed (Scott, 2001; Tanaka *et al.*, 2006). What is more, endophytic microorganisms can live inside every plant tissue and may be both intracellular and intercellular. Endophytes have been found in all plant species growing all over the world, and each and every plant acts as a host to one or more endophytic species (Arnold, 2007). The growth habitat and environmental conditions of the host plant affect the diversity and size of the endophytic populations and unique or extreme growth conditions may yield novel endophytic leads with interesting properties (Firáková *et al.*, 2007).

Dark septate endophytic fungi (DSE) are often found to be dominant in the roots of boreal forest tree species (Grünig *et al.*, 2008). They are characterized by melanized and septate hyphae and are extensively distributed in the coniferous forests of the northern hemisphere (Jumpponen & Trappe, 1998). The most frequent DSE in forest ecosystems belong to the *Philocephala fortinii* s.l. – *Acephala applanata* species complex (PAC) as up to 80% of fine roots in forest stands can be colonized by them

(Grünig *et al.*, 2008). Many of the DSE and PAC species have been shown to suppress root pathogens, accelerate root turnover and mineralization and to induce resistance to abiotic stress (Mandyam & Jumpponen, 2005; Schulz, 2006; Grünig *et al.*, 2008; Tellenbach *et al.*, 2013).

A good example of symbionts in extreme growth habitats are the endophytic fungi of Scots pine (*Pinus sylvestris* L.) seedlings in drained peatlands. Drained peatlands are harsh environments where seedlings grow under intense abiotic stress caused by high variability in the levels of temperature and soil water content as well as solar radiation. There is evidence that endophytes affect the growth and survival of the host plant by enhancing their tolerance towards biotic and abiotic stress (Waller *et al.*, 2005; Rodriguez *et al.*, 2009; Nagabhyru *et al.*, 2013). Many of the bioactive metabolites generated by endophytes have antimicrobial activity, thus protecting the host plant from phytopathogenic microorganisms (Aly *et al.*, 2010) and additionally, the secondary metabolites produced by endophytic fungi may offer potential for fields such as pharmacology and medicine (Gutierrez *et al.*, 2012). The endophytes isolated from the roots of Scots pine seedlings in extreme habitats could potentially contain compounds with interesting functional properties.

The produced bioactive metabolites could be utilized in many fields and their variety is vast. The compounds isolated from endophytic fungi belong to diverse chemical groups, which include the Amadori compounds, peptides, opine amino acids, alkaloids, phenols, steroids, isocoumarins, benzopyranones, terpenoids, xanthenes and quinones (Tan & Zou, 2001; Schulz *et al.*, 2002; Tienaho *et al.*, 2019). Endophytic organisms can also produce the same therapeutic compounds as the host plant (Aly *et al.*, 2010; Zhao *et al.*, 2010), which is especially useful in the case of slow growing and rare plants in extreme environments. The therapeutic potential could be antibiotic, antifungal, anti-algal and antiviral (Strobel *et al.*, 2004; Dai *et al.*, 2009). Metabolites have also been found to act as antidiabetic and immunosuppressive agents and in some cases also as insecticides (Strobel *et al.*, 2004). Additionally, endophytes provide cytotoxic, chemo-preventive, anti-metastatic and antitumor properties for the treatment of various types of cancer (Strobel *et al.*, 2004; Gutierrez *et al.*, 2012).

Antioxidant or free radical scavenging compounds have also been found in endophytic fungi. For example, pestacin and isopestacin have been found in cultures of *Pestalotiopsis microspora* (Strobel *et al.*, 2004) and graphis lactone A has been isolated from *Cephalosporium* sp. (Gunatilaka, 2006). Isopestacin has been found to scavenge superoxide and hydroxyl radicals in solutions using electron spin resonance measurements (Strobel *et al.*, 2002). Pestacin has been analyzed using a total

oxyradical scavenging capacity (TOSC) assay and has been found to have 11 times greater antioxidant activity than the vitamin E derivative trolox (Harper *et al.*, 2003). For graphis lactone A, free radical scavenging was studied using DPPH and hydroxyl radical assays and antioxidant activities were established using linoleic acid and human low-density lipoprotein models (Song *et al.*, 2005). However, a literature review showed that the full potential of endophytes as a source of antioxidant species for therapeutic purposes has not been utilized even though oxidative stress is involved in the pathogenic processes of many diseases (see **Chapter 2.3**).

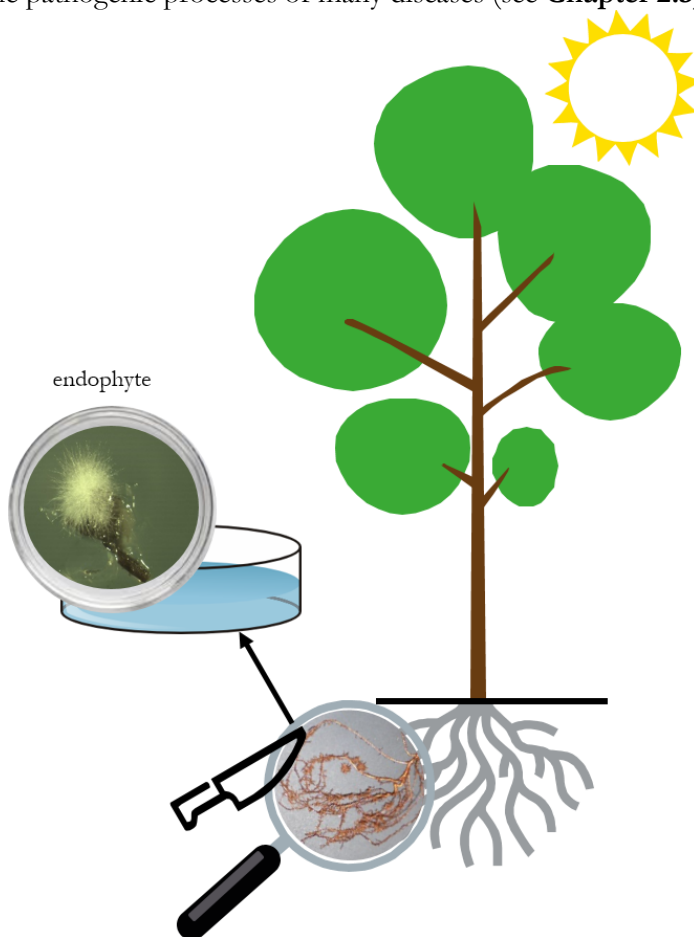


Figure 1. Endophytic fungi live inside the Scots pine roots. After isolation, the endophyte emerges from the cut and surface sterilized root tip on a growth medium. Mycorrhizas in comparison can exist outside the plant host and often form fruiting bodies.

2.2 Bioluminescent bacterial biosensors

A biosensor is described as an analytical device with a biological element connected to a physical device which generates a measurable signal proportional to the concentration of the investigated analyte (Su *et al.*, 2010). This produced signal can be monitored in numerable ways, including electrochemical, optical, acoustical, mechanical, calorimetric and electronic detection.

Optical detection is usually based on fluorescent, luminescent or colorimetric signals, which are produced as a response of microorganisms to a target compound in a dose-dependent manner. Optical detection is widely used with whole-cell microbial biosensors which have been genetically modified by fusing a genetic regulatory element (promoter) with a reporter gene from another organism. Due to environmental stimuli, the inducible gene activates, which results in a reporter gene expression by increasing (lights on) or decreasing (lights off) the monitored signal (Elad *et al.*, 2008). For the induction, the analyte of interest must be able to enter the microbial cell. All organisms have survival mechanisms to overcome and cope with stress situations induced by damaging material inside the cells and on cell membranes. The control elements of these mechanisms can be transferred from one cell to another to create living microbial biosensors with a combination of reporter genes, which leads to sensitive, real-time reporting of the cell environment. Such sensors can be used for example in the detection of antimicrobial agents, heavy metals, oxidants, such as reactive oxygen species (ROS) and endocrine disruptors (Galluzzi & Karp, 2006; Belkin *et al.*, 1996a).

In a toxic environment, bacterial cells react with several defense mechanisms by initiating gene transcriptions at specific promoter DNA sites. These promoter regulons respond to different stress situations and therefore the activation of a certain regulon can provide information about the current environmental hazards of the cell (Dempfle, 1991). By fusing bioluminescent reporter genes from bioluminescent organisms such as marine bacteria or fireflies with the desired promoter regulons of the bacteria, a stress-specific luminescent light signal can be observed (Gui *et al.*, 2017). In order to detect the luminescent light signal, the examined substance or sample material must be able to enter the bacterial cell, thus, the method provides information on the bioavailability as well as bioactivity of the tested material. This light signal is also easy to measure and quantify automatically in a continuous manner (Michelini *et al.*, 2005).

Recombinant *Escherichia coli* strains DPD2511 (*katG':lux*) (Belkin *et al.*, 1996a) and DPD2794 (*recA':lux*) (Vollmer *et al.*, 1997) can be utilized in the search of

bioactive and bioavailable products. The *katG* regulon is activated due to oxidative stress whereas *recA* responds to DNA damage in the bacteria. The *E. coli* DPD2511 strain (Belkin *et al.*, 1996a) has been constructed by fusing the *katG* (catalase) gene of the strain with the luminescence (*lux*) genes from marine *Aliivibrio fischeri* (former *Vibrio fischeri*) bacteria. The bioavailable oxidant can enter through the *E. coli* cell membrane and bind to the regulatory protein OxyR, which promotes the transcription and translation of the reporter genes. With the *lux* gene expression, this produces an increase in the emission of luminescent light. The schematic model of the function is shown in **Figure 2**. Thus, the normal defense mechanism against oxidizing agents produces an easily monitored response. When using intact living biosensors, the bioactivity and bioavailability of a chosen sample material can be detected simultaneously in a simple, cost-effective and rapid manner, which makes the assays more suitable for high-throughput screening (HTS) (Galluzzi & Karp, 2006).

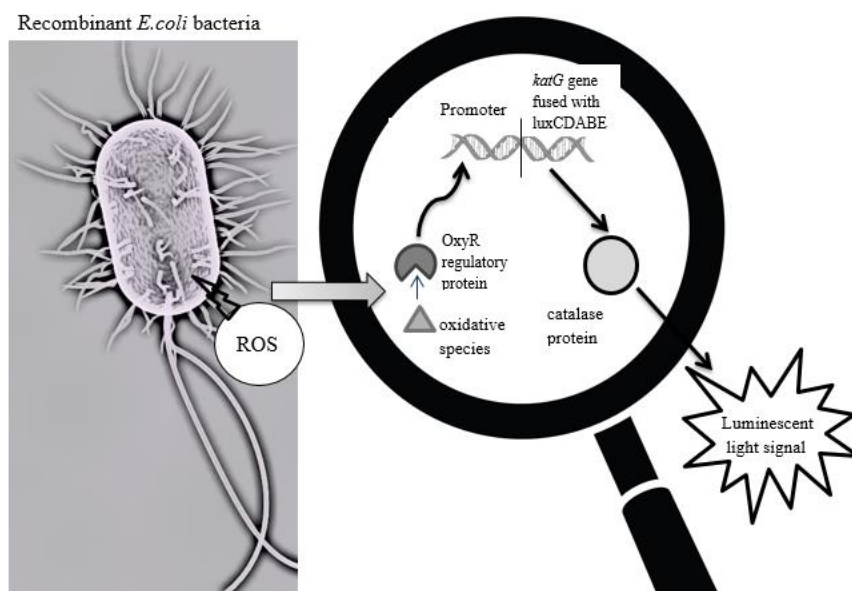


Figure 2. The schematic model of the function of *E. coli* DPD2511 biosensor. Reactive oxygen species (ROS) induce a luminescent light signal.

When antioxidant activity is measured, the bacterial cells are exposed to an oxidant such as hydrogen peroxide (H_2O_2), and the experiment is set to measure whether samples prevent the stress reaction. In other words, the method measures the *in vivo* inhibition capacity of the antioxidant against H_2O_2 . The *E. coli* DPD2511 strain has

been previously used to screen the antioxidant properties of the medicinal plants of Philippines and validated against the 1,1-diphenyl-2-picrylhydrazyl (DPPH) radical scavenging assay by Bartolome *et al.*, (2006).

The *E. coli* DPD2794 biosensor is similar except that it responds to the multiple mechanisms of genotoxicity via SOS responsive *recA* region. The term SOS is used because the response indicates cellular reaction to DNA damage induced distress. These mechanisms include UV radiation induced stress and other direct DNA damaging mutagens, as well as indirect DNA damaging agents such as ROS producing oxidants (Min *et al.*, 1999). Watt *et al.*, (2007) used the *E. coli* DPD2794 sensor to screen for antibacterial activity in herbal tinctures and they concluded that the method was usable in the field of natural substance extracts.

Kim *et al.*, (2019) used a panel of stress-responsive recombinant luminescent bacteria to detect the cytotoxicity of natural compounds to utilize in the prescreening for drug discovery. Each strain responded to a different type of cellular damage and therefore could provide an insight into the damaging mechanism. They proposed that these methods could be used as a substitution for human cell cytotoxicity tests, which often require special handling. Although a few reports exist, where these sensors have been utilized in screening the biological activity of natural substances and extracts, comprehensive analyses have not been established on the usability of these methods. With nature-derived extracts, features such as the color or turbidity could compromise the reliability of the results when using traditional microbial growth inhibition assays relying on absorbance screening. Additionally, conventional often tedious and time-consuming antibacterial assays are usually not sensitive enough to be used to detect the bioactivity of fractionated nature-derived extracts with the very low concentrations of active substances.

2.3 Antioxidants against oxidative stress

Among oxidants, the reactive oxygen species (ROS), which are often free radicals or peroxides, can exist in ionic (such as hydroxyl radicals, superoxide anions) or molecular (such as hydrogen peroxide (H₂O₂) or singlet oxygen) states in biological systems (Huang *et al.*, 2019). During normal metabolic processes, such as cellular respiration, the cells of aerobic organisms produce ROS as a by-product. However, ROS can cause destructive damage of DNA, proteins, carbohydrates and lipids and are thus major contributors to the process of aging and age-related degenerative

diseases such as cancer, mutagenesis, atherosclerosis, hypertension and ischemia-reperfusion as well as overall inflammation (Ames *et al.*, 1993; Liguori *et al.*, 2018).

Antioxidants are substances, which significantly reduce or prevent oxidation even in low concentrations (Co *et al.*, 2012). Some compounds that enhance endogenous activity instead of neutralizing free radicals are also called antioxidants (Kurutas, 2016). Then again, antioxidants in food systems are used to maintain the nutrient level, texture, color, taste, freshness, functionality, aroma and appeal by retarding lipid peroxidation and the production of secondary products relating to it (Samaranayaka & Li-Chan, 2011; Wilson *et al.*, 2017). In dermatology, topical antioxidants are used because of their broad biological activity. They might also possess anti-inflammatory, UV protective and anti-carcinogenic activities, which increase their beneficial potential (Poljsak *et al.*, 2013). Antioxidants often play an important role in preventing or alleviating chronic diseases caused by oxidants. Metabolites with antioxidant activity are therefore interesting for the perspective of numerous fields.

Antioxidants act through different chemical mechanisms: hydrogen atom transfer (HAT), single electron transfer (SET) and the ability to chelate transition metals (Apak *et al.*, 2013; Santos-Sánchez *et al.*, 2019). Several tests have been developed for these measurements. For example, the oxygen radical absorbance capacity (ORAC-FL) assay is based on the inhibition of peroxy radical (ROO•) induced oxidation of a fluorescent molecule and the reaction mechanism is based on HAT (Santos-Sánchez *et al.*, 2019). In the ferrous oxidation in the xylenol orange (FOX) reagent method, the antioxidant needs to inhibit the Fenton reaction, where H₂O₂ oxidizes Fe(II) into Fe(III) and yields highly oxidizing hydroxyl radicals or oxidoiron(IV)-compounds (FeO²⁺) (Koppenol & Hider, 2019). The ferric iron forms a colored complex causing a change in the sample absorbance. The antioxidant therefore acts as a transition metal chelator and inhibits the Fenton reaction (Apak *et al.*, 2013).

With endophytes, the levels of ROS produced by the host plant have been shown to affect the relationship between the host and the endophyte (Tanaka *et al.*, 2006). This interaction can vary from mutualistic to exploitative or from saprobic to parasitic (Hyde & Soyong, 2008). ROS production is one of the initial defense mechanisms for the plant host cells against microbial infection, thus, the successful colonization by an endophyte requires defeating them (Koskimäki *et al.*, 2016). It can therefore be suggested that endophytes produce secondary metabolites which are specifically effective towards oxidative stress.

In plants and other aerobic organisms, ROS production is caused by biotic and abiotic stress conditions or other circumstances, where the redox homeostasis is

disrupted, inducing oxidative stress damage (Greene, 2002). However, ROS also function as signaling molecules in regulating the normal growth and adaptation to stress. The balance and mechanisms behind these contrasting roles of ROS in plants are not fully known (Krishnamurthy & Rathinasabapathi, 2013). It is known that low ROS levels are necessary for basic biological processes in the cells, but higher levels lead to irreversible DNA damage and prolonged exposure eventually leads to programmed cell death (Huang *et al.*, 2019). For example, hydrogen peroxide is an uncharged molecule, which is capable of diffusing across biological membranes and therefore has a signaling function in the cells (Mullineaux *et al.*, 2000; Greene, 2002). In small concentrations, it plays an important role in response to biotic and abiotic stresses by reinforcing the plant cell wall, phytoalexin production and enhancement of resistance (Quan *et al.*, 2008). In high concentrations, hydrogen peroxide acts as an oxidizing agent, which can damage enzymes and proteins with active thiol groups (Engwa, 2018). Peroxyl radicals then again cause the peroxidation of unsaturated lipids in the membranes of biological systems (Engwa, 2018).

In normal conditions, excessive ROS in plants and the human body can be scavenged by various antioxidant defense mechanisms, which can be divided into enzymatic (specific) and non-enzymatic (non-specific) defense systems (Apel & Hirt, 2004; Demidchik, 2015). Superoxide dismutase (SOD), catalase, ascorbate peroxidase and glutathione peroxidases belong to the enzymatic systems, whereas the non-enzymatic systems primarily consist of low molecular weight antioxidants. In plants, these include compounds such as glutathione, proline, ascorbic acid, α -tocopherols, carotenoids, flavonoids, tannins and polyamines (Apel & Hirt, 2004; Engwa, 2018; Huang *et al.*, 2019; Dumont & Rivoal, 2019). Superoxide and H_2O_2 can be broken down by SOD, catalase and peroxidases but not the hydroxyl radical, which is extremely reactive. However, low molecular weight antioxidants, such as *myo*-inositol, sorbitol, mannitol and proline have been shown to be able to scavenge hydroxyl radicals, at least *in vitro* (Bohnert & Jensen, 1996).

2.4 Biological UV protection

Ultraviolet radiation (UV-R) is a part of the electromagnetic spectrum with wavelengths from 10 to 400 nm. Thus, it is below the visible region of light (400-780 nm) but above X-rays. UV-R is often divided into three ranges according to their wavelength: UV-C, UV-B and UV-A (**Figure 3**). Out of these, UV-C radiation has the shortest wavelength and highest energy making it germicidal but on the other

hand it is completely absorbed by the ozone layer of the atmosphere. UV-B and UV-A can enter through the layer and all organisms and sensitive surfaces require protection from excess amounts of these radiation ranges.

While plants need solar radiation for photosynthesis, both chlorophyll and DNA are easily damaged by high intensities of direct sunlight (Glime, 2017). Consequently, plants have developed multiple defense mechanisms against excess radiation. For example, flavonoid and other polyphenolic compound accumulation, development of a thick cuticle and reflective wax production in conifers prevent or alleviate the harming physiological effects of the radiation (Kinnunen *et al.*, 2001). Out of these, polyphenols protect the plant from solar radiation and additionally scavenge UV-R generated ROS (Stevanato *et al.*, 2014). The protection capacity is linked to the absorption wavelengths of the polyphenols as well as antioxidant properties (Stevanato *et al.*, 2014). UV-R induced skin damage can be alleviated with antioxidants when they are present in relevant concentrations at the site of the damage and during the exposure causing oxidative stress (Poljsak *et al.*, 2013). The effect of UV damage can be monitored with a bacterial biosensor *E. coli* DPD2794, which has been shown to react to both direct and indirect DNA damaging agents including ROS producing oxidative species (Min *et al.*, 1999). Plants also protect chlorophylls and DNA through pigmentation, which acts as a filter that absorbs light (Glime, 2017). These usually red or dark pigments are caused by compounds such as anthocyanins, which are a form of flavonoids (Glime, 2017).

Sunscreen products can be divided into chemical or physical products according to the mode of action. Chemical sunscreens are usually synthetic aromatic compounds conjugated with a carbonyl group. They protect the skin from the damaging effect of UV radiation by absorbing high energy UV rays and releasing lower energy rays. However, UV absorption may activate the cosmetic sunscreens and they can consequently interact with the molecules of the skin, causing adverse reactions, such as dermatitis or photosensitivity reactions (Stevanato *et al.*, 2014). Chemical sunscreens have also been shown to cause adverse environmental impacts. For example, oxybenzone was found to be genotoxic towards coral planulae and, thus, the sale of sunscreen products containing it was recently banned in Hawaii (Downs *et al.*, 2016). The maximum amount of oxybenzone in sunscreen products is also restricted in Europe (the European Commission published Regulation (EU) 2017/238). Sunscreen components have also been demonstrated to induce coral bleaching by promoting viral infections in hard coral and their symbiotic algae (Danovaro *et al.*, 2008). The other mode of action, physical sunscreens, are used as topical physical barriers and can have a visible white appearance. This visible

whiteness of the skin can be minimized by reducing the particle size of the screening compounds, but there has also been discussion about nanoparticle accumulation in the environment (Kockler *et al.*, 2014; Lu *et al.*, 2018).

These factors indicate an urgent need for safer, broad-spectrum, UV protection compounds derived from natural sources for use in the dermatology, cosmetics and coating industries. Natural sources could offer environmentally safer and anti-inflammatory compounds with UV inhibitory and antioxidant activities.

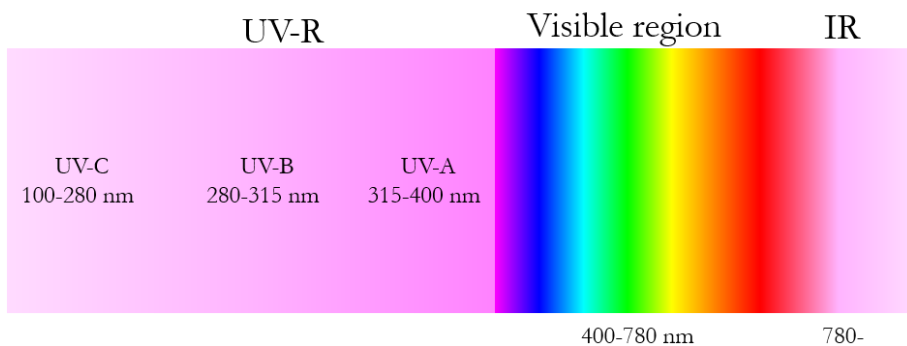


Figure 3. The light electromagnetic spectrum. With shorter wavelengths, the frequency and energy are higher. Thus, UV-C is particularly harming towards living beings.

2.5 Antibacterial agents and antibiotics

Antibiotics and antibacterial agents are sometimes referred to as synonyms used to describe agents that kill or inhibit bacteria. However, antibiotics are often considered more potent and can additionally be effective in killing or inhibiting fungi (microorganisms as a whole). Whereas antibacterial compounds kill, slowdown and inhibit the growth of bacteria alone. Generally, all antibiotics are antibacterial but not all antibacterial agents are antibiotic.

Natural products produced by bacteria and fungi have traditionally been the dominant source of clinically used antibiotics and antibacterials (Wright, 2014). The reason for this is that bacteria and fungi as well as their metabolites have evolved in such a way that they are able to enter the cells of other competitive microorganisms. Thus, they bear the desired bioavailability as well as bioactivity. Additionally, antibacterial compounds derived from microbial sources are likely to be able to modulate multiple virulence factors simultaneously. These virulence factors contain toxin and siderophore production, biofilm secretion and other such properties,

which are not essential to the cell growth but required to accomplish infection (Wright, 2014).

The modern era of antibiotics started when Sir Alexander Fleming discovered penicillin from mold in 1928 (Ventola, 2015). Since then the effectiveness of antibiotics has risen and fallen due to increased resistance in the bacteria. It has been suggested that inappropriate over-prescriptions of antibiotics as well as their extensive use in agriculture has been a major influence in the phenomenon (Ventola, 2015). However, even without considering the increased resistance, current antibiotics often have adverse effects and difficulties with dosing as well as restrictions of use for children, for example (Payne *et al.*, 2007). Consequently, there is a large need for new antibacterial and antibiotic substances that are effective, have minor environmental impacts and have low toxicity for surface coatings and medicines. For example, endophytic fungi have been found to produce metabolites that are able to kill or inhibit the action of a wide variety of microorganisms such as phytopathogens but also fungi and bacteria that are harmful to human beings (Strobel *et al.*, 2004).

3 RESEARCH OBJECTIVES

The main goal of this work was to screen for antioxidant and antibacterial bioactivities and UV protection potential from the forest-derived plant and fungus extracts. This was done by establishing biosensor methods using bacterial *E. coli* biosensors DPD2511 and DPD2794. We also used other methodologies, such as antioxidant tests and human cell models for a more diverse understanding of the activities. Additionally, the identification of the relevant metabolites found in bioactive extracts was carried out for endophytic fungi extracts. The identification process is needed in order to gain concrete benefits from the obtained bioactivities for potential future commercial applications. The specific objectives are summarized below:

- To study whether the stress-responsive luminescent *E. coli* biosensors are usable in the screening for bioactivities and UV protection potential in forest-derived extracts. (Papers **I**, **II** and **IV**)
- To assess whether it is possible to improve the antioxidant screening method published by Bartolome *et al.*, (2006) through enhanced HTS-potential. (Paper **I**)
- To investigate if *E. coli* biosensors can be used in the screening for UV protection. (Paper **II**)
- To characterize the metabolites or main metabolite groups responsible for potential bioactivities found in Scots pine root-associated endophytic fungi extracts. (Papers **III** and **IV**)

4 MATERIALS AND METHODS

For detailed information, see Papers **I-IV**. The different analyses and methods used are shown in **Table 1** and a general workflow chart of forest-derived extract screening is presented in **Figure 4**.

Table 1. Summary of the analyzed properties and methods used to investigate them. In addition, the forest-derived biomass tested with the methodology is shown.

Analysis	Method used	Forest-derived biomass	Paper
Antioxidant activity	<i>E. coli</i> DPD2511; H ₂ O ₂ inhibition (Chapter 4.5 and 4.6.1)	Spruce inner bark; Endophytic fungi	I, IV
	SCAV (Chapter 4.7.1)	Endophytic fungi	IV
	ORAC (Chapter 4.7.2)	Endophytic fungi	IV
	Cell model tests (Chapter 4.7.3)	Endophytic fungi	IV
UV protection	<i>E. coli</i> DPD2794; biological or physical protection (Chapter 4.5 and 4.6.2)	Pine needles	II
	Absorbance screening (Chapter 4.6.2.1)	Pine needles	II
Antibacterial activity	<i>E. coli</i> DPD2511; oxidative stress (Chapter 4.5 and 4.6.3)	Endophytic fungi	IV
	<i>E. coli</i> DPD2794; genotoxic effects (Chapter 4.5 and 4.6.3)	Endophytic fungi	IV
Metabolite identification	LC-MS; Data bases, literature (Chapter 4.4)	Endophytic fungi	III, IV

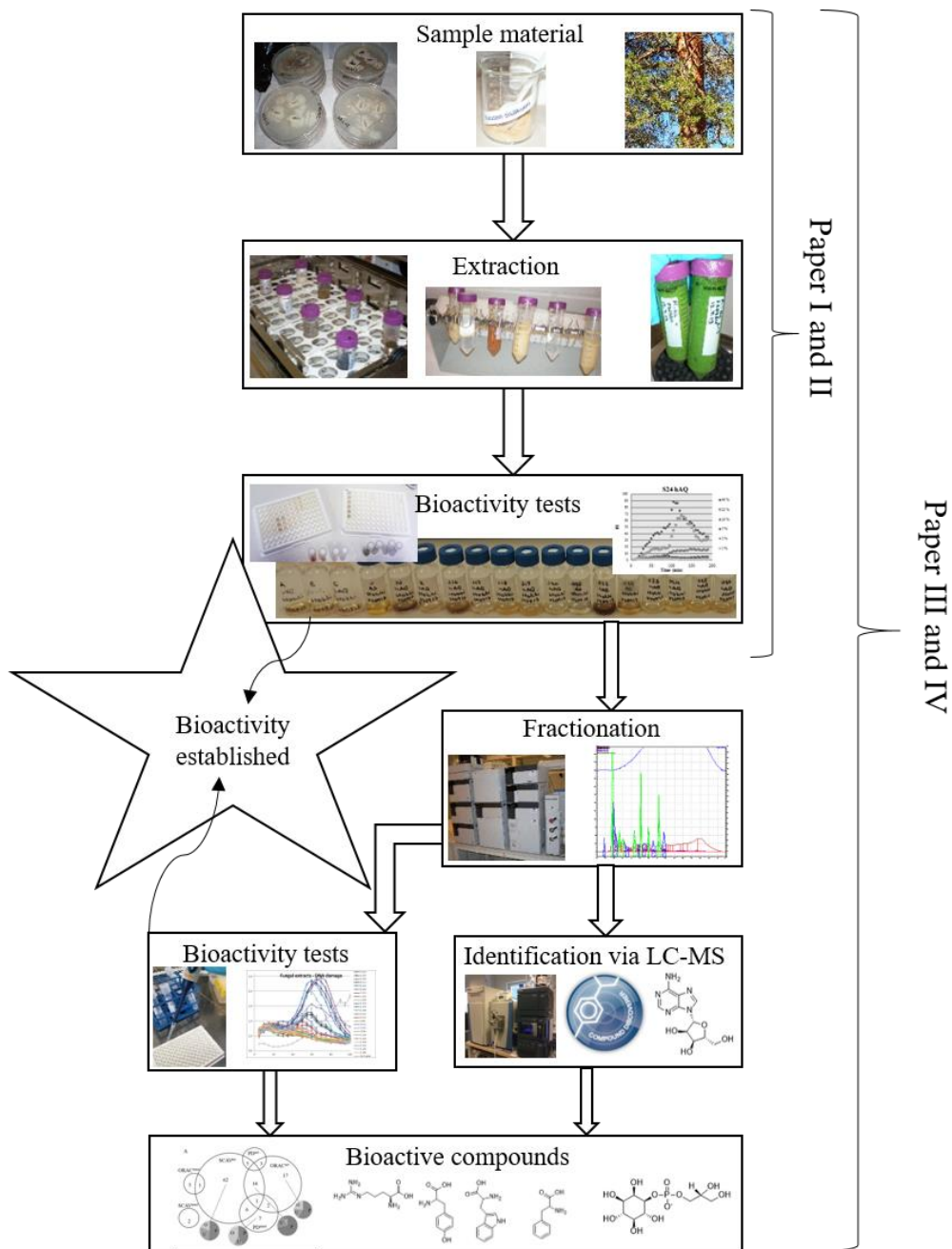


Figure 4. The workflow of this study. Bioactivity is either UV protection potential or antioxidant or antibacterial activity.

4.1 Sample pre-handling

The forest-derived sample material used in this study were the inner bark of Norway spruce (*Picea abies* (L.) Karst.) (Latva-Mäenpää *et al.*, 2013; Paper **I**), Scots pine (*Pinus sylvestris* L.) needles (Paper **II**) and endophytic fungi species isolated from the roots of 8-year-old Scots pine seedlings (Papers **III** and **IV**). The fungal species were identified using molecular methods and will be stored in the microbe and yeast library collection of Natural Resources Institute Finland. The species used in this study are *Acephala applanata* (A) and *Philocephala fortinii* (R) as well as *Humicolopsis cephalosporioides/Coniochaeta mutabilis* (S16). The identification of PAC species using the ITS region is challenging (Grünig *et al.*, 2008) and S16 identification has some uncertainty with two equally possible matches. The pure cultures of the fungus mycelium were cultivated on a solid Hagem agar above a cellophane membrane on Petri dishes (**Figure 5**).



Figure 5. The pure cultures of endophytic fungi growing on a cellophane membrane on Petri dishes.

4.2 Extraction

Endophytic fungal mycelium and spruce inner bark were extracted with hot water (**Table 2**). Water extraction is generally considered a green extraction methodology which is both environmentally friendly and safe to handle, as water is nonpoisonous and nonflammable (Chemat *et al.*, 2019). Water has been used in the extraction of food and natural products for centuries despite that it is known to be a poor solvent

for nonpolar and in some cases semi-polar compounds (Chemat *et al.*, 2019). Other advantages of using water are that it leaves no harmful residues to the extraction material and therefore the need for harsh solvent removal techniques possibly causing chemical transformations in the extract is removed (Ollanketo *et al.*, 2002). We used elevated temperature to improve the efficiency of extraction process. Higher temperatures have shown to decrease the polarity by disintegrating the hydrogen bond network (Chemat *et al.*, 2019). One disadvantage is the possible effects on heat-sensitive compounds. Ethanol and methanol are examples of alternatives that could have been used for extractions. In a study comparing the compounds extracted from sage (*Salvia officinalis*) with water (hydrodistillation), ethanol and methanol, it was concluded that because water is the most polar solvent, it extracted the most polar compounds (Ollanketo *et al.*, 2002). Methanol is the least polar out of these and it extracted the least polar compounds as expected, whereas ethanol (70%) extracted the polar compounds and some of the less polar ones (Ollanketo *et al.*, 2002). However, the highest antioxidant activity was measured with samples extracted with ethanol (Ollanketo *et al.*, 2002). One interesting perspective for future investigations could also be the use of water–organic solvent mixtures and pressurization. For example, Co *et al.* (2012) found that pressurized fluid extraction with ethanol and water gave higher antioxidant capacity from spruce bark (*Picea abies*) samples than obtained with water or ethanol separately. The solvent choice should always be pondered through the extracted material, target molecules and the intended future application area.

Table 2. The used extraction methods.

Extraction	Biomass	Paper
Hot-water extraction	Spruce inner bark	I (supplementary)
	Endophytic fungi	III, IV
Methanol extraction (100%)	Pine needles	II

Fresh frozen pine needles were ground with the help of liquid nitrogen and extracted with 100% methanol (**Table 2**). Here, pure methanol extraction was preferred over water extraction because it results in high polyphenol contents and primary metabolites such as amino acids and sugars are not present to the same extent in methanol extracts. The dried extraction products were dissolved in methanol and water so that the highest methanol concentrations for the tested extracts were 1.4% (an absorbance-based protection) and 0.9% (a bioactivity-based protection).

4.3 Fractionation of the fungal extracts

Fractionation is a process in which a sample mixture is divided into smaller quantities (fractions) according to their physical or chemical characteristics. Fractionation was performed with a semi-preparative Shimadzu Prominence high-performance liquid chromatography system using polarity to separate the fractions with a Waters XBridge reverse phase C18 column. The purpose was to focus on the bioactive fractions and identify their potentially bioactive metabolites.

4.4 LC-MS and identification

In Papers **III** and **IV** samples were analyzed using an ultra-high-performance liquid chromatograph coupled to a photodiode array detector and a hybrid quadrupole-Orbitrap mass spectrometer. Masses were scanned at the mass to charge ratio (m/z) 150-2000 and abundances over 1×10^7 were considered. The data was analyzed using Thermo Xcalibur Qual Browser software and processed using Compound Discoverer 2.1 SP1. The processing flow 'Untargeted Metabolomics Workflow' was applied with maximum element counts of $100 \times C$, $200 \times H$, $100 \times O$, $10 \times N$ ($10 \times S$, $10 \times P$). ChemSpider and KEGG databases were chosen for the identification. In addition, the SciFinder Scholar database was used with the Occurrence substance role and the highest number of references to scale down possible compound hits.

4.5 Bacterial strains and cultivation

Two genetically modified *E. coli* bacterial strains were used: *E. coli* DPD2511 (Belkin *et al.*, 1996a) and *E. coli* DPD2794 (Vollmer *et al.*, 1997). They are both stress-responsive strains, for which exposure to stimuli generates a measurable increase in luminescent light production, which can be monitored optically. An example of the luminescence signal is shown in **Figure 6** with a *Trifolium* sp. leaf over Lysogeny agar (LA) with a bacterial culture of *E. coli* DPD2794. **Figure 6a** shows the luminescence produced using a Xenogen IVIS imaging device after 16 hours of incubation at 30°C. The scale on the right shows the intensity of luminescence production with red meaning the highest and purple meaning the lowest stress-induced signal. **Figure 6b** shows a normal photograph of the same plate.

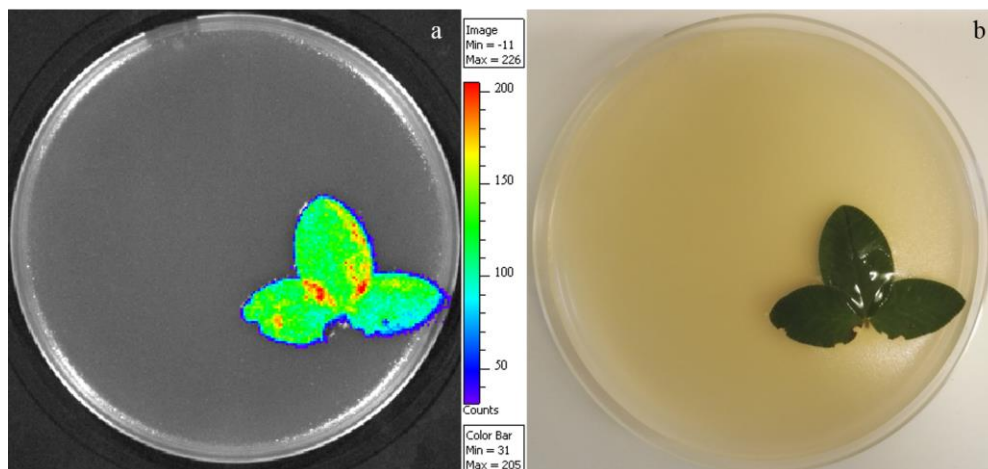


Figure 6. *Trifolium* sp. leaf on the same Petri dish as *E. coli* DPD2794 bacteria. The luminescence light production is shown after 16 hours of incubation using a Xenogen IVIS imaging device.

Both strains were used for two different biosensor methodologies, which are summarized in **Table 3**. LA growth plates supplemented with ampicillin and a potassium phosphate buffer were used. For antioxidant and antibacterial bioactivity testing, a single colony of the strain was inoculated into a liquid Lysogeny Broth (LB) medium supplemented with ampicillin and a potassium phosphate buffer. For UV protection testing, a single colony of the strain was inoculated into a liquid glucose-enriched M9 minimal medium supplemented with ampicillin. The growth medium was changed because LB was found to absorb UV radiation and interfered with the measurements. The inoculations were then incubated for approximately 16 h (overnight) in a shaker at 30°C at 300 rpm, after which the luminescence was measured with a microplate reader. The cell culture producing the highest signal was chosen for the measurements. The optical density at 600 nm was measured to be approximately 0.1 for the bacterial suspensions corresponding to 1×10^8 colony forming units/mL.

Table 3. Bacterial strains and the biosensor methodologies used.

Bacterial strain	Method	Paper
<i>E. coli</i> DPD2511	H ₂ O ₂ inhibition (antioxidant)	I, IV
	Oxidative stress (antibacterial)	(I), IV
<i>E. coli</i> DPD2794	Genotoxicity (antibacterial)	IV
	UV protection: biological and physical shield	II

4.6 Biosensor measurements

All the luminescence measurements were conducted using a Chameleon multilabel reader. The luminescence was measured in counts per second (CPS) 20 times every 5 min, and between the screens the plate was kept at 30°C and shaken. The results are expressed in induction factors (IF) calculated by dividing the CPS values of the samples by the value of the negative control (water). The abbreviation IF is used in this thesis, but both FI (fold induction) and IF (induction factor) abbreviations can be used to describe the induction compared with water blank. Coefficient of variation (CV%) was calculated for the three replicates and expressed as the error bars in the figures.

4.6.1 Antioxidant screening using *E. coli* DPD2511

Hydrogen peroxide (H₂O₂) was chosen as the oxidant for the antioxidant measurements (Paper I). It is a well-known producer of harmful hydroxyl radicals and has been reported to work well with this biosensor (Belkin *et al.*, 1996a; Belkin *et al.*, 1996b; Min & Gu, 2004). The optimum concentration was determined in Paper I by comparing the induced signal of concentrations from 0.25 mM to 4 mM and the concentration of 4 mM H₂O₂ was found to be optimal. The IF values of the samples were compared to those for H₂O₂ and lower values at the same time point were considered an indication of activity. Ascorbic acid (C-vitamin) was chosen for the reference antioxidant. The antioxidant effect is dose-dependent and 5-10 mg/mL of ascorbic acid provides approximately the same inhibition-% above 70. The constant concentration of H₂O₂ (oxidant) was added into each well with ascorbic acid (positive control, antioxidant) in a potassium phosphate buffer. Finally, the chosen cell culture was added to each well of an opaque white microplate. Sterile water in a phosphate buffer was used as the negative control.

4.6.2 UV protection screening using *E. coli* DPD2794

The bacterial strain *E. coli* DPD2794 has been found to be sensitive towards ultraviolet radiation and to give a dose-dependent luminescent signal in response to it in previous studies (Belkin *et al.*, 1996b; Vollmer *et al.*, 1997). However, a novel methodology to screen the UV protection potential of reference substances and forest-derived samples using this biosensor is described in Paper II. There are two

possible modes of use: (i) for biological protection, in which the sample substance is placed in direct contact with the biosensor cells and (ii) for physical protection, in which the sample substance is placed on a separate microplate. The biological protection method also provides simultaneous information about the sample substance cytotoxicity.

The validation of the method was conducted using several reference compounds as positive controls. Water and appropriate solvents were used as negative controls. TiO₂ (<5 µm particle size and predominantly rutile) was chosen to act as a known UV shield control because it is extensively used in sunscreen products worldwide. An LB growth medium was used as the positive control when in direct contact with the cells because it absorbs UV wavelengths. To verify the effectiveness of the UV-R dose used, the induced signals of UV-R were compared to signals induced using a known antibiotic ciprofloxacin, which specifically targets bacterial DNA. It is also widely known that antioxidants can prevent damage induced by UV-R by targeting the induced production of ROS in the cell. Therefore, the known antioxidants L-ascorbic acid and astaxanthin were used to test this protection mechanism. Additionally, because oxybenzone was found to be harmful for coral planulae and its effect further to be increased by the exposure to UV light (Downs *et al.*, 2016), it was tested as well. Oxybenzone has adverse effects towards coral and fish (Downs *et al.*, 2016; Danovaro *et al.*, 2008; Dinardo & Downs, 2017). Oxybenzone has also been shown to cause contact or photo contact allergies or even urticarial reactions in humans (Dinardo & Downs, 2017).

4.6.2.1 Absorbance measurements

Absorbance screening measurements were used as a complementary method (Paper **II**). The absorbance of 100 µL sample substance triplicates in translucent microplates was evaluated. Thermo Scientific Varioskan Flash Reader in its absorbance scan mode at 5 nm intervals for the wavelength area of 200-900 nm was used. Absorbance value averages were calculated and error bars show the standard deviations of the sample triplicates (Paper **II**). The extraction liquids methanol and water were used as negative controls.

4.6.3 Antibacterial screening with biosensors

Antibacterial screening with biosensors was conducted using *E. coli* DPD2511 to screen for oxidative stress and *E. coli* DPD2794 for DNA damage. For the oxidative stress assay (Paper **I** and **IV**), the chosen cell culture was added to each well of an opaque white microplate containing the dilutions of the H₂O₂ (positive control) or sample or sterile water (negative control). Instead, ciprofloxacin was used as a positive control for the bacterial DNA damaging agent measurements. The luminescence was measured as described before.

4.7 Other bioactivity measurements

Other bioactivity measurements were used as a complement and comparison to the biosensor methodologies in Paper **IV**. These included two microplate methodologies for antioxidant screening (hydrogen peroxide scavenging (SCAV) and oxygen radical absorbance capacity (ORAC)) and two human cell line tests (PD= Parkinson's disease and AMD= age-related macular degeneration).

4.7.1 Hydrogen peroxide scavenging, SCAV

The SCAV method sets out to measure the H₂O₂ scavenging capacity of a sample substance before it oxidizes an iron complex (**Figure 7**). It provides colorimetric results, which can be measured through the absorbance of the solution. A SCAV test was performed using the FOX reagent method by Hazra *et al.*, (2008) and Jiang *et al.*, (1990) with minor modifications in Paper **IV**. The sample absorbance values are compared with the control figure drawn with the sodium pyruvate (positive control) and the results are expressed as %-inhibition.

4.7.2 Oxygen radical absorbance capacity, ORAC

The oxygen radical absorbance capacity (ORAC) assay measures the oxidative dissociation of fluorescein in the presence of peroxy radicals (ROO•), which causes a reduction in the fluorescence signal. The antioxidant's protective ability is based on the inhibition of the breakdown of fluorescein caused by the peroxy radicals (**Figure 7**). The assay was modified from the method described by Huang *et al.*,

(2002) and Prior *et al.*, (2003) and carried out in a 96-well format with two technical replicates of each sample on a plate (Paper IV). The results are expressed as Trolox (positive control) equivalents ($\mu\text{mol TE/L}$).

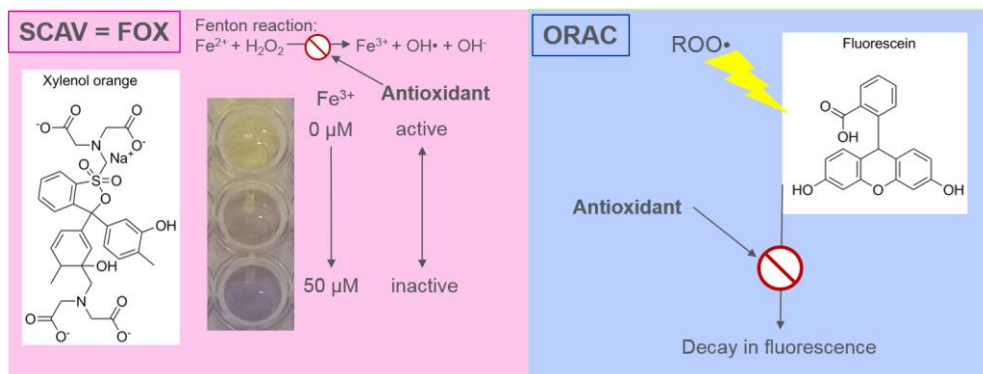


Figure 7. Schematic model of function for the hydrogen peroxide scavenging (SCAV also the ferrous oxidation in xylenol orange (FOX) reagent method) and oxygen radical absorbance capacity (ORAC) tests

4.7.3 Oxidative stress related diseases

Among reactive oxygen species (ROS) related diseases, age-related macular degeneration (AMD) is a major cause of vision impairment in elderly people worldwide. It is characterized by a progressive loss of vision due to the degenerative and neovascular changes in the central region of the retina, the macula (Kaarniranta *et al.*, 2005). Chronic oxidative stress and inflammation are strongly linked to AMD pathogenesis. In the oxidative stress reaction, the ROS primarily attack the retinal pigment epithelium (RPE) and can eventually damage the photoreceptors of the RPE layer leading to a permanent loss of vision (Klimanskaya *et al.*, 2004). Additionally, oxidative stress and aging play a major role in the neuron degeneration in the Parkinson's disease (PD) leading to mitochondrial dysfunction and even cell death (Dias *et al.*, 2013). Given the severity and socio-economic impact of these widely spread diseases, there is an enormous need for the development of new therapeutics for oxidative stress related diseases. These human cell line test protocols are described in Paper IV.

4.8 Statistical methods

In paper **II**, the statistical significance of the results was measured using a two-tailed t-test using Microsoft Office Excel 2016. The principal component analysis (PCA) and clustering analysis in Paper **IV** were performed with the SAS Enterprise Guide 7.4. (SAS).

5 RESULTS AND DISCUSSION

The focus of this study is on screening antioxidant and antibacterial bioactivities and examining the UV protection potential of forest-derived extracts. This was done using bacterial *E. coli* biosensors DPD2511 and DPD2794. Additionally, the relevant metabolites found in bioactive endophytic fungal extracts were identified using LC-MS. This section focuses on the results of forest-derived extract and fraction screening and metabolite identification. Detailed results can be found in Papers **I-IV**.

5.1 Bacterial biosensor results

Two stress-responsive bacterial biosensors were used to investigate their suitability for screening antioxidant, antibacterial and UV protective activities from forest-derived extracts and fractions.

5.1.1 Antioxidant and antibacterial activity, *E. coli* DPD2511

E. coli DPD2511 sensor was used for detecting two bioactivity types: oxidative stress towards bacteria (antibacterial activity) and the H₂O₂ inhibition potential (antioxidant activity) (**Table 3**). From these, the antioxidant activity methodology was developed in Paper **I**, whereas the oxidative stress methodology has been reported in the literature (Belkin *et al.*, 1996a; Belkin *et al.*, 1996b).

In order to test the suitability of the methodology for forest-derived materials, spruce inner bark (Paper **I**) and endophytic fungal extracts and fractions (Paper **IV**) were used. **Figure 8a** shows the dose-dependent antioxidant effect obtained from spruce inner bark extract.

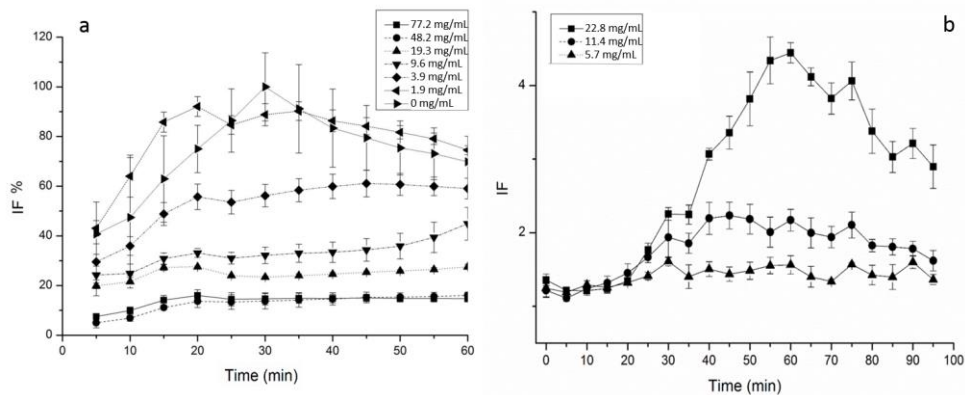


Figure 8. (a) Example data obtained from Norway spruce (*Picea abies* [L.] Karst) inner bark extract. Dilutions are dry weights of the extract in water. H₂O₂ (shown in the figure as 0 mg/mL) was used as the negative control. The error bars are the CV% of the sample triplicates in the microplate. (b) shows the resulting diagram when induction factors of the fungus R fraction 2 dilutions are drawn against time when measured with the *E. coli* DPD2511 biosensor responding to oxidative stress. The error bars are the CV% of the sample triplicates in the microplate. H₂O₂ was used as the negative control. IF = induction factor compared with water blank.

Repeatable and reliable results were obtained from the assay in a microplate format. Thus, it can be concluded that it was possible to improve the antioxidant methodology published by Bartolome *et al.*, (2006) via enhanced HTS potential. H₂O₂ was used as the negative and ascorbic acid as the positive controls.

For the antibacterial activity measurements (Paper IV), the same sensor was used for screening the oxidative stress production of endophytic fungi fractions with H₂O₂ as a positive control and water as a negative control. An example is shown in **Figure 8b**. It was found that even though the fractionated samples have extremely low concentrations, the sensor was sensitive enough to detect antibacterial oxidative effects. However, the signal magnitudes were reduced as well.

5.1.2 UV protective and antibacterial activity, *E. coli* DPD2794

E. coli DPD2794 sensor was used for detecting two bioactivity types: distress or SOS-reaction dependent genotoxicity to the bacteria (antibacterial activity) and UV protection potential (**Table 3**). Out of these, the UV protection methodology was developed in Paper II, whereas the genotoxicity methodology has been reported in the literature (Belkin *et al.*, 1996b; Vollmer *et al.*, 1997).

One potential source of safe and sustainable UV protective compounds are nature-derived substances. The UV protection test methodology developed in Paper II was tested using a *Pinus sylvestris* L. needle methanol extract (Pi_{Ne}) and the results are shown in Paper II, Figure 5. Pine needles are exposed to the UV-R from the sun and therefore, they are expected to possess UV protective activity as also demonstrated with this technique. The Pi_{Ne} at a concentration of 5.0 mg/mL protects the biosensor cells from the adverse effects of the UV-R, as its IF in 100 min measurement is lower than that of the unprotected sample (Figure 5a and b (Paper II)). In addition, this protective capacity is almost equal to that of TiO₂ concentration of 0.80 mg/mL, which was used as a positive control. Methanol extractable polyphenols are known for their antioxidant activities, which can correspond to the biological shielding potential shown in Figure 5c, Paper II. The highest content of Pi_{Ne} (3.3 mg/mL) exhibits biological UV-R protective properties for the biosensor cells. This is demonstrated in the 100 min measurement results, where the IF for the Pi_{Ne} is lower than that for the unprotected cells. However, the IF of the Pi_{Ne} is higher than that of the positive LB control, which indicates that it is not as effective in the protection as the LB control. Forest-derived substances are potentially less harmful to the environment. In addition, they pose no similar risk of accumulation as mineral-based physical sunscreen nanoparticles because they are degradable and as in this case of pine needles, sustainably derived from a waste-stream of forestry. Although the biological shielding in this technique was not as high as with LB control substance, the methanol extracts are likely to be rich in polyphenols and flavonoids, which have been widely reported to have antioxidant properties (Sowndhararajan & Kang, 2012).

For antibacterial activity measurements (Paper IV), the same sensor was used for screening genotoxicity or DNA damage caused to the biosensor cells by endophytic fungal fractions with ciprofloxacin as a positive control and water as negative control (for results, see **Chapter 5.2.1**).

5.1.3 Color effect of berry extracts

Bacterial stress-responsive biosensors were also used to investigate berry water-extracts (**unpublished data**) with the same procedures which were discussed in **Chapter 4.5**. The berry extracts used were bilberry, lingonberry, blackcurrant, cranberry and cloudberry extracts (**Figure 9a**).

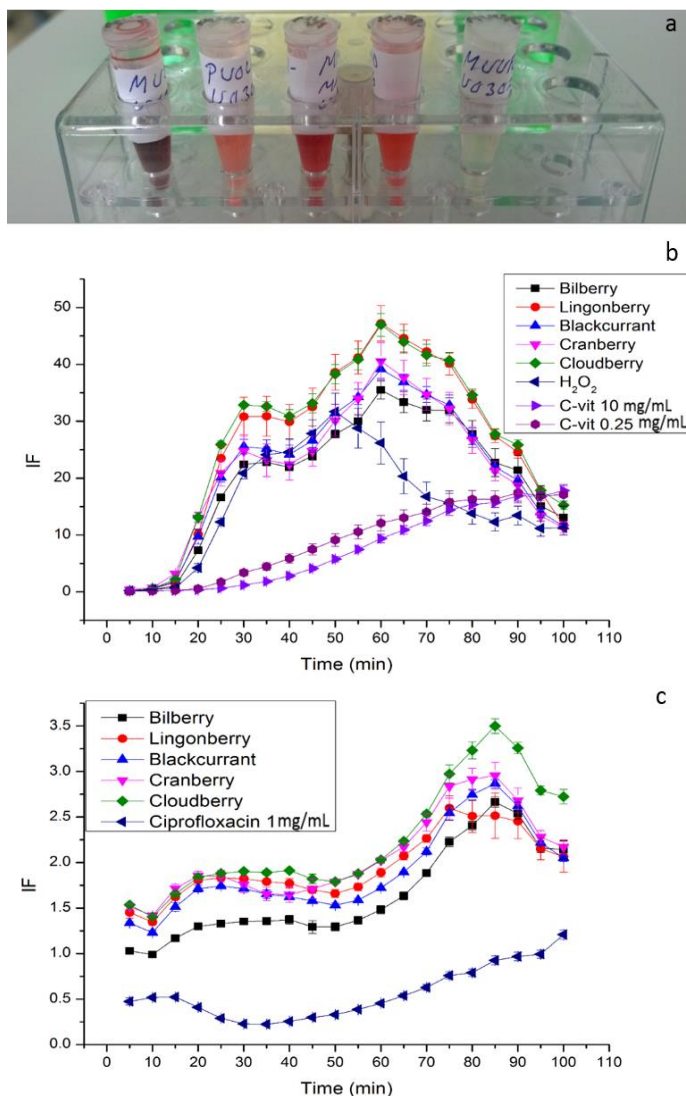


Figure 9. (a) The original berry extract content of 0.1 g/mL is strongly colored in majority of the extracts. Thus, the extracts are diluted to obtain 1:10, 1:20 and 1:40 (v/v) of the original solution. From left to right: bilberry, lingonberry, black currant, cranberry and cloudberry extracts. (b) The antioxidant test results with 1:10 dilution are shown. Extract is considered an antioxidant if it produces lower IF signals than H₂O₂ (negative) control in a given measurement time point. C-vitamin was used as positive control. For example, with bilberry, blackcurrant and cranberry all of the used dilutions of berry extracts the H₂O₂ oxidative effect seems to be inhibited at time point 50 minutes. (c) Cloudberry extract 1:10 dilution seems to induce highest luminescence signals with bacterial DNA damage responsive biosensor. Ciprofloxacin (positive control) content of 1 mg/mL is highly toxic to the cells. The error bars are the CV% of the sample triplicates in the microplate.

Because some of the extracts are strongly colored and therefore likely to interfere with the luminescence emission, the original stock content of 0.1 g/L was diluted 1:10, 1:20 and 1:40 (v/v) fold for each extract. However, the dilutions were not sufficient to remove the effect of the color completely. The berry extracts indicated low oxidative stress, with maximum IF values between 1.6 and 2.0 (data not shown). Antioxidant results showed that the highest effects, meaning that even the smallest content used (2.5 mg/mL) gave IF values below that of the H₂O₂ control, were obtained with the bilberry, blackcurrant and cranberry extracts (**Figure 9b**). However, these are also the most strongly colored extracts (see **Figure 9a**), which is important to consider when analyzing the results. The highest DNA damage test IF values were obtained using a cloudberry extract (**Figure 9c**). The color may affect the results and suppress the obtained signals of strongly colored extracts. Preferably, the absorbance of the extracts should be measured as suggested by Bartolome *et al.*, (2006). Another solution is suggested by Lappalainen *et al.*, (2001), where automatic color correction is achieved by using each sample as a reference for itself.

The bilberry, blackcurrant and cranberry extracts are rich in plant flavonoids. Bilberry and blackcurrant extracts are rich in anthocyanins, whereas cranberries are known to contain quercetin derivatives (Häkkinen *et al.*, 1999). Quercetin derivatives and anthocyanins are known antioxidants (Zhang *et al.*, 2011a; Martín *et al.*, 2017). Cloudberry contains many ellagitannin compounds, which are polymeric esters of glucose with ellagic acid (Puupponen-Pimiä *et al.*, 2016). Ellagitannins have been shown to act as antioxidants and to cause antimicrobial effects (Yoshida *et al.*, 2010; Puupponen-Pimiä *et al.*, 2016).

5.1.4 Bacterial biosensor discussion

The results obtained show that bacterial biosensor methodologies are usable in screening the bioactivities from forest-derived extracts, as expected. Similar results were obtained by Kim *et al.*, (2019). They concluded that the use of stress-responsive biosensor methodologies could be utilized for nature-derived drug screening and this could particularly be of use in the prescreening for drug discovery. They proposed that the prescreening response of a bacterial strain could be used to indicate cytotoxicity, which would reduce the need for resources compared to costly and rather laborious human cell line screening. Previously, Kim *et al.*, (2000) used the stress-responsive strain panel to screen for endocrine disturbing chemicals and even though the sensors are not designed to be responsive to these agents, they could be

used to study the cellular mechanisms of their toxicity. In addition, Hartono *et al.*, (2014) showed that toxicity of the endocrine disruptor bisphenol A could be detected from wastewater even if adsorbed into carbon nanotube beads, which emphasizes the sensitivity of the methodologies.

Belkin *et al.*, (1996a) constructed the *E. coli* DPD2511 strain and they proposed that it could be used to monitor cellular mechanisms in response to oxidative stress *in vivo* and in real-time. This methodology could be used in assaying the oxidant and antioxidant properties of food additives and other chemicals of interest as well as screening for environmental hazards of different media. They validated the sensor using organic peroxides, redox cycling agents, alcohols, cigarette smoke and hydrogen peroxide. *E. coli* DPD2794 has been shown to be effective in detecting various types of DNA damaging agents. These include direct DNA damaging agents such as mitomycin C, which inhibits DNA synthesis, and UV irradiation, which destroys nucleic acids by removing oxygen-containing groups, and indirect DNA damaging agents such as oxidants (Min *et al.*, 1999; Belkin *et al.*, 1996b; Vollmer *et al.*, 1997). Quite recently, the same biosensor was also used in a biosensor panel to model the harmful effects of artificial sweeteners on the gut microbiota by Harpaz *et al.*, (2018). They found that two toxicity response patterns could be detected with high enough concentrations. These were the induction or inhibition of the luminescent signal. Inhibition was only detected with exposure to sucralose but the *E. coli* DPD2794 responded to acesulfame K with an induced luminescence signal, which supports the earlier reports of the genotoxicity of this most used artificial sweetener. The similar luminescence signal quenching effect with higher concentrations of toxins was earlier discussed by Ismailov & Aleskerova, (2015) in their review paper. They offer an explanation that the screened stress-response induced effect is overlapped by the cytotoxicity of the sample and, thus, the magnitude of the signal is suppressed.

It was observed in Paper I that an increase in the sample concentration increases the lag time before the response peak maximum is reached. Therefore, with higher concentrations the required measurement time is also increased. According to Gu & Choi, (2001) the phenomenon may be linked to growth rate retardation.

Stress-responsive recombinant biosensors can be used for sensitive and selective toxicity screening of various sample types from different sources. For example, they have been used to screen toxic agents from industrial wastewater and river water to act as early-warning indicators of environmental pollution (Belkin *et al.*, 1996b; Vollmer *et al.*, 1997; Gu & Choi, 2001). Additionally, other environmental pollutants,

such as nanoparticles and pesticides have been investigated using these sensors (Pham *et al.*, 2004; Li *et al.*, 2013).

The obtained results are likely to be of interest in the fields of natural product utilization, such as dermatology, cosmetics and fortified or functional foods, for example. However, in order to gain the full potential from the antioxidant methodology in HTS format, it should be transferred into 384-, 1536-, 3456- or 9600-well format with automatic liquid handling. The biosensor *E. coli* DPD2511 seems to suffer from occasional instability in the luminescence production. In fact, whole-cell biosensors can become unstable over time due to the cell leakage or diffusion (Gui *et al.*, 2017). Thus, they could require reconstruction or improvement using synthetic biology after a period of use. Additionally, Min & Gu, (2004) found that the damage caused by H₂O₂ is very promptly repaired in *E. coli* bacteria, which can suggest the potential adaptability of the strain. Thus, other compounds or higher concentrations of the oxidant could be experimented with to see if the problem is due to cell mutation or resistance towards a certain oxidative agent. Additionally, it could be examined if addition of small volumes of ethanol with H₂O₂, could be used to increase the light production (Belkin *et al.*, 1996a). With the *E. coli* DPD2794 strain, the inhibition and induction effects should both be considered as shown by Harpaz *et al.*, (2018), thus, further emphasizing the need for both positive and negative control sample usage in the measurement.

The instability of the biosensors could result in the signals not being directly comparable between the measurements. The same effect was discovered by Watt *et al.*, (2007) with the *E. coli* DPD2794 strain. They propose that the block effect of each plate could be reduced by changing the experimental set-up in a way that one microplate would have one replicate of a sample and a number of microplates would be measured and then compared. One additional limitation is that a dark, reddish coloring of the samples, such as with berry extracts (**Chapter 5.1.3**), could reduce the luminescent signal results and the extracts and samples should therefore be diluted. This is caused by the fact that luminescence is produced within the wavelength of 493 nm, which corresponds to the visible region of the electromagnetic spectrum. The same effect was identified by Bartolome *et al.*, (2006) and they proposed that sample absorbance should be investigated to minimize the opportunity for its interference with the signals. Lappalainen *et al.*, (2001) suggest an alternative methodology, where color correction is achieved by using each sample as a reference for itself. Although these sensors have high sensitivity and selectivity, complex sample matrices could also mask the signal coming from the analyte or metabolite of interest (Gui *et al.*, 2017).

In Paper **II**, two methodologies were established for UV protection screening using *E. coli* DPD2794 bacterial biosensor. These methodologies could be utilized for example in the fields of dermatology and cosmetics. With the polymerase chain reaction cabinet (PCR) as the UV irradiation source (Paper **II**), the UV radiation was 254 nm, which corresponds to the UV-C region of UV light. It is completely shielded out of sunlight by the atmosphere. However, it was concluded that this methodology is easily transferrable from the PCR-cabinet to any standard UV-R emitting setting. Nevertheless, it should be tested and optimized for other settings separately. This is because the sensitivity of the bacterial strain could also be affected when changing radiation wavelengths. The *E. coli* DPD2794 strain is constructed so that it is sensitive to genotoxicity, and UV radiation damages the DNA of living beings by removing oxygen groups. The shorter the wavelength of the radiation, the higher frequency and energy it carries. While the *E. coli* biosensors have been found to be extremely sensitive, it is likely that by using longer wavelengths (UV-B and UV-A region) the irradiation time needs to be increased. However, as the irradiation time in Paper **II** was the most suitable at 30 seconds, the total measurement time is not likely to exceed critical limits for usability. The biological shield methodology is more sensitive to the solvent used and bacterial cells should always be tested with the used solvent concentration as a control. It is also important to notice that special and rather expensive UV-transparent microplates have to be used in the physical shield method because most of the radiation is otherwise blocked by the microplate itself. The irradiation source also needs to be placed directly above the microplates, to ensure the even distribution of the radiation in the microplate wells.

In many of the referred articles, the biosensors have been used together as a panel of multiple biosensors. The advantages of this technique include that toxicity towards bacteria can be detected and the induction of a certain strain or multiple strains can provide information about the type of damage caused (Gu & Choi, 2001). When using the same species, such as two *E. coli* strains here, the effect of the input cell concentration is not relevant, but if several bacterial or microbial species are used this needs to be acknowledged (Wolfe, 2018). Furthermore, the competition over the nutritional sources and possible inhibition effects, which could lead to the suppression of the signal produced, need to be considered when using a mixture of microbial species together.

Table 4. Summary of advantages and disadvantages of stress-responsive bacterial biosensors in forest-derived sample screening.

Advantages
<ul style="list-style-type: none"> • Sensitivity – can be used for small concentration samples • Selectivity but also multiple possible fields of use • Easy and cost-effective measurements • Rapid real-time response • Simultaneous information about the bioavailability and bioactivity of the sample. • Usable as panels of biosensors to obtain information about multiple stressors and the mechanisms of action simultaneously. • Can be used to obtain information about the cytotoxicity as well as antibacterial effects depending on the use.
Disadvantages
<ul style="list-style-type: none"> • Complex samples can cause matrix effect and cause signal ambiguity. • High concentration of toxins can interfere with the signal induction via quenching effect or inhibition as well as increase the required measurement time. • Strong colored sample can interfere with the luminescent signal. • Comparability between measurements should be ensured with statistically significant amount of repetitions. • Inhibition and induction effects should both be considered – verification with positive and negative controls is important. • Possible instability caused over time by cell leaking or diffusion of the whole-cell biosensor.

In conclusion, it is proposed that these bacterial stress-responsive sensors are the most usable in activity/inactivity screening with small concentration of forest-derived extracts, or preferably fractionated samples to reduce the possible sample matrix effect and induction delay phenomenon. Additionally, the comparison between sample activities should only be done within the same measurement samples or after a statistically significant number of measurement replications. While bacterial biosensors are concluded usable in the context of forest-derived extracts, it is important to regard that they only depict a part of the bioactivity spectrum and some important activities can only be detected using mammalian or human cell lines. Therefore, the biosensor methodologies should be considered merely indicative of the interesting features that should be further verified with cell lines prior to use in

various applications. Additionally, biosensors produce a change in the luminescence production as a response to a stimulus, and the results are always interpretations of the cause of reaction. This causes a completely different degree of certainty of the results when compared with standard analytical techniques, such as liquid chromatography with tandem mass spectrometry (LC-MS/MS), which can be used to verify metabolite identities. The advantages and disadvantages of the used stress-responsive bacterial biosensors are summarized in **Table 4**.

5.2 Bioactive metabolites of endophytic fungi

In order to describe the bioactive metabolites, the information gained from the bioactivity tests and LC-MS identification results for the active fractions were combined. These two results will be first presented separately and then combined using statistical methods. Finally, the results will be discussed and summarized.

5.2.1 Bioactivities of endophytic fungi extracts and fractions

Seven different bioactivity tests were conducted for endophytic fungi extracts and five of these tests additionally for their fractions. All the bioactivity test results are summarized in **Table 5**. Biosensor tests were introduced in **Chapters 4.5, 4.6** and **5.1** and other bioactivity measurements in **Chapter 4.7**. The cultivation codes of the fungi are used in the table and the fungal species were identified using the closest GenBank matches of the ITS-regions which were A= *Acephala applanata*, R= *Phialocephala fortinii* and S16= *Humicolopsis cephalosporioides*/*Coniochaeta mutabilis* (see Paper **III**). First two are common dark septate endophytic (DSE) species found in boreal forest tree roots. The S16 identification is slightly uncertain and two possible matches are equal: *H. cephalosporioides* has been classified as a DSE-like fungi and *C. mutabilis* has been found in plants but also to act as a human and animal pathogen. Only the active fractions are shown in **Table 5**.

Table 5. The bioactivities of endophytic fungi extracts and fractions. Human cell line tests were only conducted for the fungal extracts. PD= Parkinson's Disease and AMD=Age related Macular Degeneration. Endophytic fungi are shown with their cultivation codes: A= *Acephala appplanata*, R= *Phialocephala fortinii*, S16= *Humicolopsis cephalosporioides/Coniochaeta mutabilis*. Only the active preparative HPLC fractions (F1–F15) are shown below each extract (19 out of 42 fractions). The observed bioactivity is indicated with + and inactivity with -. Cells are left empty when the fraction was not tested. For the biosensor tests the samples were considered active if IF>1 or a %-inhibition rise during 10-50 minutes of measurement. SCAV= Hydrogen peroxide scavenging, 0.62-2.1 mg/mL sodium pyruvate equivalent = active. ORAC = Oxygen radical absorbance capacity, >500 μ mol TE/L = active. The samples were tested in triplicates except in ORAC, where duplicates were used

	Oxidative stress with <i>E. coli</i> DPD2511	Antioxidant activity with <i>E. coli</i> DPD2511	DNA damage with <i>E. coli</i> DPD2794	SCAV	ORAC	PD	AMD
A	-	+	+	+	+	+	-
F2	+	-	+	+	-		
F3	+	+	+	+	-		
F5	-	+	+	+	-		
F13	-	+	-	-	-		
R	-	+	+	+	+	-	-
F2	+	-	+	+	-		
F3	+	+	+	-	-		
F4	-	+	+	+	-		
F7	+	-	-	+	-		
F10	-	+	+	+	-		
F11	+	-	-	-	-		
F13	-	+	-	-	-		
F14	-	+	+	+	-		
F15	-	+	-	+	-		
S16	+	+	+	+	+	-	-
F1	-	+	-	+	-		
F2	+	-	+	-	+		
F3	+	+	-	-	+		
F7	+	-	-	-	+		
F13	-	+	+	+	+		
F14	+	-	-	+	+		

In the whole-cell bacterial biosensor tests, the fractions were considered active if the induction factors (an induction increase compared with water blank) (IF>1) of the

fraction rose above one in a dose responsive manner. In the case of antioxidant activities, a rise in the %-inhibition was considered to indicate activity when it occurred during 10 to 50 minutes of the measurement because before 10 minutes the temperature is not fully stabilized and it was concluded in Paper I that the differences between sample triplicates started to increase significantly after 50 minutes in Paper I (Tienaho *et al.*, 2015).

The fractions active in the SCAV test gave values between 0.62 to 2.1 mg/mL of sodium pyruvate equivalents. These correspond to approximately 1–10%-inhibition of H₂O₂. The ORAC test of the fractions gave values ranging from less than 10 to over 2000 μ mol TE/L and here the values over 500 were considered active.

Cell model tests were conducted for the extracts alone and no activity was detected in the case of AMD, whereas the *A. applanata* extract (cultivation code A) showed activity in the PD cell model test (max inhibition activity-% 40).

5.2.2 Bioactive metabolites from endophytic fungi

In Paper III, endophytic fungal extract metabolites are shown, and the identifications are justified with different confidence levels. The retention order of the identified compounds was also compared with the literature when appropriate. The number of identified metabolites was 220 (Paper III, Table 2) and 98 were left unidentified (Paper III, Supplementary Table S1). In addition to the main metabolites, minor ones were also present, however, the intensity limit was set at 1×10^7 , and the peaks with lower intensities were not included. Among the identified metabolites, the majority were amino acids, peptides or their derivatives. In fact, 55% of all the identified compounds were dipeptides. Additionally, amino acid quinones and Amadori compounds were tentatively identified. Amadori compounds are Maillard reaction products where an amino acid is attached to a pentose or hexose sugar group. Nucleobases, nucleosides, nucleotides and their derivatives were also detected, and these are all well-known primary metabolites. Cholines, siderophores, sugars, sugar alcohols and disaccharides as well as some common metabolites were identified among with few matches of known endophyte or plant metabolites. Because all the peptides and some other compounds could not be verified using reference compounds, they are shown with all the potential options shown in the table footnotes (Paper III, Table 2). Some ionization induced fragmentation occurred at the ion source, but fragmentation was not used. The discovered fragments are described in detail in Paper III.

The confidence of the identification was divided into four levels according to the metabolomics standards initiative (MSI) (Sumner *et al.*, 2007; Dunn *et al.*, 2013). Level 1 is for confidently identified compounds, where an authentic chemical standard was analyzed under the same analysis conditions. Level 2 is for putatively annotated compounds, where physicochemical properties and spectral similarities with public spectral libraries as well as listed references (in Paper **III**, Table 2) were used. Level 3 is for putatively annotated compound classes, where characteristic physicochemical properties or spectral similarities of compound classes are used to confirm identity. Unidentified compounds are classified as level 4 compounds, which are unidentified and unclassified but can be differentiated based upon spectral data.

In Paper **IV**, the metabolites found in the bioactive fractions are shown (Paper **IV**, Supplementary Table S2) and these are combined with the bioactivity information in Table 2 of Paper **IV**, which shows the metabolites found in either active or inactive fractions and extracts. Of the initial 330 compounds, 177 (54%) are shown in Table 2 (paper **IV**). The unidentified metabolites are shown with their exact measured masses. Most of the metabolites are the same as in Paper **III**. Some of the compounds from the extracts were potentially concentrated during the fractionation and drying process and therefore the contents of the compounds can be higher than found in the extracts.

Most of the identified metabolites in the bioactive fractions belong to the compound group peptides with 83 dipeptide or peptide matches and 9 derivatives such as acetyl- or phenylacetyl amino acids. This group therefore represents 52% of the 177 metabolites. Additionally, a further 51 unidentified compounds, which represent 29% of the metabolites, potentially influence the bioactivity of the fungal fractions. Other compounds such as nucleosides and nucleotides, Amadori compounds and sugars were also found to be among the compounds of potential bioactive interest, representing 19% of the metabolites.

In order to combine the bioactivity and metabolome results, three methodologies were used. First, the grouping of the metabolites and activities from Paper **IV** Table 2 into a visual form was done using Venn diagrams (**Figure 10**). Compound groups are presented as P= peptide, O= other and U= unknown. However, because there were five bioactivity tests and they are all presented with activity and inactivity, it is impossible to draw a comprehensive single Venn diagram without ambiguities.

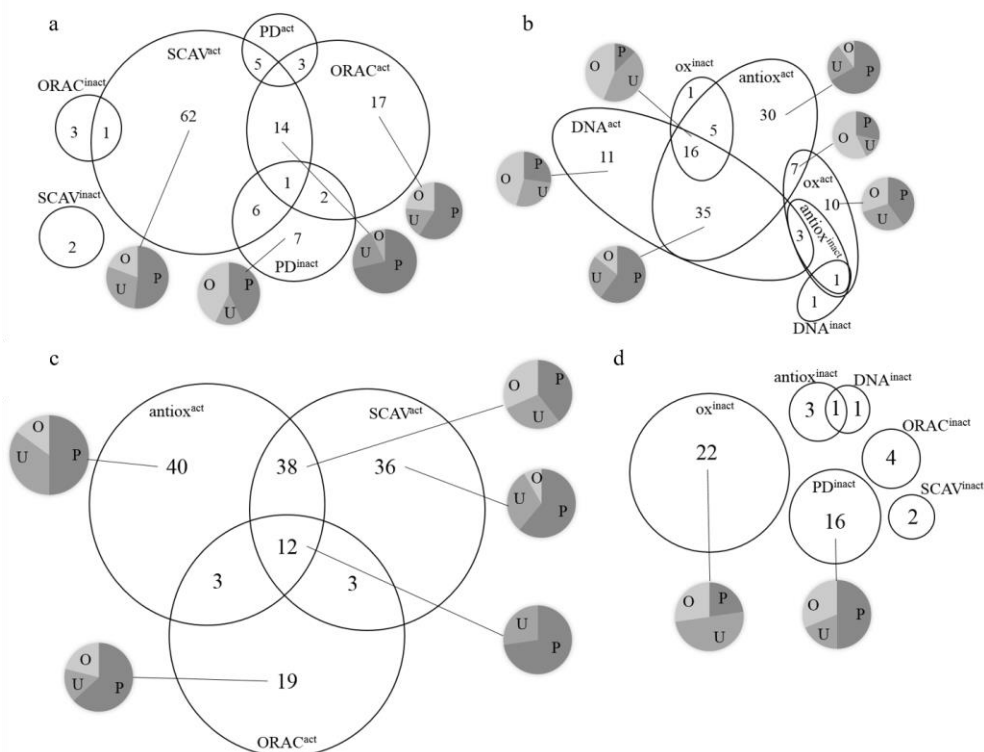


Figure 10. The Venn diagrams about the metabolite distribution to the different fractions and extracts with bioactivities and inactivities. (a) Organized according to the ORAC and SCAV and cell model for Parkinson's disease (PD) activities and inactivities. (b) Organized according to the biosensor tests with *E. coli* DPD2511 oxidative stress (ox) and antioxidant (antiox) as well as *E. coli* DPD2794 DNA damage (DNA). (c) Organized according to the *E. coli* DPD2511 oxidative stress (ox), SCAV and ORAC. (d) Organized according to the metabolites found only in inactive fractions and extracts. The pie charts show roughly the type of metabolites that were found: P= peptides, O= other and U= unknown.

Additionally, principal component analysis (PCA) and component clustering were used. PCA was found to be effective with four factors explaining 79% of the total variance (See Paper IV, Supplementary table S3B). The first principal component (PC) linked together metabolites from ORAC and SCAV active fractions. Additionally, metabolites from DNA damage biosensor fractions seem to be linked to this PC (with a semi-strong loading of 0.43). The second PC linked together metabolites from antioxidant biosensor test active fractions and DNA damage biosensor test active fractions. Principal components PC3 and PC4 were formed with the oxidative stress biosensor test and the Parkinson's disease (PD) cell model test, respectively.

The activities were divided into 19 clusters containing from one to 52 metabolites with different bioactivities and intensities of the metabolites (see Paper **IV**, Table 2). The most informative content was achieved in clusters with bioactivity in only one of the antioxidant test methods (**Figure 11**). Three clusters contained 13 metabolites which were found only in the SCAV test active fractions. The other three clusters contained 16 metabolites exclusively from the antioxidant active biosensor test (antiox^{act}) fractions and one cluster contained ten metabolites found only from the ORAC active fractions (Paper **IV**, Table 2). These antioxidant active clusters all had tentative identifications of dipeptides with Leu or Ile amino acid residues. SCAV test active clusters potentially contained six of these dipeptides (Leu or Ile and Thr, Ser, Gln, Met, Ala, or Glu). Biosensor antioxidant test active clusters potentially contained four dipeptides with Leu or Ile (Leu or Ile and Glu, Val, Leu, or Asp) and ORAC test active cluster contained three (Leu or Ile and Asp, Arg or Lys) (**Figure 11**).

When considering these tentative identifications, all the active clusters potentially contain Leu or Ile amino acids with negatively charged side chains (Asp and Glu), although differences can also be seen. The SCAV test active clusters potentially contained Leu or Ile amino acids with polar uncharged (Thr, Ser, Gln) and hydrophobic (Met and Ala) side chains. Biosensor antiox^{act} potential Leu or Ile dipeptide identifications suggest hydrophobic (Val and Leu) side chains, and ORAC active fractions suggest positively charged (Arg and Lys) side chains. Both SCAV and biosensor antioxidant test active fractions were, thus suggesting hydrophobic side chains. Both tests measure the inhibition of the H₂O₂. However, the difference between them is that the SCAV test measures the ability of a compound to scavenge the H₂O₂ before it oxidizes an iron complex (**Figure 7**), and in the biosensor test, the active compound must be able to protect the bacterial biosensor strain from the harmful effects of H₂O₂ *in vivo*.

The compound groups found in the active and inactive fractions and their reported bioactivities are introduced next. Compared with the number of secondary metabolites, the number of identified primary metabolites was large.

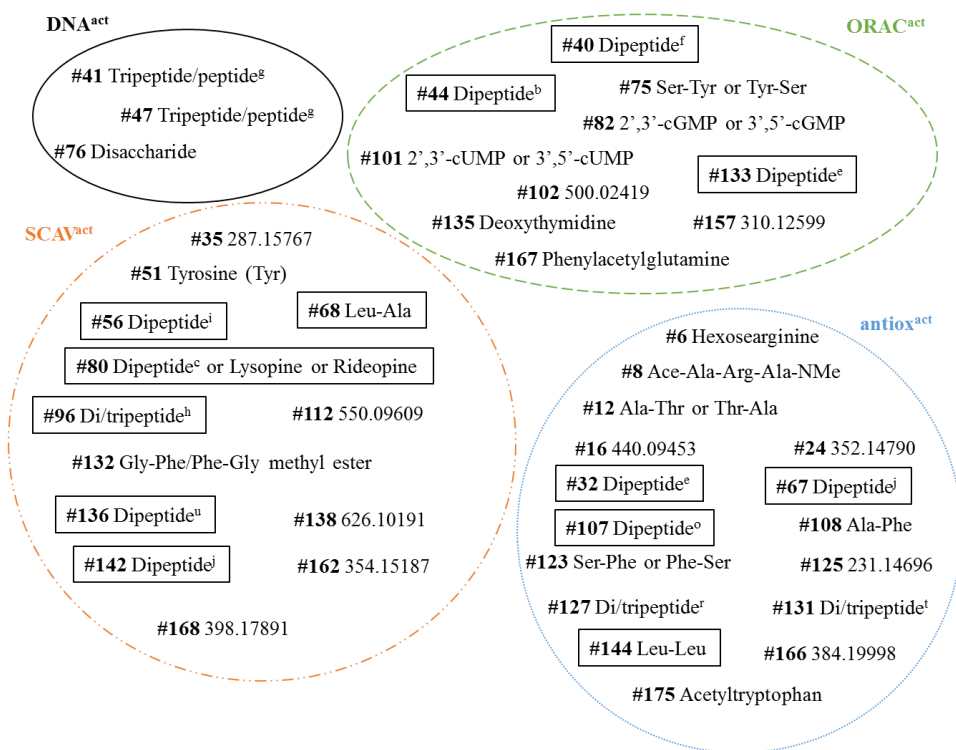


Figure 11. The clusters with compounds found from fractions with only one activity: DNA^{act}, ORAC^{act}, SCAV^{act} or antiox^{act} are shown, compound numbers, clusters and activities are shown in Table 2, Paper IV. See also Table 2, Paper IV footnotes for the identities of peptides. The framed compounds have potential Leu or Ile containing dipeptide matches in common, which are shown on the right. The side chain properties vary with these potential matches.

5.2.2.1 Amino acids and peptides

Five m/z values corresponding to free amino acids were detected: arginine, valine, tyrosine, phenylalanine and tryptophan (Paper III and IV). Large amounts of arginine were detected in the endophytic fungi extracts and fractions and it could be identified in different peaks of the chromatogram. This indicates that it is bound to many of the metabolites. Arginine is commonly used as a nitrogen storage because it has the highest nitrogen to carbon ratio out of all 22 proteinogenic amino acids (Figure 12) (Winter *et al.*, 2015). Nitrogen is often a limiting resource for plant growth since it is needed for nucleic acid and protein synthesis. Additionally, arginine is used in the production of nitric oxide and polyamines in plants and both nitric

oxide and polyamines play a crucial role in the responses to abiotic and biotic stress (Winter *et al.*, 2015).

The free amino acid valine (Val) was detected by the [2M+H]⁺ ion and found in the PD inactive extracts (Paper IV, Table 2). Unlike humans, plants and fungi are able to synthesize branched amino acids, such as valine, leucine and isoleucine, and valine is catabolized into several important molecules in fungi, such as pyruvate, propionate and succinate (Gupta & Pramer, 1970; Binder, 2010). Hydrophobic amino acids (Val, Leu and Ile, **Figure 12**) at the N terminus of peptides show antioxidant properties by increasing the interaction between peptides and fatty acids (Chen *et al.*, 1995).

Fungi and plants also synthesize phenylalanine through the shikimic acid pathway (Hyun *et al.*, 2011). Phenylalanine is used as a source of carbon and nitrogen, but some fungal species have also been shown to be able to degrade it into cinnamic acids, which are important intermediates in the formation of a variation of phenolic compounds with antimicrobial activities (Hyun *et al.*, 2011; Guzman, 2014). Tyrosine (Tyr) was detected in SCAV active fractions and extracts (Paper IV, Table 2). Tyrosine has been previously found to have antioxidant activity in the ORAC assay and this activity could be explained by the capacity of the phenolic groups to serve as hydrogen donors (Hernández-Ledesma *et al.*, 2005). The oxygen radical captures phenolic hydrogen resulting in the formation of a more stable phenoxyl radical. In fact, nucleophilic sulfur-containing side chains (Cys and Met) and aromatic side chains (Trp, Tyr and Phe) donate their hydrogen easily and are therefore potential antioxidants, but they can also all have pro-oxidative properties in certain conditions (**Figure 12**) (Carrasco-Castilla *et al.*, 2012). Additionally, histidine (His) is susceptible to oxidative reactions and has metal chelating properties because of its imidazole group, which is susceptible to oxidative reactions (Carrasco-Castilla *et al.*, 2012). Histidine-containing peptides have even been reported with higher antioxidant activity than histidine itself because of the increase in hydrophobicity and resulting higher interaction between peptides and fatty acids (Chen *et al.*, 1995). Especially acidic (Asp, Glu) but also basic (Arg, His, Lys) amino acid residues have been proposed to play a significant role in metal chelation and, thus, provide protection from lipid peroxidation (Saiga *et al.*, 2003).

Interestingly in our study, tryptophan was found to be active in SCAV and ORAC tests as an authentic standard compound, but it was found in both active and inactive fractions of the bioactivity tests (Paper IV, Supplementary Table S2). This could be because tryptophan and compounds including it have been found to contain interesting curative properties, but some are toxic instead or have been found to

increase oxidative stress in certain conditions (Le Floc'h *et al.*, 2011; Carrasco-Castilla *et al.*, 2012; Nongonierma *et al.*, 2015). Peptides containing antioxidant amino acids Trp, Tyr, Phe, Cys, Met, Asp, Glu, Val, Leu, Ile, Arg, Lys or His were commonly found in SCAV^{act}, ORAC^{act}, DNA^{act} and/or antiox^{act} fractions in Paper IV (Table 2). Only three potential and tentative matches for peptides containing antioxidant counterparts were found in fractions with oxidative activities (Paper IV, Table 2). #14 (Ala-Glu or Glu-Ala or Heliopine) was found in ox^{act} fractions; #42 (Di/tripeptide^h: potentially contains Leu, Ile, Val or Lys but also, the ethyl ester of Ala-Ala-Ala is possible) was found in ox^{act}, antiox^{inact} and DNA^{inact} fractions and #59 (Acetylglutamic acid) was found in ox^{act} fractions. These three identifications are tentative and could thus be explained by other compound matches.

Dipeptides were the most abundant class of compounds in the endophytic fungi extracts and fractions. Plant associated microorganisms have been reported to produce a variety of nitrogen containing compounds, such as cyclic peptides and peptides (Zhang *et al.*, 2006; Gunatilaka, 2006; Wang *et al.*, 2017a; Li *et al.*, 2018a). In Paper IV, the different peptides and peptide derivatives also formed a majority of the compounds only found in the antioxidant fractions and extracts (**Figure 10**). Indeed, peptides with antioxidant and other bioactivities have also been quite widely discussed in the literature (Chen *et al.*, 1996; Hernández-Ledesma *et al.*, 2005; Wang *et al.*, 2016a; Dang & Süßmuth, 2017; Sánchez & Vásquez, 2017). The antioxidant activity of peptides is usually caused by the chelation of transition metals and scavenging of free radicals (Carrasco-Castilla *et al.*, 2012). Antimicrobial peptides have been found to be active against both Gram-positive and Gram-negative bacteria and they can possess other benefits for health such as anti-inflammatory properties (Hilchie *et al.*, 2013; Chen *et al.*, 2019). Glutathione (Table 2, Paper IV) is an antioxidant peptide with sulfur-containing side chains, which is used in the non-enzymatic antioxidant defense mechanism of plants and is known to be present in high concentrations in fungi (Pocsi *et al.*, 2004). Endophytes also use antioxidant substances such as glutathione to overcome reactive oxygen species (ROS) production, which is the initial protection method of a plant against microbial invasion (Hilchie *et al.*, 2013; Koskimäki *et al.*, 2016). In Paper IV, glutathione was found in the fractions which were active in the biosensor antioxidant test and the SCAV test (antiox^{act} and SCAV^{act}).

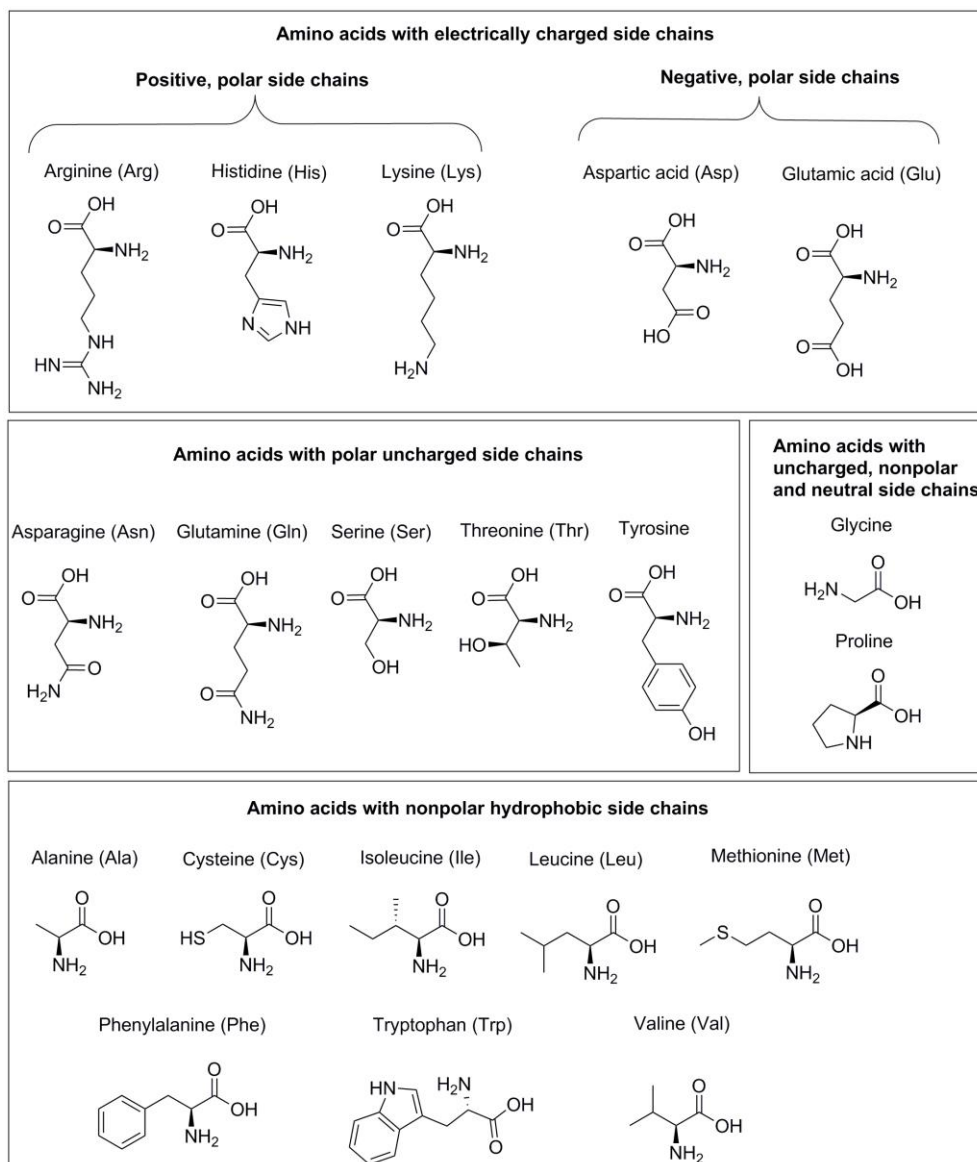


Figure 12. Amino acid side chain properties; out of the 22 proteinogenic amino acids, selenocysteine (Sec) and pyrrolysine (Pyl) have been omitted from the figure because masses suitable for peptides containing them were not discovered.

Many peptides have also been reported showing antimicrobial and antiviral properties (Salas *et al.*, 2015; Bondaryk *et al.*, 2017; Dang & Süßmuth, 2017; Sánchez & Vásquez, 2017; Kombrink *et al.*, 2018). Additionally, cyclo(3-OH-Pro-Tyr) (see Paper III and IV) was also found to have toxicity against the pest mite *Tetranychus*

urticae by Li *et al.*, (2018a). In Paper **IV**, cyclo(3-OH-Pro-Tyr) is one possible identification (MSI3) for Peptide type compound^s (#130), which have been found in fractions which were active in the biosensor antioxidant test. Then again, Kang *et al.*, (2011) found dipeptide Leu-Glu to have protective activity against UV-B induced photoinflammation. In this study, Leu-Glu is one potential compound explaining Dipeptideⁱ (see Table 2, Paper **IV**), which was found in fractions with antioxidant activities (antiox^{act}, SCAV^{act}, ORAC^{act} and antiox^{act}+DNA^{act}). Protection from ROS, which are produced by UV radiation in the skin, is one property which increases the protective capacity of sunscreen products (Poljsak *et al.*, 2013). This was verified using ascorbic acid and astaxanthin in the biological UV protection test in Paper **II** (Tienaho *et al.*, 2018).

5.2.2.2 Osmolytes and siderophores

Free amino acids and dipeptides can also act as signaling molecules and have antioxidant and buffering properties in human body (Fonteh *et al.*, 2007). Whereas plants accumulate compounds such as proline (Pro), glycine betaine and choline-*O*-sulfate in their cells, as a response to different abiotic stress situations (Ozden *et al.*, 2009). These are known as osmolytes, which accumulate in the cells as a response to osmotic stress to protect proteins from destruction (Hagihara *et al.*, 2012). Amino acid Pro, for example, is one of the most common compatible osmolytes in plants suffering from dehydration caused stress (Yoshida *et al.*, 1997). Whereas, choline-*O*-sulfate is synthesized widely in nature by plants, lichens, algae, fungi and even some bacterial species (Hagihara *et al.*, 2012), it has been shown to accumulate in plant cells under saline stress (Rivoal & Hanson, 1994) and it provides a source of sulfur and choline, which is essential nutrient with vitamin-like effects (Hagihara *et al.*, 2012). In fungi, choline-*O*-sulfate acts as the storage of sulfur, which is an essential metabolite for the growth of filamentous fungi (Spencer *et al.*, 1968; Markham *et al.*, 1993). In Paper **IV**, proline was found mainly linked in peptides and choline-*O*-sulfate was found in both active and inactive fractions. Proline-containing peptides were found in antiox^{act}, DNA^{act}, SCAV^{act} and/or ORAC^{act} fractions and some were found also in ox^{act} and some in ox^{inact} fractions. In fact, dehydration can cause oxidative stress and the free-radical damage is often targeted at the DNA of the organism (Franca *et al.*, 2007). Proline has also been shown to scavenge OH-radicals *in vitro* (Bohnert & Jensen, 1996).

One exact mass and molecular formula corresponding to *cis*- and/or *trans*-fusarinine siderophore was found with two retention times in Paper **III**. The *cis*- and

trans-fusarinine backbones are very common in many fungal siderophores (Holinsworth & Martin, 2009; Bertrand *et al.*, 2010). Siderophores are low molecular weight compounds that are used for iron uptake and storage and they have been found to be important in the maintenance of plant–fungi symbioses and for the establishment of virulence (Haas *et al.*, 2008; Kajula *et al.*, 2010; Wright, 2014). Fungi and other microorganisms have been found to produce siderophores in aerobic growth conditions during periods of iron limitation (Holinsworth & Martin, 2009). Iron is essentially required for the growth and proliferation in both bacteria and fungi, and siderophores provide cells with nutritional iron (Abdalla & Matasyoh, 2014). In DSE fungi, it was found that these species can acidify their growth environment and produce siderophores to increase the micronutrient uptake to both members of the symbiont, indicating the association to be mutualistic rather than pathogenic (Bartholdy *et al.*, 2001). In Paper **IV**, siderophores were found in both active and inactive fractions and therefore can be found from the supplementary material.

5.2.2.3 Amadori compounds, amino acid quinones and opine amino acids

Amadori compounds are formed in the Maillard reaction, where naturally occurring reducing sugars and amino acids are joined nonenzymatically (Ryu *et al.*, 2001). Hexosearginine, hexosevaline, pentoseproline, hexoseaminobutyric acid and deoxyhexosethreonine were among the tentative identifications in Paper **III**. Amadori compounds have also been previously found in fungal species (Yoshida *et al.*, 2005). Hexosearginine and specifically fructosylarginine has been identified in aged garlic and red ginseng and it has been shown to act as an effective antioxidant (Ide *et al.*, 1999; Ryu *et al.*, 2001; Joo *et al.*, 2008). The presence of fructosylarginine in the endophytic fungal extracts and fractions was verified using a synthesized reference compound. However, the antioxidant activity could not be verified in SCAV and antioxidant biosensor tests (data not shown, the synthesis route of fructosylarginine and results will be published elsewhere). Because of their ability to bind iron and other heavy metals, Amadori compounds in general have been proposed to contain antioxidant properties (Gill *et al.*, 1996). These Maillard reaction products have also proven antimicrobial properties and fructose-amino acids have indicated more biological activity compared to glucose-amino acids (Wu *et al.*, 2014). Hexoseaminobutyric acid has the same molecular formula as hexoseaminoisobutyric acid and both are thus possible identifications. Aminoisobutyric acids are rare in nature and can only be found in peptaibols, which are antibiotic antifungal peptides

produced by soil fungi (Huang *et al.*, 1995). Additionally, aminobutyric acid has a somewhat similar structure to hydroxybutyric acid, which has been reported with hydroxyl radical scavenging activity. Methyl esterified dimers and trimers of hydroxybutyric acid were found to protect bacteria from hydroxyl radicals (Koskimäki *et al.*, 2016). In Paper **IV**, hexosearginine was identified in the fractions which were active in the biosensor antioxidant test (antiox^{act}). Hexosevaline was tentatively identified in antiox^{act}, DNA^{act} and SCAV^{act} fractions and deoxyhexosethreonine and pentoseproline were tentatively identified in ox^{inact}, antiox^{act}, DNA^{act} and SCAV^{act} fractions.

Abenquines are simple aminobenzoquinones substituted with different amino acids. Quinones have been reported in endophytic fungi (Gouda *et al.*, 2016). Schulz *et al.*, (2011) stated that aminobenzoquinones are widely distributed in nature but abenquines are rare. However, their structure is related to fungal pigments lepiotaquinone and lilacinone (Schulz *et al.*, 2011). Because more than one possible amino acid quinone masses were detected in Paper **III** and they have been isolated from the rhizosphere bacteria, there is a possibility that root-colonizing fungi of the rhizosphere could produce these metabolites. However, the confidence level is putative identification (MSI2). Abenquine C or N-[4-(acetylamino)-3,6-dioxo-1,4-cyclo-hexa-dien-1-yl]-l-valine and N-[4-(acetylamino)-3,6-dioxo-1,4-cyclohexadien-1-yl]-leucine (abenquine B1) and -isoleucine (abenquine B2) have been isolated from the *Streptomyces* sp. bacteria (Schulz *et al.*, 2011; Nain-Perez *et al.*, 2017). Abenquines have been found to contain weak activity against bacteria and fungi (*E. coli*, *Lactobacillus casei*, *Bacillus subtilis*, *Trichophyton rubrum*, *T. mentagrophytes* and *Microsporum canis*), and stronger activity against bloom-forming cyanobacteria (*Synechococcus elongatus*) (Schulz *et al.*, 2011; Nain-Perez *et al.*, 2017). In Paper **IV**, abenquine C was found in both active and inactive fractions (found from the supplementary material) but abenquine B1 and B2 are among the tentatively identified matches of Peptide type compound^v, which was found in SCAV test active fractions.

Opines were among the tentatively identified metabolites in the fungal extracts and fractions. They are conjugates of amino acids and common carbonyl compounds of primary metabolism, such as pyruvate, α -ketoglutarate or glucose (Chilton *et al.*, 2001). They are formed by crown gall tumors caused by various rhizosphere bacteria of *Rhizobiaceae* sp. in a wide variety of hosts, including *Pinus* sp. (Kemp, 1978; Stomp *et al.*, 1990). It has been shown that other soil bacteria and even fungi can also utilize opines as their sole source of carbon and energy (Beauchamp *et al.*, 1990; Savka *et al.*, 1996). Heliopine is a conjugate of glutamine and pyruvate, whereas rideopine is derived from polyamine putrescine (Chilton *et al.*, 2001). Lysopine is a condensation

product of lysine and pyruvate (Kemp, 1978). However, valinopine has been detected from the poisonous mushroom *Clitocybe acromelalga* and is suggested to be a fungal toxin (Fushiya *et al.*, 1996). Saccharopine has also been isolated from different mushroom species and is a precursor of lysine in the fungal α -amino adipate pathway (Fushiya *et al.*, 1996; Xu *et al.*, 2006). Savka *et al.*, (1996) showed that opines can move through the plant and even spread to the soil as exudates and thus affect the microbial growth around the plant. Some opines have been shown to pose antagonistic effects on herbivorous larvae and cause allelopathy against weed seeds, which suggests that they are beneficial to the plant hosts (Savka *et al.*, 1996). Gall formation and opine synthesis were studied in co-cultivation experiments with *Pinus* species and *Agrobacterium tumefaciens* (Stomp *et al.*, 1990). It was found that bacteria were able to transfer DNA into pine species (including Scots pine) but the number of gall tumors decreased over time. The authors also stated that the formation of opines should not be taken as the sole evidence of transformation by *Agrobacterium* as some opine species have been identified from uncolonized plants with arginine feeding (Stomp *et al.*, 1990). In Paper **IV**, saccharopine was found in ox^{act}, antiox^{inact} and DNA^{act} fractions and heliopine was found in ox^{act} fractions. Lysopine or rideopine were found in antiox^{act}, DNA^{act} and SCAV^{act} fractions and valinopine was tentatively identified in ox^{inact}, antiox^{act}, DNA^{act} and SCAV^{act} fractions. It seems that all potential identifications possess some antibacterial activity, which could be caused by the antagonism between microbial species in the soil environment, where the amount of nutrients is limited.

5.2.2.4 Common metabolites

Some common metabolites were identified from the extracts and fractions. Glycerophosphoinositol is found in both plants and fungi and it is a major deacylation product of lipid metabolism (Prior *et al.*, 1993; van der Rest *et al.*, 2002). Most commonly, the inositol is in its *myo*-D-inositol chemical form, which has been shown to scavenge hydroxyl radicals, *in vitro* (Bohnert & Jensen, 1996). Glycerophosphorylcholine is a part of phosphatidylcholine, which is a type of phospholipid in lecithin. Lecithin is a major component of the phospholipid membrane which is also found in plant tissue (Markham *et al.*, 1993). These compounds are closely related to each other and in Paper **IV**, these were found in both active and inactive fractions. Methylcitric acid was also found in both active and inactive fractions (Paper **IV**) but it was found to have ORAC activity by Jayaprakasha *et al.*, (2007).

Of the nucleobases, guanine and isoguanine or oxyadenine were detected, which are the only ones with a molecular mass above the detection limit of 150 Da. Isoguanine is a purine analog, which is formed in the direct oxidation of adenine (Cheng *et al.*, 2012; Karalkar *et al.*, 2017). Guanine was found in SCAV^{act} and PD^{inact} fractions and Isoguanine or Oxyadenine as identified in PD^{inact} fractions in Paper **IV**. Of the DNA bases, guanine is most easily oxidized and the presence of 8-hydroxydeoxyguanosine has been considered a marker of hydroxyl radical induced oxidative damage to DNA (Wang *et al.*, 2014). The mass of this compound responds to that of the guanosine isomer in Paper **III** and **IV**. Dinesh *et al.*, (2012) reviewed activities of purine analogues and many derivatives of adenine and guanine have been found to contain antimicrobial and antiviral properties.

Nucleosides were also detected, and they contain a nucleobase with a pentose sugar unit: ribose or deoxyribose. Cytidine, pseudouridine, uridine, adenosine, guanosine isomer, deoxyguanosine, methylthymidine, and deoxythymidine were tentatively identified in Paper **III**, and the presence of cytidine, uridine and adenosine were verified with authentic standards. Methylthymidine has been used as an indicator of microbial presence in wastewater (Ruble *et al.*, 1984). In the parasitic fungus *Cordyceps sinensis* found in caterpillars, the most bioactive principles were found to be water-soluble nucleosides, exo-polysaccharides, sterols and proteins (Shashidhar *et al.*, 2013). For example, adenosine, guanosine and cordycepin were detected and found to contain pharmacological activities such as anti-cancer and pharmacokinetic effects (Shashidhar *et al.*, 2013). Adenosine is an adenine riboside, which has also been shown to induce growth in plant meristem cultures (Ries *et al.*, 1990; Pirttilä, 2011). Additionally, cytokinins are adenine derivative plant hormones, which are known to induce plant growth (Osugi & Sakakibara, 2015). Adenosine was found in this study to be abundant in the fungal extracts. It was found in both inactive and active fractions with high intensities (Paper **IV**, Supplementary Table S2). However, the mass of adenine is 135 Da, which is too low for detection in the used methodology. Nucleosides and nucleotides are vital for all living cells and are involved in many key biological processes (Huang *et al.*, 2014). Different derivatives of nucleosides and nucleotides have been found to have antimicrobial, herbicidal and insecticidal properties (Isono, 1988). Especially marine-derived nucleosides have been investigated widely because of their unique and biologically active properties, and these include marine fungi derived molecules (Huang *et al.*, 2014). Pseudouridine was found in ox^{act}, antiox^{act} and SCAV^{inact} fractions and uridine in antiox^{act}, DNA^{act} and SCAV^{act} fractions in Paper **IV**. Deoxyguanosine (whose mass and formula correspond to 8-hydroxydeoxyguanosine, which is an oxidation product of guanine)

was found in $\text{antiox}^{\text{act}}$ fractions and deoxythymidine in ORAC^{act} fractions in Paper IV. Tentatively identified uridine analogue, 5-methoxycarbonylmethyluridine was found in the ox^{inact} , $\text{antiox}^{\text{act}}$, DNA^{act} , SCAV^{act} and PD^{act} fractions.

Nucleotides are nucleosides joined with at least one phosphate group and they were tentatively identified in the extracts and fractions. Nucleotides have both antioxidant and pro-oxidative properties (Richter & Fischer, 2006). In fact, purine adenine nucleotides were concluded to have biphasic effects (including first pro-oxidant and then antioxidant phases) in the Fenton reaction, where iron is oxidized in the presence of hydrogen peroxide and forms highly reactive hydroxyl radicals (Richter & Fischer, 2006). The order of inhibitory or antioxidant potency was found to be adenosine diphosphate (ADP) > adenosine monophosphate (AMP) > adenosine triphosphate (ATP) > adenosine, whereas phosphates are generally considered pro-oxidants (Richter & Fischer, 2006). Adenosine monophosphate (AMP) or deoxyguanosine monophosphate (dGMP), cyclic uridine monophosphate (cUMP), deoxyribose adenosine monophosphate (dAMP), cyclic adenosine diphosphate ribose (cADPR), cyclic guanosine monophosphate (cGMP) and two exact masses and molecular formulae corresponding to dinucleotides were identified in Paper III. AMP or dGMP was found in PD^{inact} fractions whereas dAMP was found in SCAV^{act} and PD^{inact} fractions in Paper IV. Dinucleosides were found in ox^{inact} , $\text{antiox}^{\text{act}}$, DNA^{act} and SCAV^{act} fractions.

Cyclic nucleotides are used as signaling metabolites in almost all organisms and they regulate a vast number of cellular processes (Bähre & Kaefer, 2014; Dittmar *et al.*, 2015; Seifert, 2016; Swieczawska *et al.*, 2018). Cyclic-GMP and cUMP were found in ORAC^{act} fractions and other possible cUMP isomer in $\text{antiox}^{\text{act}}$, DNA^{act} and SCAV^{act} fractions. Cyclic nucleotides have been proposed to be among potential contributors towards the antioxidant nature of *Ziziphus jujuba* fruits (Wang *et al.*, 2016b). ADP-ribosyl groups are formed on target proteins as a response to DNA damage and poly(ADPR) polymerase enzyme homologs, which catalyze the reaction, have also been found in fungi (Semighini *et al.*, 2006). Cyclic ADPR was found in ox^{inact} , $\text{antiox}^{\text{act}}$, DNA^{act} and SCAV^{act} fractions in Paper IV. The intracellular signaling responses of plants to nitric oxide (NO) have been shown to generate cGMP and cADPR (Neill *et al.*, 2003). NO induces stress-related processes in plants, such as defense mechanisms' gene induction and programmed cell death but also stomatal closure, seed germination and root development (Neill *et al.*, 2003).

In addition, nicotinamide riboside (NR) and nicotinamide adenine dinucleotide (NAD) were tentatively identified. NR was found in the $\text{antiox}^{\text{act}}$, DNA^{act} and SCAV^{act} fractions whereas NAD was found in the ox^{act} and ORAC^{act} fractions in

Paper **IV**. NR is a naturally occurring form of vitamin B₃ (niacin) and its amide-form (nicotinamide), which is a key component in the production of NAD (Conze *et al.*, 2016; Fricker *et al.*, 2018). NAD either exists in its oxidized (NAD⁺) or reduced (NADH) form and can also be synthesized from tryptophan in prokaryotic and eukaryotic organisms (Lin & Guarente, 2003). NAD has been thought to have signaling and transcriptional regulator roles in ageing and some human diseases, such as Parkinson's disease (Lin & Guarente, 2003). In fact, NAD⁺ is essential for all organisms because of the redox maintenance and as a source of ADP-ribosyl groups, which retard aging, for example (Bieganowski & Brenner, 2004).

Sugar-nucleotides, such as uridine diphosphate (UDP)-glucose and UDP-galactose as well as UDP-galactosamine and UDP-glucosamine were also discovered in Paper **III**. UDP-glucosamines and UDP-galactosamines are important precursors of the bacterial and fungal cell wall (Maruyama *et al.*, 2007). Sugar nucleotides are donors of sugar groups in the biosynthesis of glycosides, polysaccharides and glycoconjugates and they are abundant in microorganisms and plants (Kariya & Namiki, 1997). They also play many important roles in fungi (El-Ganiny *et al.*, 2010; Li *et al.*, 2015). UDP-galactose was found in DNA^{act} fractions and UDP-galactosamine and UDP-glucosamine were found in ox^{act} and antiox^{act} fractions in Paper **IV**. Sugar-nucleotides are formed by sugars or sugar derivatives and nucleoside mono- or diphosphates and they are essential intermediates in carbohydrate metabolism and glycoconjugate biosynthesis (Wagner *et al.*, 2009).

The presence of mannitol and fucose was confirmed using authentic standards in Paper **III**. Mannitol is widely distributed in filamentous fungi and it is stored in the fungal hyphae as a carbon source (Landi *et al.*, 2017). Mannitol is sugar alcohol, which can be oxidized to form mannose, and polysaccharides which are rich in mannose have been proposed to increase the antioxidant capacity of fungal species, such as *Inonotus obliquus*, *Pleurotus eryngii* and *Hirsutella* sp. (including *C. sinensis*) (Wang *et al.*, 2017b). Additionally, mannitol itself has been shown to scavenge OH-radicals *in vitro* (Bohnert & Jensen, 1996). Fucose appears to represent a prominent feature in protein-linked glycans in the fungal kingdom (Grass *et al.*, 2010). Fucose-enriched exopolysaccharides exhibit anticancer and anti-inflammatory activities and are used in the cosmetic industry as skin moisturizers (Cescutti *et al.*, 2005).

Furthermore, disaccharides were tentatively identified. Mass and molecular formula responds for example to the one isolated from pathogenic fungal species *Claviceps africans*, with fructofuranose and arabinose backbones (Bogo *et al.*, 2006) were tentatively identified in the fungal extracts and fractions. Some polysaccharides of fungal species have been found to have antioxidant activity, such as a

heteropolysaccharide isolated from the fruiting bodies of *C. sinensis* (Zhang *et al.*, 2011b). Additionally, *Fusarium* sp. has yielded water-extractable polysaccharides with antioxidant activity (Li *et al.*, 2012). Deoxyhexoses are produced in fungi by pyranose oxidases, which have been reported among lignin-degrading fungi (Giffhorn, 2000), for example. Pyranose oxidases provide H₂O₂ for the lignin-decomposing peroxidases in white rot fungi (Giffhorn, 2000). Dehydrohexose has also been previously reported in evergreen Carob trees (*Ceratonia siliqua*) (Farag *et al.*, 2019). Disaccharides were found in DNA^{act} fractions and dehydrohexose was tentatively identified in ox^{act} and antiox^{act} fractions in Paper **IV**. Deoxyhexose was found in ox^{inact}, antiox^{act}, DNA^{act} and SCAV^{act} fractions.

5.2.2.5 Specialized metabolites

Among the tentatively identified compounds, phomone A and B are enantiomeric α -pyrone dimers isolated from the endophytic fungus *Phoma* sp. YN02-p-3 and have showed no activity against three human cell lines (Hill & Sutherland, 2017; Sang *et al.*, 2017). Blumeoside C, which is an iridoid glucoside isolated from *Fagraea blumei* (Cuendet *et al.*, 1997) has the same molecular formula. Cuendet *et al.*, (1997) discovered that blumeoside A elutes later than blumeoside C, which is in accordance with the findings in Paper **III**, Table 2. Blumeoside A displayed antioxidant activity in a DPPH test by Cuendet *et al.* (1997). In Paper **IV**, phomone A or B or blumeoside C were found in PD^{inact} fractions.

Asperulosidic acid and its stereoisomer were tentatively identified (MSI2) from the extracts and fractions and they have been isolated from the plant *Hedyotis diffusa* using water extraction (Li *et al.*, 2008). According to Friscic *et al.*, (2016), asperulosidic acid elutes later than mannitol using reversed-phase liquid chromatography as in our study. Asperulosidic acid has also been isolated from *Vernonia cinerea* with ethanol (Alara *et al.*, 2018) and its structural isomers have been isolated from *Morinda coreia* and *Saprosma scortechinii* with methanol (Kanchanapoom *et al.*, 2002; Ling *et al.*, 2002). Asperulosidic acid or isomer was found in the SCAV^{act} fractions (Paper **IV**).

Furthermore, exact masses corresponding to orsellinic acid esters were found, which have been isolated from the endophytic *Chaetomium* sp. fungus (Bashyal *et al.*, 2005; Schlörke & Zeeck, 2006; Gutierrez *et al.*, 2012; Xu *et al.*, 2014). However, orsellinic acid ester globosumone B was not included in Table 2 (Paper **III**) because of the chosen intensity limit of 1×10^7 . It was found in R fungus fractions with higher intensities and therefore it was included in Supplementary Table S2 of Paper **IV**. Globosumone B has been found to be moderately active against four

human cancer lines (Bashyal *et al.*, 2005). Orsellinic acid esters have been found to have cytotoxic, antibacterial and antiviral activities (Xu *et al.*, 2014).

Two tentative identifications (MSI3) with possible triterpene saponin structures were obtained with the molecular formula C₃₅H₅₀O₁₂. Such triterpene saponins, could for example be Dianthosaponin F, which has been isolated from *Dianthus japonicus* with methanol (Nakano *et al.*, 2011), and Celosin F, which has been isolated from *Celosia argentea* with 50% ethanol (Wu *et al.*, 2011). Celosin F has been reported to have anti-inflammatory activity by inhibiting NO production (Wu *et al.*, 2011). Saponins have been reported with wide pharmacological bioactivities and antioxidant activity (Desai *et al.*, 2009). They also act as antifungal, antimicrobial and antiviral agents (Desai *et al.*, 2009). Saponins were found in ox^{act}, SCAV^{act} and ORAC^{act} fractions in Paper IV.

Linamarin is a toxic cyanogenic glucoside isolated from cassava (*Manihot esculenta*) roots (Sulyok *et al.*, 2015). Ramulosin derivatives have been previously isolated from the endophytic fungi *Nigrospora* sp. which is present in the branches of the *Garcinia nigrolineata* tree (Gutierrez *et al.*, 2012). A ramulosin derivative was found to have mild antibacterial activity against *Staphylococcus aureus* and methicillin-resistant *S. aureus* (MRSA) by Sommart *et al.*, (2008). In Paper IV, the tentative identification of a ramulosin derivative was found in antiox^{act} and SCAV^{act} fractions and potential Linamarin was identified in antiox^{act}, DNA^{act} and SCAV^{act} fractions and there was another match in the ox^{inact} fractions.

5.2.3 Bioactive metabolites of endophytic fungi discussion

Various compounds and compound groups with bioactivities were found in endophytic fungal extracts. Endophytes have indeed been studied widely for their bioactive metabolites and many reviews have been published concerning the issue (Tan & Zou, 2001; Schulz *et al.*, 2002; Strobel, 2003; Strobel *et al.*, 2004; Gunatilaka, 2006; Zhang *et al.*, 2006; Firáková *et al.*, 2007; Aly *et al.*, 2010; Gutierrez *et al.*, 2012; Mousa & Raizada, 2013; Nisa *et al.*, 2015; Strobel, 2018, for example). Less examined water extracts were chosen as the subject of this study. Endophytic fungi species were identified according to their GenBank matches of ITS-regions and were A= *Acephala applanata*, R= *Phialocephala fortinii* and S16= *Humicolopsis cephalosporioides/Coniochaeta mutabilis*. The first two are dark, septate endophytic (DSE) species belonging to the PAC species complex commonly occurring in boreal forest tree roots. The identification of PAC species using the ITS region is challenging (Grünig

et al., 2008) and S16 identification has some uncertainty with two equally possible matches: *H. cephalosporioides* has been classified a DSE-like fungi and *C. mutabilis* has been found in plants but also to act as a human and animal pathogen.

Sterile fungal mycelia were grown on a Hagem agar growth medium, which was suitable for the growth of the selected fungus species and was simple to prepare. The same growth medium was used for all fungus species, without species-specific optimization because all of the fungal species grew well on the medium. This is reasonable for the screening of the metabolites and comparison of the fungal species. For potential further applications, the optimization of the growth conditions and nutrition should be considered due to factors that affect the metabolism in microbes: i.e. the pH, temperature, incubation period, type of microbe used, growth dynamics, and microbial internal physiology (Waqas *et al.*, 2014; Gonzáles-Menéndez *et al.*, 2018). Additionally, it should be acknowledged that the sterile mycelium outside the host and without induced stress conditions is likely to behave differently than in natural growth conditions. For affirmation of the effect on the host plant survival, co-cultivation studies should be conducted.

Water extraction was chosen in this study, because of the ease of its usability for the biosensor tests with minimal solvent effects, as well as the fact that water is a green solvent with minimal environmental and human health risks. While this proved to be favorable in the context of bioactivity tests, it complicated the identification process. This is because water extracts include all water-soluble organic molecules, such as sugars, nucleosides and peptides. For example, peptides are generally not visible in UV detection, which was used for the fractionation of the extracts. In order to make peptides and amino acids visible in a photo diode array (PDA) detector, they should be chemically modified or derivatized into fluorescent or electrochemically active products (Walker & Mills, 1995). However, factors such as the unstableness, expensiveness and toxicity of derivatives, incomplete derivatization reactions and inadequate chromatographic separations complicate the amino acid analysis (Kambhampati *et al.*, 2019). Additionally, as the bioactivities of the collected fractions were to be tested, the derivatization would have likely altered the bioactivities and complicated the identification process. Extraction solutions with varying polarities could also be tested for differences in functional properties. In addition, filtering or other separation methods could be utilized for the purification of the samples.

The drying process can also alter the metabolic profile and biological activities of the extracts and fractions. For example, freeze-drying among other drying methods was shown to affect the antioxidant activity, phenolic contents and number of

volatiles and cyclic nucleotides of *Ziziphus jujube* fruits (Wang *et al.*, 2016b). The metabolite profile can also be affected by seasonal, climatic and geographical factors (Gouda *et al.*, 2016). These factors were minimized in this study by using sterile mycelium. The fungal species were handled, extracted and examined similarly and therefore differences in the metabolome and bioactivity were caused by the fungi themselves.

The biological activity of the extracts and fractions were assessed with biosensor methodologies, which have limitations listed in **Table 4**. Additionally, the ORAC and SCAV methods have their limitations. For example, the ORAC method repeatability was questioned by Thaipong *et al.*, (2006). Additionally, the FOX reagent method has been criticized for its narrow linear range and low reproducibility (Meisner & Gebicki, 2009). By combining and comparing the results from several tests with different mechanisms, it was hypothesized that a broader view of the antioxidant and bioactive potential could be obtained. However, the used methodologies are set to measure only two of three antioxidant mechanisms: hydrogen atom transfer (HAT) by ORAC and transition metal chelation ability by SCAV. The single electron transfer (SET) mechanism is not covered. This could have been tested by choosing a test mechanism, such as the ferric reducing absorbance capacity (FRAP), which measures the antioxidant's ability to reduce iron in a colorimetric manner (Benzie & Strain, 1996; Thaipong *et al.*, 2006). In addition, in this study, all the methods were only used for activity/inactivity screening and fingerprint analysis. In order to be able to compare the signal magnitudes and activity levels, the assays should be repeated a statistically significant number of times. Additionally, different strains of the fungal species should be investigated before discussing species-specific characteristics.

The identification process also has uncertainties. The mass to charge ratio (m/z) range of 150-1000 Da was chosen for device calibration and predicted metabolite masses. For the identification of amino acids and other primary metabolites the minimum m/z value was, however, too low for the detection of many common low molecular weight compounds. The use of fragmentation or tandem mass spectrometry could have eased the identification process and verified the amino acid order of the peptide identifications. Desportes *et al.*, (2000) discussed these aspects from the perspective of wine but the same implies for the fungal species of this study: the peptides occur in an extremely complex mixture together with proteins, amino acids and a multitude of peptide-unrelated substances such as phenolic compounds, which are likely to interfere with the peptide isolation. These factors make it difficult to isolate and identify the peptides in complex solutions. Even with tandem mass

techniques (MS/MS), the number of fragment peaks with short peptide sequences make it problematic to use protein databases because the short peptides can correspond to a number of potential sequences with the same molecular mass (Le Maux *et al.*, 2015). In order to confirm that the identified metabolites are not formed during handling and testing, it was verified that the metabolites found in the active fractions were also present in the extracts. The use of a more comprehensive product library could also reduce the large number of unidentified metabolites in the identification process.

The detection limit of the mass spectrometric data was chosen to be 1×10^7 of intensity with the maximum intensities $>1 \times 10^9$ in the total ion chromatograms. This limits the number of metabolites detected, which was also necessary because of their vast quantities. However, the bioactive metabolites are not always the most abundant ones, and this could lead to losing the metabolites of interest. For example, in *Hoodia gordonii* the pregnane glycoside P57, which has been thought to be responsible for anti-obesity effects, has been found to be only a very small portion of the administrated extract and various other potentially active glycosides have later been identified from it (Vermaak *et al.*, 2011).

Various studies have shown a connection between oxidative stress and drought in plants (Jaleel *et al.*, 2007; Miller *et al.*, 2010; Obata & Fernie, 2012). Endophytic fungi and DSE species are known to improve the host plant's stress tolerance and growth and to increase the water and nutrient intake (Terhonen *et al.*, 2014; Suroño *et al.*, 2017; Suroño *et al.*, 2018; Vergara *et al.*, 2018; Li *et al.*, 2018b) but less is known about the mechanism behind the phenomenon. The effects of the DSE on phytohormone production or the root biomass extension resulting in increased water and nutrient intake have been proposed as the answers (Li *et al.*, 2018b; White *et al.*, 2019). We were not able to elucidate any separate compounds which could be responsible for the found bioactivities. Additionally, it was found that the fungal extracts and fractions contain a plethora of metabolites, which may have synergistic effects. For example, Willför *et al.*, (2003) found that in conifer knotwood extracts, the antioxidant potency was higher than that of the predominant pure compounds. Similar findings about the additive and synergetic effects of phytochemicals have also been noted by others (Boik *et al.*, 2009; Zhu *et al.*, 2018). Thus, likewise there is a high possibility that synergetic effects of the compounds could be responsible for the antioxidant and antibacterial activities found in this study. In conclusion, the synergetic effects of various bioactive metabolites produced by the endophytic symbionts could offer an additional explanation to the mechanism behind the increasing stress tolerance of the host plant.

6 CONCLUSIONS

The antioxidant and antibacterial properties as well as UV protection potential of forest-derived extracts were investigated using genetically modified bacterial *E. coli* biosensors. In addition, the bioactivities of endophytic fungi extracts and fractions were screened and the metabolites found in bioactive extracts and fractions were identified using LC-MS. The following conclusions can be drawn:

- Two new methodologies were introduced using *E. coli* biosensors DPD2511 and DPD2794. The methodologies were validated using reference compounds as well as found usable in forest-derived extract screening.
- A previously described antioxidant method was improved with HTS potential in a microplate format.
- A UV protection test for both physical and biological shielding potential was developed.
- Stress-responsive bacterial biosensors are usable in the screening of forest-derived extract bioactivities with certain limitations.
- A major proportion of the metabolome of three endophytic fungi species isolated at the same time and from the same ecological niche and host, were similar. The small differences in the metabolome could indicate that the metabolite production variance is limited when using sterile mycelium under steady nutrient supply.
- Endophytes produce a wide variety of antioxidant and antibacterial metabolites. The synergetic, additional or antagonistic effects of these various metabolites produced by the endophytic symbionts could potentially contribute to enhanced stress-resistance, survival and growth of the host plant.

Based on the obtained results, bacterial biosensors could be used in activity/inactivity type of screening with small concentrations of forest-derived extracts or preferably fractionated samples to reduce the possible complex sample matrix signal ambiguity effect and induction delay phenomenon. Additionally, the comparison between sample activities should only be done within measurements or after a statistically significant number of measurement replications.

The acquired results support the previous information about the endophytic fungi producing various bioactive metabolites. Endophytes are known to increase plant growth and stress resistance, while the underlying mechanism has not been fully established. The production of antioxidant and antimicrobial metabolites by the endophyte may partly contribute to the enhanced survival of the host. However, this proposition can only be established via co-cultivation studies with the symbiont and the host plant. With the vast number of metabolites which are present in the plant or fungus extracts, all compounds may synergistically affect the bioactive properties. Therefore, bioactivity cannot be attributed to only one effective compound even if it is found in high amounts in the extract.

Several ideas for future perspectives arise from the results of this study. Firstly, the growth media and nutrition sources were not optimized for the endophytic fungi used in this study. This optimization could increase bioactive metabolite production and even result in completely novel metabolites with interesting properties. The optimization process is often laborious and time consuming, but the benefits prevail these challenges. Secondly, extraction liquid should be evaluated for future applications. In order to obtain secondary and novel metabolites, ethanol could be evaluated as a reasonably safe alternative for water. This change should, however, be pondered thoroughly from the view of the subsequent test methodologies. For example, in the case of biosensor methodologies, the use of ethanol would create a need for further dilution of already small concentration samples when using fractionated extracts. Furthermore, the identification process would have been eased with the use of fragmentation and different m/z range parameters. This and the use of more comprehensive product libraries would have increased the number of identified metabolites as well as added confidence to the identified ones. Finally, in order to be able to say that the metabolite production in fact increases the host plant stress-resistance, co-cultivation studies should be conducted instead of using sterile mycelium.

The tremendous potential of bioactive metabolites produced by endophytic fungi is demonstrated in this thesis. However, the large-scale production of biomass and component purification are challenges, which need to be solved before the efficient

commercial scale use of bioactive compounds from endophytes is possible. Thus, future research on bioactive compound utilization could additionally lean towards molecular biology tools for determining the biological mechanisms behind bioactive metabolite production. These mechanisms could be transferred to fast-growing microbes that can be grown in large-scale reactors. For example, bioactive peptides could be produced using biotechnological tools and processes to meet increasing needs for various purposes in environmental, cosmetic, health and food industry applications.

REFERENCES

Abdalla MA, Matasyoh JC (2014). Endophytes as producers of peptides: an overview about the recently discovered peptides from endophytic microbes. *Natural Products and Bioprospecting*, 4: 257–270.

Alara OR, Abdurahman NH, Ukaegbu CI, Azhari NH, Kabbashi NA (2018). Metabolic profiling of flavonoids, saponins, alkaloids, and terpenoids in the extract from *Vernonia cinerea* leaf using LC-Q-TOF-MS. *Journal of Liquid Chromatography & Related Technologies*, 41: 722–731.

Aly AH, Debbab A, Kjer J, Proksch P (2010). Fungal endophytes from higher plants: a prolific source of phytochemicals and other bioactive natural products. *Fungal Diversity*, 41(1): 1–16.

Ames BN, Shigenaga MK, Hagen TM (1993). Oxidants, Antioxidants, and the Degenerative Diseases of Aging. *Proceedings of the National Academy of Sciences of the United States of America*, 90(17): 7915–7922.

Apel K, Hirt H (2004). Reactive oxygen species: metabolism, oxidative stress, and signal transduction. *Annual Review of Plant Biology*, 55: 373–399.

Arnold AE (2007). Understanding the diversity of foliar endophytic fungi: progress, challenges, and frontiers. *Fungal Biology Reviews*, 21(2): 51–66.

Bartholdy B, Berreck M, Haselwandter K (2001). Hydroxamate siderophore synthesis by *Phialocephala fortinii*, atypical dark septate fungal root endophyte. *BioMetals*, 14: 33–42.

Bartolome A, Bernadette M, Pastoral IL, Sevilla III F (2006). Antioxidant assay using genetically engineered bioluminescent *Escherichia coli*. In: Savitsky A, Wachter R (Eds.), *Proc. of SPIE Vol. 6098, Genetically Engineered Probes for Biomedical Applications*, San Jose, California, USA.

- Bashyal BP, Wijeratne EMK, Faeth SH, Gunatilaka AAL (2005). Globosumones A–C, cytotoxic orsellinic acid esters from the Sonoran desert endophytic fungus *Chaetomium globosum*. *Journal of Natural Products*, 68: 724–728.
- Beauchamp CJ, Chilton WS, Dion P, Antoun H (1990). Fungal catabolism of crown gall opines. *Applied and Environmental Microbiology*, 56(1): 150–155.
- Belkin S, Smulski DR, Vollmer AC, Van Dyk TK, LaRossa RA (1996a). Oxidative stress detection with *Escherichia coli* harboring a *katG':lux* fusion. *Applied and Environmental Microbiology*, 62: 2252–2256.
- Belkin S, Van Dyk TK, Vollmer AC, Smulski DR, LaRossa R (1996b). Monitoring subtoxic environmental hazards by stress-responsive luminous bacteria. *Environmental Toxicology and Water Quality*, 11: 179–185.
- Benzie IFF, Strain JJ (1996). The ferric reducing ability of Plasma (FRAP) as a measure of “antioxidant power”: the FRAP assay. *Analytical Biochemistry*, 239: 70–76.
- Bertrand S, Duval O, Helesbeux J-J, Larcher G, Richomme P (2010). Synthesis of the *trans*-fusarinine scaffold. *Tetrahedron Letters*, 51: 2119–2122.
- Bieganowski P, Brenner C (2004). Discoveries of nicotinamide riboside as a nutrient and conserved *NRK* genes establish a Preiss-Handler independent route to NAD⁺ in fungi and humans. *Cell*, 117: 495–502.
- Binder S (2010). Branched-chain amino acid metabolism in *Arabidopsis thaliana*. *The Arabidopsis book*, 8: e0137.
- Bogo A, Mantle PG, Casa RT, Guidolin AF (2006). The structures of the honeydew oligosaccharides synthesized by *Claviceps africana*. *Summa Phytopathologica*, 32: 16–20.
- Bohnert HJ, Jensen RG (1996). Strategies for engineering water-stress tolerance in plants. *Trends in Biotechnology* 14(3): 89–97.
- Boik J, Kirakosyan A, Kaufman PB, Seymour EM, Spelman K (2009). Interactions of bioactive plant metabolites: synergism, antagonism, and additivity. In: Kirakosyan

A, Kaufman PB (Eds.), Recent Advances in Plant Biotechnology, Chapter 10. Springer Science, New York, USA.

Bondaryk M, Staniszewska M, Zielinska P, Urbanczyk-Lipkowska Z (2017). Natural antimicrobial peptides as inspiration for design of a new generation antifungal compounds. *Journal of Fungi*, 3: 1–36.

Bähre H, Kaefer V (2014). Measurement of 2',3'-cyclic nucleotides by liquid chromatography–tandem mass spectrometry in cells. *Journal of Chromatography B*, 964: 208–211.

Carrasco-Castilla J, Hernández-Álvarez AJ, Jiménez-Martínez C, Jacinto-Hernández C, Alaiz M, Girón-Calle J, Vioque J, Dávila Ortiz G (2012). Antioxidant and metal chelating activities of peptide fractions from phaseolin and bean protein hydrolysates. *Food Chemistry*, 135: 1789–1795.

Cescutti P, Kallioinen A, Impallomeni G, Toffanin R, Pollesello P, Leisola M, Eerikäinen T (2005). Structure of the exopolysaccharide produced by *Enterobacter amnigenus*. *Carbohydrate Research*, 340: 439–447.

Chemat F, Vian MA, Ravi HK, Khadhraoui B, Hilali S, Perino S, Tixier AF (2019). Review of alternative solvents for green extraction of food and natural products: panorama, principles, applications and prospects. *Molecules*, 24: 3007.

Chen H-M, Muramoto K, Yamauchi F (1995). Structural analysis of antioxidative peptides from soybean β -conglycinin. *Journal of Agricultural and Food Chemistry* 43: 574–578.

Chen H-M, Muramoto K, Yamauchi F, Nokihara K (1996). Antioxidant activity of designed peptides based on the antioxidant peptide isolated from digests of a soybean protein. *Journal of Agricultural and Food Chemistry*, 44: 2619–2623.

Chen YC, Lin KYA, Lin CC, Lu TY, Lin YH, Lin CH, Chen KF (2019). Photoinduced antibacterial activity of NRC03 peptide-conjugated dopamine/nano-reduced graphene oxide against *Staphylococcus aureus*. *Photochemical & Photobiological Sciences*, 18: 2442–2448.

Cheng Q, Gu J, Compaan KR, Schaefer HF (2012) Isoguanine formation from adenine. *Chemistry: A European Journal*, 18: 4877–4886.

Chilton WS, Petit A, Chilton M-D, Dessaux Y (2001). Structure and characterization of the crown gall opines heliopine, vitopine and ridéopine. *Phytochemistry*, 58: 137–142.

Chow S-C (2014). Bioavailability and bioequivalence in drug development. *Wiley Interdisciplinary Reviews: Computational Statistics*, 6(4): 304–312.

Co M, Fagerlund A, Engman L, Sunnerheim K, Sjöberg PJR, Turner C (2012). Extraction of antioxidants from spruce (*Picea abies*) bark using eco-friendly solvents. *Phytochemical Analysis*, 23: 1–11.

Conze DB, Crespo-Barreto J, Kruger CL (2016). Safety assessment of nicotinamide riboside, a form of vitamin B₃. *Human and Experimental Toxicology*, 35(11): 1149–1160.

Cragg GM, Newman DJ (2013). Natural products: a continuing source of novel drug leads. *Biochimica et Biophysica Acta*, 1830(6): 3670–3695.

Cuendet M, Hostettmann K, Potterat O, Dyatmiko W (1997). Iridoid Glucosides with Free Radical Scavenging Properties from *Fagraea blumei*. *Helvetica Chimica Acta*, 80: 1144–1152.

Dai J, Krohn K, Draeger S, Schulz B (2009). New Naphthalene-Chroman Coupling Products from the Endophytic Fungus, *Nodulisporium* sp. from *Erica arborea*. *European Journal of Organic Chemistry*, 2009(10): 1564-1569.

Dang T, Süßmuth RD (2017). Bioactive peptide natural products as lead structures for medicinal use. *Accounts of Chemical Research*, 50: 1566–1576.

Danovaro R, Bongiorno L, Corinaldesi C, Giovannelli D, Damiani E, Astolfi P, Greci L, Pusceddu A (2008). Sunscreens cause coral bleaching by promoting viral infections. *Environmental Health Perspectives* 116: 441–447.

Demple B (1991). Regulation of bacterial oxidative stress genes. *Annual Review of Genetics*, 25: 315–337.

Demidchik V (2015). Mechanisms of oxidative stress in plants: From classical chemistry to cell biology. *Environmental and Experimental Botany*, 109: 212–228.

Desai SD, Desai DG, Kaur H (2009). Saponins and their biological activities. *Pharma Times*, 41(3): 13–16.

Desportes C, Charpentier M, Duteurtre B, Maujean A, Duchiron F (2000). Liquid chromatographic fractionation of small peptides from wine. *Journal of Chromatography A*, 893: 281–291.

Dias V, Junn E, Mouradian MM (2013). The role of oxidative stress in Parkinson's disease. *Journal of Parkinson's Disease*, 3: 461–491.

DiNardo J, Downs CA (2017). Dermatological and environmental toxicological impact of the sunscreen ingredient oxybenzone/benzophenone-3. *Journal of Cosmetic Dermatology*, 17: 15–19.

Dinesh S, Shikha G, Bhavana G, Nidhi S, Dileep S (2012). Biological activities of purine analogues: a review. *Journal of Pharmaceutical and Scientific Innovation*, 1(2): 29–34.

Dittmar F, Abdelilah-Seyfried S, Tschirner SK, Kaever V, Seifert R (2015). Temporal and organ-specific detection of cNMPs including cUMP in the zebrafish. *Biochemical and Biophysical Research Communications*, 468: 708–712.

Downs C, Kramarsky-Winter E, Segal R, Fauth J, Knutson S, Bronstein O, Ciner F, Jeger R, Lichtenfeld Y, Woodley C, Pennington P, Cadenas K, Kushmaro A, Lova Y (2016). Toxicopathological effects of the sunscreen UV filter, oxybenzone (Benzophenone-3), on coral planulae and cultured primary cells and its environmental contamination in Hawaii and the U.S. Virgin Islands. *Archives of Environmental Contamination and Toxicology*, 70: 265–288.

Dumont S, Rivoal J (2019). Consequences of oxidative stress on plant glycolytic and respiratory metabolism. *Frontiers in Plant Science*, 10: 166.

Dunn WB, Erban A, Weber RJM, Creek DJ, Brown M, Breiting R, Hankemeier T, Goodacre R, Neumann S, Kopka J, Viant MR (2013) Mass appeal: metabolite

identification in mass spectrometry-focused untargeted metabolomics. *Metabolomics* 9(1): 44–66.

Elad T, Lee JH, Belkin S, Gu MB (2008). Review: Microbial whole-cell arrays. *Microbial Biotechnology*, 1(2): 137–148.

El-Ganiny AM, Sheoran I, Sanders DA, Kaminskyj SG (2010). *Aspergillus nidulans* UDP-glucose-4-epimerase UgeA has multiple roles in wall architecture, hyphal morphogenesis, and asexual development. *Fungal Genetics and Biology*, 47: 629–635.

Engwa GA (2018). Free radicals and the role of plant phytochemicals as antioxidants against oxidative stress-related diseases. In: Asao T, Asaduzzaman M (Eds.), *Phytochemicals*, IntechOpen, DOI: 10.5772/intechopen.76719.

Ertl P, Schuhmann T (2019). A systematic cheminformatics analysis of functional groups occurring in natural products. *Journal of Natural Products*, 82: 1258–1263.

Farag MA, El-Kersh DM, Ehrlich A, Choucry MA, El-Seedi H, Frolov A, Wessjohann LA, Shokry M, Frolov A (2019). Variation in *Ceratonia siliqua* pod metabolome in context of its different geographical origin, ripening stage and roasting process. *Food Chemistry*, 283: 675–687.

Firáková S, Šturdíková M, Múčková M (2007). Bioactive secondary metabolites produced by microorganisms associated with plants. *Biologia*, 62(3): 251–257.

Fonteh AN, Harrington RJ, Harrington MG (2007). Quantification of free amino acids and dipeptides using isotope dilution liquid chromatography and electrospray ionization tandem mass spectrometry. *Amino acids*, 32: 203–212.

Franca MB, Panek AD, Eleutherio ECA (2007). Oxidative stress and its effects during dehydration. *Comparative Biochemistry and Physiology, Part A*, 146: 621–631.

Fricker RA, Green AL, Jenkins SI, Griffin SM (2018). The influence of nicotinamide on health and disease in the central nervous system. *International Journal of Tryptophan Research*, 11: 1–11.

Frisic M, Bucar F, Pilepic KH (2016). LC-PDA-ESI-MS analysis of phenolic and iridoid compounds from *Globularia* spp. *Journal of Mass Spectrometry*, 51: 1211–1236.

Fushiya S, Matsuda M, Yamada S, Nozoe S (1996). new opine type amino acids from a poisonous mushroom, *Clitocybe acromelalga*. *Tetrahedron*, 52(3): 877–886.

Galluzzi L, Karp M (2006). Whole cell strategies based on *lux* genes for high throughput applications toward new antimicrobials. *Combinatorial Chemistry & High Throughput Screening*, 9: 501–514.

Giffhorn F (2000). Fungal pyranose oxidases: occurrence, properties and biotechnical applications in carbohydrate chemistry. *Applied Microbiology and Biotechnology*, 54: 727–740.

Gill I, López-Fandiño R, Jorba X, Vulfson EN (1996). Biologically active peptides and enzymatic approaches to their production. *Enzyme and Microbial Technology*, 18: 162–183.

Glime JM (2017). Light: Effects of High Intensity. In: Glime JM. (Ed.), *Bryophyte Ecology*. Chapter 9-3. Volume 1. *Physiological Ecology*. Available at <http://digitalcommons.mtu.edu/bryophyte-ecology/>.

González-Menéndez V, Crespo G, de Pedro N, Diaz C, Martín J, Serrano R, Mackenzie TA, Justicia C, Reyes González-Tejero M, Casares M, Vicente F, Reyes F, Tormo JR, Genilloud O (2018). Fungal endophytes from arid areas of Andalucía: high potential sources for antifungal and antitumoral agents. *Nature Scientific Reports*, 8: 9729.

Gouda S, Das G, Sen SK, Shin H-S, Patra JK (2016). Endophytes: A treasure house of bioactive compounds of medicinal importance. *Frontiers in Microbiology*, 7: 1538.

Grass J, Pabst M, Kolarich D, Pörtl G, Léonard R, Brecker L, Altmann F (2010). Discovery and structural characterization of fucosylated oligomannosidic N-glycans in mushrooms. *Journal of Biological Chemistry*, 286: 5977–5984.

Greene R (2002). Oxidative stress and acclimation mechanisms in plants. The Arabidopsis Book, 1: e0036.

Grünig CR, Queloz V, Sieber TN, Holdenrieder O (2008). Dark septate endophytes (DSE) of the *Phialocephala fortinii* s.l. – *Acephala applanata* species complex in tree roots: Classification, population biology, and ecology. Botany, 86: 1355–1369.

Gu MB, Choi SH (2001). Monitoring and classification of toxicity using recombinant bioluminescent bacteria. Water Science and Technology, 43(2): 147–154.

Gui Q, Lawson T, Shan S, Yan L, Liu Y (2017). The application of whole cell-based biosensors for use in environmental analysis and in medical diagnostics. Sensors, 17: 1623.

Gunatilaka AAL (2006). Natural products from plant-associated microorganisms: distribution, structural diversity, bioactivity, and implications of their occurrence. Journal of Natural Products, 69(3): 509–526.

Gupta RK, Pramer D (1970). Metabolism of valine by the filamentous fungus *Arthrobotrys conoides*. Journal of Bacteriology, 103(1): 131–139.

Gutierrez RMP, Gonzalez AMN, Ramirez AM (2012). Compounds derived from endophytes: a review of phytochemistry and pharmacology. Current Medicinal Chemistry, 19(18): 2992–3030.

Guzman JD (2014). Natural cinnamic acids, synthetic derivatives and hybrids with antimicrobial activity. Molecules, 19: 19292–19349.

Haas H, Eisendle M, Turgeon BG (2008). Siderophores in fungal physiology and virulence. Annual Review of Phytopathology, 46: 149–187.

Hagihara M, Takei A, Ishii T, Hayashi F, Kubota K, Wakamatsu K, Nameki N (2012). Inhibitory effect of choline-*O*-sulfate on amyloid formation of human islet amyloid polypeptide. FEBS Open Bio 2: 20–25.

Harpaz D, Yeo LP, Cecchini F, Koon THP, Kushmaro A, Tok AIY, Marks RS, Eltzov E (2018). Measuring artificial sweeteners toxicity using a bioluminescent bacterial panel. Molecules, 23: 2454.

Harper JK, Arif AM, Ford EJ, Strobel GA, Porco Jr JA, Tomer DP, Oneill KL, Heider EM, Grant DM (2003). Pestacin: a 1,3-dihydro isobenzofuran from *Pestalotiopsis microspora* possessing antioxidant and antimycotic activities. *Tetrahedron*, 59(14): 2471–2476.

Hartono MR, Marks RS, Chen X, Kushmaro A (2014). Hybrid multi-walled carbon nanotubes-alginate-polysulfone beads for adsorption of bisphenol-A from aqueous solution. *Desalination and Water Treatment*, 1–17.

Hawksworth DL (2001). The magnitude of fungal diversity: the 1.5 million species estimate revisited. *Mycological Research*, 105(12): 1422–1432.

Hazra B, Biswas S, Mandal N (2008). Antioxidant and free radical scavenging activity of *Spondias pinnata*. *BMC complementary and alternative medicine*, 8(1): 63.

Hernández-Ledesma B, Dávalos A, Bartolomé B, Amigo L (2005). Preparation of antioxidant enzymatic hydrolysates from α -lactalbumin and β -lactoglobulin. Identification of active peptides by HPLC-MS/MS. *Journal of Agricultural and Food Chemistry*, 53: 588–593.

Hilchie AL, Wuerth K, Hancock REW (2013). Immune modulation by multifaceted cationic host defense (antimicrobial) peptides. *Nature Chemical Biology*, 9: 761–768.

Hill RA, Sutherland A (2017). Hot off the press. *Natural Product Reports*, 34: 338–342.

Holinsworth B, Martin JD (2009). Siderophore production by marine-derived fungi. *BioMetals*, 22: 625–632.

Huang Q, Tezuka Y, Kikuchi T, Nishi A, Tubaki K, Tanaka K (1995). Studies of metabolites of mycoparasitic fungi II. Metabolites of *Trichoderma koningii*. *Chemical and Pharmaceutical Bulletin*, 43(2): 223–229.

Huang D, Ou B, Hampsch-Woodill M, Flanagan JA, Prior RL (2002). High-throughput assay of oxygen radical absorbance capacity (ORAC) using a multichannel liquid handling system coupled with a microplate fluorescence reader in 96-well format. *Journal of Agricultural and Food Chemistry*, 50(16): 4437–4444.

Huang R-M, Chen Y-N, Zheng Z, Gao C-H, Su X, Peng Y (2014). Marine nucleosides: structure, bioactivity, synthesis and biosynthesis. *Marine Drugs*, 12: 5817–5838.

Huang H, Ullah F, Zhou D-X, Yi M, Zhao Y (2019). Mechanisms of ROS regulation of plant development and stress responses. *Frontiers in Plant Science*, 10: 800.

Hyde KD, Soyong K (2008). The fungal endophyte dilemma. *Fungal Diversity*, 33: 163–173.

Hyun MW, Yun YH, Kim JY, Kim SH (2011). Fungal and plant phenylalanine ammonia-lyase. *Mycobiology*, 39(4): 257–265.

Häkkinen S, Heinonen M, Kärenlampi S, Mykkänen H, Ruuskanen J, Törrönen R (1999). Screening of selected flavonoids and phenolic acids in 19 berries. *Food Research International*, 32: 345–353.

Ide N, Lau BHS, Ryu K, Matsuura H, Itakura Y (1999). Antioxidant effects of fructosyl arginine, a Maillard reaction product in aged garlic extract. *Journal of Nutritional Biochemistry*, 10: 372–376.

Ismailov, AD, Aleskerova LE (2015). Photobiosensors containing luminescent bacteria. *Biochemistry (Moscow)*, 80(6): 733–744.

Isono K (1988). Nucleoside antibiotics: structure, biological activity, and biosynthesis. *The Journal of Antibiotics*, XLI(12): 1711–1739.

Jackson CM, Esnouf MP, Winzor DJ, Duewer DL (2007). Defining and measuring biological activity: applying the principles of metrology. *Accreditation and Quality Assurance*, 12: 283–294.

Jaleel CA, Manivannan P, Sankar B, Kishorekumar A, Gopi R, Somasundaram R, Panneerselvam R (2007). Induction of drought stress tolerance by ketoconazole in *Catharanthus roseus* is mediated by enhanced antioxidant potentials and secondary metabolite accumulation. *Colloids and Surfaces B*, 60: 201–206.

Jayaprakasha GK, Mandadi KK, Poulouse SM, Jadegoud Y, Gowda GAN, Patil BS (2007). Inhibition of colon cancer cell growth and antioxidant activity of bioactive

compounds from *Poncirus trifoliata* (L.) Raf. Bioorganic & Medicinal Chemistry, 15: 4923–4932.

Jiang Z-Y, Woollard ACS, Wolff SP (1990). Hydrogen peroxide production during experimental protein glycation. FEBS 268: 69–71.

Joo K-M, Park C-W, Jeong H-J, Lee SJ, Chang IS (2008). Simultaneous determination of two Amadori compounds in Korean red ginseng (*Panax ginseng*) extracts and rat plasma by high-performance anion-exchange chromatography with pulsed amperometric detection. Journal of Chromatography B, 865: 159–166.

Jumpponen A, Trappe JM (1998). Dark septate endophytes: a review of facultative biotrophic root-colonizing fungi. New Phytologist, 140: 295–310.

Kaarniranta K, Ryhänen T, Karjalainen H, Lammi M, Suuronen T, Huhtala A, Kontkanen M, Teräsvirta M, Uusitalo H, Salminen A (2005). Geldanamycin increases 4-hydroxynonenal (HNE)-induced cell death in human retinal pigment epithelial cells. Neuroscience Letters, 382: 185–190.

Kajula M, Tejesvi MV, Kolehmainen S, Mäkinen A, Hokkanen J, Mattila S, Pirttilä A-M (2010). The siderophore ferricrocin produced by specific foliar endophytic fungi *in vitro*. Fungal Biology, 114: 248–254.

Kambhampati S, Li J, Evans BS, Allen DK (2019). Accurate and efficient amino acid analysis for protein quantification using hydrophilic interaction chromatography coupled tandem mass spectrometry. Plant Methods, 15: 46.

Kanchanapoom T, Kasai R, Yamasaki K (2002). Iridoid and phenolic glycosides from *Morinda coreia*. Phytochemistry, 59: 551–556.

Kang Y-A, Na J-I, Choi H-R, Choi J-W, Kang H-Y, Park K-C (2011). Novel anti-inflammatory peptides as cosmeceutical peptides. Peptides, 32: 2134–2136.

Karalkar NB, Khare K, Molt R, Benner SA (2017). Tautomeric equilibria of isoguanine and related purine analogs. Nucleosides, Nucleotides & Nucleic Acids, 31: 1–19.

Kariya M, Namiki H (1997). HPLC of phenylthiocarbonyl labelled uridine-diphosphate-hexosamine. *Chromatographia* 46: 5–11.

Kemp JD (1978). *In vivo* synthesis of crown gall-specific *Agrobacterium tumefaciens*-directed derivatives of basic amino acids. *Plant Physiology*, 62: 26–30.

Kim SW, Choi SH, Min J, Gu MB (2000). Toxicity of endocrine disrupting chemicals (EDCs) using freeze-dried recombinant bioluminescent bacteria. *Biotechnology and Bioprocess Engineering*, 5: 395–399.

Kim EJ, Seo HB, Gu MB (2019). Prescreening of natural products in drug discovery using recombinant bioluminescent bacteria. *Biotechnology and Bioprocess Engineering* 24: 264–271.

Kingston DGI (2011). Modern natural products drug discovery and its relevance to biodiversity conservation. *Journal of Natural Products*, 74(3): 496.

Kinnunen H, Huttunen S, Laakso K (2001). UV-absorbing compounds and waxes of Scots pine needles during a third growing season of supplemental UV-B. *Environmental Pollution*, 112: 215–220.

Klimanskaya I, Hipp J, Rezai KA, West M, Atala A, Lanza R (2004). Derivation and comparative assessment of retinal pigment epithelium from human embryonic stem cells using transcriptomics. *Cloning and stem cells*, 6(3): 217–245.

Kockler J, Oelgemöller M, Robertson S, Glass BD (2014). Influence of titanium dioxide particle size on the photostability of the chemical UV-filters butyl methoxy dibenzoylmethane and octocrylene in a microemulsion. *Cosmetics*, 1: 128–139.

Kombrink A, Tayyrov A, Essig A, Stöckli M, Micheller S, Hintze J, van Heuvel Y, Dürig N, Lin C-W, Kallio PT, Aebi M, Künzler M (2018). Induction of antibacterial proteins and peptides in the coprophilous mushroom *Coprinopsis cinerea* in response to bacteria. *ISME Journal*, 13: 588–602.

Koppenol WH, Hider RH (2019). Iron and redox cycling. Do's and don'ts. *Free Radical Biology and Medicine*, 133: 3–10.

Koskimäki JJ, Kajula M, Hokkanen J, Ihantola E-L, Kim JH, Hautajärvi H, Hankala E, Suokas M, Pohjanen J, Podolich O, Kozyrovska N, Turpeinen A, Pääkkönen M, Mattila S, Campbell BC, Pirttilä A-M (2016). Methyl-esterified 3-hydroxybutyrate oligomers protect bacteria from hydroxyl radicals. *Nature Chemical Biology*, 12(5): 332.

Krishnamurthy A, Rathinasabapathi B (2013). Oxidative stress tolerance in plants: Novel interplay between auxin and reactive oxygen species signaling. *Plant Signaling & Behavior*, 8(10): e25761.

Kurutas EB (2016). The importance of antioxidants which play the role in cellular response against oxidative/nitrosative stress: current state. *Nutrition Journal*, 15: 71.

Landi N, Pacifico S, Ragucci S, Di Giuseppe AM, Iannuzzi F, Zarrelli A, Piccolella S, Di Maro A (2017). Pioppino mushroom in southern Italy: An undervalued source of nutrients and bioactive compounds. *Journal of the Science of Food and Agriculture*, 97: 5388–5397.

Lappalainen J, Juvonen R, Nurmi J, Karp M (2001). Automated color correction method for *Vibrio fischeri* toxicity test. Comparison of standard and kinetic assays. *Chemosphere*, 45(4–5): 635–641.

Latva-Mäenpää H, Laakso T, Sarjala T, Wähälä K, Saranpää P (2013). Variation of stilbene glucosides in bark extracts obtained from roots and stumps of Norway spruce (*Picea abies* [L.] Karst.). *Trees-Structure and Function*, 27: 131–139.

Le Floc'h N, Otten W, Merlot E (2011). Tryptophan metabolism, from nutrition to potential therapeutic applications. *Amino Acids*, 41: 1195–1205.

Le Maux S, Nongonierma AB, FitzGerald RJ (2015). Improved short peptide identification using HILIC-MS/MS: retention time prediction model based on the impact of amino acid position in the peptide sequence. *Food Chemistry*, 173: 847–854.

Li C, Xue X, Zhou D, Zhang F, Xu Q, Ren L, Liang X (2008). Analysis of iridoid glucosides in *Hedyotis diffusa* by high-performance liquid chromatography/electrospray ionization tandem mass spectrometry. *Journal of Pharmaceutical and Biomedical Analysis*, 48: 205–211.

- Li P, Lu S, Shan T, Mou Y, Li Y, Sun W, Zhou L (2012). Extraction optimization of water-extracted mycelial polysaccharide from endophytic fungus *Fusarium oxysporum* Dzf17 by response surface methodology. *International Journal of Molecular Sciences* 13(5): 5441–5453.
- Li F, Lei C, Shen Q, Li L, Wang M, Guo M, Huang Y, Nie Z, Yao S (2013). Analysis of copper nanoparticles toxicity based on a stress-responsive bacterial biosensor array. *Nanoscale*, 5: 653–662.
- Li M, Chen T, Gao T, Miao Z, Jiang A, Shi L, Ren A, Zhao M (2015). UDP-glucose pyrophosphorylase influences polysaccharide synthesis, cell wall components, and hyphal branching in *Ganoderma lucidum* via regulation of the balance between glucose-1-phosphate and UDP-glucose. *Fungal Genetics and Biology*, 82: 251–263.
- Li X-Y, Wang Y-H, Yang J, Cui W-Y, He P-J, Munir S, He P-F, Wu Y-X, He Y-Q (2018a). Acaricidal activity of cyclopeptides from *Bacillus amyloliquefaciens* W1 against *Tetranychus urticae*. *Journal of Agriculture and Food Chemistry*, 66: 10163–10168.
- Li X, He X, Hou L, Ren Y, Wang S, Su F (2018b). Dark septate endophytes isolated from a xerophyte plant promote the growth of *Ammopiptanthus mongolicus* under drought condition. *Nature Scientific Reports*, 8: 7896.
- Liguori I, Russo G, Curcio F, Bulli G, Aran L, Della-Morte D, Gargiulo G, Testa G, Cacciotore F, Bonaduce D, Abete P (2018). Oxidative stress, aging and diseases. *Clinical Interventions in Aging*, 13: 757–772.
- Lin S-J, Guarente L (2003). Nicotinamide adenine dinucleotide, a metabolic regulator of transcription, longevity and disease. *Current Opinion in Cell Biology*, 15: 241–246.
- Ling S-K, Komorita A, Tanaka T, Fujioka T, Mihashi K, Kouno I (2002). Iridoids and Anthraquinones from the Malaysian Medicinal Plant, *Saprosma scortechinii* (Rubiaceae). *Chemical and Pharmaceutical Bulletin*, 50: 1035–1040.
- Lu J, Tian S, Lv X, Chen Z, Chen B, Zhu X, Cai Z (2018). TiO₂ nanoparticles in the marine environment: impact on the toxicity of phenanthrene and Cd²⁺ to marine zooplankton *Artemia salina*. *Science of the Total Environment*, 615: 375–380.

Mandyam K, Jumpponen A (2005). Seeking the elusive function of the root-colonizing dark septate endophytic fungi. *Studies of Mycology*, 53: 173–189.

Markham P, Robson GD, Bainbridge BW, Trinci APJ (1993). Choline: Its role in the growth of filamentous fungi and the regulation of mycelial morphology. *FEMS Microbiology Reviews*, 104: 287–300.

Martín J, Kuskoski EM, Navas MJ, Asuero AG (2017). Antioxidant Capacity of Anthocyanin Pigments, Flavonoids - From Biosynthesis to Human Health, Goncalo C. Justino, Eds., IntechOpen, DOI: 10.5772/67718. Available from: <https://www.intechopen.com/books/flavonoids-from-biosynthesis-to-human-health/antioxidant-capacity-of-anthocyanin-pigments>

Maruyama D, Nishitani Y, Nonaka T, Kita A, Fukami TA, Mio T, Yamada-Okabe H, Yamada-Okabe T, Miki K (2007). Crystal structure of uridine-diphospho-N-acetylglucosamine pyrophosphorylase from *Candida albicans* and catalytic reaction mechanism. *Journal of Biological Chemistry*, 282: 17221–17230.

Meisner P, Gebicki JL (2009). Determination of hydroperoxides in aqueous solutions containing surfactants by the ferrous oxidation-xylenol orange method. *Acta Biochimica Polonica*, 56(3): 523–527

Michelini E, Leskinen P, Virta M, Karp M, Roda A (2005). A new recombinant cell-based bioluminescent assay for sensitive androgen-like compound detection. *Biosensors and Bioelectronics*, 20: 2261–2267.

Miller G, Suzuki N, Ciftci-Yilmaz S, Mittler R (2010). Reactive oxygen species homeostasis and signaling during drought and salinity stresses. *Plant, Cell and Environment*, 33: 453–467.

Min J, Kim EJ, LaRossa RA, Gu MB (1999). Distinct responses of a *recA::luxCDABE Escherichia coli* strain to direct and indirect DNA damaging agents. *Mutation Research*, 442: 61–68.

Min J, Gu MB (2004). Adaptive responses of *Escherichia coli* for oxidative and protein damage using bioluminescence reporters. *Journal of Microbiology and Biotechnology*, 14(3): 466–469.

Mousa WK, Raizada MN (2013). The diversity of anti-microbial secondary metabolites produced by fungal endophytes: an interdisciplinary perspective. *Frontiers in Microbiology*, 4: 65.

Mullineaux P, Ball L, Escobar C, Karpinska B, Creissen G, Karpinski S (2000). Are diverse signalling pathways integrated in the regulation of *Arabidopsis* antioxidant defence gene expression in response to excess excitation energy? *Philosophical transactions of the Royal Society of London. Series B, Biological sciences*, 355(1402): 1531–1540.

Nagabhyru P, Dinkins RD, Wood CL, Bacon CW, Schardl CL (2013). Tall fescue endophyte effects on tolerance to water-deficit stress. *BMC plant biology*, 13: 127.

Nain-Perez A, Barbosa LCA, Maltha CRÁ, Forlani G (2017). Natural abenquines and their synthetic analogues exert algicidal activity against bloom-forming cyanobacteria. *Journal of Natural Products*, 80: 813–818.

Nakano T, Sugimoto S, Matsunami K, Otsuka H (2011). Dianthosaponins A—F, triterpene saponins, flavonoid glycoside, aromatic amide glucoside and γ -pyrone glucoside from *Dianthus japonicus*. *Chemical & Pharmaceutical Bulletin*, 59: 1141–1148.

Neill SJ, Desikan R, Hancock JT (2003). Nitric oxide signaling in plants. *New Phytologist*, 159: 11–35.

Newman DJ, Cragg GM (2016). Natural products as sources of new drugs from 1981 to 2014. *Journal of Natural Products*, 79: 629–661.

Nisa H, Kamili AN, Nawchoo IA, Shafi S, Shameem N, Bandh SA (2015). Fungal endophytes as prolific source of phytochemicals and other bioactive natural products: a review. *Microbial Pathogenesis*, 82: 50–59.

Nongonierma AB, FitzGerald RJ (2015). Milk proteins as a source of tryptophan-containing bioactive peptides. *Food & Function*, 6: 2115.

Obata T, Fernie AR (2012). The use of metabolomics to dissect plant responses to abiotic stresses. *Cellular and Molecular Life Sciences*, 69: 3225–3243.

O'Brien HE, Parrent JL, Jackson JA, Moncalvo J, Vilgalys R (2005). Fungal community analysis by large-scale sequencing of environmental samples. *Applied and Environmental Microbiology*, 71(9): 5544–5550.

Ollanketo M, Peltoketo A, Hartonen K, Hiltunen R, Riekkola M-L (2002). Extraction of sage (*Salvia officinalis* L.) by pressurized hot water and conventional methods: antioxidant activity of the extracts. *European Food Research and Technology*, 215: 158–163.

Osugi A, Sakakibara H (2015) Q&A: How do plants respond to cytokinins and what is their importance? *BMC Biology*, 13: 102.

Ozden M, Demirel U, Kahraman A (2009). Effects of proline on antioxidant system in leaves of grapevine (*Vitis vinifera* L.) exposed to oxidative stress by H₂O₂. *Scientia Horticulturae*, 119: 163–168.

Payne DJ, Gwynn MN, Holmes DJ, Pompliano DL (2007). Drugs for bad bugs: confronting the challenges of antibacterial discovery. *Nature Reviews, Drug discovery*, 6(1): 29–40.

Pham CH, Min J, Gu MB (2004). Pesticide induced toxicity and stress response in bacterial cells. *Bullet of Environmental Contamination and Toxicology*, 72: 380–386.

Pirttilä AM (2011). Endophytic bacteria in tree shoot tissues and their effects on host. In: Pirttilä AM, Frank AC (Eds.), *Endophytes of Forest Trees: Biology and Applications*, Forestry Sciences Vol. 80, Heidelberg: Springer Verlag: 139–149.

Pocsi I, Prade RA, Penninckx MJ (2004). Glutathione, Altruistic metabolite in fungi. *Advances in Microbial Physiology*, 49.

Poljsak B, Dahmane R, Godic A (2013). Skin and antioxidants. *Journal of Cosmetic and Laser Therapy*. 15(2): 107–113.

Prior SL, Cunliffe BW, Robson GD, Trinci APJ (1993). Multiple isomers of phosphatidyl inositol monophosphate and inositol bis- and trisphosphates from filamentous fungi. *FEMS Microbiology Letters*, 110: 147–152.

Prior RL, Hoang H, Gu L, Wu X, Bacchiocca M, Howard L, Hampsch-Woodill M, Huang D, Ou B, Jacob R (2003). Assays for hydrophilic and lipophilic antioxidant capacity (oxygen radical absorbance capacity (ORAC)) of plasma and other biological and food samples. *Journal of Agricultural and Food Chemistry*, 51: 3273–3279

Puupponen-Pimiä R, Nohynek L, Juvonen R, Kössö T, Truchado P, Westerlund-Wikström B, Leppänen T, Moilanen E, Oksman-Caldentey K-M (2016). Fermentation and dry fractionation increase bioactivity of cloudberry (*Rubus chamaemorus*). *Food Chemistry*, 197(15):950–958.

Quan LJ, Zhang B, Shi WW, Li HY (2008). Hydrogen peroxide in plants: a versatile molecule of the reactive oxygen species network. *Journal of Integrative Plant Biology* 50(1): 2–18.

van der Rest B, Boisson A-M, Gout E, Bligny R, Douce R (2002). Glycerophosphocholine metabolism in higher plant cells. Evidence of a new glyceryl-phosphodiester phosphodiesterase. *Plant Physiology*, 130: 244–255.

Richter Y, Fischer B (2006). Nucleotides and inorganic phosphates as potential antioxidants. *Journal of Biological Inorganic Chemistry*, 11: 1063.

Ries S, Wert V, O’Leary NFD, Nair M (1990). 9- β -L(+) Adenosine: A new naturally occurring plant growth substance elicited by triacontanol in rice. *Plant Growth Regulation*, 9: 263–273.

Rivoal J, Hanson AD (1994). Choline-O-sulfate biosynthesis in plants. *Plant Physiology*, 106: 1187–1193.

Rodriguez RJ, White JF, Arnold AE, Redman RS (2009). Fungal endophytes: diversity and functional roles. *The New Phytologist*, 182(2): 314–330.

Ruble PA, Merkel SM, Faust MA, Miklas J (1984). Distribution and activity of bacteria in the headwaters of the Rhode River Estuary, Maryland, USA. *Microbial Ecology*, 10: 243–255.

Ryu K, Ide N, Matsuura H, Itakura Y (2001). N α -(1-Deoxy-D-fructos-1-yl)-L-Arginine, an antioxidant compound identified in aged garlic extract. *The Journal of Nutrition*, 131: 972S–976S.

Saiga A, Tanabe S, Nishimura T (2003). Antioxidant activity of peptides obtained from porcine myofibrillar proteins by protease treatment. *Journal of Agricultural and Food Chemistry*, 51: 3661–3667.

Salas CE, Badillo-Corona JA, Ramirez-Sotelo G, Oliver-Salvador C (2015). Biologically active and antimicrobial peptides from plants. *Biomed Research International*, 102129.

Samaranayaka AGP, Li-Chan ECY (2011). Food-derived peptidic antioxidants: a review of their production, assessment, and potential applications. *Journal of Functional Foods*, 3: 229–254.

Sánchez A, Vázquez A (2017). Bioactive peptides: A review. *Food quality and safety*, 1: 29–46.

Sang X-N, Chen S-F, Chen G, An X, Li S-G, Lu X-J, Zhao D, Bai J, Wang H-F, Pei Y-H (2017). Two pairs of enantiomeric α -pyrone dimers from the endophytic fungus *Phoma* sp. YN02-P-3. *RSC Advances*, 7: 1943–1946.

Santos-Sánchez NF, Salas-Coronado R, Villanueva-Cañongo C, Hernández-Carlos B (2019). Antioxidant compounds and their antioxidant mechanism. *IntechOpen*, DOI: 10.5772/intechopen.85270.

Savka MA, Black RC, Binns AN, Farrand SK (1996). Translocation and exudation of tumor metabolites in crown galled plants. *Molecular Plant-Microbe Interactions*, 9(4): 310–313.

Schulz B, Boyle C, Draeger S, Römmert A, Krohn K (2002). Endophytic fungi: a source of novel biologically active secondary metabolites. *Mycological Research*, 106(9): 996–1004.

Schulz B (2006). Mutualistic interactions with fungal root endophytes. In: Schulz BJE, Boyle CJC, Sieber TN (Eds.), *Microbial Root Endophytes*, 1st edition; Springer Science & Business Media: Berlin, Germany, pp. 261–279.

Schulz D, Beese P, Ohlendorf B, Erhard A, Zinecker H, Dorador C, Imhoff JF (2011). Abenquines A–D: aminoquinone derivatives produced by *Streptomyces* sp. strain DB634. *The Journal of Antibiotics*, 64: 763–768.

Schlörke O, Zeeck A (2006). Orsellides A–E: an example for 6-deoxyhexose derivatives produced by fungi. *European Journal of Organic Chemistry* 2006: 1043–1049.

Scott B (2001). Epichloë endophytes: fungal symbionts of grasses. *Current Opinion in Microbiology*, 4(4): 393–398.

Seifert R (2016). Distinct Signaling Roles of cIMP, cCMP, and cUMP. *Structure*, 24: 1627–1628.

Semighini CP, Savoldi M, Goldman GH, Harris SD (2006). Functional characterization of the putative *Aspergillus nidulans* poly(ADP-ribose) polymerase homolog PrpA. *Genetics*, 173: 87–98.

Shashidhar MG, Giridhar P, Udaya Sankar K, Manohar B (2013). Bioactive principles from *Cordyceps sinensis*: a potent food supplement – a review. *Journal of Functional Foods*, 5: 1013–1030.

Sommart U, Rukachaisirikul V, Sukpondma Y, Phongpaichit S, Sakayaroj J, Kirtikara K (2008). Hydronaphthalenones and a dihydroramulosin from the endophytic fungus PSU-N24. *Chemical & Pharmaceutical Bulletin*, 56: 1687–1690.

Song YC, Huang WY, Sun C, Wang FW, Tan RX (2005). Characterization of Graphislactone A as the Antioxidant and Free Radical-Scavenging Substance from the Culture of *Cephalosporium* sp. IFB-E001, an Endophytic Fungus in *Trachelospermum jasminoides*. *Biological and Pharmaceutical Bulletin*, 28(3): 506–509.

Sowndhararajan K, Kang SC (2012). Free radical scavenging activity from different extracts of leaves of *Bauhinia vahlia* Wight & Arn. *Saudi Journal of Biological Sciences*, 20: 319–325.

Spencer B, Hussey EC, Orsi BA, Scott JM (1968). Mechanism of choline O-sulphate utilization in fungi. *Biochemical Journal*, 106: 461–469.

Stevanato R, Bertelle M, Fabris S (2014). Photoprotective characteristics of natural antioxidant polyphenols. *Regulatory Toxicology and Pharmacology* 69: 71–77.

Stomp A-M, Loopstra C, Chilton WS, Sederoff RR, Moore LW (1990). Extended host range of *Agrobacterium tumefaciens* in the genus *Pinus*. *Plant Physiology*, 92: 1226–1232.

Stone J, Bacon C, White J (2000). An Overview of Endophytic Microbes: Endophytism defined. In: Bacon CW and White JF Jr. (Eds.), *Microbial endophytes*, Marcel Dekker Inc., New York, USA, pp. 3–29.

Strobel G, Ford E, Worapong J, Harper JK, Arif AM, Grant DM, Fung PCW, Ming Wah Chau R (2002). Isopestacin, an isobenzofuranone from *Pestalotiopsis microspora*, possessing antifungal and antioxidant activities. *Phytochemistry*, 60(2): 179–183.

Strobel GA (2003). Endophytes as sources of bioactive products. *Microbes and Infection*, 5: 535–544.

Strobel G, Daisy B, Castillo U, Harper J (2004). Natural products from endophytic microorganisms. *Journal of Natural Products*, 67(2): 257–268.

Strobel G (2018). The emerge of endophytic microbes and their biological promise. *Journal of Fungi*, 4: 57.

Su L, Jia W, Hou C, Lei Y (2011). Microbial biosensors: A review. *Biosensors and Bioelectronics*, 26: 1788–1799.

Sulyok M, Beed F, Boni S, Abass A, Mukunzi A, Krska R (2015). Quantitation of multiple mycotoxins and cyanogenic glucosides in cassava samples from Tanzania and Rwanda by an LC-MS/MS-based multi-toxin method. *Food Additives & Contaminants: Part A*, 32: 488–502.

Sumner LW, Amberg A, Barrett D, Beale MH, Beger R, Daykin CA, Fan TW-M, Fiehn O, Goodacre R, Griffin JL, Hankemeier T, Hardy N, Harnly J, Higashi R, Kopka J, Lane AN, Lindon JC, Marriott P, Nicholls AW, Reily MD, Thaden JJ, Viant MR (2007). Proposed minimum reporting standards for chemical analysis chemical analysis working group (CAWG) metabolomics standards initiative (MSI). *Metabolomics*, 3(3): 211–221.

- Surono, Narisawa K (2017). The dark septate endophytic fungus *Phialocephala fortinii* is a potential decomposer of soil organic compounds and a promoter of *Asparagus officinalis* growth. *Fungal Ecology*, 28: 1–10.
- Surono, Narisawa K (2018). The inhibitory role of dark septate endophytic fungus *Phialocephala fortinii* against Fusarium disease on the *Asparagus officinalis* growth in organic source conditions. *Biological Control*, 121: 159–167.
- Swiezawska B, Duszyn M, Jaworski K, Szmidt-Jaworska A (2018). Downstream Targets of Cyclic Nucleotides in Plants. *Frontiers in Plant Science*, 9: 9.
- Tan RX, Zou WX (2001). Endophytes: a rich source of functional metabolites. *Natural Product Reports*, 18(4): 448–459.
- Tanaka A, Christensen MJ, Takemoto D, Park P, Scott B (2006). Reactive Oxygen Species Play a Role in Regulating a Fungus-Perennial Ryegrass Mutualistic Interaction. *The Plant Cell*, 18(4): 1052–1066.
- Tellenbach C, Sumarah MW, Grünig CR, Miller JD (2013). Inhibition of *Phytophthora* species by secondary metabolites produced by the dark septate endophyte *Phialocephala europaea*. *Fungal Ecology*, 6: 12–18.
- Terhonen E, Keriö S, Sun H, Asiegbu FO (2014). Endophytic fungi of Norway spruce roots in boreal pristine mire, drained peatland and mineral soil and their inhibitory effect on *Heterobasidion parviporum* *in vitro*. *Fungal Ecology*, 9: 17–26.
- Thaipong K, Boonprakob U, Crosby K, Cisneros-Zevallos L, Byrne DH (2006). Comparison of ABTS, DPPH, FRAP, and ORAC assays for estimating antioxidant activity from guava fruit extracts. *Journal of Food Composition and Analysis*, 19: 669–675.
- Tienaho J, Sarjala T, Franzén R, Karp M (2015). Method with high-throughput screening potential for antioxidative substances using *Escherichia coli* biosensor *katG::lux*. *Journal of Microbiological Methods*, 118: 78–80.
- Tienaho J, Poikulainen E, Sarjala T, Muilu-Mäkelä R, Santala V, Karp M (2018). A bioscreening technique for ultraviolet irradiation protective natural substances. *Photochemistry and Photobiology*, 94: 1273–1280.

- Tienaho J, Karonen M, Muilu-Mäkelä R, Wähälä K, Leon Denegri E, Franzén R, Karp M, Santala V, Sarjala T (2019). Metabolic Profiling of Water-Soluble Compounds from the Extracts of Dark Septate Endophytic Fungi (DSE) Isolated from Scots Pine (*Pinus sylvestris* L.) Seedlings Using UPLC-Orbitrap-MS. *Molecules*, 24: 2330.
- Ventola CL (2015). The antibiotic resistance crisis, Part 1: Causes and threats. *Pharmacy and Therapeutics*, 40(4): 277–283.
- Vergara C, Araujo KEC, Alves LS, Souza SR, Santos LA, Santa-Catarina C, Silva KD, Pereira GMD, Xavier GR, Zilli JÉ (2018). Contribution of dark septate fungi to the nutrient uptake and growth of rice plants. *Brazilian Journal of Microbiology*, 49: 67–78.
- Vermaak I, Hamman JH, Viljoen AM (2011). Hoodia gordonii: an up-to-date review of a commercially important anti-obesity plant. *Planta Medica*, 77: 1149–1160.
- Vollmer A, Belkin S, Smulski D, Van Dyk T, LaRossa R (1997). Detection of DNA damage by use of *Escherichia coli* carrying *recA'::lux*, *uvrA'::lux*, or *alkA'::lux* reporter plasmids. *Applied and Environmental Microbiology*, 63: 2566–2571.
- Wagner GK, Pesnot T, Field RA (2009). A survey of chemical methods for sugar-nucleotide synthesis. *Natural Product Reports*, 26: 1172–1194.
- Walker V, Mills GA (1995). Quantitative methods for amino acid analysis in biological fluids. *Annals of Clinical Biochemistry*, 32: 28–57.
- Waller F, Achatz B, Baltruschat H, Fodor J, Becker K, Fischer M, Heier T, Hückelhoven R, Neumann C, von Wettstein D, Franken P, Kogel K (2005). The endophytic fungus *Piriformospora indica* reprograms barley to salt-stress tolerance, disease resistance, and higher yield. *Proceedings of the National Academy of Sciences of the United States of America*, 102(38): 13386–13391.
- Wang X, Chen R, Sun L, Yu Z (2014). Study of the antioxidant capacities of four antioxidants based on oxidizing guanine in a composite membrane. *International Journal of Electrochemical Science*, 9: 6834–6842.

- Wang Q, Huang Y, Qin C, Liang M, Mao X, Li S, Zou Y, Jia W, Li H, Ma CW, Huang Z (2016a). Bioactive peptides from *Angelica sinensis* protein hydrolysate delay senescence in *Caenorhabditis elegans* through antioxidant activities. *Oxidative Medicine and Cellular Longevity*, 2016: 3956931.
- Wang R, Ding S, Zhao D, Wang Z, Wu J, Hu X (2016b). Effect of dehydration methods on antioxidant activities, phenolic contents, cyclic nucleotides, and volatiles of jujube fruits. *Food Science and Biotechnology*, 25(1): 137–143.
- Wang X, Lin M, Xu D, Lai D, Zhou L (2017a). Structural diversity and biological activities of fungal cyclic peptides, excluding cyclodipeptides. *Molecules*, 22: 2069.
- Wang Q, Wang F, Xu Z, Ding Z (2017b). Bioactive mushroom polysaccharides: a review on monosaccharide composition, biosynthesis and regulation. *Molecules*, 22: 955.
- Waqas M, Khan AL, Lee I-J (2014). Bioactive chemical constituents produced by endophytes and effects on rice plant growth. *Journal of Plant Interactions*, 9(1): 478–487.
- Watt K, Christofi N, Young R (2007). The detection of antibacterial actions of whole herb tinctures using luminescent *Escherichia coli*. *Phytotherapy Research*, 21: 1193–1199.
- White JF, Kingsley KL, Zhang Q, Verma R, Obi N, Dvinskikh S, Elmore MT, Verma SK, Gond SK, Kowalski KP (2019). Review: Endophytic microbes and their potential applications in crop management. *Pest Management Science*, 75: 2558–2565.
- Willför SM, Ahotupa MO, Hemming JE, Reunanen MH, Eklund PC, Sjöholm RE, Eckerman CS, Pohjamo SP, Holmbom BR (2003). Antioxidant activity of knotwood extractives and phenolic compounds of selected tree species. *Journal of Agricultural and Food Chemistry*, 51: 7600–7606.
- Wilson D (1995). Endophyte: The Evolution of a Term, and Clarification of Its Use and Definition. *Oikos*, 73(2): 274–276.

Wilson DW, Nash P, Buttar HS, Griffiths K, Singh R, De Meester F, Horiuchi R, Takahashi T (2017). The role of food antioxidants, benefits of functional foods, and influence of feeding habits on the health of the older person: an overview. *Antioxidants*, 6: 81.

Winter G, Todd CD, Trovato M, Forlani G, Funck D (2015). Physiological implications of arginine metabolism in plants. *Frontiers in Plant Science*, 6: 534.

Wolfe BE (2018). Using cultivated microbial communities to dissect microbiome assembly: challenges, limitations, and the path ahead. *mSystems*, 3: e00161-17.

Wright GD (2014). Something old, something new: revisiting natural products in antibiotic drug discovery. *Canadian Journal of Microbiology*, 60: 147–154.

Wu Q, Wang Y, Guo M (2011). Triterpenoid saponins from the seeds of *Celosia argentea* and their anti-inflammatory and antitumor activities. *Chemical & Pharmaceutical Bulletin*, 59: 666–671.

Wu S, Hu J, Wei L, Du Y, Shi X, Zhang L (2014). Antioxidant and antimicrobial activity of Maillard reaction products from xylan with chitosan/ chitooligomer/ glucosamine hydrochloride/ taurine model systems. *Food Chemistry*, 148: 196–203.

Xu H, Andi B, Qian J, West AH, Cook PF (2006). The α -amino adipate pathway for lysine biosynthesis in fungi. *Cell Biochemistry and Biophysics*, 46: 43–64.

Xu G-B, Wang N-N, Bao J-K, Yang T, Li G-Y (2014). New orsellinic acid esters from fungus *Chaetomium globosporum*. *Helvetica Chimica Acta*, 97: 151–159.

Yahya NA, Attan N, Wahab RA (2018). An overview of cosmeceutically relevant plant extracts and strategies for extraction of plant based bioactive compounds. *Food and Bioproducts Processing*, 112: 69–85.

Yoshida Y, Kiyosue T, Nakashima K, Yamaguchi-Shinozaki K, Shinozaki K (1997). Regulation of levels of proline as an osmolyte in plants under water stress. *Plant and Cell Physiology*, 38(10): 1095–1102.

Yoshida N, Takatsuka K, Katsuragi T, Tani Y (2005). Occurrence of fructosyl-amino acid oxidase-reactive compounds in fungal cells. *Bioscience, Biotechnology, and Biochemistry*, 69(1): 258–260.

Yoshida T, Amakura Y, Yoshimura M (2010) Structural features and biological properties of ellagitannins in some plant families of the order Myrtales. *International Journal of Molecular Sciences*, 11: 79–106.

Zhang HW, Song YC, Tan RX (2006). Biology and chemistry of endophytes. *Natural Product Reports*, 23: 753–771.

Zhang M, Swarts SG, Yin L, Liu C, Tian Y, Cao Y, Swarts M, Yang S, Zhang SB, Zhang K, Ju S, Olek DJ, Schwartz L, Keng PC, Howell R, Zhang L, Okunieff P (2011a). Antioxidant Properties of Quercetin. In: LaManna J, Puchowicz M, Xu K, Harrison D, Bruley D (Eds.), *Oxygen Transport to Tissue XXXII. Advances in Experimental Medicine and Biology*, vol. 701. Springer, Boston, MA

Zhang J, Yu Y, Zhang Z, Ding Y, Dai X, Li Y (2011b). Effect of polysaccharide from cultured *Cordyceps sinensis* of immune function and anti-oxidation activity of mice exposed to ⁶⁰Co. *International Immunopharmacology*, 11: 2251–2257.

Zhao J, Zhou L, Wang J, Shan T, Zhong L, Liu X, Gao X (2010). Endophytic fungi for producing bioactive compounds originally from their host plants. In: Méndez-Vilas A (Ed.), *Current Research, Technology and Education Topics in Applied Microbiology and Microbial Biotechnology*, No.2, Vol.1, Formatex Research Center, Badajoz, Spain.

Zhu Y, Yao Y, Shi Z, Everaert N, Ren G (2018). Synergistic effect of bioactive anticarcinogens from soybean on anti-proliferative activity in MDA-MB-231 and MCF-7 human breast cancer cells *in vitro*. *Molecules*, 23: 1557.

PUBLICATIONS

PUBLICATION

I

**Method with High-Throughput Screening Potential for Antioxidative
Substances Using *Escherichia coli* Biosensor *katG*'::*lux***

Jenni Tienaho, Tytti Sarjala, Robert Franzén and Matti Karp

Journal of Microbiological Methods, 118, pp. 78–80
<http://dx.doi.org/10.1016/j.mimet.2015.08.018>

**Reprinted with the kind permission from the Journal of Microbiological
Methods. © 2015 Elsevier.**



Note

Method with high-throughput screening potential for antioxidative substances using *Escherichia coli* biosensor *katG':lux*Jenni Tienaho^{a,b,*}, Tytti Sarjala^b, Robert Franzén^a, Matti Karp^a^a Department of Chemistry and Bioengineering, Tampere University of Technology, Korkeakoulunkatu 8, FI-33101 Tampere, Finland^b Natural Resources Institute Finland (Luke), Parkano Research Unit, Kaironiementie 15, FI-39700 Parkano, Finland

ARTICLE INFO

Article history:

Received 16 June 2015

Received in revised form 19 August 2015

Accepted 24 August 2015

Available online 29 August 2015

Keywords:

Antioxidative activity

Bacterial biosensor

Bioscreening

Microplate technique

ABSTRACT

A new method is described for the rapid real-time screening of antioxidative properties using a recombinant *Escherichia coli* DPD2511 biosensor. This microplate technique, without time-consuming pre-incubations and handling, has potential for a high-throughput search of bioactive compounds. Special emphasis was given to obtaining highly reliable and repeatable results.

© 2015 Elsevier B.V. All rights reserved.

When using intact living biosensors, both bioactivity and bioavailability of a chosen sample material can be detected simultaneously in a simple, cost-effective and rapid manner, which makes the assays more suitable for high-throughput screening (HTS) (Galluzzi and Karp, 2006). These effects can be monitored continuously and without long incubation or handling times. The *Escherichia coli* strain DPD2511 (Belkin et al., 1996) has been constructed by fusing the *katG* (catalase) genes of the strain to the luminescence (*lux*) genes from the *Vibrio fischeri* bacteria. The bioavailable oxidant is able to enter through the *E. coli* cell membrane and bind to the regulatory protein OxyR which promotes the transcription and translation of the reporter genes. With the *lux* gene fusion this produces an increase in luminescent light emission, which can be measured and quantified in a continuous manner (Michellini et al., 2005). Thus, the normal defense mechanism signaling against oxidizing agents produces an easily monitored response. When antioxidative activity is measured, the bacteria are exposed to an oxidant such as hydrogen peroxide (H_2O_2), and the experiment is set to measure whether samples prevent the stress reaction. In other words the method measures the inhibition capacity of the antioxidant against H_2O_2 . The strain was used to screen antioxidative properties of medicinal plants used in the Philippines and validated against the DPPH assay by Bartolome et al. (2006). We describe a microplate technique of the screening method with an improved HTS potential.

The bacteria were preserved in 15% glycerol at $-80\text{ }^\circ\text{C}$. Working stock was prepared by inoculating Luria Agar growth-plates supplemented with $100\text{ }\mu\text{g/ml}$ of ampicillin and 10 vol.% of 1 M potassium phosphate buffer. The plates were cultivated overnight at $30\text{ }^\circ\text{C}$ before storing in $4\text{ }^\circ\text{C}$. Cultivations were discarded after a week from inoculation as they lose their sensitivity during prolonged storing (Kim and Gu, 2003). A single colony of the strain was inoculated into 5 ml of liquid Luria Broth medium supplemented with $100\text{ }\mu\text{g/ml}$ of ampicillin and 10 vol.% of 1 M potassium phosphate buffer and incubated for approximately 16 h in a shaker at $30\text{ }^\circ\text{C}$ and 300 rpm, after which the luminescence was measured with a Chameleon Multilabel (Hidex Oy, Finland) microplate reader. The cell culture producing the highest signal was chosen for the measurement.

For the assay with H_2O_2 , $100\text{ }\mu\text{l}$ of the chosen cell culture was added to each well of an opaque white microplate (Thermo Electron Corporation, Finland) containing $50\text{ }\mu\text{l}$ of fourfold dilutions of the H_2O_2 and $50\text{ }\mu\text{l}$ of sterile water. Sterile water was also used as a negative control. Luminescence was measured in counts per seconds (CPS) 20 times every 5 min and between the screenings the plate was shaken and kept at $30\text{ }^\circ\text{C}$. CPS values vary depending on the date and chosen culture. Thus, the results are expressed in induction factors (FI) calculated by dividing the CPS values of the samples by the value of the negative control. For the ascorbic acid (AA) measurements, a constant concentration of 4 mM of H_2O_2 was used in each well and $50\text{ }\mu\text{l}$ of sterile water was replaced with AA concentrations in the 1 M potassium phosphate buffer. Sterile water with the phosphate buffer was used as the negative control.

Tryptone, yeast extract and agar were obtained from Lab M Limited, UK. Sodium salt of ampicillin was obtained from Sigma-Aldrich, USA.

* Corresponding author.

E-mail addresses: jenni.tienaho@tut.fi, jenni.tienaho@luke.fi (J. Tienaho), tytti.sarjala@luke.fi (T. Sarjala), robert.franzen@tut.fi (R. Franzén), matti.karp@tut.fi (M. Karp).

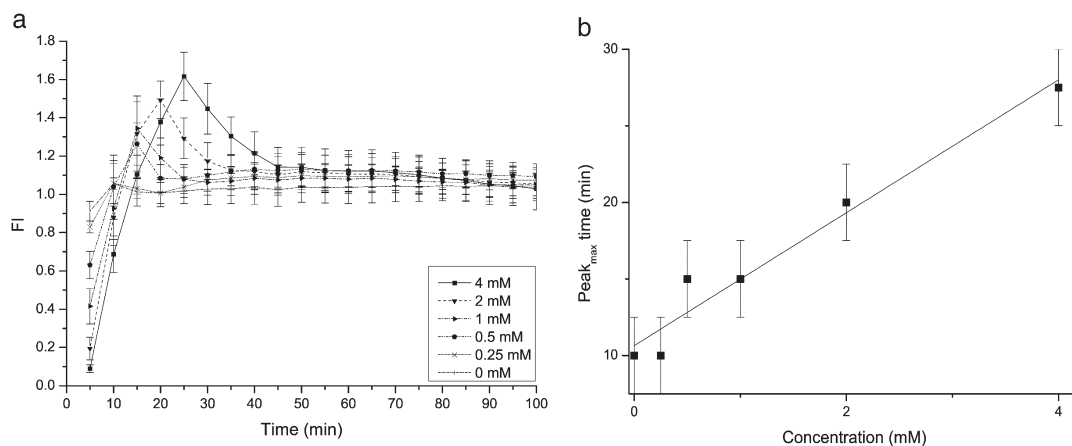


Fig. 1. (a) Luminescence produced by the H₂O₂ concentrations (mM) in FI represented with a 5 measurement average with CV% between measurements as the error bars. (b) The lag time before the peak maximum increases as the concentration increases. As the reading device measures the luminescence emitted every 5 min, the error bars are a constant ± 2.5 min for every peak_{max} time value.

Sodium chloride, KH₂PO₄ and H₂O₂ were from Merck KGaA, Germany and L-ascorbic acid and K₂HPO₄ were from VWR International, USA.

The results of the H₂O₂ assay are shown in Fig. 1a. The FI values were directly proportional to the sample concentration used but also the lag time before the FI maximum increased with the concentration (Fig. 1b). For this reason the experiment was continued for 100 min even though the rise in signal could be detected in less than 20 min. The temperature stabilized at 30 °C after the first 10–15 min and therefore the error before this time can give higher values. The coefficient of variation (CV%) of the four parallel concentrations on the plate was constantly under 10%. Repeatability of the method is also high as the CV% of the results between 5 alternate measurements gave no higher values than 10%. Because the concentration of 4 mM of H₂O₂ gave the highest factor of induction values, this concentration was selected for the antioxidative activity measurements.

The results for the first 50 min of the experiment with AA are shown in Fig. 2a. All of the AA concentrations were able to inhibit some of the light induction produced by the H₂O₂ concentration of 4 mM for 50 min. After this time the signals began to rise exponentially, which

is probably due to the toxic effects of H₂O₂ overcoming the inhibition effect of the AA concentrations. In Fig. 2b the %inhibition (Eq. (1)) (Bartolome et al., 2006) of the AA concentrations is shown at the time point 25 min. The CV% of the sample quadruplicates in the microplate was not higher than 11% from 10 to 45 min. The highest value of error was produced by three of the highest concentrations at the time point 20 or 25 min. Otherwise it was well over 10% between the same time limits. At 50 min as the signal starts to rise, the error also rises.

$$\% \text{inhibition} = \frac{L_{\text{solvent}} - L_{\text{ascorbic acid}}}{L_{\text{solvent}}} \times 100 \quad (1)$$

The method was also used to screen antioxidative activities from various extracts (fungal mycelium extracts, Scots pine and Norway spruce tissue extracts and pure stilbene compounds) from Finnish forests and the example figure is presented in the supplementary figure. In conclusion, the results obtained in this study show that the developed method using recombinant *E. coli* harboring *katG*::*lux* fusion is suitable

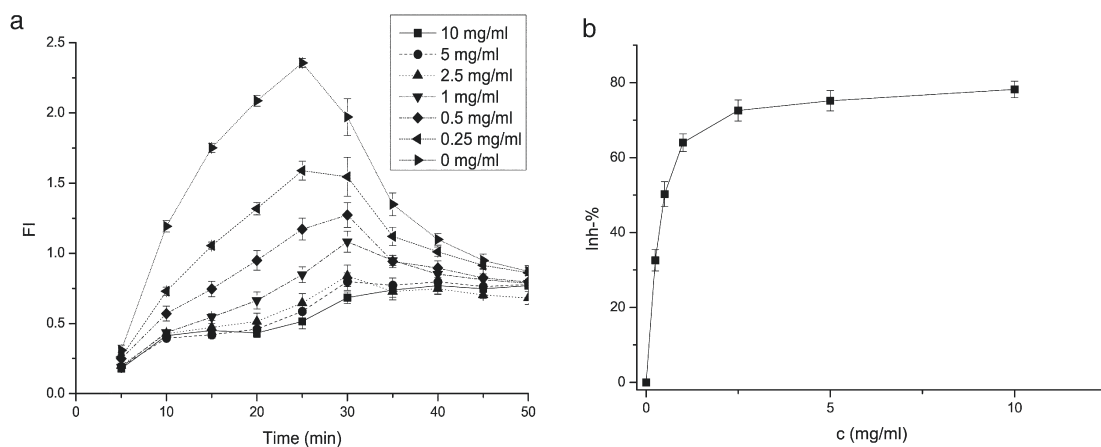


Fig. 2. (a) The antioxidative activity of the AA concentrations measured with the *E. coli* sensor. The error bars are the CV% of the sample quadruplicates in the microplate. (b) The %inhibition of AA shown at 25 min. The error bars are calculated from the standard deviation of the sample quadruplicates in the microplate.

to screen for the antioxidative properties of sample material in a simple, rapid and reliable manner, and it embodies real HTS potential.

Conflict of interest

The authors declare no conflict of interest.

Acknowledgments

Dr. LaRossa has kindly provided the *Escherichia coli* DPD2511 strain. M. Karp acknowledges the sabbatical year funding from the Finnish Cultural Foundation (Suomen Kulttuurirahasto). Authors also acknowledge P. Fairchild for the language check of this manuscript.

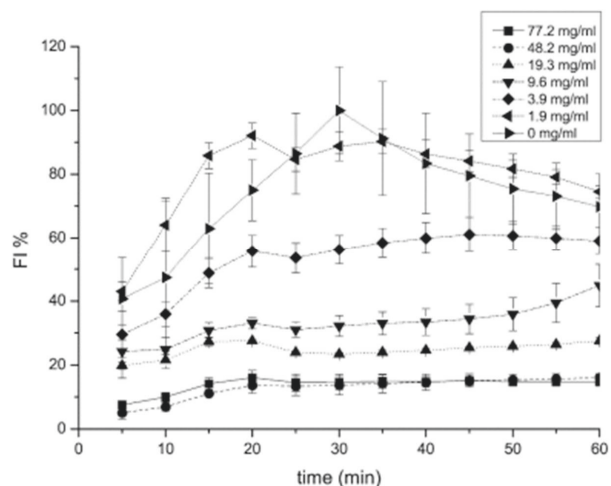
Appendix A. Supplementary data

Supplementary data to this article can be found online at <http://dx.doi.org/10.1016/j.mimet.2015.08.018>.

References

- Bartolome, A., Bernadette, M., Pastoral, I.L., Sevilla III, F., 2006. In: Savitsky, A., Wachter, R. (Eds.), Antioxidant Assay Using Genetically Engineered Bioluminescent *Escherichia coli*. Proc. of SPIE Vol. 6098, Genetically Engineered Probes for Biomedical Applications <http://dx.doi.org/10.1117/12.643950>.
- Belkin, S., Smulski, D.R., Vollmer, A.C., Van Dyk, T.K., LaRossa, R.A., 1996. Oxidative stress detection with *Escherichia coli* harboring a katG::lux fusion. Appl. Environ. Microbiol. 62, 2252–2256. [http://dx.doi.org/10.1016/S0956-5663\(97\)87068-6](http://dx.doi.org/10.1016/S0956-5663(97)87068-6).
- Galluzzi, L., Karp, M., 2006. Whole cell strategies based on lux genes for high throughput applications toward new antimicrobials. Comb. Chem. High Throughput Screen. 9, 501–514. <http://dx.doi.org/10.2174/13862070677935351>.
- Kim, B.C., Gu, M.B., 2003. A bioluminescent sensor for high throughput toxicity classification. Biosens. Bioelectron. 18, 1015–1021. [http://dx.doi.org/10.1016/S0956-5663\(02\)00220-8](http://dx.doi.org/10.1016/S0956-5663(02)00220-8).
- Michelini, E., Leskinen, P., Virta, M., Karp, M., Roda, A., 2005. A new recombinant cell-based bioluminescent assay for sensitive androgen-like compound detection. Biosens. Bioelectron. 20, 2261–2267. <http://dx.doi.org/10.1016/j.bios.2004.10.018>.

Appendix A. Supplementary data



Supplementary figure. Example data obtained from Norway spruce (*Picea abies* [L.] Karst) inner bark extract with water as the extraction solvent. Concentrations are dry weights of the extract in water. As the extract is likely to contain many compounds with different mechanisms of antioxidative activity, the figure produced varies from pure substances such as H_2O_2 (shown in the figure with 0 mg/ml). Also multiple peak maxima were detected, which supports the idea of several antioxidative substances within the extract. The error bars are the CV% of the sample triplicates in the microplate.

PUBLICATION II

A Bioscreening Technique for Ultraviolet Irradiation Protective Natural Substances

Jenni Tienaho, Emmi Poikulainen, Tytti Sarjala, Riina Muilu-Mäkelä, Ville Santala
and Matti Karp

Photochemistry and Photobiology, 94, pp. 1273–1280

<http://dx.doi.org/10.1111/php.12954>

**Reprinted with the kind permission from Photochemistry and Photobiology.
© 2018 Wiley Online Library.**

1 **A Bioscreening Technique for Ultraviolet Radiation Protective Natural Substances**

2

3 Jenni Tienaho ^{*1,2}, Emmi Poikulainen ¹, Tytti Sarjala ², Riina Muilu-Mäkelä ², Ville Santala ¹, Matti

4

Karp ¹

5

6 ¹. Laboratory of Chemistry and Bioengineering, Tampere University of Technology,

7

Korkeakoulunkatu 8, FI-33101 Tampere, Finland

8

². Natural Resources Institute Finland (Luke), Production systems, Kaironientie 15, FI-39700

9

Parkano, Finland

10

11

12

13

*Corresponding author email: jenni.tienaho@tut.fi; jenni.tienaho@luke.fi (Jenni Tienaho)

14

15 **ABSTRACT**

16

17 Ultraviolet radiation (UV-R) has genotoxic and aging effects on skin, and sunscreens are used to
18 alleviate the damage. However, sunscreens contain synthetic shielding agents that can cause harmful
19 effects in the environment. Nature-derived substances may have potential as replacement materials for
20 the harmful sunscreen chemicals. However, screening of a broad range of samples is tedious, and often
21 requires a separate genotoxicity assessment. We describe a simple microplate technique for the
22 screening of UV protective substances using a recombinant *Escherichia coli* biosensor. We can detect
23 both absorbance-based and bioactivity-based shields with simultaneous information about the sample
24 genotoxicity. With this technique, a controversial sunscreen compound, oxybenzone offers physical or
25 absorbance-based shield but appears genotoxic at higher concentrations (3.3 mg/ml). We also
26 demonstrate that pine needle extract (Pi_{Ne}) shields the biosensor from UV-R in a dose-dependent manner
27 without showing genotoxicity. The physical shield of 5 mg/ml Pi_{Ne} is similar to that of one of the most
28 common UV-shielding compound TiO₂ concentration 0.80 mg/ml. The bioactivity-based shield of Pi_{Ne}
29 also reaches the extent of the physical shield with the highest concentration (3.3 mg/ml). To conclude,
30 our technique is suitable in detecting the UV-shielding potential of natural substances, and gives
31 simultaneous information on genotoxicity.

32 INTRODUCTION

33

34 Ultraviolet radiation (UV-R) is the main environmental cause of photo induced skin aging by the
35 process of producing free radicals, such as reactive oxygen species (ROS) in the skin cells. ROS
36 stimulate inflammatory process, initiate DNA damage and cause oxidative damage to cellular lipids,
37 proteins and carbohydrates [1]. UV-R can also cause skin cancer by inducing carcinogenic effects. To
38 alleviate these adverse consequences, sunscreen use is widely encouraged. Based on their mechanism
39 of action, most sunscreen compounds used today can be separated into “physical sunscreens” or
40 minerals, and “chemical sunscreens”. Physical shielding compounds, such as titanium dioxide (TiO₂)
41 and zinc oxide (ZnO), reflect, scatter and absorb UV-R. Chemical sunscreen compounds, such as
42 oxybenzone, octinoxate, avobenzone or *para*-amino benzoic acid (PABA), contain alternating single
43 and double bonds in their structure, which allows them to absorb the high energy UV-R and release
44 UV-R with lower energy [2]. This process makes the radiation less damaging.

45 Both of these shielding compound groups have been found to have disadvantages. Physical sunscreens
46 can cause a bleaching effect, which is unsightly but can be reduced by decreasing the particle size of
47 the mineral used [3]. However, the use of non-degradable and accumulating nanoparticles are causing
48 emerging concern among the environmental scientists [4]. Chemical UV filters also possess harmful
49 environmental impacts. For example, (2-hydroxy-4-methoxyphenyl)-phenylmethanone (oxybenzone)
50 has been shown to be genotoxic to coral planulae [5]. Sunscreen components have also been
51 demonstrated to induce coral bleaching by promoting viral infections to hard coral and their symbiotic
52 algae [6]. There is therefore an urgent need to replace sunscreen chemicals with more environmentally
53 friendly options. This could be achieved by using nature-derived substances with UV inhibition or
54 shielding properties. The screening of vast amount of substances is, however, tedious and often requires
55 a separate evaluation of the genotoxicity.

56 For the simultaneous assessment of genotoxicity, living whole-cell microbial biosensors have been
57 proven to be useful. Living whole-cell microbial biosensors can detect both bioactivity and
58 bioavailability of a selected sample material simultaneously, and the produced real-time response can

59 be quantified and monitored in a continuous manner. For example, the *Escherichia coli* (*E.coli*) strain
60 DPD2794 [7] has been constructed by fusing the SOS-responsive *recA* gene promoter of the bacteria
61 with the luminescent *luxCDABE* genes of marine *Vibrio fischeri* bacteria. The resulting *recA':lux*
62 reporter plasmid produces an increase in the luminescent light emission in the presence of bioavailable
63 genotoxic DNA damaging agents.

64 Sassanfar et al. [8] concluded that UV-R induces about 10-fold transcription of *recA*. This was later
65 confirmed by Vollmer et al. [7] using the *E.coli* DPD2794 biosensor. They also found that the sensor
66 was extremely sensitive and effective when compared to the conventional methodologies, such as the
67 Ames test. Here, we have applied the biosensor to develop a microplate technique with high-throughput
68 screening (HTS) potential, which can be easily used with any laboratory equipment emitting continuous
69 UV-R, such as a standard Polymerase Chain Reaction (PCR) cabinet. PCR cabinets are designed for
70 nucleic acid amplification and UV-R is used to prevent sample contamination.

71 Synthesis of UV-absorbing compounds in epidermal layers of plant leaves are one of the several
72 mechanisms in plants to protect themselves against UV radiation. Needles of conifer species are known
73 to be well protected from UV radiation [9, 10]. For example, Scots pine needles have been reported to
74 accumulate UV-B inducible flavonoids for shielding the inner cell layers [11]. Scots pine needles also
75 comprise a vast resource of renewable side stream biomass in forestry to be utilized for novel purposes,
76 and therefore, were selected as a suitable testing material for the method development.

77 Some nature-derived UV filters are already in use. The mechanism by which many of these work is
78 based on secondary metabolites acting as antioxidant or anti-inflammatory agents, thereby alleviating
79 the harmful effects of UV radiation [12]. One commercially used example of a nature-derived chemical
80 sunscreen compound is PABA, which can be found in yeast, bacteria and plants. However, its use has
81 been banned in many countries as it can cause allergic reactions and irritation [13]. This highlights the
82 need for simultaneous genotoxicity assessment.

83 Current testing models for sunscreen products can be divided into *in vivo* and *in vitro* models, from
84 which only *in vivo* testing involving irradiation of human subjects have been validated and is currently

85 in use for the official solar protection factor (SPF) testing [14]. In addition to spectrophotometric *in*
86 *vitro* methods, approaches with simultaneous information on sample genotoxicity have also been
87 developed with human cell cultivations [15]. However, the use of bacterial biosensor cells increases the
88 HTS potential of the developed technique for a wide range of sample material with regard to time- and
89 cost efficiency.

90 In this study, we introduce a microplate technique with improved HTS potential for the UV-shield
91 detection of various sample material using the *E.coli* DPD2794 biosensor. With the developed and
92 optimized technique, both physical shielding and biological shielding – where the UV shielding effect
93 of sample material is measured in contact with biosensor cells – can be detected and compared simply
94 and rapidly, without any need for a separate genotoxicity assessment. We also demonstrate that the
95 technique is suitable for the screening of natural product extracts in order to replace the harmful
96 chemicals used in the sunscreen products with natural, sustainable and less damaging biochemical UV
97 protectants.

98 **MATERIALS AND METHODS**

99

100 **Chemicals and samples:** Tryptone, yeast extract, and agar were obtained from Labema, Finland; NaCl,
101 KH₂PO₄ and dimethyl sulfoxide (DMSO) from Merck KGaA, Germany; Sodium salt of ampicillin,
102 TiO₂ (< 5µm particle size and predominantly rutile), astaxanthin and CaCl₂ were from Sigma-Aldrich,
103 USA; and K₂HPO₄ from VWR International, USA. M9 Minimal Salts mixture (containing Na₂HPO₄•7
104 H₂O, KH₂PO₄, NaCl and NH₄Cl) has been purchased from Sigma LifeSciences, Sigma-Aldrich, USA.
105 MgSO₄ and L-ascorbic acid were obtained from J.T. Baker, USA, and D-glucose was from Amresco,
106 USA. Ethanol was obtained from Altia, Finland and ciprofloxacin from Bayer, Germany. Finally,
107 oxybenzone was obtained from TCI, Japan.

108

109 **Bacterial strains and cultivation:** Recombinant bacterial strain *E. coli* DPD2794 (*recA'*::*lux*)
110 previously described by Vollmer et al. [7] was used in this study (a kind gift by Dr. Robert A. LaRossa
111 from DuPont Company Central Research and Development, Wilmington, USA). The bacteria were

112 preserved in 15-% glycerol at -80 °C. The working stock was prepared by inoculation in Lysogeny Agar
113 (LA) (tryptone 10 g/L; yeast extract 5 g/L; NaCl 10 g/L and agar 15 g/L) growth-plates supplemented
114 with 100 µg/ml of ampicillin and 100 mM of sterile and filtered potassium phosphate buffer, pH 7.0.
115 The plates were cultivated overnight at 30 °C before being stored at 4 °C. A single colony of the strain
116 was inoculated into 5 ml of liquid glucose-enriched M9 minimal medium (11.3 g/liter M9 salts, 0.1 mM
117 CaCl₂, 1 mM MgSO₄, and 0.2 % (w/v) anhydrous D-Glucose) supplemented with 100 µg/ml of
118 ampicillin. It was then incubated for approximately 16 hours in a shaker at 30 °C and 300 rpm, after
119 which the luminescence was measured with a Chameleon Multilabel (Hidex Oy, Finland) microplate
120 reader to verify the activity of the biosensor. Optical density at 600 nm was measured to be
121 approximately 0.1 for the bacterial suspensions corresponding to 1×10^8 CFU/ml.

122

123 **Sample preparation:** The needle samples of Scots pine (*Pinus sylvestris* L.) were collected from a
124 mature living pine from the western Finland during late June 2013. The needles of the previous of the
125 current (c+1) growing seasons were separated and weighed. Needles were frozen at -80 °C and ground
126 in a mortar with the help of liquid nitrogen before adding to sealed and previously weighed
127 polypropylene test tubes. Pure methanol extraction was chosen, because it has been reported to give
128 high polyphenol content [16] and primary metabolites such as amino acids and sugars are not present
129 in methanol extracts. For the extraction procedure 27 ml of methanol (Methanol for liquid
130 chromatography, LiChrosolv®, Merck KgaA, Germany) was mixed to 1.75 g of the needle powder by
131 vortexing. Extraction tube was then put to the rotamixer (Rotamixer, Type MMVI4, Heto-Holten A/S,
132 Denmark) at full power (30 rpm) for 60 minutes. Extraction tube was then centrifuged at +4 °C and
133 8200 g for 10 minutes after which the supernatant was collected to a new polypropylene tube and finally
134 filtered through nylon syringe filter (0.20 µm, Nylon 66 Filter Membrane from Supelco by Sigma-
135 Aldrich Co, USA) to a previously weighed and sterile polypropylene test tube. Aliquot of methanol
136 without needle material went through the same extraction procedure simultaneously as control sample.
137 Finally, the extraction product was dried using a vacuum centrifuge with a cooling unit (Rotational-
138 Vacuum-Concentrator RVC 2-18, Cold Trap CT 02-50 SR, Martin Christ Gefriertrocknungsanlagen
139 GmbH, Germany) before storing at -80 °C.

140

141 The dry and frozen methanol extract of pine needles was dissolved into methanol and double distilled
142 water (DDW) (1:2.7) to achieve a stock solution of 100 mg/ml of dried extraction product. This stock
143 solution was further diluted in DDW to achieve concentrations of 0.1; 0.5; 1.0 and 5.0 mg/ml for the
144 physical shield testing and 0.17; 0.33; 1.7 and 3.3 mg/ml per microplate well for the biological shield
145 tests. The difference in the concentrations chosen for the physical and biological shield tests is due to
146 the stronger effect of the sample material when in direct contact with the bacterial biosensor cells.
147 Hence, the sample concentrations for the biological test were kept slightly lower. The maximum
148 concentration of the UV filters allowed in cosmetic products according to the EU Cosmetics Regulation
149 list (Regulation (EC) 1223/2009) goes from 2 % to 25 % of the cosmetic product mass. We use a
150 concentration maximum of 1 % for the potential UV protective samples, which lays below these
151 regulated maximum values. The highest methanol concentrations for the extracts were 1.4 % for 5
152 mg/ml and 0.9 % for 3.3 mg/ml. The sample solutions were stored in -20 °C and covered from the light.

153

154 **Irradiation source:** DNA/RNA UV-cleaner cabinet (UVC/T-AR DNA/RNA UV-CLEANER BOX,
155 BIOSAN company, Latvia) was used as the irradiation source for the experiments. This equipment was
156 chosen because it is widely available in laboratories, and so requires no expensive investments.
157 However, the developed technique can be adapted to any other continuous UV-R emitting setting and
158 is therefore highly modifiable. The distance between the bottom of the microplate and the UV source
159 was 48.5 cm for all of the measurements. The wavelength of the UV irradiation was validated using
160 AvaSpec – ULS2048L StarLine Versatile Fiber-optic Spectrometer (Avantes, Apeldoorn, Netherlands),
161 and it was that of a normal mercury UV lamp with a maximum wavelength of approximately 254 nm.
162 Irradiation dose of the used cabinet was also measured using Ophir Laser thermal sensor 3A-PF-12
163 detector (Ophir Optronics Solutions Ltd, Jerusalem, Israel) with a 12 mm aperture.

164

165 **Biological protection and bioactivity:** With this technique, the sample volume of 50 µl of the potential
166 UV protective substance concentrations were pipetted in triplicates into an opaque white 96 well
167 microplates (Greiner Bio-one GmbH, Austria). The volume of 100 µl of the bacterial inoculation in M9

168 minimal media was then pipetted into the same microplate wells. For the sake of comparability a clear
169 UV-transparent microplate (Corning® 96 well plates, half-area, polystyrene flat bottom, UV-Vis-
170 transparent between 220 and 1600 nm, Corning Inc., USA) containing 100 µl of water was added above
171 the plate before irradiation. In order to stabilize the UV-R dose, the lamp, acting as a UV source, was
172 left on for approximately 30 minutes before irradiation. The plates were then moved to a DNA/RNA
173 UV-cleaner cabinet into a previously optimized place, and irradiated for 30 seconds with direct UV
174 light. Some wells of the plate covered with aluminum foil sheet, for the negative control signals. After
175 the irradiation period 100 µl of Lysogeny Broth (LB) medium was added into the wells for nutrition
176 and the luminescent light signal was measured in counts per second (CPS) using a Chameleon
177 Multilabel (Hidex Oy, Finland) microplate reader in 10-minute intervals for a total of 180 minutes with
178 a shaking between the measurements.

179

180 **Physical protection and absorbance:** This technique was otherwise similar to that of biological
181 protection except that 100 µl of the different concentrations of the potential UV protective substances
182 were pipetted in triplicates into clear UV transparent microplates in a way that the total liquid volume
183 of the microplate wells remained the same. The 100 µl of bacterial inoculation in M9 minimal media
184 was then added similarly into another separate opaque white microplate and the plates were then
185 handled and irradiated as above.

186

187 **Absorbance measurements:** The absorbance of 100 µl of sample substance triplicates in translucent
188 microplate (Sarstedt AG & Co, Germany) was evaluated using Thermo Scientific Varioskan Flash
189 Reader (Thermo Fischer Scientific, Thermo Electron Co. USA) in the absorbance scan mode with 5 nm
190 intervals for the wavelength area of 200-900 nm. Absorbance value averages were calculated and error
191 bars are the standard deviations of the sample triplicates.

192

193 **Result analysis:** All figures have been drawn using Origin 8 data analysis and graphic workspace
194 (OriginLab Corp., USA). Because CPS values can vary depending on the date and chosen culture, all
195 of the results, except for the absorbance measurements, are expressed in induction factors (IF), which

196 have been calculated by dividing the sample triplicate CPS values averages with those of negative
197 controls. Error bars have been calculated from the standard deviations of the sample IF triplicates. A
198 two-tailed t-test was also conducted to confirm the statistical significance of the results within the
199 measurement plates using Microsoft Office Excel 2016 (Microsoft Co., USA).

200

201 **RESULTS AND DISCUSSION**

202 The wavelength of the UV irradiation was that of normal mercury lamp with a maximum in the 254 nm
203 UV wavelength area and the irradiation dose rate was found to be approximately $190 \mu\text{W}/\text{cm}^2$. The
204 place of the microplate was optimized in the UV-cleaner cabinet to give the highest signal to
205 background ratio and lowest errors between sample triplicates. The place was obtained when the plate
206 was situated at 20 cm from the opening and 26 cm from the left face of the cabinet (see **Figure 1a**). It
207 was also found that the best irradiation time giving the maximum signal was 30 seconds and this time
208 was used for the measurements throughout (**Figure 1b**), making the irradiation dose $5.7 \text{ mJ}/\text{cm}^2$. The
209 Standard Erythema Dose (SED) has been proposed by Commission Internationale de l'Eclairage [17]
210 as UV-R dose equivalent of $100 \text{ J}/\text{m}^2$ or $10 \text{ mJ}/\text{cm}^2$ [18], and the used irradiation dose in this study is
211 57 % of this. The incubation time is the time after exposure at which the luminescence signals were
212 monitored every 10 minutes for 180 minutes, whereas the exposure time is the seconds of UV-R
213 exposure. We can see that 30 seconds of irradiation gives the highest signal in the higher measurement
214 times, and therefore, it has been chosen for the measurements. From the **Figure 1c**, we can see how the
215 UV transparent clear microplate is put directly on top of the white opaque microplate with biosensor
216 cells for the time of the UV exposure. The sample is placed into the clear plate above, for the physical
217 measurements, and into the white microplate below, for the biological shield measurements.

218

<Figure1>

219

220 We also tested to see whether the distance from the lamp height of the plate would affect the signal. We
221 used a standard adjustable laboratory equipment jack (Lab Jack Swiss Boy 110 MR, Rudolf Grauer AG,
222 Degersheim, Switzerland) for this. We found that the height of the plate was approximately directly
223 proportional to the signal (See Supporting materials, **Figure S1**). However, the normal table height was

224 chosen for the measurements because it was the easiest to maintain, and the luminescent light signal
225 produced was not efficiently lower than that of the highest setting.

226 TiO_2 (< 5 μm particle size and predominantly rutile) was chosen to act as a known UV-shield control,
227 because it is extensively used in sunscreen products worldwide. However, TiO_2 is insoluble in water,
228 and was dissolved into 96 % ethanol to prepare 1 M solution and further diluted with DDW for
229 concentrations of 0.80; 8.0; 80 and 800 $\mu\text{g}/\text{ml}$. The ethanol percentages of the final solutions were
230 0.00032 % to 3.2 %. TiO_2 has been shown to possess antimicrobial effects [19] and also the uneven
231 distribution of small insoluble particles could affect the microbial cell functions. Therefore, among cells
232 the control used was LB growth medium, because it absorbs the UV-R wavelengths. The LB was diluted
233 with DDW to get dry matter concentrations of 0.01; 0.09; 0.93 and 9.3 mg/ml per microplate well. The
234 results obtained from these standard substances are shown in the **Figure 2a** (TiO_2) and **2b** (LB) from
235 where we can see that they provide UV protection in a dose dependent manner with all of the LB
236 concentrations except the lowest of 0.01 mg/ml of dry matter concentration and with the highest 800
237 and 80 $\mu\text{g}/\text{ml}$ of TiO_2 .

238 <Figure2>

239

240 To verify the effectiveness of the UV-R dose used, we also compared the induced signals of UV-R to
241 that induced with a known antibiotic ciprofloxacin (50 mg/ml stock solution was diluted to DDW to
242 achieve concentrations of 0.001; 1.0; 3.8; 5.5 and 7.5 mg/ml per microplate well). Ciprofloxacin
243 specifically targets the bacterial DNA and the obtained results can be seen in the **Figure 3a**. From the
244 figure, we can see that the exposure time of 30 seconds gives approximately the same luminescence
245 light signal induction factor at the time point of 100 minutes after exposure time with the ciprofloxacin
246 concentration of 0.001 mg/ml. With higher concentrations of ciprofloxacin, it seems that the light signal
247 produced starts to decrease, which is probably due to cell death, and therefore reduction in the sum of
248 the luminescent light signal produced by the bacteria in the microplate well. These results show that the
249 UV-R dose chosen is effective enough to be comparable with the genotoxic effects towards the bacteria
250 caused by a known antibiotic.

<Figure3>

251

252

253 It is also widely known that antioxidants can prevent the damage induced by UV-R by targeting the
254 induced production of ROS in the cell. The known antioxidants L-ascorbic acid (0.17; 0.33; 0.83; 1.7
255 and 3.3 mg/ml per microplate well in DDW) and astaxanthin (5 mg/ml solution was prepared in DMSO,
256 and DDW was used to achieve concentrations of 0.017; 0.17; 1.7; 17 and 170 $\mu\text{g/ml}$ per microplate
257 well) were used to test this protection mechanism in the developed methodologies. From the **Figure 3b**
258 can be seen, that ascorbic acid seems to give biological shield against UV light in a dose-dependent
259 manner and **Figure 3c** shows that ascorbic acid concentrations also absorb the UV wavelengths under
260 300 nm. However, the shielding effect is not as clear in the case of astaxanthin (**Figure 3d**). Astaxanthin
261 also seems to induce the luminescence production with all but the lowest concentrations (0.017 and
262 0.17 $\mu\text{g/ml}$ per microplate well) implying genotoxic properties. However, as astaxanthin stock was
263 dissolved into DMSO, the solvent used most likely causes this observation. The astaxanthin
264 concentrations used were from 1.7×10^{-5} mg/ml to 0.17 mg/ml, and they consequently contain from
265 0.0003 % to 3.3 % DMSO, and this could produce enough toxicity in the higher concentrations. In fact,
266 due to this result, we tested that the biosensor can stand no larger concentrations than 2 % of DMSO
267 without it effecting the cells (data not shown). DMSO has also previously been found to possess
268 bacteriostatic properties [20]. From the absorbance of these substances, we can see that DMSO itself
269 absorbs in the UV area (**Figure 3e**) but in the biological shield technique (**Figure 3d**), the shielding
270 effect is lost due to genotoxicity. The sample with the highest concentration of astaxanthin (170 $\mu\text{g/ml}$)
271 at 100 min of the measurement gave better shield for the biosensor than the LB control, as the IF of the
272 astaxanthin sample was smaller than the unprotected cells (0 $\mu\text{g/ml}$) and the LB control (p-values <
273 0.0001). According to the results, also the sample with 3.3 mg/ml ascorbic acid shields the biosensor
274 from the UV-R better than the LB control. The lower IF of the ascorbic acid sample than that of LB or
275 non-shielded biosensor cells (p-values < 0.0001) indicates statistically significant shielding. This
276 observation of antioxidants causing UV shielding effects is not surprising as UV-R causes ROS
277 formation. Astaxanthin has been referred as the most effective antioxidant but unfortunately the

278 insolubility to water causes it to be not as preferable source of shield according to our technique. By
279 adding antioxidant material into sunscreens the risks caused by UV-R can, however, be alleviated.

280

281 Because oxybenzone has been found to be harmful towards coral planulae and its effect was found to
282 be increased by the exposure to UV light [5], we were curious on finding out, how it would affect our
283 genotoxicity sensitive biosensor. The oxybenzone stock of 50 mg/ml was prepared by dissolving
284 oxybenzone into 96 % ethanol. Further dilutions of 10 and 0.1 mg/ml were prepared into DDW for the
285 physical shield testing whereas concentrations of 0.03 and 3.33 mg/ml per microplate well were used
286 for the biological activity test (consequently they contained 0.63 to 6.3 % of ethanol). As expected, we
287 found that oxybenzone possesses physical UV-shield (**Figure 4a**) whereas biological shielding effect
288 (**Figure 4b**) is overtaken by the genotoxicity of the chemical and the ethanol concentrations do not
289 explain these observations, when biosensor cells are exposed to both oxybenzone and UV-R. In the
290 **Figure 4c** the physical and biological shield from **Figures 4a** and **4b** of the sample are drawn at the
291 time point 100 min. From **Figure 4c** we can see that the physical shield shows dose-dependent behavior,
292 but as the bacterial cells are already harmed by the oxybenzone itself (dark biological effect shows dose
293 dependent rise in luminescence signal levels), adding UV exposure significantly increases the
294 luminescent light signal production indicating severe DNA damage instead of shielding effect. At 100
295 min of the measurement, the UV exposed oxybenzone (3.3 mg/ml) caused more DNA damage to the
296 biosensor cells than the unexposed oxybenzone with same concentration, as its signal is higher than that
297 of the unexposed (p-value < 0.0001). This 3.3 mg/ml oxybenzone concentration at 100 min
298 measurement time also caused more damage to the biosensor cells than the mere UV exposure (p-value
299 = 0.002). This information indicates that these results represent statistical significance. The results
300 underline that, while oxybenzone has physical UV-shielding effect, it is also harmful to the biosensor
301 cells and similar adverse results have been previously reported in the case of coral and fish [5, 6, 21].
302 Oxybenzone has also been shown to cause contact or photocontact allergy or even urticarial reactions
303 with humans [21].

304

<Figure4>

305

306 A potential source to obtain safe and sustainable UV-shielding compounds is nature-derived substances.
307 The methodology was tested using *Pinus sylvestris* L. needle extract (Pi_{Ne}) and the results are shown in
308 the **Figure 5**. Pine needles are exposed to the UV-R from the sun and therefore, they are expected to
309 possess UV inhibitory activity, which we were able to demonstrate with our technique. **Figure 5a** and
310 **5b** correspond to the physical absorbance based shield, and we can see that they absorb in the UV area.
311 The Pi_{Ne} with concentration 5.0 mg/ml protects the biosensor cells from adverse effects of the UV-R,
312 as its IF in 100 min measurement is lower than that of the unprotected sample (p-value < 0.0001). In
313 addition, this protective capacity is similar to that of a commercially used sunscreen chemical TiO₂
314 concentration 0.80 mg/ml, which was used as a control (p-value = 0.1683, tested for difference in
315 means). Methanol extractable polyphenols are known for their antioxidant activities, which can
316 correspond to the biological shielding potential shown in the **Figure 5c**. The highest concentration of
317 Pi_{Ne} (3.3 mg/ml) exhibits biological UV-R protective properties for the biosensor cells. This is
318 demonstrated in the 100 min measurement results, where the IF for the Pi_{Ne} is lower than that for the
319 unprotected cells (p-value = 0.001). However, the IF of the Pi_{Ne} is higher than that of the LB control (p-
320 value < 0.0001), which indicates that it is not as effective in the protection as the LB control. In the
321 **Figure 5d**, the comparison of the effectiveness of the physical and biological shielding mechanisms
322 show that the absorbance based (physical) shield is the main factor corresponding to the UV inhibition
323 of the used extract concentrations whereas we cannot detect any genotoxicity. Nature-derived
324 substances are therefore potentially less harmful to the environment and they also pose no similar risk
325 of accumulation to the environment as mineral based physical sunscreen nanoparticles because they are
326 degradable and, as in this case of needles, sustainably derived from a waste-stream of forestry. Although
327 the biological shielding in our technique was not as high as with control substance LB, the methanol
328 extracts are most likely rich in polyphenols and flavonoids, which have been widely reported to have
329 antioxidant properties [16]. These results should, however, be considered to be merely indicative of the
330 applicability of the technique developed. For a more comprehensive analysis of the UV protection
331 capacity of the selected needle material, test should be performed with a broad range of needle material
332 samples gathered from various environments and at different times of year.

333

<Figure5>

334

335 In conclusion, it is important to obtain safe, sustainable and environmentally friendly UV-shielding
336 compounds. Our methodology can be utilized and is also highly modifiable to be used in the high-
337 throughput screening of various natural products for UV-R induced damage preventive substances and
338 it gives simultaneous information about the genotoxic effects of the sample substance.

339 **ACKNOWLEDGEMENTS**

340 The European Regional Development Fund has supported this work (project code A71142). The town
341 of Parkano and SASKY municipal education and training consortium also contributed to funding this
342 work, along with Natural Resources Institute Finland and Tampere University of Technology. We wish
343 to thank Dr. Matti Virkki for the help with the wavelength and UV dose measurements and analyzes as
344 well as Dr. Praveen Ramasamy, who kindly offered us the astaxanthin powder-Dr. Robert A. LaRossa
345 from DuPont Company Central Research and Development, kindly provided the *E.coli* DPD2794
346 bacterial strain.

347

348 **CONFLICTS OF INTEREST**

349 The authors declare that they have no conflicts of interest.

350

351 **SUPPORTING MATERIALS**

352 Additional supporting information may be found online in the Supporting Information section at the
353 end of the article: **Figure S1**. The effect of the plate distance from the irradiation source.

354

355 **REFERENCES**

356 1. Pillai, S., C. Oresajo and J. Hayward (2005) Ultraviolet radiation and skin aging: roles of reactive
357 oxygen species, inflammation and protease activation, and strategies for prevention of inflammation
358 induced matrix degradation – a review. *Int. J. Cosmet. Sci.* 27, 17–34.

- 359 2. Heinrich, U., H. Tronnier, D. Kockott, R. Kuckuk and H. M. Heise (2004) Comparison of sun
360 protection factors determined by an *in vivo* and different *in vitro* methodologies: a study with 58
361 different commercially available sunscreen products. *Int. J. Cosmet. Sci.* 26, 79–89.
- 362 3. Kockler, J., M. Oelgemöller, S. Robertson and B. D. Glass (2014) Influence of Titanium Dioxide
363 Particle Size on the Photostability of the Chemical UV-Filters Butyl Methoxy Dibenzoylmethane and
364 Octocrylene in a Microemulsion. *Cosmetics*. 1, 128–139.
- 365 4. Lu, J., S. Tian, X. Lv, Z. Chen, B. Chen, X. Zhu and Z. Cai (2018) TiO₂ nanoparticles in the marine
366 environment: Impact on the toxicity of phenanthrene and Cd²⁺ to marine zooplankton *Artemia salina*.
367 *Sci. Total. Environ.* 615, 375–380.
- 368 5. Downs, C., E. Kramarsky-Winter, R. Segal, J. Fauth, S. Knutson, O. Bronstein, F. Ciner, R. Jeger,
369 Y. Lichtenfeld, C. Woodley, P. Pennington, K. Cadenas, A. Kushmaro and Y. Lova (2016)
370 Toxicopathological Effects of the Sunscreen UV Filter, Oxybenzone (Benzophenone-3), on Coral
371 Planulae and Cultured Primary Cells and Its Environmental Contamination in Hawaii and the U.S.
372 Virgin Islands. *Arch. Environ. Contam. Toxicol.* 70, 265–288.
- 373 6. Danovaro, R., L. Bongiorni, C. Corinaldesi, D. Giovannelli, E. Damiani, P. Astolfi, L. Greci and A.
374 Pusceddu (2008) Sunscreens Cause Coral Bleaching by Promoting Viral Infections. *Environ. Health*
375 *Perspect.* 116, 441–447.
- 376 7. Vollmer, A. C., S. Belkin, D. R. Smulski, T. K. Van Dyk and R. A. LaRossa (1997) Detection of
377 DNA damage by use of *Escherichia coli* carrying *recA':::lux*, *uvrA':::lux*, or *alkA':::lux* reporter
378 plasmids. *Appl. Environ. Microbiol.* 63, 2566–2571.
- 379 8. Sassanfar, M. and J. Roberts (1991) Constitutive and UV-mediated activation of RecA protein:
380 combined effects of *recA441* and *recF143* mutations and of addition of nucleosides and adenine. *J.*
381 *Bacteriol.* 173, 5869–5875.
- 382 9. Day, T. A., T. C. Vogelmann and E. H. (1992) Are some plant life forms more effective than others
383 in screening out ultraviolet-B radiation? *Oecologia*. 92, 513–519.

- 384 10. Hoque, E. and G. Remus (1999) Natural UV-Screening Mechanisms of Norway Spruce (*Picea*
385 *abies* [L.] Karst.) Needles. Photochem. Photobiol. 69, 177–192.
- 386 11. Schnitzler J.-P., T. P. Jungblut, C. Feicht, M. Köfferlein, C. Langebartels, W. Heller and H.
387 Sandermann (1997) UV-B induction of flavonoid biosynthesis in Scots pine (*Pinus sylvestris* L.)
388 seedlings. Trees. 11, 162–168.
- 389 12. Saewan, N. and A. Jimtaisong (2015) Natural products as photoprotection. J. Cosmet. Dermatol.
390 14, 47–63.
- 391 13. Wong, T. and D. Orton (2011) Sunscreen allergy and its investigation. Clin. Dermatol. 29, 306–
392 310.
- 393 14. Cole, C. (2014) Sunscreens – what is the ideal testing model? Photodermatol. Photoimmunol.
394 Photomed. 30, 81–87.
- 395 15. Schuch, A. P., M. C. S. Moraes, T. Yagura and C. F. M. Menck (2014) Highly Sensitive
396 Biological Assay for Determining the Photoprotective Efficacy of Sunscreen. Environ. Sci. Technol.
397 48, 11584–11590.
- 398 16. Sowndhararajan, K. and S. C. Kang (2012) Free radical scavenging activity from different
399 extracts of leaves of *Bauhinia vahlii* Wight & Arn. Saudi J. Biol. Sci. 20, 319–325.
- 400 17. Commission Internationale de l’Eclairage (1997) Standard Erythema Dose, a Review. Technical
401 Report CIE 125-1997. CIE Central Bureau, Vienna, Austria.
- 402 18. IARC Working Group on the Evaluation of Carcinogenic Risk to Humans (2012) Solar and
403 Ultraviolet Radiation. In Radiation - IARC Monographs on the Evaluation of Carcinogenic Risks to
404 Humans, No. 100D. pp. 35-102. International Agency for Research on Cancer, Lyon, France.
- 405 19. Besinis, A. T., De Peralta and R. D. Handy (2014) The antibacterial effects of silver, titanium
406 dioxide and silica dioxide nanoparticles compared to the dental disinfectant chlorhexidine on
407 *Streptococcus mutans* using a suite of bioassays. Nanotoxicology. 8, 1–16.

408 20. Wood, D. C. and J. Wood (1975) Pharmacologic and Biochemical Considerations of Dimethyl
409 Sulfoxide. Ann. N. Y. Acad. Sci. 243, 7–19.

410 21. DiNardo, J. and C. A. Downs (2017) Dermatological and environmental toxicological impact of
411 the sunscreen ingredient oxybenzone/benzophenone-3. J. Cosmet. Dermatol. 17, 15–19.

412 LIST OF FIGURE LEGENDS

413 **Figure 1.** The optimal place of the microplate in the UV-cleaner cabinet for obtaining the highest signal
414 to background ratio and smallest errors between triplicate measurements **(a)**. The exposure time signals
415 at 30 minutes, 100 minutes and 180 minutes of incubation after exposure to UV-R **(b)**. Clear UV
416 transparent microplate placed directly over the opaque white microplate with the biosensor bacteria. In
417 physical shield measurements, the sample is put on a clear plate, and in biological shield measurements
418 on a white plate **(c)**

419 **Figure 2.** Luminescence produced by the *E.coli* DPD2794 biosensor, when exposed to 30 seconds of
420 UV light while protected by **(a)** TiO₂ concentrations with physical protection measurement (in a
421 separate UV plate) and **(b)** LB concentrations with biological protection (in contact with bacterial cells)
422 measurement

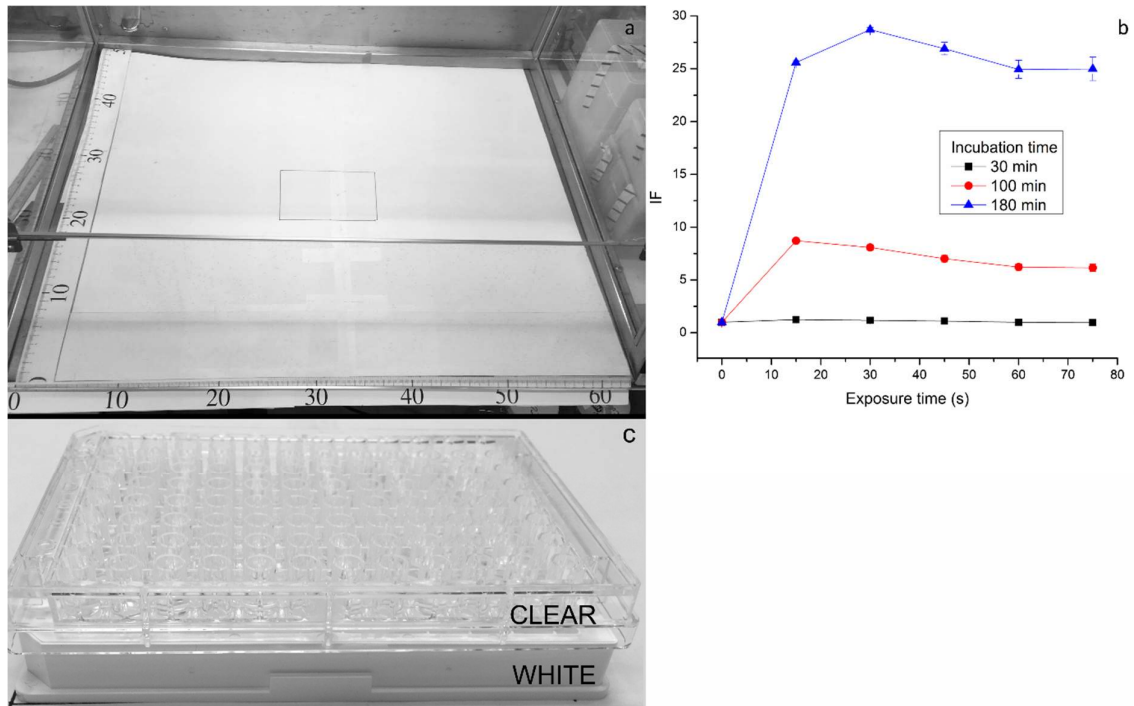
423 **Figure 3.** The comparison of the effect of the UV-R dose of 30 seconds to that of ciprofloxacin
424 concentrations **(a)**. The luminescence signals produced by *E.coli* DPD2794 when exposed to 30 seconds
425 of UV radiation whilst protected by antioxidant agent ascorbic acid **(b)** and astaxanthin **(d)**
426 concentrations as well as LB controls. All substances have been measured with contact with the
427 bacterial cells (biological effect). The absorbance of the ascorbic acid **(c)** and astaxanthin **(e)** and the
428 corresponding controls in the different wavelength areas

429 **Figure 4.** UV shielding effects and genotoxicity of oxybenzone. Physical **(a)** and biological **(b)**
430 shielding and their comparison at the time point 100 min **(c)**. In addition to other figures, the dark
431 biological effect was added in which the cells have not been UV-irradiated

432 **Figure 5.** Luminescent light signal produced when *E.coli* DPD2794 cells were exposed to 30 seconds
433 of UV radiation and protected by pine needle methanol extract concentrations (Pi_{Ne}). The physical shield
434 results **(a)**, the absorbance of the sample in the different wavelength areas **(b)**, the biological shield
435 results **(c)** and the comparison of the methods **(d)** is shown with the used sample concentrations

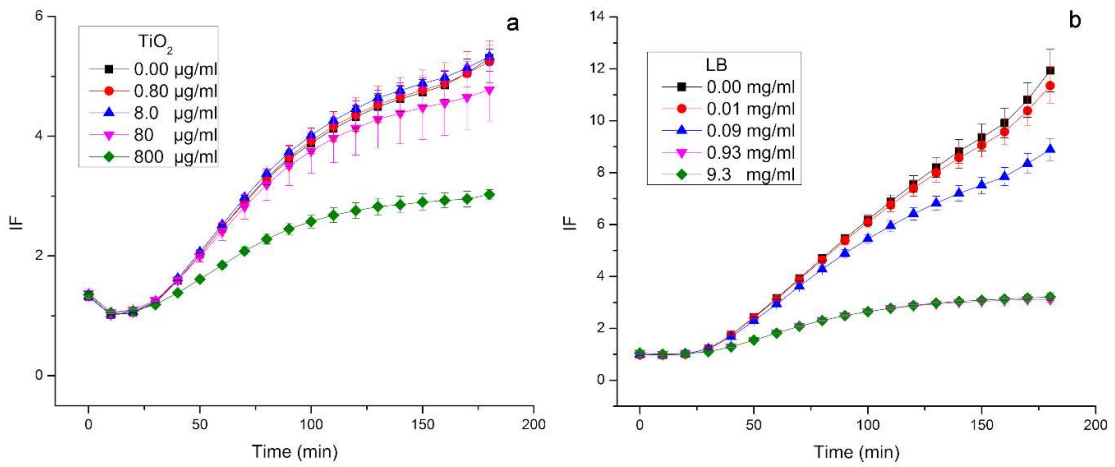
436 **Supplementary Figure.** The effect of the plates distance from the irradiation source. Height is
437 expressed as the distance from the cabinet base. At the time point of 100 minutes incubation after
438 irradiation, the height of 0 cm gives the lowest error bars and the luminescence differences between
439 height levels is not as significant **(a)**. The luminescent light emission signals behave rather alike in all
440 of the measurement time points **(b)**

441 Figure 1



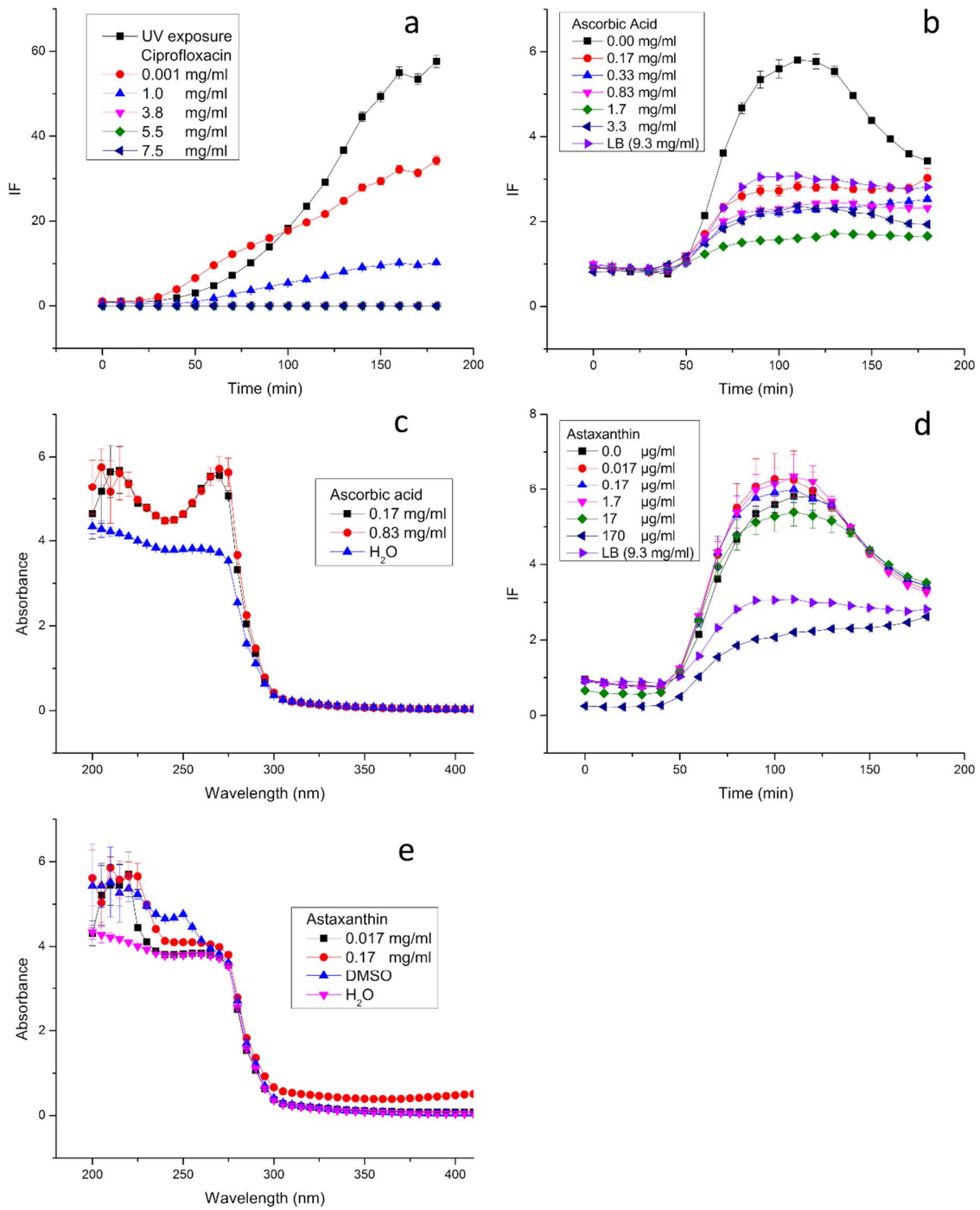
442

443 Figure 2

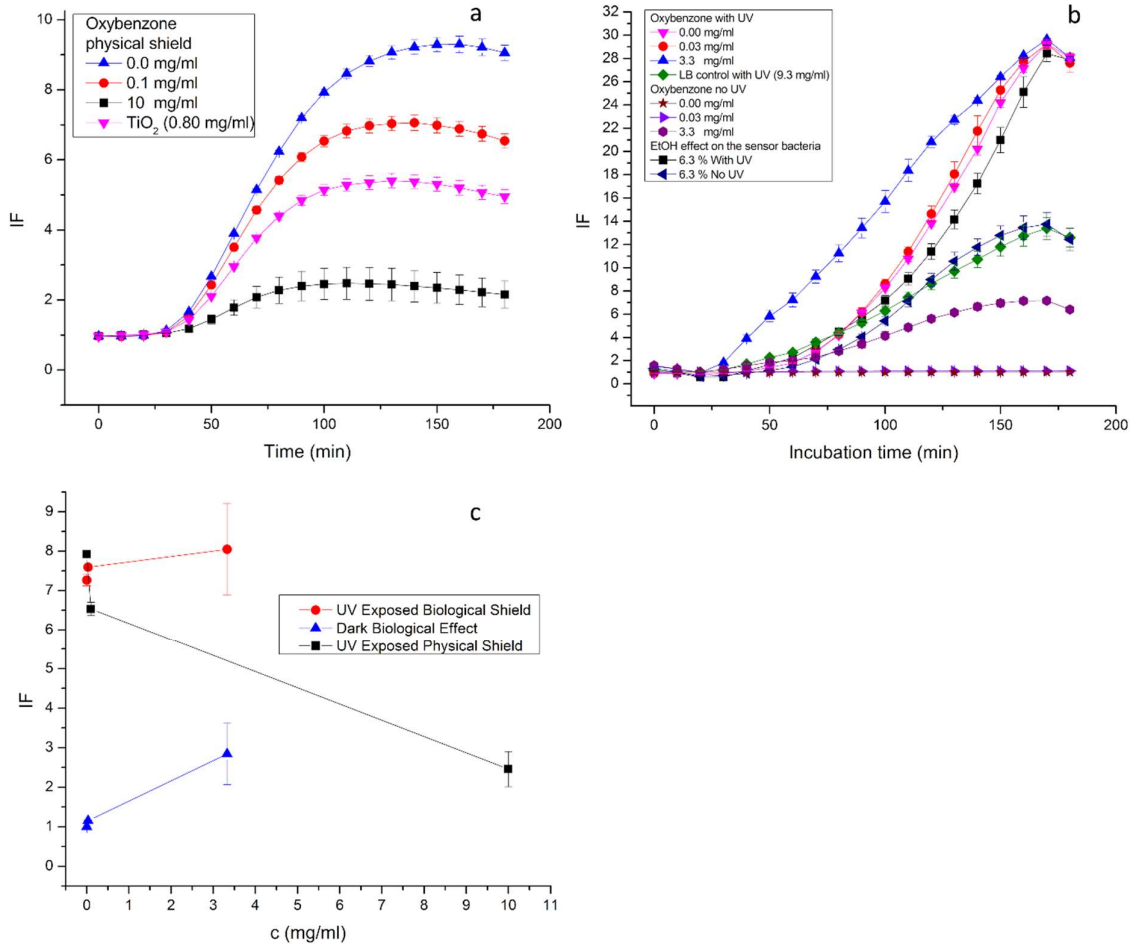


444

445 Figure 3

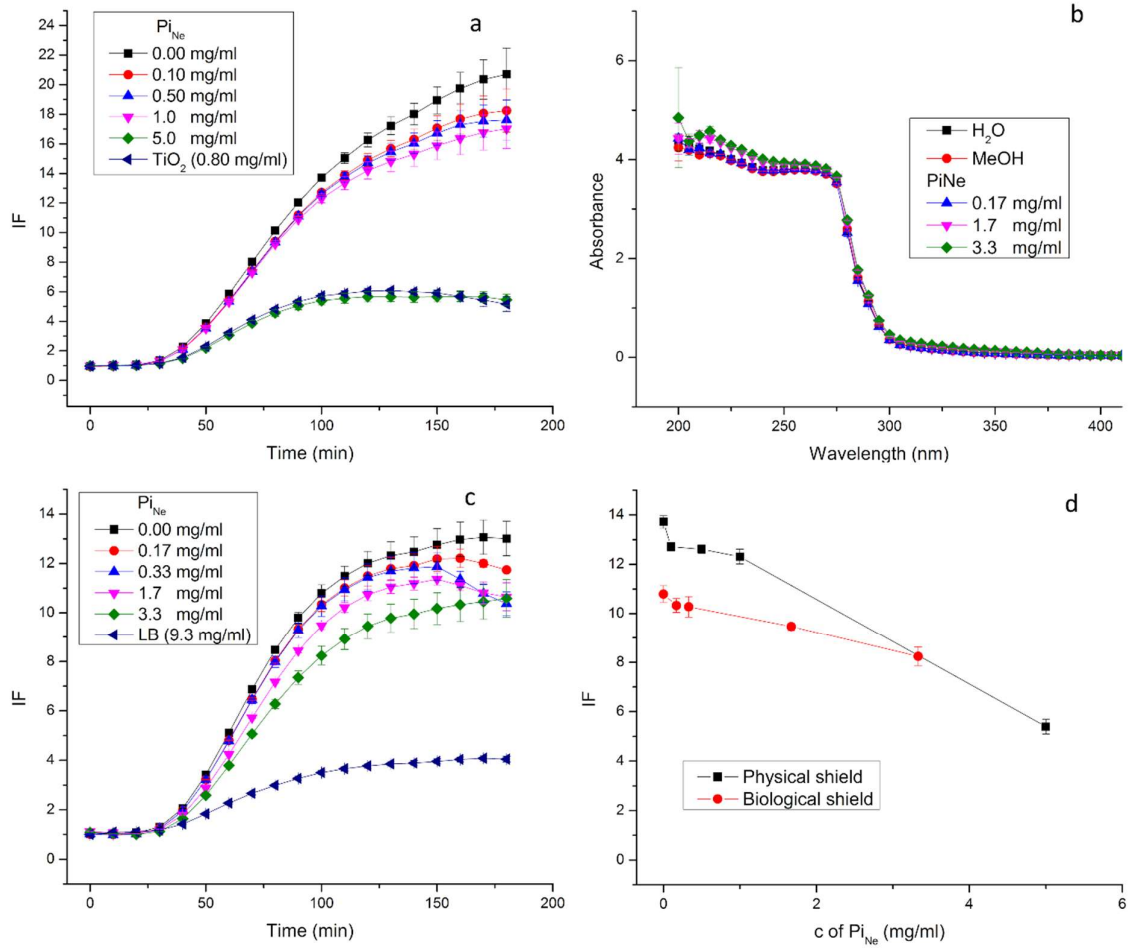


447 Figure 4



448

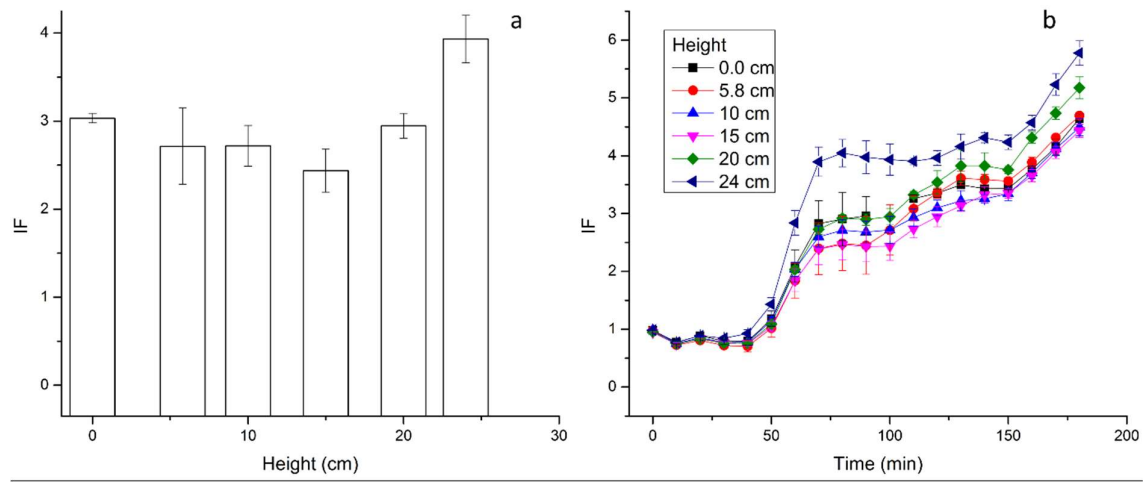
449 Figure 5



450

451

452 Supplementary figure S1



453

PUBLICATION
III

Metabolic Profiling of Water-Soluble Compounds from the Extracts of Dark Septate Endophytic Fungi (DSE) Isolated from Scots Pine (*Pinus sylvestris* L.) Seedlings Using UPLC-Orbitrap-MS

Jenni Tienaho, Maarit Karonen, Riina Muilu-Mäkelä, Kristiina Wähälä, Eduardo Leon Denegri, Robert Franzén, Matti Karp, Ville Santala and Tytti Sarjala

Molecules, 24, 2330
<http://dx.doi.org/10.3390/molecules24122330>

Reprinted from MDPI, © 2019 The Authors (Open access)



Article

Metabolic Profiling of Water-Soluble Compounds from the Extracts of Dark Septate Endophytic Fungi (DSE) Isolated from Scots Pine (*Pinus sylvestris* L.) Seedlings Using UPLC–Orbitrap–MS

Jenni Tienaho ^{1,2,*} , Maarit Karonen ³, Riina Muilu–Mäkelä ², Kristiina Wähälä ⁴, Eduardo Leon Denegri ⁴, Robert Franzén ⁵, Matti Karp ¹, Ville Santala ¹ and Tytti Sarjala ²

¹ Faculty of Natural Sciences and Engineering, Tampere University, FI-33101 Tampere, Finland; karpmatti1@gmail.com (M.K.); ville.santala@tuni.fi (V.S.)

² Natural Resources Institute Finland (Luke), FI-00791 Helsinki, Finland; riina.muilu-makela@luke.fi (R.M.-M.); tytti.sarjala@luke.fi (T.S.)

³ Natural Chemistry Research Group, Department of Chemistry, University of Turku, FI-20014 Turku, Finland; maarit.karonen@utu.fi

⁴ Department of Chemistry, University of Helsinki, FI-00014 Helsinki, Finland; kristiina.wahala@helsinki.fi (K.W.); eleondenegri@outlook.com (E.L.D.)

⁵ School of Chemical Engineering, Department of Chemistry and Materials Science, Aalto University, FI-00076 Espoo, Finland; robert.franzen@aalto.fi

* Correspondence: jenni.tienaho@tuni.fi or jenni.tienaho@luke.fi; Tel.: +358-29-532-4986

Received: 24 May 2019; Accepted: 22 June 2019; Published: 25 June 2019



Abstract: Endophytes are microorganisms living inside plant hosts and are known to be beneficial for the host plant vitality. In this study, we isolated three endophytic fungus species from the roots of Scots pine seedlings growing on Finnish drained peatland setting. The isolated fungi belonged to dark septate endophytes (DSE). The metabolic profiles of the hot water extracts of the fungi were investigated using Ultrahigh Performance Liquid Chromatography with Diode Array Detection and Electron Spray Ionization source Mass Spectrometry with Orbitrap analyzer (UPLC–DAD–ESI–MS–Orbitrap). Out of 318 metabolites, we were able to identify 220, of which a majority was amino acids and peptides. Additionally, opine amino acids, amino acid quinones, Amadori compounds, cholines, nucleobases, nucleosides, nucleotides, siderophores, sugars, sugar alcohols and disaccharides were found, as well as other previously reported metabolites from plants or endophytes. Some differences of the metabolic profiles, regarding the amount and identity of the found metabolites, were observed even though the fungi were isolated from the same host. Many of the discovered metabolites have been described possessing biological activities and properties, which may make a favorable contribution to the host plant nutrient availability or abiotic and biotic stress tolerance.

Keywords: endophytes; endophytic fungi; *Acephala applanata*; *Phialocephala fortinii*; *Humicolopsis cephalosporioides*; *Coniochaeta mutabilis*; Scots pine; metabolites; UPLC–MS; peptides

1. Introduction

Endophytes are bacterial or fungal microorganisms that colonize a wide variety of plant tissues during at least some period of their lifecycle. Endophytic infection is considered inconspicuous, the infected host tissues are at least transiently symptomless, and the microbial colonization is internal [1,2]. Endophytes have been isolated from all of the studied plant species [3]. However, it has been estimated that only 1–2% of the known 300,000 plant species have been studied for their endophytes [4].

The relationship between the host and the endophyte can have many forms ranging from saprobic to parasitic and from exploitative to mutualistic. Endophytic fungi and bacteria have been shown to improve the health of the host plant by improving the biotic and abiotic stress tolerance due to phytohormone production, and host's nutrient uptake [5–8]. The endophytes have also been shown to produce toxic chemicals preventing attacks by insects and herbivores [9,10].

Dark septate endophytic fungi (DSE) are often dominant in the roots of tree species [11] and characterized with melanized and septate hyphae. These Ascomycetous conidial or sterile endophytic fungi colonize the roots of many higher plant species widely in the northern hemisphere and are extensively distributed in coniferous boreal forests [12]. The most frequent DSE in natural forest ecosystems in the northern hemisphere belong to the *Phialocephala fortinii* s.l.–*Acephala applanata* species complex (PAC) and up to 80% of fine roots in forest stands can be colonized by them [11]. Studies have shown that DSE and PAC species induce resistance to abiotic stress, accelerate root turnover and mineralization, and suppress root pathogens [11,13–15].

The metabolic profiling of endophytes has revealed novel compounds possessing interesting bioactive properties to be utilized in future. For example, during the years 1995 to 2011, at least 313 novel compounds were isolated and identified from bacterial and fungal endophytic microorganisms [16]. These were found possessing interesting properties, for example as agrochemicals, antiparasitics and in the field of pharmacology. Additionally, in the previous studies of Scots pine bacterial endophytes, they have been shown to produce efficient antioxidant and antimicrobial compounds [17]. Water extraction has been previously found effective in yielding bioactive principles from microorganisms. For example, water-soluble nucleosides, exopolysaccharides, peptides, proteins and sterols showed also bioactive properties in the caterpillar parasitic fungus *Cordyceps sinensis* [18].

In this study, we explored three common endophytic fungal isolates from conifer roots and their aqueous extracts using LC–MS methodologies. The endophytic fungal species used in this study were isolated from the roots of eight-year-old Scots pine seedlings growing in a Finnish drained peatland setting. The growth conditions for trees and especially young seedlings in drained peatlands are harsh due to the extreme variability in temperature, solar radiation, variability in soil ground water level (drought/flood) and poor nutrition. The northern peatlands are rather unexplored environments as regards their endophytes. Scots pine is one of the most economically important and common tree species in Finland and the boreal zone in general. In spite of that, a limited number of studies has been published about its endophytic symbionts. In fact, to our knowledge, this is the first time that the metabolic profile of water extracted Scots pine root associated endophytic fungi belonging to DSE is investigated. However, under this kind of continuously strenuous growth conditions, the associated endophytes may play a role in enhancing the survival of the host trees by producing effective metabolites with interesting bioactivities. Moreover, we decided to use UPLC–Orbitrap–MS as UPLC enables fast and sensitive analyses with ultra-high performance for complex samples, and Orbitrap has a high resolving power and is thereby suitable for the accurate mass measurements and characterization of compounds.

2. Results and Discussion

2.1. Identification of the Endophytic Fungal Isolates

The taxonomic identification of the isolated fungal strains (A, R, and S16) was made by comparing the ITS (Internal Transcribed Spacer) region with the best GenBank Blast matches (Table 1). According to the DNA sequencing of ITS1, 5.8S and ITS2 rDNA regions, A and R strains belong to PAC. ITS region of the S16 strain matched with the two species *Humicolopsis cephalosporioides* and *Coniochaeta mutabilis*. The alignments of the S16 strain together with its best GenBank matches are presented in Supplementary Figure S1. PAC species cannot be reliably separated using only the ITS regions which emphasizes the need for complementing sequencing methods in order to validate the results [11]. However, the strain A had 100% identity together with *Acephala applanata* strain (AY078147.1), whereas

strain R was more similar with *Phialocephala fortinii* strains (see alignments in Supplementary Figure S2). *Humicolopsis cephalosporioides* and *Coniochaeta mutabilis* can be considered as DSE-like fungi [19]. Previously, *Coniochaeta* were considered as *Lecytophora* sp. [20]. The phylogenetic tree (Figure 1) is rooted with *Coniochaeta mutabilis*. Fungal species used in this study are to be joined into the microbe and yeast library collection of Natural Resources Institute Finland.

Table 1. The endophytic fungus isolates and NCBI information about the best match and our identification.

Strain (GenBank Accession NO.)	GenBank Accession NO. for the Best Match	Max Identity (%)/Query Coverage (%)	Our Description for the Strain	Order	Class	Phylum
A (KM068384)	AY078147.1	100/98	<i>Acephala applanata</i>	Helotiales	Leotiomycetes	Ascomycota
R (KJ649992)	AB671499.2	100/100	<i>Phialocephala fortinii</i>	Helotiales	Leotiomycetes	Ascomycota
S16 (KJ649998)	KC128659	99/98	<i>Humicolopsis cephalosporioides</i>			Ascomycota
	DQ93680	99/98	<i>Coniochaeta mutabilis</i>	Coniochaetales	Sordariomycetes	Ascomycota



Figure 1. The Neighbor-Joining topology of ITS1, 5.8S and ITS2 rDNA sequences of root endophyte strains A, R and S16 from Scots pine and those obtained from GenBank. The phylogenetic tree was rooted with the *Coniochaeta mutabilis*.

2.2. Identification of the Metabolites

We were able to identify 220 metabolites from three fungal extracts (Table 2) and 98 compounds were left unidentified (Supplementary Table S1). Identification was mainly based on the exact masses and the molecular formula observed. It was performed with Thermo Compound Discoverer software and SciFinder Scholar database with the substance role Occurrence and the highest number of references to scale down possible compound hits. Compound Discoverer hits were also run through SciFinder database to verify that the identified products have been found in natural sources. The references shown in Table 2 were used to complement the identification and additionally 39 authentic standards were examined. Metabolites, whose presence and identity were verified with authentic standards, are marked with the reliability of three stars. The majority of the identified metabolites belonged to the group of amino acids, dipeptides and peptides. In addition to the main metabolites, minor ones were also present but the intensity limit of the peaks in the ion chromatogram was set at 1×10^7 , and the peaks with intensities lower than that were not included.

Table 2. The identified metabolites from the aqueous endophytic fungi extracts. Metabolomics Standards Initiative (MSI) was used to define the metabolite identification confidence [21,22]. Level 1 is for confidently identified compounds, where an authentic chemical standard was analyzed under same analysis conditions. Level 2 is for putatively annotated compounds, where physicochemical properties and spectral similarities with public spectral libraries as well as listed references were used. Level 3 is for putatively annotated compound classes, where characteristic physicochemical properties or spectral similarities of compound classes are used to confirm identity. Unidentified compounds are shown in the Supplementary Table S1 and their identification is level 4: unidentified and unclassified but can be differentiated based upon spectral data. Listed references were used to confirm the identification for example by similar findings from natural sources and further justifications are described after the table. If the observed intensity of the metabolite in the total ion chromatogram is over 1×10^7 , metabolite is marked with x under the corresponding fungal extract. nd = not detected. RDB = ring-double bond equivalent.

#ID	RT	[M + H] ⁺	[M - H] ⁻	Exact Mass		RDB	Molecular Formula	Compound	Class	MSI	References	Fungal Extract		
				Measured	Calculated							Error	A	R
1	0.46	175	173	174.11199	174.11168	1.8	C ₆ H ₁₀ O ₂ N ₄	Arginine	Amino acid	1	[23–26]	x	x	x
2	0.49	337	335	336.16316	336.16450	-4.0	C ₆ H ₁₀ O ₂ N ₄	Hexosearginine	Amadori	1	[27–29]	x	x	x
3	0.51	335	333	334.06709	334.06650	1.8	C ₆ H ₁₀ O ₂ P	Glycero-phospho-inositol	Common metabolite	2	[30,31]	x	-	x
4	0.52	372	370	371.22764	371.22810	-1.2	C ₆ H ₁₀ O ₂ N ₇	Acce-Ala-Avg-Ala-NMe	Peptide	2		x	x	x
5	0.53	183	181	182.07875	182.07904	-1.6	C ₃ H ₄ O ₆	Mannitol	Hexitol	1	[24,26,32]	x	x	x
6	0.53	246	244	245.14851	245.14879	-1.1	C ₃ H ₉ O ₃ N ₃	Ala-Avg or Avg-Ala	Dipeptide	2		-	x	x
7	0.54	nd	165	166.04668	166.04774	-6.4	C ₃ H ₁₀ O ₆	Pentonic acid	Pentonic acid	3	[26]	x	x	x
8	0.54	nd	195	196.05748	196.05831	-4.2	C ₃ H ₁₂ O ₇	Hexonic acid	Hexonic acid	3	[26]	x	x	x
9	0.54	218	216	217.10586	217.10626	-1.8	C ₈ H ₁₅ O ₃ N ₃	Ala-Gln	Dipeptide	1		-	-	x
10	0.55	203	201	202.14253	202.14298	-2.2	C ₈ H ₁₅ O ₂ N ₄	Dimethylarginine	Amino acid derivative	2	[25,33]	x	x	x
11	0.55	219	217	218.08984	218.09027	-2.0	C ₈ H ₁₅ O ₂ N ₂	Ala-Glu or Glu-Ala or Heliopeine	Dipeptide or Opine amino acid	2	[34]	-	-	x
12	0.55	244	242	243.08558	243.08552	0.2	C ₉ H ₁₃ O ₂ N ₃	Cytidine	Nucleoside	1	[25,26,35–40]	x	x	x
13	0.55	248	246	247.11641	247.11682	-1.7	C ₉ H ₁₇ O ₂ N ₃	Gln-Thr or Thr-Gln	Dipeptide	2		-	-	x
14	0.55	258	nd	257.10240	257.10282	-3.0	C ₈ H ₂₀ O ₂ NP	Glycero-phosphoryl-choline	Choline	2	[25,41]	x	x	x
15	0.56	191	189	190.09479	190.09536	-3.0	C ₇ H ₁₀ O ₂ N ₂	Ala-Thr or Thr-Ala	Dipeptide	2	[23,24,26]	x	x	x
16	0.56	235°	nd	234.15747	234.15796	-2.1	C ₁₀ H ₂₂ O ₂ N ₂	Valine	Amino acid	2		-	-	x
17	0.56	253	251	252.12182	252.12224	-1.7	C ₁₀ H ₁₆ O ₂ N ₄	His-Pro or Pro-His	Dipeptide	2		-	-	x
18	0.56	266	264	265.11662	265.11615	1.8	C ₁₀ H ₁₆ O ₂ N ₄	Hexoseaminobutyric acid	Amadori	3		-	-	x
19	0.57	205	203	204.11052	204.11101	-2.4	C ₈ H ₁₆ O ₂ N ₂	Sec-Val or Val-Ser	Dipeptide	2	[42]	x	x	-
20	0.58	187	185	186.10007	186.10044	-2.0	C ₈ H ₁₆ O ₂ N ₂	Pro-Ala	Dipeptide	2		-	-	x
21	0.58	198	196	197.07971	197.08004	-1.7	C ₈ H ₁₃ O ₂ N ₃	Acetylhistidine	Amino acid derivative	2		-	-	x
22	0.58	219	217	218.12640	218.12666	-1.2	C ₉ H ₁₈ O ₂ N ₂	Dipeptide ^a or Lysopine or Ridoopine	Dipeptide or Opine amino acid	3/2	[34,43]	x	x	x
23	0.58	246	244	245.13727	245.13756	-1.2	C ₁₀ H ₁₉ O ₄ N ₂	Dipeptide ^b	Dipeptide	3		x	x	x
24	0.58	260	258	259.18913	259.18959	-1.8	C ₁₂ H ₂₅ O ₂ N ₃	Dipeptide ^c	Dipeptide	3		x	x	x
25	0.59	184	nd	183.05615	183.05653	-2.1	C ₈ H ₁₃ O ₂ N ₃	Choline-O-sulphate	Choline	1	[41,44]	x	x	x
26	0.60	233	231	232.10553	232.10592	-1.7	C ₉ H ₁₆ O ₂ N ₂	Asp-Val or Val-Asp	Dipeptide	2		x	x	x
27	0.60	335	333	334.06584	334.06650	-2.0	C ₉ H ₁₉ O ₁₁ P	Glycero-phospho-inositol	Common metabolite	2	[30,31]	x	x	x
28	0.61	165	163	164.06831	164.06848	-1.0	C ₃ H ₄ O ₅	Fucose	Hexose	1	[45]	-	-	x
29	0.64	191	189	190.09482	190.09536	-2.8	C ₇ H ₁₀ O ₂ N ₂	Ala-Thr or Thr-Ala	Dipeptide	2		x	x	-
30	0.64	219	217	218.12619	218.12666	-2.2	C ₉ H ₁₈ O ₂ N ₂	Dipeptide ^d or Lysopine or Ridoopine	Dipeptide or Opine amino acid	3/2	[34,45]	-	-	x
31	0.64	nd	217	218.08980	218.09027	-2.2	C ₈ H ₁₅ O ₂ N ₂	Ala-Glu or Glu-Ala or Heliopeine	Dipeptide or Opine amino acid	2	[34]	-	-	x
32	0.64	nd	565	566.05592	566.05502	1.6	C ₁₂ H ₂₁ O ₂ N ₂ P ₂	UDP-galactose	Nucleotide sugar	2	[46,47]	x	x	x
33	0.65	217	215	216.12187	216.12224	-1.7	C ₈ H ₁₆ O ₂ N ₄	Acetylarginine	Amino acid derivative	2	[26]	x	x	x
34	0.66	255	nd	254.08980	254.09027	-1.8	C ₁₁ H ₁₉ O ₂ N ₂	Nicotinamide riboside	Pyridine nucleoside	2	[48]	x	x	-
35	0.67	152	150	151.04914	151.04941	-1.7	C ₅ H ₅ O ₂ N ₅	Guanine	Nucleobase	1	[35,38]	-	-	x

Table 2. Contd.

#ID	RT	[M + H] ⁺	[M - H] ⁻	Exact Mass			Molecular Formula	RDB	Compound	Class	MSI	References	Fungal Extract	
				Measured	Calculated	Δm (ppm)							A	S16
36	0.67	247	245	246.12114	246.12157	-1.7	C ₁₀ H ₁₈ O ₈ N ₂	3	Dipeptide ^d	Dipeptide	3		x	x
37	0.68	219	217	218.08995	218.09027	-1.5	C ₈ H ₁₄ O ₈ N ₂	2	Ala-Glu or Glu-Ala or Heliopeine UDP-galactosamine	Dipeptide or Opine amino acid Nucleotide sugar	2	[34]	-	-
38	0.68	608	606	607.08235	607.08157	1.3	C ₁₇ H ₂₆ O ₁₇ N ₃ H ₂	8		Nucleotide sugar	2	[45,49]	x	x
39	0.69	247	245	246.12112	246.12157	-1.8	C ₁₀ H ₁₈ O ₈ N ₂	3	Dipeptide ^d	Dipeptide	3		x	x
40	0.69	288	286	287.19514	287.19574	-2.1	C ₁₀ H ₁₈ O ₈ N ₂	3	Dipeptide ^d	Dipeptide	3		x	x
41	0.71	189	187	188.07948	188.07971	-1.2	C ₇ H ₁₂ O ₇ N ₂	4	Acetylglutamate	Amino acid derivative	2	[50]	x	x
42	0.72	193	191	192.02628	192.02701	-3.8	C ₈ H ₁₂ O ₇	4	Isocitrate	Common metabolite	2	[26,29]	-	-
43	0.72	280	278	279.13127	279.1318	-1.9	C ₁₁ H ₂₀ O ₈ N ₂	2	Hexosevaline	Amadori	2	[26,29]	-	-
44	0.73	246	244	245.13705	245.13756	-2.1	C ₁₀ H ₁₆ O ₈ N ₂	3	Dipeptide ^b	Dipeptide	3		x	x
45	0.74	348	346	347.06339	347.06309	-2.0	C ₁₆ H ₁₆ O ₁₃ N ₂ P	8	AMP or dGMP	Nucleotide	2	[51,53]	-	-
46	0.74	nd	565	566.05580	566.05502	1.4	C ₁₂ H ₁₂ O ₇ N ₂ P ₂	8	UDP-glucose	Nucleotide sugar	2	[46,47,53,54]	x	x
47	0.77	204	nd	203.11554	203.11576	-1.1	C ₉ H ₁₂ O ₈ N ₂	2	Acetylserine	Common metabolite	2	[50,55]	x	x
48	0.77	219	217	218.12622	218.12666	-2.0	C ₈ H ₁₆ O ₈ N ₂	2	Dipeptide ^e or Lysopine or Ridopeine	Dipeptide or Opine amino acid	3/2	[34,43]	x	x
49	0.77	333	331	332.13261	332.13320	-1.8	C ₁₂ H ₂₀ O ₈ N ₄	5	Tripeptide/peptide ^f	Tripeptide or peptide	3		x	-
50	0.78	205	203	204.11084	204.11101	-0.8	C ₈ H ₁₆ O ₈ N ₂	2	Ser-Val or Val-Ser	Dipeptide	2		x	x
51	0.78	608	606	607.08248	607.08157	1.5	C ₁₇ H ₂₇ O ₁₇ N ₃ H ₂	8	UDP-glucoseamine	Nucleotide sugar	2	[46,49]	x	x
52	0.80	187	185	186.10017	186.10044	-1.5	C ₈ H ₁₄ O ₈ N ₂	3	Ala-Pro	Dipeptide	1	[24,26]	x	x
53	0.80	193	191	192.02628	192.02701	-3.8	C ₈ H ₁₂ O ₇	4	Citric acid	Common metabolite	3		x	x
54	0.80	260	258	259.18922	259.18959	-2.0	C ₁₂ H ₂₀ O ₈ N ₂	2	Dipeptide ^e	Dipeptide	3		x	x
55	0.81	315	313	314.12205	314.1213	2.4	C ₁₁ H ₂₂ O ₁₀	1	Disaccharide	Disaccharide	3	[56]	-	-
56	0.81	189	187	188.11563	188.11609	-2.4	C ₈ H ₁₆ O ₈ N ₂	3	Dipeptide ^e	Dipeptide	3		x	x
57	0.81	288	286	287.19523	287.19574	-1.8	C ₁₀ H ₂₀ O ₈ N ₂	3	Dipeptide ^e	Dipeptide	3		x	x
58	0.81	333	331	332.13261	332.13320	-1.8	C ₁₂ H ₂₀ O ₈ N ₄	5	Tripeptide/peptide ^f	Tripeptide or peptide	3		x	-
59	0.82	219	217	218.12630	218.12666	-1.7	C ₈ H ₁₆ O ₈ N ₂	2	Dipeptide ^a or Lysopine or Ridopeine	Dipeptide or Opine amino acid	3/2	[34,43]	x	-
60	0.84	260	258	259.15272	259.15321	-1.9	C ₁₁ H ₂₀ O ₈ N ₃	3	Dipeptide ^b or Lysopine or Ridopeine	Di-/Tripeptide	3		x	x
61	0.85	219	217	218.12633	218.12666	-1.5	C ₈ H ₁₆ O ₈ N ₂	2	Ridopeine	Dipeptide or Opine amino acid	3	[34,43]	x	x
62	0.85	233	231	232.14292	232.14231	-6.3	C ₁₀ H ₂₀ O ₈ N ₂	2	Dipeptide ^g	Dipeptide	3		x	x
63	0.85	260	258	259.18870	259.18959	-3.4	C ₁₂ H ₂₀ O ₈ N ₂	2	Dipeptide ^g	Dipeptide	3		x	x
64	0.86	221	219	220.08778	220.08817	-1.8	C ₈ H ₁₆ O ₈ N ₂ S	2	Cys-Val or Val-Cys or Met-Ala	Dipeptide	2		x	x
65	0.86	245	243	244.06948	244.06954	-0.2	C ₉ H ₁₂ O ₈ N ₂	5	Pseudouridine	Nucleoside	2	[25,35]	-	-
66	0.86	247	245	246.12114	246.12157	-1.7	C ₁₀ H ₁₈ O ₈ N ₂	3	Dipeptide ^d	Dipeptide	3		x	x
67	0.87	182	180	181.07374	181.07389	-0.8	C ₈ H ₁₂ O ₇	5	Tyrosine	Amino acid	1	[23–26,35]	x	x
68	0.87	nd	205	206.04209	206.04266	-2.8	C ₇ H ₁₀ O ₇	3	Methylsuccinic acid	Common metabolite	2	[57,58]	x	x
69	0.89	260	258	259.15288	259.15321	-1.3	C ₁₁ H ₂₀ O ₈ N ₃	3	Di-/Tripeptide ^h	Di-/Tripeptide	3		x	-
70	0.91	190	188	189.06334	189.06372	-2.0	C ₈ H ₁₂ O ₈ N ₂	2	Acetylglutamic acid	Amino acid derivative	2		x	x
71	0.91	233	231	232.14152	232.14231	-3.4	C ₁₀ H ₂₀ O ₈ N ₂	2	Dipeptide ^g	Dipeptide	3		x	x
72	0.91	260	258	259.18907	259.18959	-2.0	C ₁₂ H ₂₀ O ₈ N ₂	2	Dipeptide ^g	Dipeptide	3		x	x
73	0.93	233	231	232.10574	232.10592	-0.8	C ₈ H ₁₆ O ₈ N ₂	2	Asp-Val or Val-Asp	Dipeptide	2		x	x
74	0.95	nd	205	206.04215	206.04266	-2.5	C ₇ H ₁₀ O ₇	4	Methylsuccinic acid	Dipeptide	2		x	x
75	0.95	218	216	217.10599	217.10626	-1.2	C ₈ H ₁₂ O ₈ N ₂	3	Acetylglutamic acid	Common metabolite	2	[57,58]	x	x
76	0.97	190	188	189.06359	189.06372	-0.7	C ₇ H ₁₂ O ₈ N ₂	3	Acetylglutamic acid	Amino acid derivative	2		-	-
77	0.97	307	305	306.02467	306.02530	-2.1	C ₁₀ H ₁₈ O ₈ N ₂ P	5	2,3'-cUMP or 3',5'-cUMP	Amino acid derivative	2	[59–62]	-	-
78	0.99	245	243	244.06915	244.06954	-1.6	C ₉ H ₁₂ O ₈ N ₂	5	Uridine	Nucleoside	1	[35,36,38,39,63]	x	x
79	0.99	288	286	287.19481	287.19574	-3.2	C ₁₀ H ₂₀ O ₈ N ₂	3	Dipeptide ^e	Dipeptide	3		x	x
80	0.99	332	330	331.06817	331.06817	-2.0	C ₁₀ H ₁₄ O ₈ N ₂ P	8	dAMP	Nucleotide	2	[52,53,64]	-	-
81	1.01	253	251	252.11056	252.11101	-1.8	C ₁₂ H ₁₆ O ₈ N ₂	6	Ala-Tyr	Dipeptide	1		x	x
82	1.03	261	259	260.13679	260.13722	-1.6	C ₁₁ H ₂₀ O ₈ N ₂	3	Dipeptide ^l	Dipeptide	3		x	x

Table 2. Contd.

#ID	RT	[M + H] ⁺	[M - H] ⁻	Exact Mass		Error	Molecular Formula	RDB	Compound	Class	MSI	References	Fungal Extract		
				Measured	Calculated								Δm (ppm)	A	R
83	1.04	203	201	202.13162	202.13174	-0.6	C ₉ H ₁₈ O ₃ N ₂	2	Leu-Ala	Dipeptide	1		x	x	x
84	1.04	215	213	214.13141	214.13174	-1.5	C ₁₀ H ₁₈ O ₃ N ₂	3	Pro-Val or Val-Pro	Dipeptide	2		x	x	x
85	1.08	221	219	220.08783	220.08817	-1.5	C ₈ H ₁₆ O ₃ N ₂ S	3	Cys-Val or Val-Cys or Met-Ala	Dipeptide	3		x	x	x
86	1.10	261	259	260.13679	260.13722	-1.6	C ₁₁ H ₂₀ O ₃ N ₂	3	Dipeptide ^d	Dipeptide	3		x	x	x
87	1.10	664	662	663.10777	663.10912	-2.0	C ₂₁ H ₂₇ O ₁₄ N ₂ H ₂	15	Nicotinamide adenine dinucleotide	Dinucleotide	2	[48]	-	-	x
88	1.11	240	238	239.15306	239.15321	-0.6	C ₁₁ H ₁₉ O ₃ N ₅	3	Di-/Tripeptide ^h	Di-/Tripeptide	3		x	-	-
89	1.17	202	nd	201.11101	201.11134	-1.6	C ₈ H ₁₅ O ₃ N ₃	3	Acetyl(methyl)-glutaminamide	Amino acid derivative	3		x	-	-
90	1.17	403	401	402.22194	402.22268	-1.8	C ₁₆ H ₃₀ O ₈ N ₆	5	Tripeptide/peptide ^h	Tripeptide or peptide	3		x	-	-
91	1.18	613	611	612.15080	612.15197	-1.9	C ₃₀ H ₅₂ O ₁₂ N ₆ S ₂	8	Glutathione dimer	Tripeptide	3	[17,55,65]	x	-	-
92	1.23	315	313	314.12193	314.12130	2.0	C ₁₁ H ₂₂ O ₁₀	1	Disaccharide	Disaccharide	2	[56]	x	x	-
93	1.24	189	187	188.11571	188.11609	-2.0	C ₈ H ₁₆ O ₃ N ₂	1	Dipeptide ^h	Dipeptide	3		x	x	x
94	1.24	269	267	268.10536	268.10592	-2.1	C ₁₂ H ₁₆ O ₃ N ₂	6	See-Tyr or Tyr-Ser	Dipeptides	3		x	x	x
95	1.30	268	266	267.09608	267.09676	-2.5	C ₁₀ H ₁₉ O ₄ N ₅	7	Adenosine	Nucleoside	1	[25,26,35–38,40,55,63]	x	x	x
96	1.33	315	313	314.12166	314.12130	1.2	C ₁₁ H ₂₂ O ₁₀	1	Disaccharide	Disaccharide	3	[56]	-	x	-
97	1.33	542	540	541.05998	541.06111	-2.1	C ₁₃ H ₂₁ O ₁₃ N ₄ H ₂	11	Cyclic ADP-ribose	Nucleotide	3	[66]	-	x	-
98	1.40	179	177	178.04742	178.04774	-1.8	C ₈ H ₁₆ O ₆	2	Dehydrohexose	Dehydro-hexose	1	[67]	x	x	x
99	1.42	221	219	220.08820	220.08817	0.1	C ₈ H ₁₆ O ₃ N ₂ S	2	Ala-Met	Dipeptide	1		-	-	x
100	1.47	346	344	345.04695	345.04744	-1.4	C ₁₀ H ₁₂ O ₇ N ₅ P	9	2',3'-cGMP or 3',5'-cGMP	Nucleotide	2	[25,38,51,59–62]	x	x	x
101	1.48	219	217	218.12633	218.12666	-1.5	C ₉ H ₁₈ O ₄ N ₂	2	Dipeptide ^a or Lysopine or Rideopeptide	Dipeptide or Opine amino acid	2/3	[34,43]	x	x	x
102	1.50	267	265	266.12611	266.12666	-2.1	C ₈ H ₁₈ O ₄ N ₂	6	Dipeptide ^d	Dipeptide	3		x	x	x
103	1.50	284	282	283.00056	283.00167	-3.9	C ₁₀ H ₁₃ O ₃ N ₅	7	Guanosine isomer	Nucleoside	2	[26,35,37,39]	x	x	x
104	1.54	346	344	345.04701	345.04744	-1.2	C ₁₀ H ₁₂ O ₇ N ₅ P	9	2',3'-cGMP or 3',5'-cGMP	Nucleotide	2	[25,38,51,59–62]	x	-	x
105	1.57	165	163	164.06821	164.06848	-1.6	C ₈ H ₁₂ O ₅	1	Deoxyhexose	Deoxyhexose	3	[68]	x	x	-
106	1.61	246	244	245.13713	245.13756	-1.7	C ₁₀ H ₁₉ O ₄ N ₃	3	Dipeptide ^b	Dipeptide	3		x	x	x
107	1.64	219	217	218.12628	218.12666	-1.7	C ₉ H ₁₈ O ₄ N ₂	2	Dipeptide ^a or Lysopine or Rideopeptide	Dipeptide or Opine amino acid	3/2	[34,43]	x	x	x
108	1.64	267	265	266.12620	266.12666	-1.7	C ₁₃ H ₁₈ O ₄ N ₂	6	Dipeptide ^d	Dipeptide	3		x	x	x
109	1.67	260	258	259.15294	259.15321	-1.0	C ₁₁ H ₂₁ O ₄ N ₂	3	Di-/Tripeptide ^h	Di-/Tripeptide	3		x	x	x
110	1.68	294	292	293.13692	293.13756	-2.2	C ₁₄ H ₁₉ O ₄ N ₅	7	Di-/Tripeptide ^h m	Di-/Tripeptide	3		x	x	x
111	1.69	233	231	232.14200	232.14231	-1.3	C ₁₀ H ₂₀ O ₄ N ₂	2	Dipeptide ^d	Dipeptide	3		x	x	x
112	1.71	281	279	280.10530	280.10592	-2.2	C ₁₆ H ₂₀ O ₄ N ₂	7	Abenquine C or enantiomer	AA quinone	3	[69,70]	x	x	x
113	1.72	189	187	188.11572	188.11609	-2.0	C ₈ H ₁₆ O ₃ N ₂	2	Dipeptide ^g	Dipeptide	3		-	-	x
114	1.74	152	150	151.04925	151.04941	-1.0	C ₈ H ₁₅ O ₃ N ₂	6	Isoguanine or Oxadenine	Nucleoside	2	[71,72]	-	-	x
115	1.74	246	244	245.13727	245.13756	-1.2	C ₁₀ H ₁₉ O ₄ N ₃	3	Dipeptide ^b	Dipeptide	3		x	x	x
116	1.74	279	277	278.12642	278.12666	-0.9	C ₁₄ H ₁₈ O ₄ N ₂	7	Pro-Tyr or Tyr-Pro	Dipeptide	3		x	x	x
117	1.74	288	286	287.19527	287.19574	-1.6	C ₁₂ H ₂₅ O ₃ N ₅	3	Dipeptide ^e	Dipeptide	3		-	-	x
118	1.75	261	259	260.13698	260.13722	-0.9	C ₁₁ H ₂₀ O ₃ N ₂	3	Fusaric acid monomer	Siderophore	2	[73–77]	-	-	x
119	1.75	268	266	267.09639	267.09676	-1.4	C ₁₀ H ₁₃ O ₄ N ₂	7	Deoxyguanosine	Nucleoside	2	[35]	x	x	x
120	1.75	318	316	317.15840	317.15869	-0.9	C ₁₃ H ₂₃ O ₃ N ₅	4	Tripeptide/peptide ^a	Tripeptide/peptide	3		x	x	x
121	1.76	166	164	165.07893	165.07898	-0.3	C ₉ H ₁₁ O ₂ N	5	Phenylalanine	Amino acid	1	[23,24,26,55]	x	x	x
122	1.76	189	187	188.11574	188.11609	-1.8	C ₈ H ₁₆ O ₃ N ₂	2	Dipeptide ^g	Dipeptide	3		-	-	x
123	1.76	260	258	259.15306	259.15321	-0.6	C ₁₁ H ₂₁ O ₄ N ₂	3	Di-/Tripeptide ^h	Di-/Tripeptide	3		-	-	x
124	1.78	257	255	256.10554	256.10592	-1.5	C ₁₁ H ₁₉ O ₃ N ₂	5	Methylthymidine	Nucleoside derivative	2	[78]	x	x	x
125	1.78	266	264	265.11577	265.11615	-1.4	C ₁₀ H ₁₉ O ₃ N ₂	2	Ala-Leu	Amadori	3	[79]	x	x	x
126	1.80	203	201	202.13164	202.13174	-0.5	C ₈ H ₁₆ O ₃ N ₂	2	Di-/Tripeptide ^h	Dipeptide	3		x	x	x
127	1.80	260	258	259.15303	259.15321	-0.7	C ₁₁ H ₂₁ O ₄ N ₂	3	Di-/Tripeptide ^h	Di-/Tripeptide	3		x	x	x
128	1.82	189	187	188.11586	188.11609	-1.2	C ₈ H ₁₆ O ₃ N ₂	2	Dipeptide ^g	Dipeptide	3		x	x	x

Table 2. Contd.

#ID	RT	[M + H] ⁺	[M - H] ⁻	Exact Mass			Molecular Formula	RDB	Compound	Class	MSI	References	Fungal Extract	
				Measured	Calculated	Δm (ppm)							A	R
129	1.82	215	213	214.13157	214.13174	-0.8	C ₁₀ H ₁₈ O ₄ N ₂	3	Pro-Val or Val-Pro	Dipeptide	2		x	x
130	1.82	233	231	232.14207	232.14231	-1.0	C ₁₀ H ₂₀ O ₄ N ₂	3	Dipeptide ¹	Nucleotide	3		x	x
131	1.85	307	305	306.02538	306.02530	0.3	C ₉ H ₁₇ O ₈ N ₂ P	7	2,3'-cUMP or 3',5'-cUMP	Nucleotide	3	[59–62]	x	x
132	1.86	260	258	259.15312	259.15321	-0.3	C ₁₁ H ₂₁ O ₄ N ₃	4	Di-/Tripeptide ^h	Di-/Tripeptide	3		x	x
133	1.86	348	346	347.16926	347.16925	0.0	C ₁₄ H ₂₅ O ₇ N ₃	4	Tripeptide ^h	Tripeptide	3		x	-
134	1.87	249	247	248.11934	248.11947	-0.5	C ₁₀ H ₂₀ O ₃ N ₂ S	2	Met-Val or Val-Met	Dipeptide	2		x	x
135	1.89	261	259	260.13682	260.13722	-1.5	C ₁₁ H ₂₀ O ₄ N ₂	6	Fusarinone monomer	Siderophore	2	[73–77]	x	x
136	1.89	281	279	280.14177	280.14231	-1.9	C ₁₄ H ₂₀ O ₄ N ₂	6	Val-Tyr	Dipeptide	1		x	x
137	1.89	295	293	294.12105	294.12157	-1.8	C ₁₄ H ₁₈ O ₄ N ₂	7	Peptide type compound ^p	Dipeptide or peptide derivative	3	[69,70]	x	x
138	1.90	318	316	317.15846	317.15869	-0.7	C ₁₄ H ₁₈ O ₄ N ₂	4	Tripeptide/peptide ^o	Tripeptide/peptide	3		x	-
139	1.90	317	315	316.09129	316.09067	2.0	C ₁₄ H ₁₈ O ₄ N ₂	7	5-methoxycarbonyl-methyluridine	Nucleoside derivative	2	[39,40]	x	-
140	1.91	229	227	228.14731	228.14739	-0.3	C ₁₁ H ₂₀ O ₃ N ₂	3	Pro-Leu	Dipeptide	1		x	x
141	1.91	247	245	246.12145	246.12157	-0.6	C ₁₀ H ₁₈ O ₄ N ₂	3	Dipeptide ^d	Dipeptide	3		x	x
142	1.95	249	247	248.11934	248.11947	-0.5	C ₁₀ H ₂₀ O ₃ N ₂ S	2	Met-Val or Val-Met	Dipeptide	2		x	x
143	1.96	231	229	230.16318	230.16304	0.6	C ₁₁ H ₂₂ O ₄ N ₂	6	Dipeptide ^d	Dipeptide	3		x	x
144	1.96	348	346	347.16933	347.16925	0.2	C ₁₂ H ₁₆ O ₄ N ₂	6	Ala-Phe	Dipeptide	1		x	x
145	1.96	348	346	347.16933	347.16925	0.2	C ₁₄ H ₂₅ O ₇ N ₃	4	Tripeptide ^o	Tripeptide	3		x	x
146	1.99	223	221	222.10043	222.10044	0.0	C ₁₁ H ₁₄ O ₄ N ₂	6	Gly-Phe	Dipeptide	1		x	-
147	1.99	246	244	245.13786	245.13756	1.2	C ₁₀ H ₁₉ O ₄ N ₂	3	Dipeptide ^b	Dipeptide	3		x	-
148	2.02	541	539	540.14854	540.14791	1.2	C ₂₄ H ₂₈ O ₁₄	11	Phomone A or B or Blumeoside C	Endophyte or plant metabolite	2	[80–82]	x	-
149	2.06	355	353	354.15349	354.15394	0.7	C ₂₄ H ₂₈ O ₁₄	7	Peptide ^r	Peptide	3		-	x
150	2.07	581	579	580.15391	580.15436	-0.8	C ₂₀ H ₂₅ O ₈ N ₁₀ P	15	Dinucleotide	Dinucleotide	3		-	x
151	2.08	229	227	228.14738	228.14739	0.0	C ₁₁ H ₂₀ O ₄ N ₂	3	Ile-Pro or Pro-Ile	Dipeptide	2		x	x
152	2.09	231	229	230.16290	230.16304	-0.6	C ₁₁ H ₂₀ O ₄ N ₂	2	Dipeptide ^d	Dipeptide	3		x	x
153	2.10	247	245	246.12100	246.12157	-2.3	C ₁₀ H ₁₈ O ₄ N ₂	3	Dipeptide ^d	Dipeptide	3		x	x
154	2.10	306	304	305.13731	305.13756	-0.8	C ₁₅ H ₁₉ O ₄ N ₃	8	Thr-Irp or Irp-Thr	Dipeptide	2		x	x
155	2.10	581	579	580.15428	580.15436	-0.1	C ₂₀ H ₂₅ O ₈ N ₁₀ P	15	Dinucleotide	Dinucleotide	3		-	x
156	2.14	318	316	317.15843	317.15869	-0.8	C ₁₃ H ₂₂ O ₄ N ₂	4	Tripeptide/peptide ^h	Tripeptide/peptide	3		x	x
157	2.15	253	251	252.11087	252.11101	-0.5	C ₁₂ H ₁₆ O ₄ N ₂	6	Phe-Ser or Ser-Phe	Dipeptide	2		x	x
158	2.15	279	277	278.12630	278.12666	-1.3	C ₁₄ H ₁₈ O ₄ N ₂	4	Pro-Irp or Irp-Pro	Dipeptide	2	[55]	x	x
159	2.19	455	453	454.15560	454.15560	-0.6	C ₁₆ H ₃₀ O ₇ N ₄ S ₂	7	Peptide ^r	Peptide	3		x	x
160	2.20	280	278	279.12166	279.12191	-0.9	C ₁₃ H ₁₇ O ₄ N ₂	4	Di/tripeptide ¹	Di-/Tripeptide	3		x	-
161	2.20	318	316	317.15861	317.15869	-0.2	C ₁₃ H ₂₃ O ₄ N ₂	4	Tripeptide/peptide ¹	Tripeptide/peptide	3		x	x
162	2.22	229	227	228.14723	228.14739	-0.7	C ₁₁ H ₂₀ O ₄ N ₂	3	Leu-Pro	Dipeptide	1		x	x
163	2.22	345	343	344.13676	344.13722	-1.3	C ₁₆ H ₂₀ O ₄ N ₂	10	Tyr-Tyr	Dipeptide	2		x	x
164	2.24	348	346	347.16899	347.16925	-0.7	C ₁₄ H ₂₀ O ₄ N ₂	4	Tripeptide ^o	Tripeptide	3		x	-
165	2.24	223	221	222.10048	222.10044	0.2	C ₁₁ H ₁₈ O ₄ N ₂	6	Phe-Gly	Dipeptide	2		x	-
166	2.26	277	275	276.11095	276.11101	-0.2	C ₁₄ H ₁₈ O ₄ N ₂	7	Peptide type compound ^h	Dipeptide/cyclodipeptide	3	[83,84]	x	x
167	2.27	294	292	293.13713	293.13756	-1.5	C ₁₄ H ₂₀ O ₄ N ₂	8	Di/tripeptide ^{an}	Di-/Tripeptide	3		x	x
168	2.27	295	293	294.15724	294.15796	-2.4	C ₁₅ H ₂₂ O ₄ N ₂	6	Leu-Tyr	Dipeptide	1		x	x
169	2.28	247	245	246.12108	246.12157	-2.0	C ₁₀ H ₁₈ O ₄ N ₂	3	Dipeptide ^d	Dipeptide	3		x	x
170	2.29	231	229	230.16275	230.16304	-1.2	C ₁₁ H ₂₂ O ₄ N ₂	6	Dipeptide ^d	Dipeptide	3		x	x
171	2.29	237	235	236.11557	236.11609	-2.2	C ₁₂ H ₁₆ O ₄ N ₂	6	Gly-Phe or Phe-Gly methyl ester	Dipeptide derivative	2		x	x
172	2.30	267	265	266.12630	266.12666	-1.3	C ₁₃ H ₁₈ O ₄ N ₂	6	Dipeptide ¹	Dipeptide	3		x	x
173	2.32	229	227	228.14739	228.14739	-0.2	C ₁₁ H ₂₀ O ₄ N ₂	3	Ile-Pro or Pro-Ile	Dipeptide	2		x	x
174	2.32	557	555	556.15074	556.14283	14.2	C ₂₄ H ₂₈ O ₁₅	11	Blumeoside A	Plant metabolite	2	[80]	-	x
175	2.34	205	203	204.08986	204.08988	-0.1	C ₁₁ H ₁₂ O ₂ N ₂	7	Tryptophan	Amino acid	1	[23–26,35]	x	x

Table 2. Contd.

#ID	RT	[M + H] ⁺	[M – H] [–]	Exact Mass		Error	Molecular Formula	RDB	Compound	Class	MSI	References	Fungal Extract		
				Measured	Calculated								Δm (ppm)	A	R
176	2.34	227	225	226.09527	226.09536	–0.4	C ₁₀ H ₁₄ O ₄ N ₂	5	Deoxythymidine	Nucleoside	2	[85]	x	-	x
177	2.34	263	261	262.13484	262.13512	–1.1	C ₁₁ H ₂₀ O ₃ N ₂	2	Dipeptide ^d	Dipeptide	3		x	x	x
178	2.35	261	259	260.13704	260.13722	–0.7	C ₁₁ H ₂₀ O ₃ N ₂	3	Dipeptide ^d	Dipeptide	3		x	x	x
179	2.37	295	293	294.15764	294.15796	–1.1	C ₁₅ H ₂₂ O ₂ N ₂	6	Dipeptide ^o	Dipeptide	3		x	x	x
180	2.38	281	279	280.10551	280.10592	–1.5	C ₉ H ₁₆ O ₂ N ₂	8	Abenquine C or enantiomer	AA quinone	2	[69,70]	x	x	x
181	2.39	277	275	276.11105	276.11101	–0.2	C ₁₄ H ₁₈ O ₂ N ₂	7	Peptide type compound ^h	Dipeptide/cyclodipeptide	3	[83,84]	x	x	x
182	2.39	295	293	294.12163	294.12157	0.2	C ₁₄ H ₁₈ O ₂ N ₂	7	Peptide type compound ^h	Dipeptide or peptide derivative	3	[69,70]	x	x	x
183	2.40	160	158	159.08949	159.08954	–0.3	C ₆ H ₈ O ₂ N	2	Acetyllysine	Amino acid derivative	2	[26]	x	x	x
184	2.41	276	274	275.12709	275.12699	0.4	C ₁₄ H ₁₇ O ₃ N ₃	8	Ala-Trp	Dipeptide	1		x	x	x
185	2.45	261	259	260.13728	260.13722	0.2	C ₁₁ H ₂₀ O ₃ N ₂	3	Dipeptide ^d	Dipeptide	3		x	x	x
186	2.45	263	261	262.13499	262.13512	–0.5	C ₁₁ H ₂₀ O ₃ N ₂	3	Dipeptide ^d	Dipeptide	3		x	x	x
187	2.46	295	293	294.15803	294.15796	0.2	C ₁₅ H ₂₂ O ₂ N ₂	6	Dipeptide ^o	Dipeptide	3		x	x	x
188	2.50	281	279	280.10603	280.10592	0.4	C ₁₃ H ₁₆ O ₃ N ₂	7	α-Asp-Phe	Dipeptide	1		x	x	x
189	2.54	245	243	244.17876	244.17869	0.3	C ₁₂ H ₂₄ O ₂ N ₂	2	Leu-Leu	Dipeptide	1		x	x	x
190	2.54	281	279	280.10582	280.10592	–0.3	C ₁₃ H ₁₆ O ₃ N ₂	7	β-Asp-Phe	Dipeptide	1		x	x	x
191	2.55	265	263	262.13402	262.13512	–4.2	C ₁₁ H ₂₀ O ₃ N ₂	2	Dipeptide ^o	Dipeptide	3		x	x	x
192	2.55	265	263	264.14735	264.14739	–0.1	C ₁₄ H ₂₀ O ₃ N ₂	6	Val-Phe or Phe-Val	Dipeptide	2		x	x	x
193	2.58	253	251	252.12127	252.12224	–3.8	C ₁₇ H ₂₀ O ₂ N ₄	8	His-Pro or Pro-His	Dipeptide	2		x	x	x
194	2.59	382	380	381.15388	381.15360	0.7	C ₁₇ H ₂₀ O ₂ N ₄	8	Tripeptide ^x	Tripeptide	3		x	x	x
195	2.60	293	291	292.10606	292.10592	0.5	C ₁₄ H ₁₈ O ₃ N ₂	8	Pyr-Tyr or Cyclo(Glu-Tyr)	Dipeptide/cyclo-dipeptide	2	[83]	x	-	-
196	2.61	192	190	191.06101	191.06162	–3.2	C ₉ H ₁₅ O ₂ N ₂	2	Acetylmethionine	Amino acid derivative	2	[26,86]	x	-	x
197	2.66	281	279	280.10557	280.10592	–1.2	C ₈ H ₁₆ O ₂ N ₂	7	Phe-Asp	Dipeptide	2		x	x	x
198	2.66	295	293	294.15748	294.15796	–1.6	C ₁₅ H ₂₂ O ₂ N ₂	6	Dipeptide ^o	Dipeptide	3		x	-	x
199	2.69	263	261	262.13505	262.13512	–0.3	C ₁₁ H ₂₀ O ₃ N ₂	2	Dipeptide ^o	Dipeptide	3		x	x	x
200	2.75	276	274	275.12715	275.12699	0.6	C ₁₄ H ₁₇ O ₃ N ₃	8	Trip-Ala	Dipeptide	2		x	x	x
201	2.75	433	431	432.12736	432.12678	1.3	C ₁₈ H ₂₄ O ₂	7	Asperulosidic acid or isomer	Plant metabolite	2	[87–91]	x	x	-
202	2.75	518	516	517.23808	517.23840	–0.6	C ₃₄ H ₅₀ O ₁₀ N ₅	7	Peptide ^g	Peptide	3		x	x	-
203	2.77	306	304	305.13740	305.13756	–0.5	C ₁₅ H ₁₉ O ₄ N ₃	8	Thr-Trip or Trip-Thr	Dipeptide	2		x	x	x
204	2.78	295	293	294.12150	294.12157	–0.2	C ₁₄ H ₁₈ O ₃ N ₂	7	Peptide type compound ^h	Dipeptide or peptide derivative	2	[69,70]	x	x	x
205	2.81	265	263	264.14732	264.14739	–0.3	C ₁₄ H ₂₀ O ₂ N ₂	6	Val-Phe or Phe-Val	Dipeptide	3		x	x	x
206	2.91	248	246	247.10475	247.10559	–3.4	C ₁₀ H ₁₇ O ₆ N	3	Pentoseproline or Valinopine or Linamarin	Amadori or Opine amino acid or Plant metabolite	2	[92–94]	x	x	x
207	2.99	287	285	286.10512	286.10526	–0.5	C ₁₄ H ₁₈ O ₇	5	Orsellinic acid ester	Plant metabolite	3	[16,95–97]	-	x	-
208	3.01	248	246	247.10585	247.10559	1.1	C ₁₀ H ₁₇ O ₆ N	3	Pentoseproline or Valinopine or Linamarin	Amadori or Opine amino acid or Plant metabolite	2	[92–94]	x	x	x

Table 2. Contd.

#ID	RT	[M + H] ⁺	[M - H] ⁻	Exact Mass			Molecular Formula	RDB	Compound	Class	MSI	References	Fungal Extract	
				Measured	Calculated	Δm (ppm)							A	S16
209	3.02	528	526	527.29613	527.29552	1.2	C ₃₄ H ₄₁ O ₈ N ₅	7	Peptide ^z	Peptide	3		-	x
210	3.11	243	241	242.12691	242.12666	1.0	C ₁₁ H ₁₈ O ₃ N ₂	4	Dipeptide [#]	Dipeptide	3		x	-
211	3.22	174	172	173.10513	173.10519	-0.3	C ₈ H ₁₅ O ₃ N	2	Acetyl/leucine or acetyl/isoleucine	Amino acid derivative	2	[26]	x	-
212	3.29	243	241	242.12608	242.12666	-2.4	C ₁₁ H ₁₈ O ₃ N ₂	4	Dipeptide [#]	Dipeptide	3		x	-
213	3.37	174	172	173.10538	173.10519	1.1	C ₈ H ₁₅ O ₃ N	2	Acetyl/leucine or acetyl/isoleucine	Amino acid derivative	2	[26]	x	-
214	3.37	663	661	662.33214	662.33023	2.9	C ₃₃ H ₅₀ O ₂	11	Saponin	Saponin	2	[98,99]	x	x
215	3.50	282	280	281.08955	281.08994	-1.4	C ₁₃ H ₁₉ O ₂	7	Phenylacetyl-glutamine	Amino acid derivative	2	[83,84]	x	x
216	3.76	277	275	276.11101	276.11101	-1.8	C ₉ H ₁₅ O ₂ N ₂	8	Peptide type, compound ^u	Dipeptide/cyclodipeptide	3		x	-
217	4.07	517	515	516.27897	516.27685	4.1	C ₂₀ H ₃₀ O ₇ N ₁₀	7	Acetyltryptophan	Peptide	3		x	-
218	4.23	247	245	246.10060	246.10044	0.7	C ₉ H ₁₅ O ₃ N ₂	8	Tripeptide/peptide ^s	Amino acid derivative	2		x	-
219	4.30	397	395	396.21529	396.21212	8.0	C ₁₇ H ₂₅ O ₈ N ₆	6	Tripeptide/peptide ^s	Tripeptide/peptide	3		x	-
220	4.95	201	199	200.10441	200.10486	-2.2	C ₁₀ H ₁₆ O ₄	2	Rumitidesin derivative	endophytic fungi metabolite	3	[16,100]	x	x

a = Dipeptide containing Leu or Ile and Ser or Thr and Val; b = Dipeptide containing Leu or Ile and Asn or Gln and Val; c = Dipeptide containing Leu or Ile and Lys; d = Dipeptide containing Leu or Ile and Asp or Glu and Val; e = Dipeptide containing Leu or Ile and Arg; f = Tripeptide containing Ala, Asp and Gln or Glu, Glu and Gly or Ala, Asn and Glu or a tetrapeptide containing Ala, Ala, Asp and Gly or Ala, Glu Gly and Gly or the methyl ester of acetylated tripeptide containing Asn, Gly and Ser; g = Dipeptide containing Leu or Ile and Gly or Ala and Val; h = Dipeptide containing Leu or Ile and Gln; or a tripeptide containing Ala, Gly and Leu or Ile; or Ala, Ala and Val; or the methyl ester of an acetylated dipeptide containing Gly or Ala and Lys; or the ethyl ester of Ala-Ala-Ala or a tripeptide containing Gly, Gly and Val; or an acetylated dipeptide containing Thr and Val; or the methyl ester of a tripeptide containing Gly, Gly and Leu or Ile; or the methyl ester of a dipeptide containing Or Asn and Leu or Ile; or Val and Gln; or the methyl ester of a tripeptide containing Ala, Gly and Val; i = Dipeptide containing Leu or Ile and Thr; j = Dipeptide containing Leu or Ile and Glu; k = Tripeptide containing Arg, Glu and Val; or Arg, Asp and Leu or Ile; or Gln, Glu and Lys or a tetrapeptide containing Ala, Ala, Asp and Lys; or Ala, Gln, Gly and Lys or a pentapeptide containing Ala, Ala, Gly, Gly and Lys; l = Dipeptide containing Phe and Thr or the methyl ester of a dipeptide containing Phe and Ser or Ala and Tyr; or the ethyl ester of a dipeptide containing Gly and Tyr; or the phenyl methyl ester of a dipeptide containing Ala and Ser; m = Dipeptide containing Gln and Phe or a tripeptide containing Ala, Gly and Phe or the methyl ester of a dipeptide containing Asn and Phe or the methyl ester of a tripeptide containing Gly, Gly and Phe or the phenyl methyl ester of a dipeptide containing Gln and Gly or the phenyl methyl ester of a tripeptide containing Ala, Gly and Gly; n = Tripeptide containing Ala, Glu and Val; or Glu, Glu and Leu or Ile; or Pro, Thr and Thr; or Ala, Asp and Leu or Ile; or an acetylated tripeptide containing Gly, Ser and Leu and Ile; or Gly, Thr and Val; or the methyl ester of a tripeptide containing Ala, Asp and Val or Asp, Gly and Leu or Ile; o = Tripeptide containing Asp, Thr and Leu or Ile; Or Glu, Ser and Leu or Ile; or Glu, Thr and Val; or the methyl ester of a tripeptide containing Asp, Thr and Val; or an acetylated tripeptide containing Ser, Thr and Val; p = Dipeptide containing Glu and Phe or Abenquine B1 or Abenquine B2; q = Dipeptide containing Leu or Ile and Val; r = Tripeptide-amide containing Pyr, Glu and Pro; s = Tetrapeptide containing Cys, Met, Thr and Thr or Met, Met, Ser and Ser; t = Dipeptide containing Asn and Phe or a tripeptide containing Gly, Gly and Phe; or a dipeptide-amide containing Asp and Phe; or an acetylated dipeptide-amide containing Gly and Tyr or the phenyl methyl ester of Gly-Gly-Gly; u = Pyr-Phe or Cyclo(3-OH-Pro-Tyr) or Acetylmethoxy-Tyr; v = Dipeptide containing Leu or Ile and Met; w = Dipeptide containing Leu or Ile and Tyr; x = Tripeptide containing Ala, Glu and Tyr; or Asp, Phe and Thr; or Glu, Phe and Ser or the methyl ester of a tripeptide containing Asp, Phe and Ser; y = Tetrapeptide containing Gln, Glu, Glu and Leu or Ile; or a pentapeptide containing Ala, Asp, Val and Val; or Asp, Pro, Ser, Ser or Leu or Ile; or Ala, Ala, Glu, Glu And Val; or Ala, Ala, Asp, Glu and Leu or Ile; or Ala, Glu, Gly and Leu or Ile; or Asp, Pro, Thr, Ser, Val; or Glu, Pro, Thr and Thr; z = Pentapeptide containing Pro, Pro, Thr, Thr and Leu or Ile; or Glu, Gly, Pro, Leu or Ile and Leu or Ile; or Ala, Asp, Pro, Leu or Ile and Leu or Ile; or Ala, Glu, Pro, Val and Leu or Ile; # = Cyclo(Glu-Leu); or Pyr and Leu or Ile; or Pyr-Val methyl ester; ° = Tetrapeptide containing Ala, Arg, Arg and Asp; or Arg, Arg, Glu and Gly; or an acetylated tetrapeptide containing Arg, Arg, Gly and Ser; § = Tripeptide containing Gln, His and Leu or Ile; or a tetrapeptide containing Ala, Gly, His and Leu or Ile; or Ala, Ala, His and Val; or an acetylated tripeptide containing Ala, His and Lys; or the methyl ester of a tripeptide containing Pyr, Arg and Pro; or a pentapeptide-amide containing Ala, Gly, Gly, Pro and Pro; ° = Is detected by the [2M + H]⁺ ion due to the used m/z range.

2.2.1. Amino Acids, Dipeptides and Peptides

Amino acids, dipeptides and tripeptides are the most abundant group of identified metabolites in Table 2, as can be expected with water extraction. With the used m/z range 150–2000, we were able to detect five amino acids: arginine, valine, tyrosine, phenylalanine and tryptophan (Figure 2). All except valine were verified with authentic standards and their retention time order is similar to that found in the literature [23,24,55]. Valine was detected by the $[2M + H]^+$ ion as its molecular weight is too low for the scan range used. Arginine was found to be the most dominant compound and it was detected with multiple retention times and the intensities up to 1×10^9 in the mass spectrum. It was also detected as a degradation product of many peptides or other structures with arginine backbone, which explains the multiple retention times. Amino acids formed potassium adducts and $[2M + H]^+$ and $[2M - H]^-$ ions were also observed for them. In addition, arginine was detected by $[3M + H]^+$ and $[3M - H]^-$ ions and tryptophan with ammonium fragment ions.

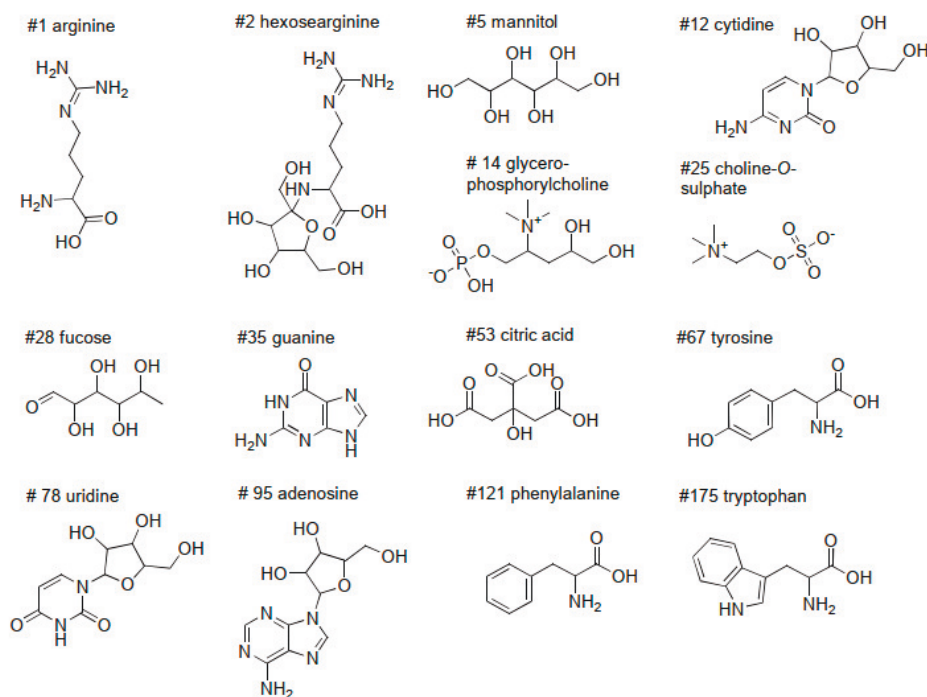


Figure 2. Structures of some of the identified compounds with #ID from Table 2.

Dipeptides were the most abundant class of compounds in our samples (Table 2) with 122 possible identifications, which represents 55% of the identified metabolites. Out of the dipeptides, 16 were verified with authentic standards (Figure 3). In addition, three tentative identifications of cyclic dipeptides were made using databases and listed references in Table 2: Cyclo(Glu-Tyr); Cyclo(3-OH-Pro-Tyr) and Cyclo(Glu-Leu) or Cyclo(Glu-Ile). Plant associated microorganisms are known to produce a variety of N-containing compounds, such as cyclic peptides and peptides [6,83,84,101].

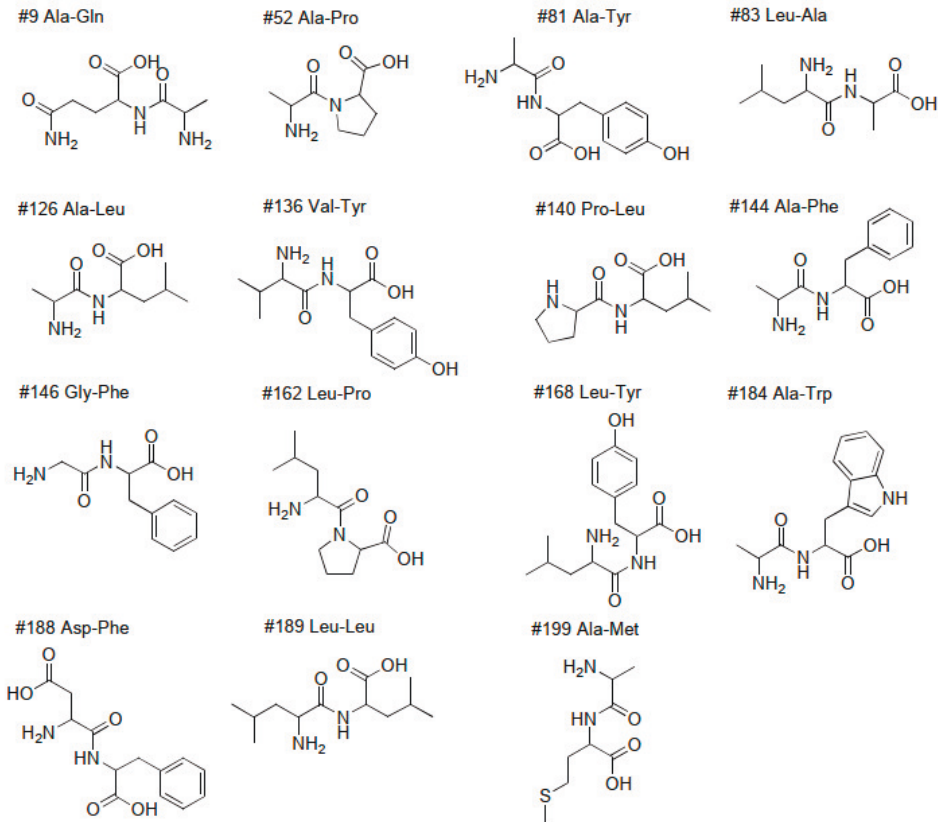


Figure 3. Dipeptides, whose presence was verified with authentic standards and #ID from Table 2.

Furthermore, 29 tripeptides and other oligopeptides were tentatively identified in our samples (Table 2) together with 14 amino acid derivatives. Small peptides and amino acids have also been identified from the tubers of *Pinellia ternate* roots [26] and some of the findings confirm the retention order of the compounds identified by databases and literature in our study. For some compounds, additional ions were detected. Ammonium adducts were typical for aceglutamide and acetylcitrulline type compounds and the sodium adduct was detected for acetylleucine and acetylisoleucine. Glutathione yielded an additional doubly charged ion. It is a peptide produced in response to several stress situations in endophytic microbes [17,65]. Its retention order in comparison to acetylcarnitine, tyrosine, adenosine, phenylalanine and tryptophan is the same as reported by Ibanez et al. [55]. Additional ions of tryptophan and its ammonium fragment were detected for acetyltryptophan and for Trp-Ala dipeptide, which strengthens the tentative identifications. The retention order of arginine, dimethylarginine, tyrosine and tryptophan was similar to that found in Liang et al. [25]. Dimethylarginine was also detected with ESI-MS by Gamał-Eldin et al. [33]. In addition, methionine and its derivatives, such as acetylmethionine have an important role in the biochemistry of plant tissues [86].

The proteins and enzymes produced by the endophytes have been reported to increase thermostability, pH-stability, UV tolerance and products with activity against pathogenic microorganisms [6]. Peptides produced by the endophytes have also been searched for new antibiotic compounds and other bioactive properties [102,103]. Antimicrobial peptides and proteins have been found to be biosynthesized immediately in response to pathogenic microorganism assault [104–106]. In this study, we detected large amounts of arginine, which is commonly used as nitrogen storage

because it has the highest nitrogen to carbon ratio out of all 21 proteinogenic amino acids [107]. Nitrogen is often a limiting resource for the plant growth since it is needed for nucleic acid and protein synthesis. Arginine is used in the production of nitric oxide and polyamines in plants as well and both play a crucial role in the responses to abiotic and biotic stress [107]. One of the cyclic dipeptides found, Cyclo(3-OH-Pro-Tyr) was reported with acaricidal activity against *Tetranychus urticae* and cyclic dipeptides have been described being active towards plant pathogens [84,108].

2.2.2. Opine Amino Acids

Four possible identifications in Table 2 were opines or N²-(1-carboxyethyl)-amino acids. Heliopine is a conjugate of glutamine and pyruvate, whereas rideopine is a product of the reductive amination of polyamine putrescine with α -ketoglutaric acid [34]. Lysopine is a condensation product of lysine and pyruvate [43]. Heliopine, rideopine and lysopine have all been detected from crown gall tumours produced by rhizosphere bacteria *Agrobacterium tumefaciens* [34,43]. Valinopine has been detected from a poisonous mushroom *Clitocybe acromelalga* and is suggested being a fungal toxin [92]. In addition, we were able to observe a compound tentatively identified as saccharopine, which is a precursor of lysine in the fungal α -amino acid pathway [109]. However, the intensities were under 1×10^7 and, thus, it was not included in Table 2.

2.2.3. Amino Acid Quinones and Amadori Compounds

Abenquine C or its enantiomer and Abenquine B1 and B2 are tentatively identified amino acid quinone derivatives in Table 2. Abenquine C or N-[4-(acetylamino)-3,6-dioxo-1,4-cyclohexadien-1-yl]-L-valine and N-[4-(acetylamino)-3,6-dioxo-1,4-cyclohexadien-1-yl]-leucine (Abenquine B1) and -isoleucine (Abenquine B2) have been isolated from the rhizosphere bacteria *Streptomyces* sp. strain DB634 [69,70]. Because more than one possible amino acid quinone masses were detected and they have been isolated from the rhizosphere, there is a possibility that root-colonizing fungi of the rhizosphere could produce these metabolites. However, the confidence level is putative identification.

Furthermore, Amadori compounds were detected. They are Maillard reaction products where amino acid is attached to a pentose or hexose sugar. Namely, hexosearginine, hexosevaline, pentoseproline, hexoseaminobutyric acid and deoxyhexosethreonine were among the tentatively identified compounds in Table 2. Out of these, the presence of hexosearginine (Figure 2) was verified with a synthetic reference compound (purity 99%) [110]. Additionally, hexosearginine's fragmentation into arginine was detected in UPLC-MS. Amadori compounds have previously been identified from fungal cultures [28] and characteristic ions similar to our findings have also been detected by Davidek et al. [93] and Wang et al. [29]. Hexoseaminobutyric acid was detected with a shorter retention time than the hexose sugar structure as also shown by Lamberts et al. [42]. Additionally, deoxyhexose amino acids have been previously detected from eukaryotic cells [79].

2.2.4. Cholines

Discovered cholines presented in Table 2 are choline-O-sulphate and glycerophosphorylcholine (Figure 2). Choline-O-sulphate has been found in relatively large amounts in fungal mycelia and has been suggested to act as a storage of sulphur, which is an essential metabolite for growth in filamentous fungi [41,44]. Glycerophosphorylcholine is a part of phosphatidylcholine, which is a type of phospholipid in lecithin. Lecithin is a major component of the phospholipid membrane also found in plant tissues [41]. The occurrence of both of these compounds was confirmed with authentic standards and they were observed as potassium adducts in the positive ionization. Glycerophosphorylcholine retention time with respect to arginine, tyrosine, adenosine and tryptophan was same as found by Liang et al. [25].

2.2.5. Nucleobases, Nucleosides, Nucleotides, and their Derivatives

Out of nucleobases, we were able to detect guanine and isoguanine or oxyadenine, which are the only ones with molecular mass over 150 Da (Table 2). The identification of guanine was confirmed by an authentic standard (Figure 2). Isoguanine is a purine analog, which is formed as a result of direct oxidation of adenine [71,72].

Nucleosides contain a nucleobase with a pentose sugar unit: ribose or deoxyribose. Cytidine, pseudouridine, uridine, adenosine, guanosine isomer, deoxyguanosine, methylthymidine, and deoxythymidine (Table 2) were tentatively identified, and the presence of cytidine, uridine and adenosine was verified with authentic standards (Figure 2). Nucleosides were discovered to form formate adducts and $[2M - H]^-$ cluster ions in negative ESI, and guanosine isomer also yielded a fragment ion responding to the detachment of pentose sugar unit. Methylthymidine has been used as an indicator of microbial presence in wastewaters [78].

Nucleotides are nucleosides joined with at least one phosphate group. We were able to tentatively identify adenosine monophosphate (AMP) or deoxyguanosine monophosphate (dGMP), cyclic uridine monophosphate (cUMP), deoxyribose adenosine monophosphate (dAMP), cyclic adenosine diphosphate ribose (cyclic ADP-ribose), cyclic guanosine monophosphate (cGMP) and two exact masses and molecular formulae corresponding to dinucleotides (Table 2). The dinucleotides exhibited a UV maximum at 258–261 nm, which in addition to the shape of the UV spectrum correlates with the literature [111]. The absorption maximum in our study was, however, broader and continued until 300 nm, which is likely caused by other compounds eluting simultaneously. Cyclic nucleotides are used as signaling metabolites in almost all organisms and they regulate a vast number of cellular processes [59–62]. The presence of the main fragment ion at m/z 152.1 was also detected with cGMP as reported in the literature [59]. ADP-ribosyl groups are formed on target proteins as a response to DNA damage and poly(ADP-ribose) polymerase enzyme homologs, which catalyze the reaction, have also been found in fungi [66]. In addition, nicotinamide riboside and nicotinamide adenine dinucleotide (NAD) were tentatively identified. NAD produced a fragment ion at m/z 540.1 in the negative ESI mode corresponding to the cleavage of nicotinamide. The retention order of the above mentioned metabolites was similar to that found in the literature [25,26,36–40,48,51–53,55,63,64,85]. Shiao et al. [35] detected nucleosides and nucleobases from the pathogenic fungus *Cordyceps sinensis* and their retention order is same as ours.

Additionally, sugar-nucleotides, such as uridine diphosphate (UDP)-glucose and UDP-galactose as well as UDP-galactosamine and UDP-glucosamine, were discovered (Table 2). UDP-glucosamines and UDP-galactosamines are important precursors of the bacterial and fungal cell wall [49]. Sugar nucleotides are donors of sugar groups in the biosynthesis of glycosides, polysaccharides and glycoconjugates, and they are abundant in microorganisms and plants [46]. They also possess many important roles in fungi [47,54].

2.2.6. Siderophores

One exact mass corresponding to *cis*- and/or *trans*-fusarinine siderophore was found with two retention times (Table 2). The *cis*- and *trans*-fusarinine backbones are very common in many fungal siderophores [75,76]. Siderophores are low molecular weight compounds that are used for iron uptake and storage and they have, for example, been found to have importance in the maintenance of plant–fungi symbioses [74,77]. Fungi and other microorganisms have been found to produce siderophores under aerobic growth conditions, where low iron availability is detected [75]. Iron is essentially required for the growth and proliferation in both bacteria and fungi and siderophores provide cells with nutritional iron [102]. In DSE fungi, it was found that these species have the ability to acidify the environment and produce siderophores to increase the micronutrient uptake to both members of the symbiont, indicating the association to be mutualistic rather than pathogenic [73]. Fusarinine monomers were also discovered with characteristic formic acid and water fragment ions.

2.2.7. Other Common Metabolites

Pentonic and hexonic acids in Table 2 were identified by their exact masses and molecular formulae according to Sun et al. [26], where they had further identified the species being ribonic and gulonic acids using MS/MS data. Glycerophosphoinositol is closely related to glycerophosphorylcholine. It is found in both plants and fungi and is a major deacylation product of lipid metabolism [30,31,55]. In addition, as with cholines, the potassium adduct was observed for it.

Acetyl coenzyme A is a central carbon and energy cycle metabolite, which is bulky and amphiphilic and, thus, cannot readily transverse biological membranes. Acetylcarnitine is used in fungi to transport the acetyl unit [50]. The retention order of acetylcarnitine in relation to tyrosine, glutathione dimer, adenosine, phenylalanine and tryptophan is also similar to that found by Ibanez et al. [55].

Isocitrate and citric acid are isomers with the same molecular formula as well as methylisocitric acid and methylcitric acid. Citric acid and isocitrate are both important intermediates in the Krebs cycle, which is the metabolic route to produce energy to the eukaryotic cells, such as in plants and fungi. The presence of citric acid was confirmed with an authentic standard (Figure 2). In addition, we observed potassium adducts with both citric acid and isocitrate, which strengthened the tentative identification of isocitrate. Methylcitrate cycle catabolizes propionate in yeast and filamentous fungi [57]. Propionate is produced during the catabolism of amino acids and fatty acid oxidation in higher eukaryotes and is toxic, thus, inhibiting the cell growth [112]. Methylcitrate cycle metabolizes it into pyruvate, which can be used as a source of carbon [58]. Methylcitric acid and methylisocitric acid are important intermediates in this cycle.

2.2.8. Sugars, Sugar Alcohols, Disaccharides

The presence of mannitol and fucose (Table 2) was confirmed using authentic standards (Figure 2). Mannitol is widely distributed in filamentous fungi and stored in the fungal hyphae as a carbon source [32]. Fucose appears to represent a prominent feature in protein-linked glycans in the fungal kingdom [45]. Additionally, disaccharides, such as the one isolated from pathogenic fungal species *Claviceps africans*, with fructofuranose and arabinose backbone [56] were found. Deoxyhexoses, then again, are produced in fungi by pyranose oxidases, which have been reported among lignin-degrading fungi [68] for example. Deoxyhexose yielded fragment ions corresponding to the cleavage of water, whereas dehydrohexose structure was detected by its sodium and ammonium adducts and by $[2M + H]^+$ and $[2M - H]^-$ ions. Dehydrohexose has also been previously reported from evergreen trees [67].

2.2.9. Endophyte or Plant Metabolites

Phomone A and B are enantiometric α -pyrone dimers isolated from the endophytic fungus *Phoma* sp. YN02-p-3 [81,82]. Blumeoside C, which is an iridoid glucoside isolated from *Fagraea blumei* [80] has the same molecular formula. Cuendet et al. [80] discovered that Blumeoside A elutes later than Blumeoside C, which is in accordance with our findings (Table 2).

Asperulosidic acid and its stereoisomer were isolated from the plant *Hedyotis diffusa* using water extraction [89]. According to Friscic et al. [90], asperulosidic acid elutes later than mannitol using reversed-phase liquid chromatography as in our study (Table 2). Asperulosidic acid has also been isolated from *Vernonia cinerea* with ethanol [91] and its structural isomers from *Morinda coreia* and *Saprosma scortechinii* with methanol [87,88].

Furthermore, we were able to find exact masses corresponding to orsellinic acid esters, which have been isolated from the endophytic *Chaetomium* sp. fungus [16,95–97]. However, orsellinic acid ester Globosumone B was not included in the Table 2 because of the chosen intensity limit 1×10^7 .

Two possible triterpene saponin structures were obtained with the molecular formula $C_{35}H_{50}O_{12}$, one could be Dianthosaponin F, which has been isolated from *Dianthus japonicus* with methanol [98], and the other Celosin F, which has been isolated from *Celosia argentea* with 50% ethanol [99].

Linamarin is a cyanogenic glucoside isolated from the cassava (*Manihot esculenta*) roots [94]. Ramulosin derivatives have been previously isolated from endophytic fungi *Nigrospora* sp. Present in the branches of *Garcinia nigrolineata* tree [16,100].

2.3. Metabolites in Fungal Extracts

We conducted a qualitative study on the screening and identification of the water-soluble metabolites from the endophytic fungi extracts. There was a high number of primary metabolites in the aqueous extracts as expected. The number of identified metabolites was almost the same with all of the fungal species, and a majority of the metabolites, 141 compounds, were detected from all of the fungal extracts (Figure 4). From the extract A (*A. applanata*), we identified 177 metabolites and out of these 12 metabolites were exclusively found in fungus A (Figure 4). These twelve were all dipeptides or peptides except the nucleoside derivative 5-methoxycarbonylmethyluridine (Table 2). From the extract of fungus R (*P. fortinii*) 184 metabolites were identified and 15 of the metabolites were found only in this extract. These included fucose, guanine, acetylcitrulline, disaccharides, dinucleotides, acetylleucine or acetylisoleucine, the endophytic fungi metabolite orsellinic acid ester and the plant metabolites blumeoside A and asperulosidic acid as well as dipeptides and peptides. From the extract of fungus S16 (*H. cephalosporioides* or *C. mutabilis*) we identified 177 metabolites and 16 of these were found in the S16 extract only. These included hexosevaline, pseudouridine, acetylglutamic acid, cUMP, NAD and saponin as well as Ala-Glu or Glu-Ala or heliopine and other dipeptides and peptides.

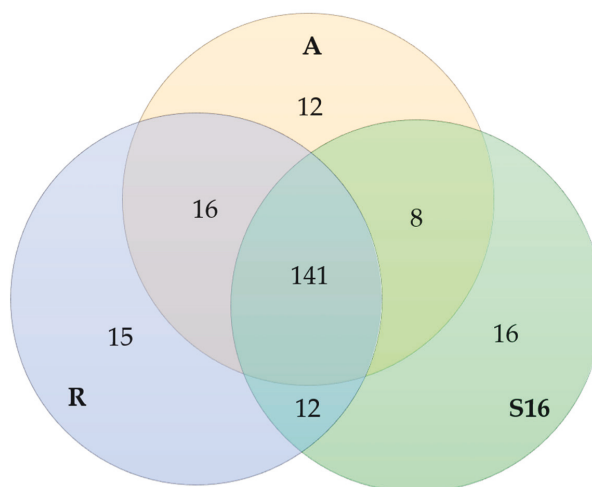


Figure 4. A Venn diagram of the 220 identified metabolites and how they are distributed among the fungal species A (*A. applanata*), R (*P. fortinii*) and S16 (*H. cephalosporioides* or *C. mutabilis*).

In this study, we identified a large number of water-soluble metabolites that may make a contribution to nutrient intake or stress-resistance of the host plant. Many of the identified compounds have been previously reported possessing interesting bioactivities. Thus, the bioactive properties of the fungal isolates and their sub-fractions are to be investigated in the future for their antimicrobial and antioxidant properties to evaluate their potential for the host plant vitality and other applications. To our knowledge, this is the first time that metabolic profiling is conducted on these Scots pine associated endophytic fungi species using water extracts. Thus, this work offers valuable reference about the metabolites of similar endophytes, which are to be discovered in the future.

3. Materials and Methods

3.1. Reagents

Ala-Phe, Ala-Tyr, Asp-Phe (methyl ester), Leu-Leu (acetate), Leu-Pro (hydrochloride), Phe-Ala, Pro-Gly, Pro-Leu, Tyr-Ala, Val-Tyr, guanine, cytidine, uridine, guanosine (hydrate), β -(-)-adenosine, D-mannitol, L-tyrosine, L-arginine (hydrochloride), L-phenylalanine, L-(-)-fucose and *trans*-3-indoleacrylic acid were obtained from Sigma-Aldrich (Saint Louis, MO, USA) each with purity $\geq 98\%$. L- α -Glycerophosphorylcholine (purity 99%) and Choline-O-sulphate (D13, purity 98%) were purchased from Carbosynth Limited, Compton, UK. DL-Ala-DL-Leu (purity $\geq 95\%$), DL-Ala-DL-Met, DL-Ala-DL-Val, L-Ala-L-Gln (HPLC grade), L-Ala-L-Trp, L-Ala-L-Pro (purity $>96\%$), Gly-L-Ile (purity $>99\%$), Gly-DL-Leu, Gly-L-Phe (HPLC grade), Gly-L-Pro (HPLC grade), DL-Leu-Gly, L-Leu-L-Tyr, DL-Leu-DL-Val, L-Leu-L-Ala (hydrate), and Salicin (HPLC grade) were obtained from TCI Europe, Zwijndrecht, Belgium, with purity $>98\%$ unless specified. L-(-)-tryptophan (purity $>99\%$) was purchased from Acros Organics/Thermo Fisher Scientific, Waltham, MA, USA. Hydrogen peroxide and citric acid (monohydrate, purity $>99\%$) were obtained from Merck KGaA, Darmstadt, Germany, and ethanol from Altia, Helsinki, Finland.

3.2. Endophytic Fungi Isolation and Identification

The fungal endophytes were originally isolated from the roots of eight-year-old Scots pine (*Pinus sylvestris* L.) trees grown on a drained peatland forest site in western Finland. Scots pine roots were washed and the root tips were examined under a dissecting microscope. The root tips showing signs of potential fungal association or mycorrhizal features were selected for surface sterilization with a short bath in 70% ethanol and 30% H₂O₂ and followed by laying on sterile Petri dishes on agar. The pure cultures of the fungus mycelium were cultivated on a solid Hagem agar [113] on Petri dishes.

The species of the fungus isolates were identified with molecular methods. DNA from the fungus mycelium was extracted using E.Z.N.A. Fungal DNA Mini Kit (Omega bio-tek, Norcross, GA, USA) according to the manufacturer's instructions. The nucleotide sequence of the Internal Transcribed Spacer (ITS) region of fungal ribosomal DNA (rDNA) was analysed in MacroGen Inc. (Amsterdam) from polymerase chain reaction (PCR) product amplified with ITS1 and ITS4 primer pair [114]. The reaction mixture of 50 μ L included, 10x enzyme buffer (Biotools B&M Labs, S.A. Madrid, Spain), 0.5 μ M each primers, 0.2 μ M dNTP mix, DNA Polymerase (5 U/ μ L) (Biotools B&M Labs, S.A. Madrid, Spain) and 1 μ L DNA template. The PCR were performed with the following conditions: initial incubation at 94 °C for 5 min followed by 25 cycles of 1 min at 94 °C, 1 min at 58 °C and 1.5 min at 72 °C. Sequences with a similarity of $>99\%$ to ITS1, 5.8S and ITS2 rDNA regions were considered as identical species [115]. ITS1, 5.8S and ITS2 regions were extracted from the fungal ITS sequences and the cleaned sequences were used for BLAST searches against GenBank/NCBI to provide taxonomic identification. The best matches from GenBank were aligned and a phylogenetic tree was generated in Geneious 6.0.6 using the Neighbor-Joining analysis (Figure 1). The sequences were deposited in GenBank with accession numbers KM068384, KJ649992 and KJ649998.

3.3. Fungal Extract Preparation

The fungal mass was collected from the surface of a cellophane membrane on agar [113] with a scalpel, stored at -80 °C, and ground in a mortar before adding to sealed, sterile and previously weighed polypropylene test tubes (BD Falcon™, VWR International Oy, Helsinki, Finland). The extraction was executed with boiling deionized and filtered (0.2 μ m, Nylon 66 Filter Membrane from Supelco by Sigma-Aldrich Co, Saint Louis, MO, USA) water. The fungal mass was mixed with equal amount of boiling deionized and filtered (0.45 μ m Nylon membrane, Supelco Analytical/Sigma Aldrich, Saint Louis, MO, USA) water (1 mL = 1 g) by vortexing. Extraction tubes were then shaken in $+95$ – 100 °C water bath (SW22, JULABO Labortechnik GmbH, Seelbach, Germany) for 15 minutes after which the tubes were cooled in an ice bath before vortexing again. Extraction tubes were then centrifuged at

+4 °C and 8200 g for 10 minutes (Eppendorf Centrifuge 5804R, Hamburg, Germany). The supernatants were collected into new polypropylene tubes and centrifuged again with the same settings. Finally, the supernatants were filtered through nylon syringe filters (0.2 µm, Cronus Filter from SMI-LabHut Ltd., Gloucester, UK) to new polypropylene tubes. Aliquots of water without fungal material were extracted simultaneously as control samples. The pH of the extracts was measured with indicator paper (scale 1–14) and it ranged from 5.5 to 7. Extracts were dried with freeze-drying equipment (VirTis BenchTop 6K with Trivac E2, D 2,5E Vacuum pump, SP Industries, Warminster, PA, USA) before storing at –80 °C. The dried extracts were dissolved in sterile purified water before analysis.

3.4. UHPLC-DAD-ESI-Orbitrap-MS

After vacuum drying, 20 µL of ethanol and 980 µL of water were added to the samples. The samples were then mixed with a vortex and filtered using 0.2 µm PTFE syringe filter prior to analyses. The samples were analyzed using an ultra-high performance liquid chromatograph coupled to a photodiode array detector (UHPLC–DAD, Acquity UPLC, Waters Corporation, Milford, MA, USA) and a hybrid quadrupole-Orbitrap mass spectrometer (Q Exactive™, Thermo Fisher Scientific GmbH, Bremen, Germany). The column was Acquity UPLC® BEH Phenyl (100 × 2.1 mm i.d.; 1.7 µm; Waters Corporation, Wexford, Ireland). The mobile phase consisted of (A) acetonitrile and (B) water and formic acid (99.9:0.1, The elution profile was as follows: 0–0.5 min, 0.1% A; 0.5–5.0 min, 0.1–30% A (linear gradient); 5.0–5.1 min, 30–90% A (linear gradient); 5.1–7.1 min, 90% A; 7.1–7.2 min, 90–0.1% A (linear gradient); 7.2–8.5 min, 0.1% A. The injection volume was 5 µL and flow rate 0.5 mL/min. The UV data was collected at 190–500 nm. The heated ESI source (H–ESI II, Thermo Fisher Scientific GmbH, Bremen, Germany) was operated both in negative and positive ion modes. The parameters for negative ionization were as follows: spray voltage was set at –3.0 kV, sheath gas (N₂) flow rate at 60 (arbitrary units), aux gas (N₂) flow rate at 20 (arbitrary units), sweep gas flow rate at 0 (arbitrary units), capillary temperature at +380 °C and S-lens RF level at 60. The parameters for positive ionization were similar, except that spray voltage was set at 3.8 kV. Orbitrap was set at a resolution of 70,000 and an automatic gain of 3×10^6 was used. Masses were scanned at *m/z* 150–2000. Pierce ESI Negative Ion Calibration Solution (Thermo Fischer Scientific Inc., Waltham, MA, USA) was used to for the calibration. The data was processed with Thermo Xcalibur Qual Browser software (Version 3.0.63, Thermo Fisher Scientific Inc., Waltham, MA, USA).

3.5. Identification

Orbitrap data was processed using Compound Discoverer 2.1 SP1 (Thermo-Fisher Scientific, Waltham, MA, USA). The processing flow ‘Untargeted Metabolomics Workflow’ was utilized. The following general settings were used for the workflow: mass tolerance = 5 ppm, intensity threshold = 30%, S/N threshold = 3, minimum peak intensity = 1×10^6 , maximum element counts = $100 \times C$, $200 \times H$, $10 \times N$, $100 \times O$, $10 \times S$ and $10 \times P$. The following settings were used for the peak detection: filter peaks = true, maximum peak width = 0.5 min, remove singlets = true, minimum # scans per peak = 5 and minimum # isotopes = 1. ChemSpider and KEGG databases were used for the identification. In addition, we used SciFinder Scholar database (American Chemical Society, CAS, Columbus, OH, USA) with substance role Occurrence and highest number of references to scale down possible compound hits.

Supplementary Materials: The following are available online. Supplementary Figure S1: Alignment of ITS region of S16 strain (KJ649998) with its best GenBank matches *Coniochaeta mutabilis* (DQ93680) and *Humicolopsis cephalosporioides* (KC128659). Supplementary Figure S2: Alignment of ITS region of A (KM068384) and R (KJ649992) strains with their best GenBank matches *Acephala appianata* (AY078147) and *Phialocephala fortinii* (AB671499.2 and AY033087), respectively. Supplementary Table S1: The unidentified metabolites.

Author Contributions: Conceptualization, M.K. (Maarit Karonen), K.W., R.F., M.K. (Matti Karp), V.S. and T.S.; Data curation, J.T. and M.K. (Maarit Karonen); Formal analysis, J.T., M.K. (Maarit Karonen), R.M.-M. and E.L.D.; Funding acquisition, R.F., M.K. (Matti Karp) and T.S.; Investigation, J.T., M.K. (Maarit Karonen), R.M.-M. and E.L.D.; Methodology, M.K. (Maarit Karonen), K.W. and T.S.; Project administration, R.F., M.K. (Matti Karp), V.S.

and T.S.; Resources, M.K. (Maarit Karonen), K.W., M.K. (Matti Karp), V.S. and T.S.; Supervision, M.K. (Maarit Karonen), K.W., R.F., M.K. (Matti Karp), V.S. and T.S.; Validation, J.T., M.K. (Maarit Karonen), K.W. and T.S.; Visualization, J.T., M.K. (Maarit Karonen) and R.M.-M.; Writing—original draft, J.T. and M.K. (Maarit Karonen); Writing—review & editing, J.T., M.K. (Maarit Karonen), R.M.-M., K.W., E.L.D., R.F., M.K. (Matti Karp), V.S. and T.S.

Funding: This research was partly funded by COST Action FA1103: Endophytes in Biotechnology and Agriculture in the form of a short-term scientific mission fund of J. Tienaho. This work has also been funded by the European Regional Development Fund (project code A71142) as well as the town of Parkano and SASKY municipal education and training consortium. Natural Resources Institute Finland and Tampere University are also warmly acknowledged for their financial support. In addition, J. Tienaho is grateful for the personal fund by Kone Foundation.

Acknowledgments: A. Käenmäki, H. Leppälampi and E. Pihlajaviita are kindly acknowledged for their technical assistance. J. Tienaho also thanks Jesús Martín and Olga Genilloud from Fundación MEDINA, Granada, Spain as well as other team members, who welcomed and guided her warmly to their daily work during her short-term scientific mission. Their help with the initial metabolite identification is also respectfully valued.

Conflicts of Interest: The authors declare no conflict of interest. The funders had no role in the design of the study; in the collection, analyses, or interpretation of data; in the writing of the manuscript, or in the decision of publishing the results.

References

1. Stone, J.K.; Bacon, C.W.; White, J. An Overview of Endophytic Microbes: Endophytism defined. In *Microbial Endophytes*, 1st ed.; Bacon, C.W., White, J.F., Jr., Eds.; Elsevier Inc.: New York, NY, USA, 2000; pp. 17–24.
2. Schulz, B.; Boyle, C. What are Endophytes? In *Microbial Root Endophytes*, 1st ed.; Schulz, B.J.E., Boyle, C.J.C., Sieber, T.N., Eds.; Springer Science & Business Media: Berlin, Germany, 2006; pp. 1–13.
3. Hyde, K.D.; Soyong, K. The fungal endophyte dilemma. *Fungal Divers.* **2008**, *33*, 163–173.
4. Strobel, G. The Emergence of Endophytic Microbes and Their Biological Promise. *J. Fungi* **2018**, *4*, 57. [[CrossRef](#)] [[PubMed](#)]
5. Waller, F.; Achatz, B.; Baltruschat, H.; Fodor, J.; Becker, K.; Fischer, M.; Heier, T.; Huckelhoven, R.; Neumann, C.; Von Wettstein, D.; et al. The endophytic fungus *Piriformospora indica* reprograms barley to salt-stress tolerance, disease resistance, and higher yield. *Proc. Natl. Acad. Sci. USA* **2005**, *102*, 13386–13391. [[CrossRef](#)] [[PubMed](#)]
6. Zhang, H.W.; Song, Y.C.; Tan, R.X. Biology and chemistry of endophytes. *Nat. Prod. Rep.* **2006**, *23*, 753–771. [[CrossRef](#)] [[PubMed](#)]
7. Rodriguez, R.J.; White, J.F., Jr.; Arnold, A.E.; Redman, R.S. Fungal endophytes: Diversity and functional roles. *New Phytol.* **2009**, *182*, 314–330. [[CrossRef](#)]
8. Nagabhyru, P.; Dinkins, R.D.; Wood, C.L.; Bacon, C.W.; Schardl, C.L. Tall fescue endophyte effects on tolerance to water-deficit stress. *BMC Plant Biol.* **2013**, *13*, 127. [[CrossRef](#)] [[PubMed](#)]
9. Tellenbach, C.; Sumarah, M.W.; Grünig, C.R.; Miller, J.D. Inhibition of *Phytophthora* species by secondary metabolites produced by the dark septate endophyte *Phialocephala europaea*. *Fungal Ecol.* **2013**, *6*, 12–18. [[CrossRef](#)]
10. Terhonen, E.; Keriö, S.; Sun, H.; Asiegbu, F.O. Endophytic fungi of Norway spruce roots in boreal pristine mire, drained peatland and mineral soil and their inhibitory effect on *Heterobasidion parviporum* in vitro. *Fungal Ecol.* **2014**, *9*, 17–26. [[CrossRef](#)]
11. Grünig, C.R.; Queloz, V.; Sieber, T.N.; Holdenrieder, O. Dark septate endophytes (DSE) of the *Phialocephala fortinii* s.l. –*Acephala applanata* species complex in tree roots: Classification, population biology, and ecology. *Botany* **2008**, *86*, 1355–1369. [[CrossRef](#)]
12. Jumpponen, A.; Trappe, J.M. Dark septate endophytes: A review of facultative biotrophic root-colonizing fungi. *New Phytol.* **1998**, *140*, 295–310. [[CrossRef](#)]
13. Mandyam, K.; Jumpponen, A. Seeking the elusive function of the root-colonising dark septate endophytic fungi. *Stud. Mycol.* **2005**, *53*, 173–189. [[CrossRef](#)]
14. Schulz, B. Mutualistic Interactions with Fungal Root Endophytes. In *Microbial Root Endophytes*, 1st ed.; Schulz, B.J.E., Boyle, C.J.C., Sieber, T.N., Eds.; Springer Science & Business Media: Berlin, Germany, 2006; pp. 261–279.
15. Tellenbach, C.; Grünig, C.R.; Sieber, T.N. Negative effects on survival and performance of Norway spruce seedlings colonized by dark septate root endophytes are primarily isolate-dependent. *Environ. Microbiol.* **2011**, *13*, 2508–2517. [[CrossRef](#)] [[PubMed](#)]

16. Gutierrez, R.M.; Gonzalez, A.M.; Ramirez, A.M. Compounds Derived from Endophytes: A Review of Phytochemistry and Pharmacology. *Curr. Med. Chem.* **2012**, *19*, 2992–3030. [[CrossRef](#)] [[PubMed](#)]
17. Koskimäki, J.J.; Kajula, M.; Hokkanen, J.; Ihantola, E.-L.; Kim, J.H.; Hautajärvi, H.; Hankala, E.; Suokas, M.; Pohjanen, J.; Podolich, O.; et al. Methyl-esterified 3-hydroxybutyrate oligomers protect bacteria from hydroxyl radicals. *Nat. Chem. Biol.* **2016**, *12*, 332–338. [[CrossRef](#)] [[PubMed](#)]
18. Shashidhar, M.; Giridhar, P.; Sankar, K.U.; Manohar, B. Bioactive principles from *Cordyceps sinensis*: A potent food supplement—A review. *J. Funct. Foods* **2013**, *5*, 1013–1030. [[CrossRef](#)]
19. Endo, N.; Dokmai, P.; Suwannasai, N.; Phosri, C.; Horimai, Y.; Hirai, N.; Fukuda, M.; Yamada, A. Ectomycorrhization of *Tricholoma matsutake* with *Abies veitchii* and *Tsuga diversifolia* in the subalpine forests of Japan. *Mycoscience* **2015**, *56*, 402–412. [[CrossRef](#)]
20. Khan, Z.; Gené, J.; Ahmad, S.; Cano, J.; Al-Sweih, N.; Joseph, L.; Chandy, R.; Guarro, J. *Coniochaeta polymorpha*, a new species from endotracheal aspirate of a preterm neonate, and transfer of *Lecythophora* species to *Coniochaeta*. *Antonie van Leeuwenhoek* **2013**, *104*, 243–252. [[CrossRef](#)]
21. Sumner, L.W.; Amberg, A.; Barrett, D.; Beale, M.H.; Beger, R.; Daykin, C.A.; Fan, T.W.-M.; Fiehn, O.; Goodacre, R.; Griffin, J.L.; et al. Proposed minimum reporting standards for chemical analysis. *Metabolomics* **2007**, *3*, 211–221. [[CrossRef](#)]
22. Dunn, W.B.; Erban, A.; Weber, R.J.M.; Creek, D.J.; Brown, M.; Breitling, R.; Hankemeier, T.; Goodacre, R.; Neumann, S.; Kopka, J.; et al. Mass appeal: Metabolite identification in mass spectrometry-focused untargeted metabolomics. *Metabolomics* **2013**, *9*, 44–66. [[CrossRef](#)]
23. Meek, J.L. Prediction of peptide retention times in high-pressure liquid chromatography on the basis of amino acid composition. *Proc. Natl. Acad. Sci. USA* **1980**, *77*, 1632–1636. [[CrossRef](#)]
24. Liu, Z.; Rochfort, S. A fast liquid chromatography–mass spectrometry (LC–MS) method for quantification of major polar metabolites in plants. *J. Chromatogr. B* **2013**, *912*, 8–15. [[CrossRef](#)]
25. Liang, K.; Liang, S.; Lu, L.; Zhu, D.; Zhu, H.; Liu, P.; Zhang, M. Metabolic variation and cooking qualities of millet cultivars grown both organically and conventionally. *Food Res. Int.* **2018**, *106*, 825–833. [[CrossRef](#)]
26. Sun, L.-M.; Zhang, B.; Wang, Y.-C.; He, H.-K.; Chen, X.-G.; Wang, S.-J. Metabolomic analysis of raw *Pinelliae* Rhizoma and its alum-processed products via UPLC-MS and their cytotoxicity. *Biomed. Chromatogr.* **2019**, *33*, e4411. [[CrossRef](#)]
27. Ryu, K.; Ide, N.; Matsuura, H.; Itakura, Y. N α -(1-Deoxy-D-fructos-1-yl)-L-Arginine, an Antioxidant Compound Identified in Aged Garlic Extract. *J. Nutr.* **2001**, *131*, 972S–976S. [[CrossRef](#)]
28. Yoshida, N.; Takatsuka, K.; Katsuragi, T.; Tani, Y. Occurrence of Fructosyl-Amino Acid Oxidase-Reactive Compounds in Fungal Cells. *Biosci. Biotechnol. Biochem.* **2005**, *69*, 258–260. [[CrossRef](#)]
29. Wang, J.; Lu, Y.-M.; Liu, B.-Z.; He, H.-Y. Electrospray positive ionization tandem mass spectrometry of Amadori compounds. *J. Mass Spectrom.* **2008**, *43*, 262–264. [[CrossRef](#)]
30. Prior, S.L.; Cunliffe, B.W.; Robson, G.D.; Trinci, A.P. Multiple isomers of phosphatidyl inositol monophosphate and inositol bis- and triphosphates from filamentous fungi. *FEMS Microbiol. Lett.* **1993**, *110*, 147–152. [[CrossRef](#)]
31. Van Der Rest, B.; Boisson, A.-M.; Gout, E.; Bligny, R.; Douce, R. Glycerophosphocholine Metabolism in Higher Plant Cells. Evidence of a New Glyceryl-Phosphodiester Phosphodiesterase. *Plant Physiol.* **2002**, *130*, 244–255. [[CrossRef](#)]
32. Landi, N.; Pacifico, S.; Ragucci, S.; Di Giuseppe, A.M.; Iannuzzi, F.; Zarrelli, A.; Piccolella, S.; Di Maro, A. Pioppino mushroom in southern Italy: An undervalued source of nutrients and bioactive compounds. *J. Sci. Food Agric.* **2017**, *97*, 5388–5397. [[CrossRef](#)]
33. Gamal-Eldin, M.A.; Macartney, D.H. Selective molecular recognition of methylated lysines and arginines by cucurbit[6]uril and cucurbit[7]uril in aqueous solution. *Org. Biomol. Chem.* **2013**, *11*, 488–495. [[CrossRef](#)]
34. Chilton, W.S.; Petit, A.; Chilton, M.-D.; Dessaux, Y. Structure and characterization of the crown gall opines heliopine, vitopine and ridéopine. *Phytochem.* **2001**, *58*, 137–142. [[CrossRef](#)]
35. Shiao, M.-S.; Wang, Z.-N.; Lin, L.-J.; Lien, J.-Y.; Wang, J.-J. Profiles of nucleosides and nitrogen bases in Chinese medicinal fungus *Cordyceps sinensis* and related species. *Bot. Bull. Acad. Sin.* **1994**, *35*, 261–267.
36. Ranogajec, A.; Beluhan, S.; Šmit, Z. Analysis of nucleosides and monophosphate nucleotides from mushrooms with reversed-phase HPLC. *J. Sep. Sci.* **2010**, *33*, 1024–1033. [[CrossRef](#)]
37. Dudley, E.; Bond, L. Mass spectrometry analysis of nucleosides and nucleotides. *Mass Spectrom. Rev.* **2014**, *33*, 302–331. [[CrossRef](#)]

38. Laourdakis, C.D.; Merino, E.F.; Neilson, A.P.; Cassera, M.B. Comprehensive quantitative analysis of purines and pyrimidines in the human malaria parasite using ion-pairing ultra-performance liquid chromatography-mass spectrometry. *J. Chromatogr. B* **2014**, *967*, 127–133. [[CrossRef](#)]
39. Li, S.; Jin, Y.; Tang, Z.; Lin, S.; Liu, H.; Jiang, Y.; Cai, Z. A novel method of liquid chromatography–tandem mass spectrometry combined with chemical derivatization for the determination of ribonucleosides in urine. *Anal. Chim. Acta* **2015**, *864*, 30–38. [[CrossRef](#)]
40. Lu, Z.; Wang, Q.; Wang, M.; Fu, S.; Zhang, Q.; Zhang, Z.; Zhao, H.; Liu, Y.; Huang, Z.; Xie, Z.; et al. Using UHPLC Q-Trap/MS as a complementary technique to in-depth mine UPLC Q-TOF/MS data for identifying modified nucleosides in urine. *J. Chromatogr. B* **2017**, *1051*, 108–117. [[CrossRef](#)]
41. Markham, P.; Robson, G.D.; Bainbridge, B.W.; Trinci, A.P. Choline: Its role in the growth of filamentous fungi and the regulation of mycelial morphology. *FEMS Microbiol. Lett.* **1993**, *104*, 287–300. [[CrossRef](#)]
42. Lamberts, L.; Rombouts, I.; Delcour, J.A. Study of nonenzymic browning in α -amino acid and γ -aminobutyric acid/sugar model systems. *Food Chem.* **2008**, *111*, 738–744. [[CrossRef](#)]
43. Kemp, J.D. In Vivo Synthesis of Crown Gall-specific *Agrobacterium tumefaciens*-directed Derivatives of Basic Amino Acids. *Plant Physiol.* **1978**, *62*, 26–30. [[CrossRef](#)]
44. Spencer, B.; Hussey, E.C.; Orsi, B.A.; Scott, J.M. Mechanism of choline O-sulphate utilization in fungi. *Biochem. J.* **1968**, *106*, 461–469. [[CrossRef](#)]
45. Grass, J.; Pabst, M.; Kolarich, D.; Pörtl, G.; Léonard, R.; Brecker, L.; Altmann, F. Discovery and Structural Characterization of Fucosylated Oligomannosidic N-Glycans in Mushrooms. *J. Boil. Chem.* **2010**, *286*, 5977–5984. [[CrossRef](#)]
46. Kariya, M.; Namiki, H. HPLC of phenylthiocarbonyl labelled uridine-diphosphate-hexosamine. *Chromatographia* **1997**, *46*, 5–11. [[CrossRef](#)]
47. El-Ganiny, A.M.; Sheoran, I.; Sanders, D.A.; Kaminsky, S.G. *Aspergillus nidulans* UDP-glucose-4-epimerase UgeA has multiple roles in wall architecture, hyphal morphogenesis, and asexual development. *Fungal Genet. Boil.* **2010**, *47*, 629–635. [[CrossRef](#)]
48. Carpi, F.M.; Cortese, M.; Orsomando, G.; Polzonetti, V.; Vincenzetti, S.; Moreschini, B.; Coleman, M.; Magni, G.; Pucciarelli, S. Simultaneous quantification of nicotinamide mononucleotide and related pyridine compounds in mouse tissues by UHPLC-MS/MS. *Sep. Sci. PLUS* **2018**, *1*, 22–30. [[CrossRef](#)]
49. Maruyama, D.; Nishitani, Y.; Nonaka, T.; Kita, A.; Fukami, T.A.; Mio, T.; Yamada-Okabe, H.; Yamada-Okabe, T.; Miki, K. Crystal Structure of Uridine-diphospho-N-acetylglucosamine Pyrophosphorylase from *Candida albicans* and Catalytic Reaction Mechanism. *J. Boil. Chem.* **2007**, *282*, 17221–17230. [[CrossRef](#)]
50. Strijbis, K.; Distel, B. Intracellular Acetyl Unit Transport in Fungal Carbon Metabolism. *Eukaryot. Cell* **2010**, *9*, 1809–1815. [[CrossRef](#)]
51. Lorenzetti, R.; Lilla, S.; Donato, J.L.; De Nucci, G. Simultaneous quantification of GMP, AMP, cyclic GMP and cyclic AMP by liquid chromatography coupled to tandem mass spectrometry. *J. Chromatogr. B* **2007**, *859*, 37–41. [[CrossRef](#)]
52. Zhang, W.; Tan, S.; Paintsil, E.; Dutschman, G.E.; Gullen, E.A.; Chu, E.; Cheng, Y.-C. Analysis of deoxyribonucleotide pools in human cancer cell lines using a liquid chromatography coupled with tandem mass spectrometry technique. *Biochem. Pharmacol.* **2011**, *82*, 411–417. [[CrossRef](#)]
53. Zhu, M.; Assmann, S.M. Metabolic Signatures in Response to Abscisic Acid (ABA) Treatment in *Brassica napus* Guard Cells Revealed by Metabolomics. *Sci. Rep.* **2017**, *7*, 12875. [[CrossRef](#)]
54. Li, M.; Chen, T.; Gao, T.; Miao, Z.; Jiang, A.; Shi, L.; Ren, A.; Zhao, M. UDP-glucose pyrophosphorylase influences polysaccharide synthesis, cell wall components, and hyphal branching in *Ganoderma lucidum* via regulation of the balance between glucose-1-phosphate and UDP-glucose. *Fungal Genet. Boil.* **2015**, *82*, 251–263. [[CrossRef](#)]
55. Ibanez, C.; Simó, C.; Garcia-Cañas, V.; Gómez-Martínez, Á.; Ferragut, J.A.; Cifuentes, A. CE/LC-MS multiplatform for broad metabolomic analysis of dietary polyphenols effect on colon cancer cells proliferation. *Electrophoresis* **2012**, *33*, 2328–2336. [[CrossRef](#)]
56. Bogo, A.; Mantle, P.G.; Casa, R.T.; Guidolin, A.F. The structures of the honeydew oligosaccharides synthesized by *Claviceps africana*. *Summa Phytopathol.* **2006**, *32*, 16–20. [[CrossRef](#)]
57. Miyakoshi, S.; Uchiyama, H.; Someya, T.; Satoh, T.; Tabuchi, T. Distribution of the Methylcitric Acid Cycle and α -Oxidation Pathway for Propionate Catabolism in Fungi. *Agric. Boil. Chem.* **1987**, *51*, 2381–2387. [[CrossRef](#)]

58. Brock, M.; Maerker, C.; Schutz, A.; Völker, U.; Buckel, W. Oxidation of propionate to pyruvate in *Escherichia coli*: Involvement of methylcitrate dehydratase and aconitase. *Eur. J. Biochem.* **2002**, *269*, 6184–6194. [[CrossRef](#)]
59. Bähre, H.; Kaever, V. Measurement of 2',3'-cyclic nucleotides by liquid chromatography–tandem mass spectrometry in cells. *J. Chromatogr. B* **2014**, *964*, 208–211. [[CrossRef](#)]
60. Dittmar, F.; Abdelilah-Seyfried, S.; Tschirner, S.K.; Kaever, V.; Seifert, R. Temporal and organ-specific detection of cNMPs including cUMP in the zebrafish. *Biochem. Biophys. Res. Commun.* **2015**, *468*, 708–712. [[CrossRef](#)]
61. Seifert, R. Distinct Signaling Roles of cCMP, cCMP, and cUMP. *Structure* **2016**, *24*, 1627–1628. [[CrossRef](#)]
62. Świeżawska, B.; Duszyn, M.; Jaworski, K.; Szmidsztajn, A. Downstream Targets of Cyclic Nucleotides in Plants. *Front. Plant Sci.* **2018**, *9*, 9. [[CrossRef](#)]
63. Contreras-Sanz, A.; Scott-Ward, T.S.; Gill, H.S.; Jacoby, J.C.; Birch, R.E.; Malone-Lee, J.; Taylor, K.M.G.; Peppiatt-Wildman, C.M.; Wildman, S.S.P. Simultaneous quantification of 12 different nucleotides and nucleosides released from renal epithelium and in human urine samples using ion-pair reversed-phase HPLC. *Purinergic Signal.* **2012**, *8*, 741–751. [[CrossRef](#)]
64. Perret, D. Of urines and purines—A life in separation science. *Nucleosides Nucleotides Nucleic Acids* **2018**, *37*, 588–602. [[CrossRef](#)]
65. Pocsí, I.; Prade, R.A.; Penninckx, M.J. Glutathione, Altruistic metabolite in fungi. *Adv. Microb. Physiol.* **2004**, *49*, 1–76. [[CrossRef](#)]
66. Semighini, C.P.; Savoldi, M.; Goldman, G.H.; Harris, S.D. Functional Characterization of the Putative *Aspergillus nidulans* Poly(ADP-Ribose) Polymerase Homolog PrpA. *Genetics* **2006**, *173*, 87–98. [[CrossRef](#)]
67. Farag, M.A.; El-Kersh, D.M.; Ehrlich, A.; Choucri, M.A.; El-Seedi, H.; Frolov, A.; Wessjohann, L.A.; Shokry, M.; Frolov, A. Variation in *Ceratonia siliqua* pod metabolome in context of its different geographical origin, ripening stage and roasting process. *Food Chem.* **2019**, *283*, 675–687. [[CrossRef](#)]
68. Giffhorn, F. Fungal pyranose oxidases: Occurrence, properties and biotechnical applications in carbohydrate chemistry. *Appl. Microbiol. Biotechnol.* **2000**, *54*, 727–740. [[CrossRef](#)]
69. Nain-Perez, A.; Barbosa, L.C.A.; Maltha, C.R.Á.; Forlani, G. Natural Abenquines and Their Synthetic Analogues Exert Algicidal Activity against Bloom-Forming Cyanobacteria. *J. Nat. Prod.* **2017**, *80*, 813–818. [[CrossRef](#)]
70. Schulz, D.; Beese, P.; Ohlendorf, B.; Erhard, A.; Zinecker, H.; Dorador, C.; Imhoff, J.F. Abenquines A–D: aminoquinone derivatives produced by *Streptomyces* sp. strain DB634. *J. Antibiot.* **2011**, *64*, 763–768. [[CrossRef](#)]
71. Cheng, Q.; Gu, J.; Compaan, K.R.; Schaefer, H.F. Isoguanine Formation from Adenine. *Chem. - A Eur. J.* **2012**, *18*, 4877–4886. [[CrossRef](#)]
72. Karalkar, N.B.; Khare, K.; Molt, R.; Benner, S.A. Tautomeric equilibria of isoguanine and related purine analogs. *Nucleosides Nucleotides Nucleic Acids* **2017**, *31*, 1–19. [[CrossRef](#)]
73. Bartholdy, B.; Berreck, M.; Haselwandter, K. Hydroxamate siderophore synthesis by *Phialocephala fortinii*, a typical dark septate fungal root endophyte. *BioMetals* **2001**, *14*, 33–42. [[CrossRef](#)]
74. Haas, H.; Eisendle, M.; Turgeon, B.G. Siderophores in Fungal Physiology and Virulence. *Annu. Rev. Phytopathol.* **2008**, *46*, 149–187. [[CrossRef](#)]
75. Holinsworth, B.; Martin, J.D. Siderophore production by marine-derived fungi. *BioMetals* **2009**, *22*, 625–632. [[CrossRef](#)]
76. Bertrand, S.; Duval, O.; Helesbeux, J.-J.; Larcher, G.; Richomme, P. Synthesis of the *trans*-fusarinine scaffold. *Tetrahedron Lett.* **2010**, *51*, 2119–2122. [[CrossRef](#)]
77. Kajula, M.; Tejesvi, M.V.; Kolehmainen, S.; Mäkinen, A.; Hokkanen, J.; Mattila, S.; Pirttilä, A.-M. The siderophore ferricrocin produced by specific foliar endophytic fungi in vitro. *Fungal Biol.* **2010**, *114*, 248–254. [[CrossRef](#)]
78. Rublee, P.A.; Merkel, S.M.; Faust, M.A.; Miklas, J. Distribution and activity of bacteria in the headwaters of the Rhode River Estuary, Maryland, USA. *Microb. Ecol.* **1984**, *10*, 243–255. [[CrossRef](#)]
79. Klinger, M.M.; A Laine, R.; Steiner, S.M. Characterization of novel amino acid fucosides. *J. Boil. Chem.* **1981**, *256*, 7932–7935.
80. Cuendet, M.; Hostettmann, K.; Potterat, O.; Dyatmiko, W. Iridoid Glucosides with Free Radical Scavenging Properties from *Fagraea blumei*. *Helvetica Chim. Acta* **1997**, *80*, 1144–1152. [[CrossRef](#)]
81. Hill, R.A.; Sutherland, A. Hot off the press. *Nat. Prod. Rep.* **2017**, *34*, 338–342. [[CrossRef](#)]

82. Sang, X.-N.; Chen, S.-F.; Chen, G.; An, X.; Li, S.-G.; Lu, X.-J.; Zhao, D.; Bai, J.; Wang, H.-F.; Pei, Y.-H. Two pairs of enantiomeric α -pyrone dimers from the endophytic fungus *Phoma* sp. YN02-P-3. *RSC Adv.* **2017**, *7*, 1943–1946. [[CrossRef](#)]
83. Wang, X.; Lin, M.; Xu, D.; Lai, D.; Zhou, L. Structural Diversity and Biological Activities of Fungal Cyclic Peptides, Excluding Cyclodipeptides. *Molecules* **2017**, *22*, 2069. [[CrossRef](#)]
84. Li, X.-Y.; Wang, Y.-H.; Yang, J.; Cui, W.-Y.; He, P.-J.; Munir, S.; He, P.-F.; Wu, Y.-X.; He, Y.-Q. Acaricidal Activity of Cyclodipeptides from *Bacillus amyloliquefaciens* W1 against *Tetranychus urticae*. *J. Agric. Food Chem.* **2018**, *66*, 10163–10168. [[CrossRef](#)]
85. Yamaoka, N.; Kudo, Y.; Inazawa, K.; Inagawa, S.; Yasuda, M.; Mawatari, K.-I.; Nakagomi, K.; Kaneko, K. Simultaneous determination of nucleosides and nucleotides in dietary foods and beverages using ion-pairing liquid chromatography–electrospray ionization–mass spectrometry. *J. Chromatogr. B* **2010**, *878*, 2054–2060. [[CrossRef](#)]
86. Sánchez, J.; Nikolau, B.J.; Stumpf, P.K. Reduction of N-Acetyl Methionine Sulfoxide in Plants. *Plant Physiol.* **1983**, *73*, 619–623. [[CrossRef](#)]
87. Ling, S.-K.; Komorita, A.; Tanaka, T.; Fujioka, T.; Mihashi, K.; Kouno, I. Iridoids and Anthraquinones from the Malaysian Medicinal Plant, *Saprosma scortechinii* (Rubiaceae). *Chem. Pharm. Bull.* **2002**, *50*, 1035–1040. [[CrossRef](#)]
88. Kanchanapoom, T.; Kasai, R.; Yamasaki, K. Iridoid and phenolic glycosides from *Morinda coreia*. *Phytochemistry* **2002**, *59*, 551–556. [[CrossRef](#)]
89. Li, C.; Xue, X.; Zhou, D.; Zhang, F.; Xu, Q.; Ren, L.; Liang, X. Analysis of iridoid glucosides in *Hedyotis diffusa* by high-performance liquid chromatography/electrospray ionization tandem mass spectrometry. *J. Pharm. Biomed. Anal.* **2008**, *48*, 205–211. [[CrossRef](#)]
90. Friščić, M.; Bucar, F.; Pilepić, K.H. LC-PDA-ESI-MS analysis of phenolic and iridoid compounds from *Globularia* spp. *J. Mass Spectrom.* **2016**, *51*, 1211–1236. [[CrossRef](#)]
91. Alara, O.R.; Abdurahman, N.H.; Ukaegbu, C.I.; Azhari, N.H.; Kabbashi, N.A. Metabolic profiling of flavonoids, saponins, alkaloids, and terpenoids in the extract from *Vernonia cinerea* leaf using LC-Q-TOF-MS. *J. Liq. Chromatogr. Relat. Technol.* **2018**, *41*, 722–731. [[CrossRef](#)]
92. Fushiya, S.; Matsuda, M.; Yamada, S.; Nozoe, S. New opine type amino acids from a poisonous mushroom, *Clitocybe acromelalga*. *Tetrahedron* **1996**, *52*, 877–886. [[CrossRef](#)]
93. Davidek, T.; Blank, I.; Kraehenbuehl, K.; Hau, J.; Devaud, S. New approaches in the analysis of Amadori compounds. In *Innovations in Analytical Flavor Research, State-of-the-Art in Flavour Chemistry and Biology, Proceedings of the 7th Wartburg Symposium, Eisenach, Germany, 21–23 April 2004*; Hofmann, T., Rothe, M., Schieberle, P., Eds.; Deutsche Forschungsanstalt für Lebensmittelchemie: Garching, Germany, 2005; Volume 4953, pp. 213–219.
94. Sulyok, M.; Beed, F.; Boni, S.; Abass, A.; Mukunzi, A.; Krska, R. Quantitation of multiple mycotoxins and cyanogenic glucosides in cassava samples from Tanzania and Rwanda by an LC-MS/MS-based multi-toxin method. *Food Addit. Contam. Part A* **2015**, *32*, 488–502. [[CrossRef](#)]
95. Bashyal, B.P.; Wijeratne, E.M.K.; Faeth, S.H.; Gunatilaka, A.A.L. Globosumones A–C, Cytotoxic Orsellinic Acid Esters from the Sonoran Desert Endophytic Fungus *Chaetomium globosum*. *J. Nat. Prod.* **2005**, *68*, 724–728. [[CrossRef](#)]
96. Schlörke, O.; Zeeck, A. Orsellides A–E: An Example for 6-Deoxyhexose Derivatives Produced by Fungi. *Eur. J. Org. Chem.* **2006**, *2006*, 1043–1049. [[CrossRef](#)]
97. Xu, G.-B.; Wang, N.-N.; Bao, J.-K.; Yang, T.; Li, G.-Y. New Orsellinic Acid Esters from Fungus *Chaetomium globosporum*. *Helvetica Chim. Acta* **2014**, *97*, 151–159. [[CrossRef](#)]
98. Nakano, T.; Sugimoto, S.; Matsunami, K.; Otsuka, H. Dianthosaponins A–F, Triterpene Saponins, Flavonoid Glycoside, Aromatic Amide Glucoside and γ -Pyrone Glucoside from *Dianthus japonicus*. *Chem. Pharm. Bull.* **2011**, *59*, 1141–1148. [[CrossRef](#)]
99. Wu, Q.; Wang, Y.; Guo, M. Triterpenoid Saponins from the Seeds of *Celosia argentea* and Their Anti-inflammatory and Antitumor Activities. *Chem. Pharm. Bull.* **2011**, *59*, 666–671. [[CrossRef](#)]
100. Sommart, U.; Rukachaisirikul, V.; Sukpondma, Y.; Phongpaichit, S.; Sakayaroj, J.; Kirtikara, K. Hydronaphthalenones and a Dihydroramulosin from the Endophytic Fungus PSU-N24. *Chem. Pharm. Bull.* **2008**, *56*, 1687–1690. [[CrossRef](#)]

101. Gunatilaka, A.A.L. Natural Products from plant-associated microorganisms: Distribution, structural diversity, bioactivity, and implications of their occurrence. *J. Nat. Prod.* **2006**, *69*, 509–526. [[CrossRef](#)]
102. Abdalla, M.A.; Matasyoh, J.C. Endophytes as Producers of Peptides: An Overview About the Recently Discovered Peptides from Endophytic Microbes. *Nat. Prod. Bioprospecting* **2014**, *4*, 257–270. [[CrossRef](#)]
103. Nisa, H.; Kamili, A.N.; Nawchoo, I.A.; Shafi, S.; Shameem, N.; Bandh, S.A. Fungal endophytes as prolific source of phytochemicals and other bioactive natural products: A review. *Microb. Pathog.* **2015**, *82*, 50–59. [[CrossRef](#)]
104. Salas, C.E.; Badillo-Corona, J.A.; Ramírez-Sotelo, G.; Oliver-Salvador, C.; Ramí Rez-Sotelo, G. Biologically Active and Antimicrobial Peptides from Plants. *BioMed Res. Int.* **2015**, *2015*, 1–11. [[CrossRef](#)]
105. Bondaryk, M.; Staniszewska, M.; Zielińska, P.; Urbańczyk-Lipkowska, Z. Natural Antimicrobial Peptides as Inspiration for Design of a New Generation Antifungal Compounds. *J. Fungi* **2017**, *3*, 46. [[CrossRef](#)]
106. Kombrink, A.; Tayyrov, A.; Essig, A.; Stöckli, M.; Micheller, S.; Hintze, J.; van Heuvel, Y.; Dürig, N.; Lin, C.-W.; Kallio, P.T.; et al. Induction of antibacterial proteins and peptides in the coprophilous mushroom *Coprinopsis cinerea* in response to bacteria. *ISME J.* **2019**, *13*, 588–602. [[CrossRef](#)]
107. Winter, G.; Todd, C.D.; Trovato, M.; Forlani, G.; Funck, D. Physiological implications of arginine metabolism in plants. *Front. Plant Sci.* **2015**, *6*, 1–14. [[CrossRef](#)]
108. Kwak, M.-K.; Liu, R.; Kim, M.-K.; Moon, D.; Kim, A.H.; Song, S.-H.; Kang, S.-O. Cyclic dipeptides from lactic acid bacteria inhibit the proliferation of pathogenic fungi. *J. Microbiol.* **2014**, *52*, 64–70. [[CrossRef](#)]
109. Xu, H.; Andi, B.; Qian, J.; West, A.H.; Cook, P.F. The α -Amino adipate Pathway for Lysine Biosynthesis in Fungi. *Cell Biophys.* **2006**, *46*, 43–64. [[CrossRef](#)]
110. Sarjala, T.; Tienaho, J.; Leon-D, E.; Wähälä, K. Antioxidant activity and bioactive properties of root-colonizing endophytic fungi. *Coniochaeta lignicola* **2019**. Manuscript in preparation.
111. Scott, J.F.; Zamecnik, P.C. SOME OPTICAL PROPERTIES OF DIADENOSINE-5'-PHOSPHATES. *Proc. Natl. Acad. Sci. USA* **1969**, *64*, 1308–1314. [[CrossRef](#)]
112. Lucas, K.A.; Filley, J.R.; Erb, J.M.; Graybill, E.R.; Hawes, J.W. Peroxisomal Metabolism of Propionic Acid and Isobutyric Acid in Plants. *J. Boil. Chem.* **2007**, *282*, 24980–24989. [[CrossRef](#)]
113. Modess, O. Zur Kenntnis der Mykorrhizabildner von Kiefer und Fichte. In *Symbolae botanicae Upsalienses*; Anonymous, Ed.; Uppsala Universitet: Uppsala, Sweden, 1941; Volume 5, pp. 1–147.
114. White, T.; Bruns, T.; Lee, S.; Taylor, J. AMPLIFICATION AND DIRECT SEQUENCING OF FUNGAL RIBOSOMAL RNA GENES FOR PHYLOGENETICS. In *PCR Protocols*; Elsevier BV: Amsterdam, The Netherlands, 1990; pp. 315–322.
115. Koukol, O.; Kolařík, M.; Kolářová, Z.; Baldrian, P. Diversity of foliar endophytes in wind-fallen *Picea abies* trees. *Fungal Divers.* **2012**, *54*, 69–77. [[CrossRef](#)]

Sample Availability: Samples of the compounds are not available from the authors.



© 2019 by the authors. Licensee MDPI, Basel, Switzerland. This article is an open access article distributed under the terms and conditions of the Creative Commons Attribution (CC BY) license (<http://creativecommons.org/licenses/by/4.0/>).

Metabolic Profiling of Water-Soluble Compounds from the Extracts of Dark Septate Endophytic Fungi (DSE) Isolated from Scots Pine (*Pinus sylvestris* L.) Seedlings Using UPLC–Orbitrap–MS

Jenni Tienaho ^{1,2,*}, Maarit Karonen ³, Riina Muilu–Mäkelä ², Kristiina Wähälä ⁴, Eduardo Leon Denegri ⁴, Robert Franzén ⁵, Matti Karp ¹, Ville Santala ¹ and Tytti Sarjala ²

¹ Faculty of Natural Sciences and Engineering, Tampere University, FI-33101 Tampere, Finland; karpmatti1@gmail.com (M.K.); ville.santala@tuni.fi (V.S.)

² Natural Resources Institute Finland (Luke), FI-00791 Helsinki, Finland; riina.muilu-makela@luke.fi (R.M.-M.); tytti.sarjala@luke.fi (T.S.)

³ Natural Chemistry Research Group, Department of Chemistry, University of Turku, FI-20014 Turku, Finland; maarit.karonen@utu.fi

⁴ Department of Chemistry, University of Helsinki, FI-00014 Helsinki, Finland; kristiina.wahala@helsinki.fi; (K.W.); eleondenegri@outlook.com (E.L.D.)

⁵ School of Chemical Engineering, Department of Chemistry and Materials Science, Aalto University, FI-00076 Espoo, Finland; robert.franzen@aalto.fi

* Correspondence: jenni.tienaho@tuni.fi or jenni.tienaho@luke.fi; Tel.: +358-29-532-4986

Table S1. The unidentified metabolites. The intensity of the metabolite in the corresponding fungi extract is shown under the fungal species codes. Intensities over 1×10^7 are shown in black whereas lower intensities with a grey color. Other ions are also shown if detected. * = Was also detected but not identified by Sun et al. [26]. nd = not detected.

#	rt	[M + H] ⁺	[M – H] ⁻	Exact Mass Measured	A	R	S16	Other Ions
1	0.40	274	272	273.96623*	5×10 ⁷	8×10 ⁶	8×10 ⁶	
2	0.40	388	386	387.94673*	3×10 ⁷	2×10 ⁶	3×10 ⁵	
3	0.40	518	516	517.90331	5×10 ⁶	2×10 ⁵	nd	
4	0.41	218	216	217.97572*	1×10 ⁷	1×10 ⁶	1×10 ⁷	
5	0.46	nd	257	258.07335	6×10 ⁶	1×10 ⁷	3×10 ⁶	
6	0.46	387	385	386.18007	7×10 ⁵	7×10 ⁶	7×10 ⁵	
7	0.47	251	249	250.02328	1×10 ⁷	3×10 ⁷	1×10 ⁷	
8	0.49	308	306	307.21086	6×10 ⁴	2×10 ⁵	7×10 ⁴	
9	0.50	nd	194	195.95317	6×10 ⁶	5×10 ⁶	1×10 ⁷	
10	0.53	219	nd	218.01907	2×10 ⁷	2×10 ⁷	7×10 ⁷	
11	0.53	329	327	328.14845	4×10 ⁷	6×10 ⁷	1×10 ⁷	
12	0.53	nd	371	372.14400	1×10 ⁷	5×10 ⁷	9×10 ⁶	
13	0.53	nd	396	397.13561	2×10 ⁶	2×10 ⁶	8×10 ⁶	
14	0.54	nd	217	218.05522	8×10 ⁸	8×10 ⁸	6×10 ⁸	
15	0.54	221	219	220.03447	2×10 ⁷	2×10 ⁸	2×10 ⁸	
16	0.54	281	279	280.05580	1×10 ⁸	1×10 ⁸	1×10 ⁸	
17	0.55	441	439	440.09453	1×10 ⁸	7×10 ⁷	7×10 ⁶	
18	0.56	353	351	352.14891	4×10 ⁵	7×10 ⁵	9×10 ⁵	
19	0.58	358	nd	357.16752	4×10 ⁸	4×10 ⁸	3×10 ⁸	
20	0.60	nd	194	195.95305	4×10 ⁷	4×10 ⁷	9×10 ⁷	
21	0.61	353	351	352.14790	7×10 ⁵	1×10 ⁶	1×10 ⁶	
22	0.70	nd	238	239.89826	2×10 ⁷	1×10 ⁷	6×10 ⁴	
23	0.70	323	321	322.13713	2×10 ⁵	2×10 ⁶	4×10 ⁵	
24	0.71	265	263	264.11391	9×10 ⁵	2×10 ⁶	4×10 ⁵	
25	0.73	286	284	287.15767	2×10 ⁸	2×10 ⁸	3×10 ⁷	
26	0.74	240	238	239.89876	2×10 ⁷	1×10 ⁷	1×10 ⁵	
27	0.81	409	407	408.17357	1×10 ⁶	4×10 ⁶	1×10 ⁶	
28	0.87	274	272	273.08436	3×10 ⁶	1×10 ⁷	6×10 ⁶	
29	0.96	274	272	273.08439	3×10 ⁶	8×10 ⁶	4×10 ⁶	
30	0.98	nd	522	523.13210	3×10 ⁵	6×10 ⁶	5×10 ⁴	
31	1.05	nd	675	676.20680	9×10 ⁵	nd	nd	
32	1.19	409	407	408.17412	1×10 ⁶	1×10 ⁶	8×10 ⁵	
33	1.21	409	407	408.17412	5×10 ⁵	3×10 ⁶	6×10 ⁵	
34	1.28	588	586	587.10512	nd	nd	9×10 ⁵	
35	1.35	240	238	239.89890	2×10 ⁶	9×10 ⁵	2×10 ⁵	
36	1.74	280	278	279.13032	4×10 ⁶	3×10 ⁶	8×10 ⁶	
37	1.75	714	712	713.21584	1×10 ⁵	nd	nd	
38	1.78	239	237	238.10523	1×10 ⁸	3×10 ⁷	3×10 ⁵	
39	1.78	550	548	549.11226	1×10 ⁷	3×10 ⁷	3×10 ⁷	1099.22937 [2M + H] ⁺ ; 1097.34277 [2M – H] ⁻
40	1.78	621	619	620.11598	8×10 ⁶	2×10 ⁷	2×10 ⁷	
41	1.79	221	219	220.09434	8×10 ⁶	2×10 ⁶	6×10 ⁵	
42	1.85	501	499	500.02419	3×10 ⁷	5×10 ⁷	6×10 ⁷	
43	1.90	430	nd	429.10509	4×10 ⁵	5×10 ⁶	6×10 ⁵	
44	1.93	219	nd	218.10373	1×10 ⁷	nd	1×10 ⁶	
45	1.98	nd	287	288.09615	1×10 ⁷	2×10 ⁷	8×10 ⁶	
46	1.98	428	426	427.56868	7×10 ⁶	2×10 ⁷	7×10 ⁶	
47	1.99	551	549	550.09609	6×10 ⁷	3×10 ⁸	2×10 ⁸	
48	2.02	430	nd	429.10518	7×10 ⁶	2×10 ⁷	7×10 ⁶	
49	2.04	2630	2628	2629.83072	1×10 ⁵	2×10 ⁵	6×10 ⁵	1315.92264 [M + 2H] ²⁺ ; 1313.90808 [M – 2H] ²⁻
50	2.04	nd	2674	2675.83414	3×10 ⁴	9×10 ⁴	2×10 ⁵	1336.90979 [M – 2H] ²⁻
51	2.05	636	634	635.11345	1×10 ⁷	3×10 ⁷	9×10 ⁶	
52	2.05	557	555	556.14305	5×10 ⁶	6×10 ⁶	7×10 ⁶	
53	2.06	284	282	283.11683	6×10 ⁶	5×10 ⁶	5×10 ⁷	
54	2.06	430	428	429.10496	3×10 ⁶	1×10 ⁷	3×10 ⁶	
55	2.09	521	519	520.22252	nd	nd	5×10 ⁶	
56	2.12	283	nd	282.07945	1×10 ⁷	3×10 ⁷	1×10 ⁷	565.16650 [2M + H] ⁺ ; 563.15295 [2M – H] ⁻
57	2.12	398	396	397.13389	8×10 ⁷	7×10 ⁷	4×10 ⁷	
58	2.12	532	530	531.13646	3×10 ⁶	1×10 ⁷	3×10 ⁶	
59	2.15	280	278	279.12977	2×10 ⁷	2×10 ⁷	5×10 ⁶	

60	2.15	379	377	378.10960	nd	7×10 ⁶	nd	
61	2.19	232	nd	231.14696	2×10 ⁸	2×10 ⁸	1×10 ⁹	
62	2.19	429	427	428.06072	3×10 ⁶	3×10 ⁷	2×10 ⁷	857.12567 [2M + H] ⁺ ; 855.11475 [2M - H] ⁻
63	2.29	532	530	531.13615	7×10 ⁶	2×10 ⁷	9×10 ⁶	
64	2.32	556	554	555.14738	3×10 ⁷	5×10 ⁷	2×10 ⁷	
65	2.34	627	625	626.10191	4×10 ⁷	2×10 ⁸	4×10 ⁷	
66	2.35	572	570	571.14232	1×10 ⁷	1×10 ⁷	1×10 ⁷	1143.28784 [2M + H] ⁺ ; 1141.27905 [2M - H] ⁻
67	2.38	435	433	434.10237	1×10 ⁶	7×10 ⁵	1×10 ⁶	
68	2.40	458	456	457.57568	1×10 ⁷	2×10 ⁷	1×10 ⁷	
69	2.49	418	416	417.59318	1×10 ⁶	3×10 ⁶	2×10 ⁶	836.18762 [2M + H] ⁺ ; 834.17896 [2M - H] ⁻
70	2.50	217	215	216.08989	nd	5×10 ⁵	nd	
71	2.61	1149	1147	1148.24490	3×10 ⁵	1×10 ⁵	2×10 ⁶	575.12973 [M + 2H] ²⁺ ; 573.11517 [M - 2H] ²⁻
72	2.62	860	858	859.19628	1×10 ⁶	1×10 ⁶	2×10 ⁶	
73	2.63	1125	1123	1124.23156	4×10 ⁵	3×10 ⁵	1×10 ⁶	563.12306 [M + 2H] ²⁺ ; 561.10850 [M - 2H] ²⁻
74	2.64	1173	1171	1172.25456	nd	nd	4×10 ⁵	587.13456 [M + 2H] ²⁺ ; 585.12000 [M - 2H] ²⁻
75	2.67	836	834	835.18477	1×10 ⁶	3×10 ⁶	3×10 ⁶	
76	2.74	289	287	288.12139	5×10 ⁵	2×10 ⁷	2×10 ⁵	
77	2.84	430	428	429.59822	3×10 ⁴	5×10 ⁴	nd	
78	2.92	297	295	296.14736	2×10 ⁸	5×10 ⁷	2×10 ⁷	314.18057 [M + NH ₃ + H] ⁺
79	2.92	1440	1438	1439.71760	5×10 ⁵	3×10 ⁷	1×10 ⁶	720.86316 [M + 2H] ²⁺ ; 718.84860 [M - 2H] ²⁻
80	2.98	311	309	310.12599	2×10 ⁸	2×10 ⁸	5×10 ⁷	328.15967 [M + NH ₃ + H] ⁺
81	3.03	217	215	216.09007	2×10 ⁷	1×10 ⁷	8×10 ⁶	
82	3.03	273	271	272.12620	2×10 ⁶	6×10 ⁶	nd	
83	3.21	341	339	340.17302	4×10 ⁸	2×10 ⁸	3×10 ⁷	358.20670 [M + NH ₃ + H] ⁺
84	3.28	355	353	354.15187	4×10 ⁸	4×10 ⁸	7×10 ⁷	372.18558 [M + NH ₃ + H] ⁺
85	3.29	nd	815	816.24794	3×10 ⁵	nd	nd	
86	3.30	386	nd	385.12025	1×10 ⁶	5×10 ⁶	3×10 ⁷	771.24628 [2M + H] ⁺ ; 769.23413 [2M - H] ⁻
87	3.46	385	383	384.19998	3×10 ⁸	1×10 ⁸	3×10 ⁷	402.23282 [M + NH ₃ + H] ⁺
88	3.53	544	542	543.19283	6×10 ⁶	2×10 ⁶	9×10 ⁵	
89	3.54	399	397	398.17891	4×10 ⁸	4×10 ⁸	1×10 ⁸	416.21155 [M + NH ₃ + H] ⁺
90	3.66	219	217	218.11531	8×10 ⁶	5×10 ⁷	9×10 ⁴	
91	3.69	429	427	428.22640	1×10 ⁸	8×10 ⁷	2×10 ⁷	
92	3.77	443	441	442.20564	2×10 ⁸	2×10 ⁸	1×10 ⁸	460.23773 [M + NH ₃ + H] ⁺
93	3.80	406	404	405.19078	6×10 ⁵	nd	nd	
94	3.90	473	471	472.25292	3×10 ⁷	5×10 ⁷	nd	490.28571 [M + NH ₃ + H] ⁺
95	4.03	883	881	882.45986	3×10 ⁶	2×10 ⁷	nd	1765.91760 [2M + H] ⁺ ; 1763.91077 [2M - H] ⁻
96	4.08	1085	1083	1084.04655	nd	7×10 ⁵	nd	
97	4.09	534	nd	533.30479	2×10 ⁷	8×10 ⁷	3×10 ⁷	
98	4.96	395	393	394.19960	nd	3×10 ⁷	nd	



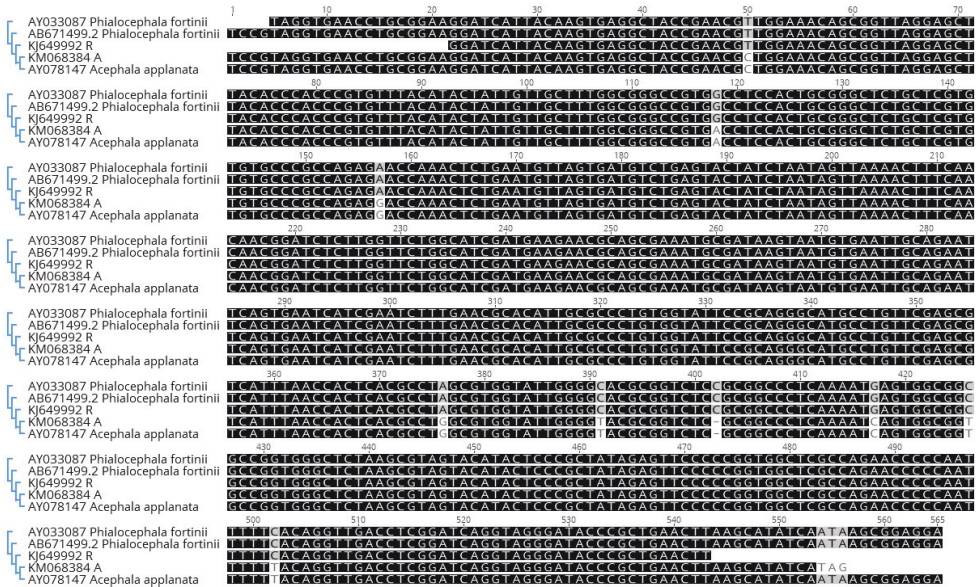


Figure S2. Alignment of ITS region of A (KM068384) and R (KJ649992) strains with their best GenBank matches *Acepheala applanata* (AY078147) and *Phialocephala fortinii* (AB671499.2 and AY033087), respectively.

Correction

Correction: Tienaho, J., *et al.* Metabolic Profiling of Water-Soluble Compounds from the Extracts of Dark Septate Endophytic Fungi (DSE) Isolated from Scots Pine (*Pinus sylvestris* L.) Seedlings Using UPLC–Orbitrap–MS. *Molecules* 2019, 24, 2330

Jenni Tienaho ^{1,2,*}, Maarit Karonen ³, Riina Muilu–Mäkelä ², Kristiina Wähälä ⁴, Eduardo Leon Denegri ⁴, Robert Franzén ⁵, Matti Karp ¹, Ville Santala ¹ and Tytti Sarjala ²

¹ Faculty of Natural Sciences and Engineering, Tampere University, FI-33101 Tampere, Finland; karpmatti1@gmail.com (M.K.); ville.santala@tuni.fi (V.S.)

² Natural Resources Institute Finland (Luke), FI-00791 Helsinki, Finland; riina.muilu-makela@luke.fi (R.M.-M.); tytti.sarjala@luke.fi (T.S.)

³ Natural Chemistry Research Group, Department of Chemistry, University of Turku, FI-20014 Turku, Finland; maarit.karonen@utu.fi

⁴ Department of Chemistry, University of Helsinki, FI-00014 Helsinki, Finland; kristiina.wahala@helsinki.fi; (K.W.); eleondenegri@outlook.com (E.L.D.)

⁵ School of Chemical Engineering, Department of Chemistry and Materials Science, Aalto University, FI-00076 Espoo, Finland; robert.franzen@aalto.fi

* Correspondence: jenni.tienaho@tuni.fi or jenni.tienaho@luke.fi; Tel.: +358-29-532-4986

Received: 26 August 2019; Accepted: 16 September 2019; Published: 6 November 2019

The authors wish to make the following corrections to this paper published in *Molecules*. Two inadvertent errors were found from Table 2 footnotes section:

Footnote k states that “k = Tripeptide containing Arg, Glu and Val; or Arg, Asp and Leu or Ile; or Gln, Gln and Lys or a tetrapeptide containing Ala, Ala, Asp and Lys; or Ala, Gln, Gly and Lys or a pentapeptide containing Ala, Ala, Gly, Gly and Lys”.

However, it should be “k = Tripeptide containing Arg, Glu and Val; or Arg, Asp and Leu or Ile; or Gln, Gln and Lys or a tetrapeptide containing Ala, Ala, Asn and Lys; or Ala, Gln, Gly and Lys or a pentapeptide containing Ala, Ala, Gly, Gly and Lys”.

Footnote n states that “n = Tripeptide containing Ala, Glu and Val; or Glu, Glu and Leu or Ile; or Pro, Thr and Thr; or Ala, Asp and Leu or Ile; or an acetylated tripeptide containing Gly, Ser and Leu and Ile; or Gly, Thr and Val; or the methyl ester of a tripeptide containing Ala, Asp and Val or Asp, Gly and Leu or Ile”.

However, it should be “n = Tripeptide containing Ala, Glu and Val; or Glu, Gly and Leu or Ile; or Pro, Thr and Thr; or Ala, Asp and Leu or Ile; or an acetylated tripeptide containing Gly, Ser and Leu or Ile; or Gly, Thr and Val; or the methyl ester of a tripeptide containing Ala, Asp and Val or Asp, Gly and Leu or Ile”.

These changes have no material impact on the conclusions of our paper. We apologize for any inconvenience to our readers.



© 2019 by the authors. Licensee MDPI, Basel, Switzerland. This article is an open access article distributed under the terms and conditions of the Creative Commons Attribution (CC BY) license (<http://creativecommons.org/licenses/by/4.0/>).

PUBLICATION
IV

**Metabolites of the Endophytic Fungi of Scots Pine (*Pinus sylvestris*) Roots:
An Abundant Source of Bioactive Compounds for Potential Utilization**

Jenni Tienaho, Maarit Karonen, Riina Muilu-Mäkelä, Janne Kaseva, Nuria de Pedro, Francisca Vicente, Olga Genilloud, Ulla Aapola, Hannu Uusitalo, Robert Franzén, Kristiina Wähälä, Matti Karp, Ville Santala and Tytti Sarjala

Submitted for publication

